Université de Lille
Faculté de Médecine

Année 2022

THESE

Pour l'obtention du grade de
DOCTEUR DE L'UNIVERSITE DE LILLE

Discipline: Aspects moléculaires et cellulaires de la biologie - MED

Présentée par
Laura Mahoney-Sánchez

Caractérisation du rôle de l'α-synucleine dans la Ferroptose, dans le contexte de la maladie de Parkinson.

Directeur de thèse: Jean-Christophe Devedjian
Soutenu le 20 Juin 2022

JURY

Pr. David Devos	Président du Jury
Dr. Solange Desagher	Rapporteur
Dr. Stephan Schildknecht	Rapporteur
Pr. Sonia Gandhi	Examinateur
Dr. James Duce	Examinateur
Dr. Jean-Christophe Devedjian	Directeur de thèse

University of Lille
Faculty of Medicine

Year 2022

THESIS

For the degree of
Philosophiae Doctor, Ph.D

Discipline: Molecular and cellular aspects of Biology - MED

Presented by
Laura Mahoney-Sánchez

Characterising the role of α-synuclein in Ferroptosis, in the context of Parkinson's Disease

---

PhD supervisor: Jean-Christophe Devedjian
Held the 20th June 2022

JURY

Pr. David Devos	President of Jury
Dr. Solange Desagher	Rapporteur
Dr. Stephan Schildknecht	Rapporteur
Pr. Sonia Gandhi	Examinateur
Dr. James Duce	Examinateur
Dr. Jean-Christophe Devedjian	PhD supervisor

To my parents

Acknowledgements

As this PhD comes to an end, I feel the need to thank everyone who has made this adventure possible. First of all, I would like to thank Prof. Régis Bordet for giving me the opportunity to conduct this research project in the laboratory he was leading before becoming the president of the University of Lille. By joining a dynamic translational unit, I was able to acquire valuable knowledge on both clinical and pre-clinical research. It's been in the "*U-1172: Troubles cognitifs dégénératifs et vasculaires, au 4ème étage Ouest*" that the magic has taken place!

Next, I would like to thank Prof. David Devos and my PhD supervisor Jean-Christophe Devedjian for the guidance, support and trust they have given me throughout these past years. You have both enabled me to grow and develop into an independent researcher of the future and for that I will always be deeply grateful. I am convinced our paths will cross again and some great science will come of it!

I would also like to thank the members of the PhD Jury and the "*rapporteurs*" for reading through this manuscript and providing their valuable feedback:

Dr. Stephan Schildknecht, thank you for being not only part of this PhD jury but also a member of the "PhD follow up committee" thus following the progression of this work from the beginning. Your input always came in handy when faced with obstacles and I could not think of anyone more suitable for assessing this PhD manuscript.

Dr. Solange Desagher, I am very grateful for the feedback on this manuscript and the always interesting discussions around α-synuclein and LUHMES cells. I am convinced the new collaboration established with Prof. David Devos and Dr. Jean-Christophe Devedjian will be fruitful and help towards addressing some unanswered questions around α-synuclein and ferroptosis.

Prof. Sonia Gandhi, I am honoured to have you as a member of this PhD jury and extremely excited to be working with you in the near future!

Finally, I would like to thank Dr. James Duce not only for being part of the PhD jury, but also the support and good advices you've given me both professionally and personally over the past years. I am deeply grateful for everything you've done for me that has allowed me to reach the end of this PhD.

Next, I would like to thank the wonderful colleagues I have worked with in the lab. Aurélie Jonneaux (future Dr. Jonneaux!), the cell culture mum. Thank you for teaching me how to take care of LUHMES cells and your immense help with CRISPR when I first arrived

in the lab. I could have never split +50 LUHMES sub-clones on my own! I wish you all the best with your own PhD project. Flore Gouel, know how much I admire and respect your dedication and hard work. You are an immense asset to this research group and I feel honoured to have worked by your side (and shared an office with!). I truly hope we will work together again in the future and unravel the cellular mechanisms governing ferroptosis in dopaminergic neurons. I would also like to thank Kelly Timmermam for the help you were always happy to offer whether it had to do with PCRs, animal care, organotypic culture or distracting me when I needed it. Keep the "*Vale!"* going! I couldn't forget the other members of the "bureau": Charlotte Laloux and Chirine El katrib. Thank you both for providing such a great environment to work in. Chirine and Marie-Amandine, all the best of luck with your final PhD year. I promise it gets easier! And finally, Laurent Puy, a PhD colleague and friend outside the lab. Thank you for all the great conversations we had. All the best for your future in research!

I also would like to thank Hind Bouchaoui, my partner in crime, soon Dr. Bouchaoui! When I'll think back at this PhD, I will remember all the normal frustration and suffering that comes with a PhD, but it will all be sweeten by the fact that you were by my side from beginning to end (China 2018 – China 2022?). Thank you for all the support and laughs you've given me these past years.

Although I am not able to mention every member of the amazing U1172 team, do know that I am deeply grateful for all the help you've all given me throughout this PhD and for the great "ambiance de travail" you create: Mary, Camille, Maud, Michèle, Tavarak, Patrick, Sandra, Julie, Olivier, Vincent, Sandrine, Romain, etc. And the list goes on!

I would like to thank Scott Ayton, who welcomed me in his lab when I was merely an undergraduate student and first introduced me to ferroptosis in 2015. It is because of you that I embarked on this PhD project.

I would also like to thank my friends in the UK, Lille and Spain who've all been extremely understanding and supportive when I missed trips or parties because of this PhD: Alec, Hattie, Lucy, Alex, Jake, Kate, Sandra, and the list goes on. In Lille, a special mention to my forever flatmates: Leslie and Marina. You two represent a big part of my life in Lille, and for that I thank you! Romain, who started as a work colleague and became a dear friend with his amazing partner Judith and adorable son, Adam. Thank you for your friendship (and don't forget you'll be invited to a Spanish wedding one day!).

Finally, I have to thank the support of my family. Mamá, Rebeca y Elena. Sois mi roca, mi referencia, mi familia. No estaría aquí escribiendo estos agradecimientos después de haber

terminado una tesis sin vuestro amor y apoyo. Gracias. And dad, thank you for everything you did for us. Your love continues to drive my motivation to work hard and become the best version of myself. I love you and miss you. Finally, I need to thank my partner, Lucas, for setting such an amazing example for me and for all the love and care you give me every day.

List of abbreviations

αKG α-ketoglutarate

α-syn α-synuclein

α-TOH α-tocopherol

aa Amino acid

AA Arachidonic acid

ACACA Acetyl-CoA Carboxylase Alpha

ACL ATP citrate lyase

ACSL4 Acyl-CoA synthetase long-chain family member 4

Acyl-DHAP Acyldihydroxyacetone phosphate

AD Alzheimer's Disease

AdA Adrenic acid

AGP 1-alkyl-glycerol-3-phosphate

AGPAT3 1-Acylglycerol-3-Phosphate O-Acyltransferase 3

AGPS Alkylglyceronephosphate

AHS Agricultural Health study

AIFM1 Apoptosis inducing factor mitochondria-associated 2

Alkyl-DHAP Alkyldihydroxyacetone phosphate

ALOX Lipoxygenases

ALS Amyotrophic lateral sclerosis

APP Amyloid precursor protein

ARE Antioxidant response element

BBB Blood brain barrier

BSO Buthionine sulfoximine

CBS Cystathionine β-synthase

ccRCC Clear-cell renal carcinoma

CI Confidence interval

CLEM Correlative light and electron microscopy

CNS Central nervous system

CoA Coenzyme-A

COMT Catechol-O-methyltransferase

CoQ10 CoenzymeQ10

COXs Cyclooxygenases

CRISPR Clustered regularly interspaced short palindromic repeats

CSF Cerebrospinal fluid

Cu-ATSM Copper(II)-diacetyl-bis(4-methylthiosemicarbazonato

DAB 3,3'-Diaminobenzidine

DAT Dopamine transporter

DBS Deep brain stimulation

DFO Deferoxamine

DFP Deferiprone

DGLA Dihomogamma-linolenic acid

DHA Docosahexaenoic acid

DHAP Dihydroxyacetone phosphate

DLB Dementia with Lewy Bodies

DLD Dihydrolipoamide dehydrogenase

DMT1 Divalent metal transporter 1

D-PUFAs Deuterated-Polyunsaturated fatty acids

ePL Alkyl-ether phospholipids

ER Endoplasmic reticulum

ESCRT Endosomal sorting complexes required for transport

Ether-PL Ether-linked phospholipids

FAR1 Fatty acyl coenzyme A reductase

FASN Fatty acid synthase
Fer-1 Ferrostatin
FPN Ferroportin
FSP1 Ferroptosis suppressor protein 1
FT Ferritin
FTMT Ferritin mitochondrial
GBA β-glucocerebrosidase
GBSSK Gey's Balanced Salt Solution + Glucose + Kynurenic acid
GCL Glutamate-cysteine ligase
GPX4 Glutathione peroxidase 4
GSH Glutathione
GNPAT Glyceronephosphate O-acyltransferase
GSL2 Glutaminase 2
GSS Glutathione synthetase
GSSG Oxidised glutathione
15-HETE 15-hydroxyeicosatetraenoic acid
HMOX1 Heme oxygenase 1
4-HNE 4-hydroxy-2-nonenal
H_2O_2 Hydrogen peroxide
HR Homologous recombination
ICP-MS Inductively-coupled plasma mass spectrometry
IKE Imidazole ketone erastin
MPTP 1-methyl,4-phenyl-1,2,3,6-tetra hydropyridine
MSA Multiple systems atrophy
MUFA Monounsaturated fatty acid
NAC n-acetylcysteine
NAC Non-amyloid beta component
iPLA2 Calcium-independent phospholipase A2
iPSC Inducible pluripotent stem cell
IRE Iron response element
Iso WT Isogenic WT
KD Knock-down
KO Knock-out
LB Lewy Body
L-DOPA Levodopa
L-Gln Glutamine
LIP Labile iron pool
LN Lewy neurites
LOH Lipid alcohols
LOOH Lipid hydroperoxides
LPCAT3 Lysophosphatidylcholine acyltransferase 3
Lpx-1 Liproxstatin
LTF Lactotransferrin
LUHMES Lund human mesencephalic
MAO-B Monoamine oxidase-B
MAPK Mitogen-activated protein kinase
MDA Malondialdehyde
mDANs Midbrain dopaminergic neurons
MFB Medial forebrain bundle
MHCII Major histocompatibility complex II
MPP^+ N-methyl-4-phenylpyridine
NADPH Nicotinamide adenine dinucleotide phosphate
NBIA Neurodegeneration with brain iron accumulation
NCOA4 Nuclear receptor coactivator 4

NGS Normal goat serum
NHEJ Non-homologous end joining
NOX NADPH oxidase
Nrf2 Nuclear factor erythroid-2-related factor 2
NT Non-transfected
O_2- Superoxide
OBS Organotypic brain slice
PD Parkinson's Disease
PE Phosphatidylethanolamine
PEBP1 Phosphatidylethanolamine-binding protein 1
PET Positron emission tomography
PEX3 Peroxisomal biogenesis factor 3
PEX14 Peroxisomal biogenesis factor 14
PI Peroxidability index
PL Phospholipids
PLA2G6 VI calcium-independent phospholipase A2 beta
PLD2 Phospholipase D2
pPL Plasmalogen
PUFA Polyunsaturated fatty acid
PVDF Polyvinylidene difluoride
QSM Quantitative susceptibility mapping
REM-8 Receptor-mediated endocytosis 8
ROS Reactive oxygen species
RR Relative risk
RTA Radical trapping agents
RT-PCR Reverse transcription polymerase chain reaction
Se Selenium
SFA Saturated fatty acid
siRNA small interfering RNA
·OH Hydroxyl radicals
6-OHDA 6-Hydroxydopa
OR Odd ratio
OS Oxidative stress
OVCAR-8 Ovarian carcinoma cells
PAF Pure autonomic failure
PAM Protospacer adjacent motif
PC Phosphatidylcholine
smNPC Small-molecule derived neuronal precursor cells
SN Substantia nigra
SNpc Substantia nigra pars compacta
SNPs Single nucleotide polymorphisms
TBI Traumatic brain injury
TCA Tricarboxylic acid
Tf Transferin
TfR1 Transferin receptor 1
TH Tyrosine hydroxylase
TMEM189 Transmembrane protein 189
VAMP2 Vesicle associated membrane protein 2
VMAT2 Vesicular dopamine transporter
VPS35 Vacuolar protein sorting
XcT- Cysteine-glutamate antiporter

List of figures

List of tables

List of supplementary figures and tables

Index

II. MATERIALS AND METHODS

4. PhD Preface

III. RESULTS

IV. GENERAL CONCLUSIONS AND DISCUSSION

VI. REFERENCES

V. ANNEXES

Abstract

Parkinson's disease (PD) is a common and progressive neurodegenerative disorder primarily affecting dopaminergic neurons in the substantia nigra pars compacta (SNpc), characterised by motor impairments as well as non-motor symptoms. While dopamine-based therapies are effective in fighting the initial stages of the disease, a lack of neuroprotective drugs means that the disease continues to progress. Along with the traditionally recognised pathological hallmarks of dopaminergic neuronal death and intracellular α-synuclein (α-syn) depositions, iron accumulation, elevated oxidative stress and lipid peroxidation damage are further conspicuous features of PD pathology. Importantly, the underlying mechanisms linking these pathological hallmarks with neurodegeneration remain unclear. Ferroptosis, a regulated iron dependent cell death pathway involving a lethal accumulation of lipid peroxides, shares several features with PD pathophysiology. Interestingly, α-syn has been functionally and pathologically linked with the metabolisms of iron and polyunsaturated fatty acids (PUFAs), suggesting a possible link between dysregulated α-syn and iron and lipid dyshomeostasis in PD pathology. This project aims to study the potential implication of α-syn in the ferroptosis pathway, thus demonstrating a pivotal interplay between α-syn and ferroptosis in PD. To this extent, we have generated stable LUHMES dopaminergic neuronal precursor cell lines with the homozygous PD-linked A53T α-syn mutation, and have knocked-out the main 140 amino-acid long α-syn isoform (140 α-syn) via CRISPR/Cas9 genome editing. We have observed that the PD-linked A53T α-syn mutation increases the sensitivity of LUHMES dopaminergic neurons to ferroptosis-induced lipid peroxidation and cell death, whilst absence of the main 140 α-syn results in ferroptosis evasion. This response was specific to ferroptosis since no difference in apoptosis sensitivity was reported. Interestingly, reducing α-syn levels by siRNA also protected dopaminergic neurons from ferroptosis to comparable levels as knocking-down the well-established pro-ferroptotic modulator acyl-CoA synthetase long chain family member 4 (ACSL4). Using small molecule derived neuronal precursor cells (smNPC) from PD patients differentiated into midbrain dopaminergic neurons (mDANs), we reproduced our findings and showed that the KO of α-syn protects mDANs against ferroptosis-induced cell death and lipid peroxidation. In addition, we showed intrinsically higher levels of lipid peroxidation and vulnerability to ferroptotic cell death in mDANs from a PD patients baring SNCA triplication.

Lipidomic analysis of the plasma membrane were conducted in LUHMES dopaminergic neurons depleted of α-syn in order to decipher the mechanism resulting in ferroptosis resistance. A reduction in PUFA contained in phosphatidylcholine (PC) and phosphatidylethanolamine (PE) phospholipids was observed upon α-syn and ACSL4 knock-down (KD), mirrored by a reduction in the peroxidability index. Surprisingly, a more selective a prominent reduction was observed in ether-phospholipids (ether-PL), a subclass of phospholipids which were recently shown to be essential for ferroptotic cell death. These results provide the first direct link between α-syn and the metabolism of ether-PL and demonstrate that the levels of endogenous α-syn can determine the sensitivity of dopaminergic neurons to ferroptosis, further strengthening the implication of ferroptosis in the pathology of PD.

Introduction - Chapter 1:

Parkinson's Disease – Two centuries of research

1.1 Introduction

Parkinson's Disease (PD) is a neurodegenerative disease that results predominantly from the loss of dopaminergic neurons in the substantia nigra pars compacta (SNpc) of the midbrain leading to a dopamine deficit in the striatum. It stands as the second most common progressive neurodegenerative disorder with an estimate of 7 to 10 million PD patients worldwide and a predicted increase as the population ages (Parkinson's Foundation). Clinically, PD patients present with motor impairments such as bradykinesia, rest tremor, rigidity and gait disorders, as well as non-motor symptoms including dysautonomia (anosmia, constipation, etc), sleep disturbances, behavioural disorders (anxiety, depression, apathy, etc) and cognitive disorders that may progress to dementia (Fearnley and Lees, 1991). These non-motor symptoms may appear in the individual several years before the onset of the characteristic motor symptoms in what is known as the prodromal phase of the disease (Postuma et al., 2012). The main pathological hallmarks of the sporadic and familial forms of PD are a predominant and progressive degeneration of the dopaminergic neurons of the SNpc associated with a systematic progressive iron accumulation, leading to a dopamine depletion in the striatum, disappearance of neuromelanin and appearance of intracellular Lewy Bodies with the major component consisting of aggregated α-synuclein (α-syn) (Dexter et al., 1989a; Schneider and Obeso, 2015; Shahmoradian et al., 2019; Spillantini et al., 1997).

Over the past two hundred years, extensive research has focused on unravelling the aetiology, physiopathology and clinical manifestation of Parkinson's disease with the common aim of better understanding the disease in order to delay the disease onset and slow the progression via neuroprotective treatments. This chapter provides an overview of the disease from the beginnings of PD's clinical description, risk factors and treatments, down to the cellular and molecular level of the disease pathology.

1.2 Clinical Description.

First described in the early 19th century, James Parkinson writes in his "Essay on the Shaking Palsy":

"Involuntary tremulous motion, with lessened muscular power, in parts not in action and even when supported; with a propensity to bend the trunk forwards, and to pass from a walking to a running pace: the senses and intellects being uninjured" (figure 1).

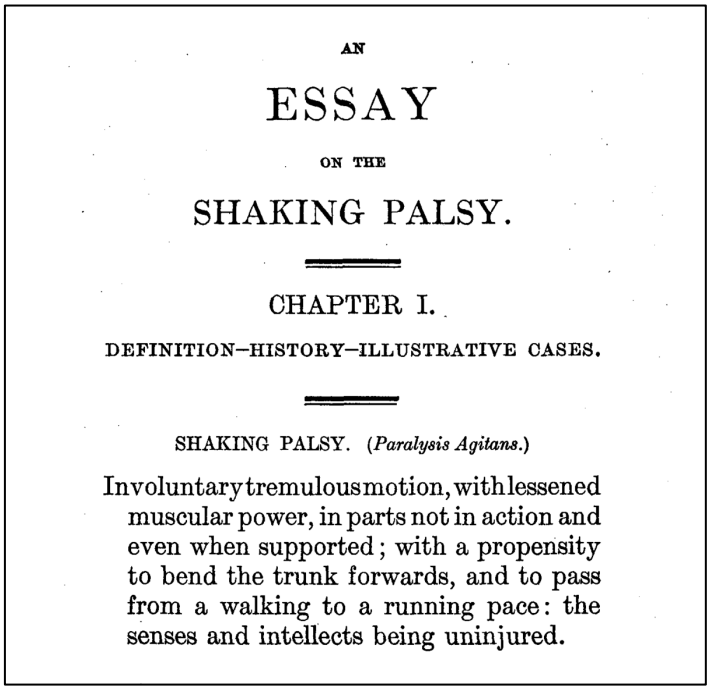

AN

ESSAY

ON THE

SHAKING PALSY.

CHAPTER I.

DEFINITION—HISTORY—ILLUSTRATIVE CASES.

SHAKING PALSY. (*Paralysis Agitans.*)

Involuntary tremulous motion, with lessened muscular power, in parts not in action and even when supported; with a propensity to bend the trunk forwards, and to pass from a walking to a running pace: the senses and intellects being uninjured.

Figure 1. James Parkinson's first description of the characteristic motor tremor of Parkinson's Disease. Extract from the first page of "An essay on the Shaking Palsy" written by James Parkinson's in 1817.

Over 50 years later, Jean-Martin Charcot provided a more thorough description of the clinical spectrum including the arthritic changes, dysautonomia and pain associated with Parkinson's Disease, and identified bradykinesia as one of the cardinal symptoms of the disease (Charcot, 1886):

> *"Long before rigidity actually develops, patients have significant difficulty performing ordinary activities: this problem relates to another cause. In some of the various patients I showed you, you can easily recognize how difficult it is for them to do things even though rigidity or tremor is not the limiting feature. Instead, even a cursory exam demonstrates that their problem relates more to slowness in execution of movement rather than to real weakness. In spite of tremor, a patient is still able to do most things, but he performs them with remarkable slowness. Between the thought and the action there is a considerable time lapse. One would think neural activity can only be effected after remarkable effort."*

Other cardinal features of Parkinson's Disease include tremor, rigidity and postural instability. Charcot also contributed towards the differentiation of Parkinson's disease from

other tremorous disorders, such as multiple sclerosis, allowing for a distinct diagnosis. Furthermore, Charcot noted two subgroups based on the clinical manifestations: the tremorous and the rigid/akinetic forms, which still today are suggested as the two major subtypes, despite there not being a consensus on the classification of Parkinson's disease subtypes (Charcot, 1886; Kalia and Lang, 2015). The course and prognosis of the disease varies depending on the subtype, in which the tremor-dominant form is often associated with a slower rate of progression and therefore less functional disability (Jankovic et al., 1990; Kalia and Lang, 2015). Moreover, it is hypothesised that the subtypes of Parkinson's disease may have distinct aetiologies and pathogenesis (Marras and Lang, 2013).

In addition to the "classic" motor symptoms previously mentioned, other motor complications are observed amongst PD patients. These include hypomimia with decreased eye blink rate, impaired upward gaze, dystonia, shuffling gait, "freezing" and speech impairments. (Jankovic, 2008).

Aside from the motor symptoms, Parkinson's Disease patients suffer several non-motor features including olfactory dysfunction, cognitive impairments, sleep disorders, autonomic dysfunction, pain, fatigue, and depression amongst others. These symptoms can precede the motor symptoms and appear up to twenty years before the diagnosis occurs with the onset of motor features (figure 2). The pathogenic neurodegeneration causing Parkinson's Disease is presumably underway during this prodromal period, which offers a valuable window for disease modifying drugs to slow the neurodegeneration, thus progression of the disease.

Progression of PD is characterised by worsening of motor symptoms which are initially managed by pharmacological dopamine treatments. These therapies only provide symptomatic relief and, as the disease progresses, the motor and non-motor symptoms become greater and complications arise due to long-term treatments. These include motor and non-motor fluctuations, dyskinesia and psychosis (Hely et al., 2005). Furthermore, in advanced-stages of the disease, several motor and non-motor symptoms become unresponsive to the treatments, including postural instability, freezing of gait and speech dysfunction. A multi-centric study assessed these motor features in 149 patients who were diagnosed with PD over 15 years earlier and reported a series of non-Levodopa(L-DOPA)-responsive problems: 50% of patients reported choking, whilst symptomatic postural hypotension and urinary incontinence occurred in 35% and 41% of patients, respectively. Freezing of gait and falls were reported in 81% on patients (Hely et al., 2005). Finally, cognitive decline and dementia is prevalent in late-stages of the disease, occurring in 83% of patients who have had PD for over 17 years (Hely et al., 2008) (Figure 2). However, there is

great phenotypic variability in terms of symptoms and age of onset of symptoms during the course of the disease, particularly during the prodromal phase. For example, some patients may start with discrete motor symptoms 10 years before diagnosis and only suffer from constipation in the advanced stage of the disease.

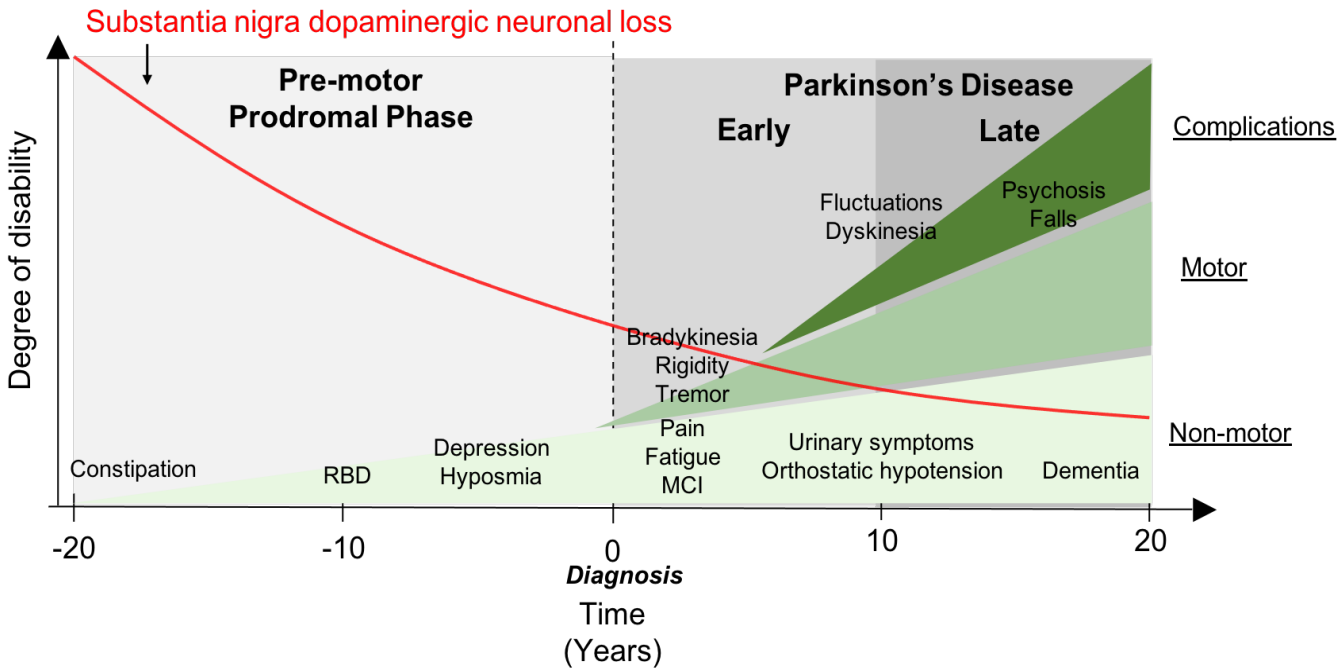

Figure 2. Clinical symptoms and progression of Parkinson's Disease.
Parkinson's Disease diagnosis is marked by the onset of motor symptoms which are associated to the loss of ~50% of dopaminergic neurons in the substantia nigra. Non-motor symptoms often precede the diagnosis in what it's known as the prodromal phase which can last up to 20 years. The prodromal phase is mainly characterised by non-motor features which evolve as the disease progresses often leading to dementia in late stages. The cardinal motor symptoms include bradykinesia, rigidity and tremor, and can be managed with symptomatic dopamine therapy. The late stages of the disease are marked by stronger motor and non-motors symptoms along with complications related to long-term treatments

With advances in treatments and increase in survival times, the later stages of the disease are often prolonged in which the combination of the motor and non-motor features in addition to the complications arising from long-term treatments lead to strong disabilities, loss of independence and eventually death (Coelho and Ferreira, 2012).

1.3 Risk factors

Parkinson's disease is considered the second most common neurodegenerative disorder after Alzheimer's Disease. The prevalence in Europe, North and South America seems to be higher when compared to countries in Africa, Asia and the Middle East. (Kalia and Lang,

2015). Age is the greatest risk factor for the disease as evident from the fact that the prevalence and incidence increase with age, reaching a peak after 80 years of age (Driver et al., 2009; Pringsheim et al., 2014). Ethnicity and gender are also considered established risk factors; in North-America, the incidence of PD is highest in Hispanic individuals, followed by non-Hispanics Whites, Asians, and lowest in Blacks (Van Den Eeden et al., 2003). Furthermore, the incidence in men is also higher than in women with a male-to-female ratio of approximately 3:2 (de Lau and Breteler, 2006).

Research has profoundly changed our knowledge on PD pathology and determinants. Whilst genetic studies have revealed the heterogeneity of PD and identified specific genes and single nucleotide polymorphisms (SNPs) associated with the pathogenesis and aetiology, epidemiological studies have contributed towards understanding the contribution of behavioural and environmental factors in disease pathogenesis and progression. The key role of such behavioural and environmental factors in modifying the risk of developing PD is strengthen by the fact that approximately 90% of PD cases have no genetic cause (Ascherio and Schwarzschild, 2016; Klein and Westenberger, 2012). An in-depth understanding of the risk factors of PD and their interactions could enable the identification of PD in its prodromal phase and therefore promote identification of biomarkers, individualisation of treatments and neuroprotective interventions before the onset of motor symptoms.

1.3.1 Genetic contributions

Although the majority of PD cases are sporadic, the contribution of genetics to PD is suggested by the fact that family history of PD or tremor increases the risk of developing the disease (Noyce et al., 2012). Furthermore, owing to the clinical and pathological similarities between genetic PD and the more common idiopathic cases, genetic PD serves as an excellent model for understanding the pathology of PD and enables the identification of at-risk individuals in the earliest phases of the disease. The crucial impact of genetics in PD pathology was first confirmed by the discovery of monogenic forms of the disease which are considered to be autosomal and dominant:

1.3.1.a Autosomal-dominant Parkinson's disease genes

SNCA, which encodes the protein α-syn, was the first identified gene to be related with autosomal-dominant PD (Polymeropoulos et al., 1997). Although the incidence of SNCA-related PD is rare, missense mutations and multiplications of the gene locus are known causes of early-onset PD with an age of onset ≤ 50 years. Patients with *SNCA* mutations initially

respond well to L-DOPA although as the disease progresses, patients often present with cognitive decline and dementia (Klein and Westenberger, 2012). Five missense mutations have been identified so far: A53T (Polymeropoulos et al., 1997), A30P (Krüger et al., 1998), E46K (Zarranz et al., 2004), H50Q (Appel-Cresswell et al., 2013) and G51D (Lesage et al., 2013). Interestingly, all point mutations are located in the amino-terminal region of the α-syn protein, which adopts an α-helical upon binding to phospholipid membranes. The mutations in *SNCA* are thought to increase the propensity of α-syn to adopt stable β sheets and exacerbate the formation of toxic oligomers (Bertoncini et al., 2005). A more in-depth overview on α-syn and the pathological contributions to PD is provided in section 1.4.1 "Lewy Body pathology in Parkinson's disease" and in chapter 3. Despite it being a rare cause of the disease, duplications and triplications of *SNCA* are also associated with increased risk of developing PD and diffuse Lewy body disease, with a later age of onset than the observed with *SNCA* mutations (Johnson et al., 2004). Interestingly, an association between *SNCA* copies (duplications vs triplication) and clinical manifestation has been suggested, where increased number of *SNCA* copies lead to earlier disease onset, more severe symptoms and faster disease progression (Fuchs et al., 2007; Ross et al., 2008).

LRRK2 encodes the leucine-rich repeat kinase 2, a protein involved in several cellular processes ranging from neurite growth and synaptic morphogenesis, to autophagy, membrane trafficking and innate immune response (Brice, 2005). Mutations in *LRRK2* is the most common cause of late-onset autosomal-dominant and sporadic PD, accounting for 4% of genetic PD, and are found in 1% of sporadic PD cases worldwide (Brice, 2005; Lesage et al., 2006; Ozelius et al., 2006). Clinically, *LRRK2*-related PD patients usually show mid-to-late onset of the disease, and progress slowly. The response to L-DOPA treatments is favourable and cognitive decline into dementia is rare. Amongst the more than 50 known *LRRK2* mutations, at least 16 of them seem to be pathogenic, including the six most recurrent mutations: p.R114C, p.R1441G, p.R1441H, p.Y1699C, p.G2019S, and p.I2020T) (Klein and Westenberger, 2012).

Missense mutations in other genes have also been proposed to mediate autosomal dominant forms of PD: *VPS35*, *DNAJC13* and *CHCHD2*. A single missense mutation in the *VPS35* gene, A620D, is responsible for a rare form of autosomal-dominant PD: *VPS35* encodes the vacuolar protein sorting 35 (VPS35), a subunit of the retromer complex that associates with endosomes responsible for the intracellular traffic of proteins and lipids between the Golgi apparatus, the endoplasmic reticulum (ER), lysosomes and the plasma membrane (Williams

et al., 2017). *DNAJC13* encodes a chaperone protein (receptor-mediated endocytosis 8 – REM-8) which, like VPS35, is also involved in mediating transmembrane protein trafficking by regulating the dynamics of clathrin coats on early endosomes. Missense mutations in *DNAJC13* therefore impair endosomal transport and have also been linked to monogenic autosomal dominant forms of PD (Vilariño-Güell et al., 2014). It is worth mentioning, that the evidence associating dysregulated endosomal receptor-sorting/recycling and PD pathology is highlighted by the aforementioned pathogenic mutations in *VPS35, LRRK2* and *DNAJC13.* Although the evidence remains unconclusive, some mutations in *EIF4G1* have also been linked to PD suggesting an impaired ability of neurons to respond to stress conditions. However, some mutation carrier exist with no apparent pathological phenotype, meaning further clinical and functional studies on *EIF4G1* are required to conclude on its implication with autosomal dominant forms of PD (Deng et al., 2015).

1.3.1.b Autosomal-recessive Parkinson's disease genes

Pathogenic mutations in *parkin*, *PINK1* and *DJ-1* are responsible for the majority of recessively inherited PD (Kalia and Lang, 2015). Mutations in *parkin* are most commonly associated with autosomal recessive PD, as evident from the fact that in patients with PD onset before 45 years of age, *parkin* mutation are found in 50% and 15% of familiar and sporadic cases, respectively (Lücking et al., 2000; Periquet et al., 2003). The *parkin* gene is the second largest gene in the human genome, which would explain the large number and wide spectrum mutations detected up to date. The *parkin* mutations which have been reported across all exons are mainly point mutations (missense and nonsense mutations), although some small indels and whole exon deletions and duplications have also been reported (Abbas et al., 1999). The parkin protein is a 465-amino acid long protein with a modular architecture. It functions as an E3 ubiquitin ligase responsible for conjugating ubiquitin proteins to lysine residues of proteins targeted for degradation via the proteasome. Unlike *parkin*, mutations in the *PINK1* gene are mainly point mutations, and are the second most common cause of autosomal-recessive early-onset PD, with a frequency that ranges from 1-9% depending on ethnicity (Healy et al., 2004; Klein et al., 2006; Rogaeva et al., 2004; Valente et al., 2004). The majority of the reported *PINK1* mutations are loss-of-function mutations affecting the kinase domain of the protein, indicating the importance of the protein's enzymatic activity in the pathogenesis of PD. Interestingly, some studies have suggested a common pathway by which PINK1 and parkin may act in synergy to sense and eliminate damaged mitochondria. PINK1 is stabilized in mitochondria with lower membrane potential, and as such, it recruits

parkin, which becomes enzymatically active and target damage mitochondria for mitophagy (Pickrell and Youle, 2015; Vranas et al., 2022; Zhang et al., 2022). Finally, despite the low frequency, *DJ-1* (or *PARK7*) is the third gene associated with autosomal-recessive PD, and is mutated in about 1-2% of early onset PD cases (Pankratz et al., 2006). DJ-1 forms a dimeric structure under physiological conditions, and is thought to act as a cellular sensor of oxidative stress (Canet-Avilés et al., 2004; Macedo et al., 2003). Most of the point mutations seem to affect the stability and dimerization status of the protein, leading to its loss of function, degradation and subsequent reduction in the neuroprotective and antioxidant functions (Takahashi-Niki et al., 2004).

1.3.1.c Genetic risk variants

In the past decade, almost 900 genetic association studies have identified further genetic risk factors or polymorphisms associated with the development of PD (van der Brug et al., 2015). Loss of function mutations in *GBA* remains the greatest genetic risk factor for developing PD. *GBA* encodes the β-glucocerebrosidase enzyme responsible for the degradation of glucocerebrosides into glucose and ceramide. Its enzymatic deficiency results in excessive storage of its substrate within lysosomes of macrophages and neurons amongst other cell types, and is responsible for Gaucher disease (Hruska et al., 2008). A large multicentric study including ~5700 PD cases and almost 5000 controls showed an odds ratio for any *GBA* mutation in PD patients vs controls of 5.43 (Sidransky et al., 2009). Variants in several Parkinson-designated (*SNCA, LRRK2, PARK16, GAK*) and other genes (*MAPT, GBA, APOE, BST1*, etc) have also been associated with an increased risk of developing PD (Klein and Westenberger, 2012), some of which are depictured in figure 3, but will not be further discussed as it is a topic beyond the scope of this thesis manuscript.

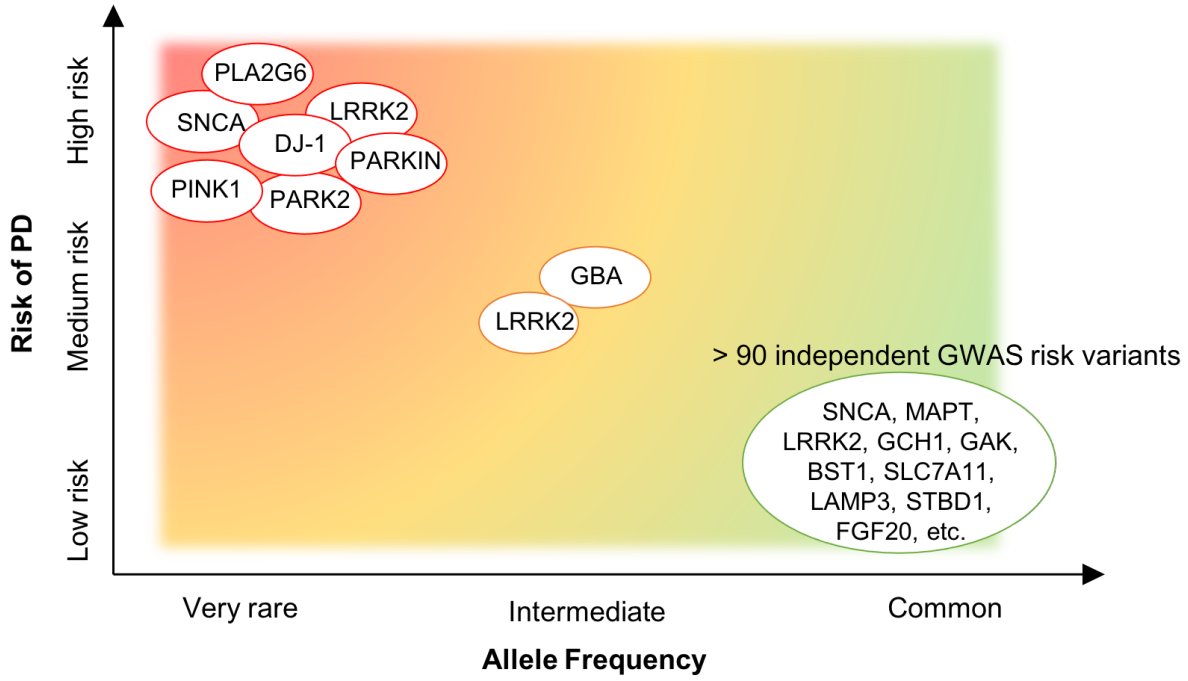

Figure 3. Schematic overview of genetic variants in Parkinson's disease grouped according to allele frequency and associated risk of Parkinson's disease. Image adapted from (Van der Brug et al., 2015).

1.3.2 Environmental contributions

Risk of developing PD is clearly multifactorial, but the elaborate interplay between the various factors remains unclear and requires further deciphering. Following an overview of the genetic contribution, section 1.3.2 will provide a brief description of some environmental contributors to increased PD risk.

1.3.2.a Pesticides

The associated risk of developing PD with the exposure to pesticides was suggested by the discovery of the neurotoxic effects of the metabolite of 1-methyl,4-phenyl-1,2,3,6-tetra hydropyridine (MPTP), which in the body is converted to the pro-parkinsonian molecule N-methyl-4-phenylpyridine (MPP^+), with a similar structure to the paraquat pesticide (Davis et al., 1979; Langston et al., 1983). A case-control study in France revealed a positive association between pesticide exposure and PD in the elderly (Baldi et al., 2003). In a longitudinal study, the relative risk (RR) of PD was shown to be increased in men who worked more than 10 years on a plantation (RR 1.7), and the RR increased as the exposure time is prolonged (RR 1.9 in men who did more than 20 years of plantation work) (Petrovitch et al., 2002). An additional study determined a stronger association with intensity rather than

duration of pesticide exposure and showed a significant association of pesticides with tremor-dominant PD in men, the most typical PD presentation (Moisan et al., 2015). The class of pesticides seems to be key in its ability to increase the risk of PD, since individuals exposed to pesticides had a 70% higher incidence of PD than those not exposed and no relation was found between risk of PD and exposure to acids/solvents, asbestos, coal or stone dust or eight other chemicals (Ascherio et al., 2006). This notion is supported by a prospective investigation in Finland which showed no association between blood concentrations of organochlorine pesticides and increased PD risk (Weisskopf et al., 2010). The Agricultural Health study (AHS) assessed whether pesticides causing mitochondrial dysfunction and/or oxidative stress are associated with PD in humans and found positive association with the use of pesticides that inhibit mitochondrial complex I such as rotenone (odds ratio (OR) = 1.7; 95% confidence interval (CI), 1.0-2.8), and with the use of pesticides like paraquat that trigger oxidative stress (OR= 2.5, 95% CI, 1.2-3.6) (Tanner et al., 2011). Overall, the evidence linking pesticide exposure to PD risk is substantial, however the molecular mechanisms behind the neurodegeneration remains uncertain.

1.3.2.b Traumatic brain injury

Evidence has shown that traumatic brain injury (TBI) can cause disruption to the blood-brain barrier (BBB), long-term brain inflammation, mitochondrial dysfunction, increased glutamate release and α-syn accumulation in the brain, all pathological features closely linked to PD (Acosta et al., 2015; Fischer et al., 2016; Marras et al., 2014). Interestingly, the associated risk appears higher soon after the injury and gradually decreases over time. A Danish study with over 13 000 PD cases revealed that the RR of PD within 3 months of concussion was 6.6 (95% CI 4.4 – 9.9), but the risk descended to 1.9, 1.8 and 1.4 between 4 and 12 months, 1 and 4 years and between 5 and 9 years, respectively (Rugbjerg et al., 2008). Similar results were obtained in a later study which included 18 000 PD cases, in which the RR for PD was 3.34 (95% CI 2.72-4.12) within 12 months following head injury, but this number decreased to 1.28 after 1-4 years, 1.18 in years 5-9 and 1.17 after 10 years (Fang et al., 2012). The early increase in PD risk in the aforementioned studies may be explained by reverse causation due to more frequent falls and head injuries in individuals with early PD. It is therefore difficult to establish whether there is a long-term increase in the risk of developing PD due to TBI. Despite the controversy from human studies, mounting pre-clinical data indicates there might indeed be an association between TBI and an increased risk of developing PD. The question remains as to whether TBI triggers PD pathology or

accelerates the pathology in at risk populations. An *in vivo* study conducted in a chronic TBI rat model revealed decreased TH positive neurons in the SNpc relative to sham control, in parallel to an increased α-syn accumulation and major histocompatibility complex II (MHCII) staining – a protein found in inflammatory microglia cells – in the ipsilateral SN compared to the contralateral SN in TBI animals or sham controls (Acosta et al., 2015). It is worth mentioning that MCHII staining, which is not normally expressed in the brain, was found in post-mortem brains of PD patients (McGeer et al., 1988). In another study, 24 month old mice subject to cortical TBI revealed a more pronounced, although transient, conformational and post-translational modifications to α-syn that may increase its pathological aggregation, when compared to mice injured at the age of 4 months (Uryu et al., 2003). These results suggest that depending on the age of the individuals and whether they were already at-risk individuals, TBI may contribute towards accelerating the pathology of PD. Further pre-clinical and clinical studies are required in order to strengthen the association between TBI and increased PD risk.

1.4 Current treatments

1.4.1 Symptomatic therapy

Current pharmacological treatments revolve around dopamine deficit in the midbrain and therefore aim to restore dopamine neurotransmission. This strategy however only offers symptomatic relief during the initial stages of the disease. The therapeutic arsenal includes the dopamine precursor L-DOPA, dopamine agonists and dopamine metabolism inhibitors (Connolly and Lang, 2014). Treatment should begin once the symptoms suffice to cause the patient disability or discomfort, and aim to improve function and quality of life (Kalia and Lang, 2015). Dopamine treatments efficiently manage bradykinesia and rigidity early in the disease, however, their efficacy becomes insufficient against more severe symptoms as the disability progresses.

Many PD drugs are associated with adverse reactions which should be taken into account when starting the treatment and prescribing them to the patients. Dopamine agonist and L-DOPA may cause nausea, daytime somnolence and oedema (Kalia and Lang, 2015). Dopamine agonists are also associated with impulse control disorders and therefore shouldn't be prescribed to patients with a history of addiction. Another side effect is hallucinations which can be especially problematic in elderly patients with cognitive impairments.

Overall, L-DOPA remains the standard most effective treatment in combination with decarboxylase inhibitors (Nagatsua and Sawadab, 2009; Yahr et al., 1969). Evidence from a randomized, double-blind, placebo-controlled trial suggested that L-DOPA slowed progression (as measured by UPDRS) between baseline and 42 weeks compared to the placebo group (Fahn et al., 2004). However, a more recent and larger study found no evidence of a disease-modifying effect of L-DOPA (Verschuur et al., 2019). Disparity in the potential neuroprotective actions of this drug may arise from L-DOPA's interference with the striatal presynaptic dopamine transporter; standardly used as a reporter for nigrostriatal degeneration by DAT SPECT in clinical trials (Fahn and Parkinson Study Group, 2005; Fahn et al., 2004). The powerful symptomatic action and short half-life of L-DOPA also weakens its clinical use with motor complications such as "wearing off" and dyskinesia occurring 4-6 years after chronic use, depending on disease severity (Agid et al., 1998, 2002; Tran et al., 2018).

1.4.2 Management of long-term therapy complications.

Complications due to long-term dopamine therapies are common features in advanced stages of the disease. These complications include both motor and non-motor fluctuations, dyskinesia and psychosis (Figure 2). Such complications are believed to be partially caused by the pulsatile stimulation of the dopamine receptors in the striatum. This phenomenon occurs in late stages of the disease once the intracerebral concentration of L-DOPA becomes linked to plasma concentrations (Connolly and Lang, 2014). To delay the onset of such complications, dopamine agonists, monoamine oxidase-B (MAO-B) inhibitors or catechol-O-methyltransferase (COMT) inhibitors are prescribed as concomitant therapies. However, an open-label randomized trial assessed the long-term effectiveness of dopamine agonists and MAO-B inhibitors over L-DOPA which failed to show any long-term benefits of a L-DOPA sparing strategy (PD Med Collaborative Group et al., 2014). In order to avoid the characteristic motor and non-motor fluctuation caused by the variable intracerebral dopamine concentrations, continuous dopaminergic stimulation is required. This can be achieved either by subcutaneous administration of the dopaminergic agonist apomorphine (Drapier et al., 2016 ; Katzenschlager R, et al., 2018) or by direct and continuous delivery of a stable concentrated L-DOPA-carbidopa gel alone (Duodopa, Abbott Laboratories) or with an ICOMT (Legicon Lobstor Pharmaceutical) into the duodenum via a percutaneous tube attached to a portable infusion pump (Olanow et al., 2014). Another approach consists in a dopaminergic stimulation by continuous intra-cerebroventricular delivery of anaerobic

dopamine via a subcutaneous tube attached to a pump. Dopamine is directly delivered into the lateral ventricle at the entrance of the third ventricle, closest to the nigrostriatal pathway. This innovative strategy showed promising results in two *in vivo* PD mouse models (MPTP and 6-hydroxydopamine, 6-OHDA) (Laloux et al., 2017) and is currently being tested in an ongoing clinical trial (DIVE – NCT04332276).

1.4.3 Surgical treatment

Surgical treatments are focused on treating the advanced-stage motor symptoms of Parkinson's Disease. Substantial number of clinical studies have shown that deep brain stimulation (DBS) of the subthalamic nucleus or to a lesser extend internal globus pallidus is effective in treating the moderate-to-severe PD motor symptoms (Kleiner-Fisman et al., 2006; Krack et al., 2003; Wenzelburger et al., 2003). In average, DBS is undertaken 10 to 13 years post PD diagnosis, once motor symptoms continue to be controlled with L-DOPA, but the motor fluctuations and dyskinesia become disabling. Interestingly, the EARLYSTIM trial showed that DBS of the subthalamic nucleus early in the course of the disease (mean disease duration 7,5 years with +3 years of motor fluctuations) let to a better improved quality of life and several secondary outcome measures compared to the best pharmacological treatments (Carmona-Torre et al., 2013; Schuepbach et al., 2013). These findings might change the current practice around delaying surgical interventions until later stages of the disease.

1.5 Pathology of Parkinson's disease

1.5.1 Lewy Body pathology in PD

Aggregated α-syn, one of the main components in intracellular Lewy Bodies (Spillantini et al., 1997), has long been considered a key pathological hallmark of the disease. As previously discussed, the relationship of α-syn to disease pathology has been confirmed by genome wide association studies, where single nucleotide polymorphisms associate with sporadic PD risk whilst confirmed mutations and duplication/triplication in the *SNCA* gene lead to various clinical manifestations ranging from classical to early onset familial PD (Zhang et al., 2018a; Blauwendraat et al., 2019). Despite the involvement of α-syn in PD pathology, the exact physiological function of this protein and the mechanisms linking it to neurodegeneration remain elusive. A more in-depth analysis on α-syn and its physiological functions is provided in chapter 4, whilst this section of the manuscript will mainly focus on Lewy body (LB) pathology.

The processes by which Lewy pathology arises and its roles in neuronal death remain elusive. The current leading hypothesis in PD research proposes that intraneuronal α-syn first adopts β-sheet rich amyloid fibrils, which are the basis of the LB (Spillantini et al., 1998). α-syn immunohistochemistry staining reveals that the process of classical LB formation follows specific stages (figure 4). Under normal conditions, α-syn staining is weakly observed in neuronal cell bodies (figure 4A). Within the first stage of LB formation, α-syn staining is observed as a diffuse and pale cytoplasmic staining representing the first observable abnormal α-syn accumulation (Kovacs et al., 2012; Kuusisto et al., 2003) (figure 4B). Next, the staining of α-syn shows an irregular shaped and uneven pattern in neurons (figure 4C), followed by a discrete staining corresponding to pale bodies (figure 4D&E) and one or more small, early LBs located in the periphery of the pale bodies (figure 4E). Finally, the "early LBs" develop into typical ring-shaped LBs with a central core and a surrounding halo (figure 4F) (Wakabayashi et al., 2013).

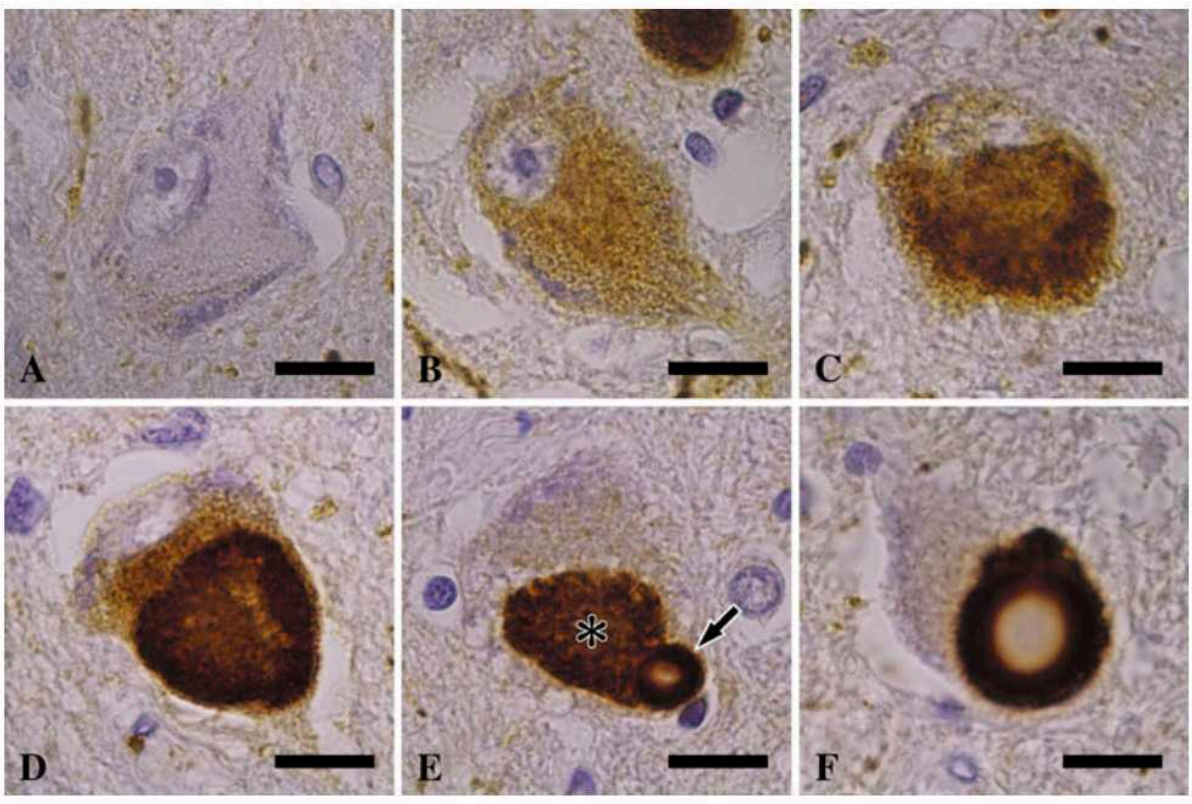

Figure 4. Immunohistochemistry staining of α-synuclein in the different maturation stages of Lewy bodies in the substantia nigra. **A.** No α-syn staining in the cytoplasm of neurons. **B.** Diffuse and pale staining. **C.** Irregular and uneven staining of α-syn. **D.** Appearance of the first pale bodies as evident from a discrete staining. **E.** Abnormal α-syn aggregates in the form of pale bodies (asterisk) and Lewy body (arrow). **F.** Ring-shaped Lewy body. Bars = 10µM. Image from (Wakabayashi et al., 2013),

Proteome studies have shown that LB composition is far more complex than simple α-syn aggregates with more than 300 proteins at the core of LB, of which approximately 90 have been confirmed by immunohistochemistry staining and are associated with α-syn, protein degradation systems, molecular chaperones or axonal damage (Wakabayashi et al., 2013). Most recently, and thanks to the advances of modern technologies for electron microscopy such as energy filters, direct electron detectors and drift-correcting software for tomography, a 3D view of the structural components of LB and Lewy neurites (LN) reveal that in addition to α-syn filaments, there is an abundance of crowded membranous material in Lewy pathology with membranes originating from vesicles and fragmented organelles including lysosomes and mitochondria (Shahmoradian et al., 2019). In addition to crowded organelles and membrane fractions in such aggregates, correlative light and electron microscopy (CLEM) also reveals a shell of mitochondria surrounding some of the inclusions. These recent findings suggest that the membrane crowding observed in Lewy pathology is modulated by α-syn, and further supports the hypothesis that impaired organellar trafficking contributes to Lewy, and more generally, PD pathogenesis (Hunn et al., 2015).

The neurodegeneration of dopaminergic neurons is associated with the appearance of LB and LN inclusions. In sporadic PD, Lewy pathology seems to occur and propagate in a sequential order throughout the different brain regions (Braak et al., 2003) (Figure 5). Most commonly, pathology is first detected in the anterior olfactory bulb and/or the dorsal motor nucleus of the vagus nerve in the medulla, and is known as Braak stages 1 and 2. At this stage, patients present non-motor symptoms such as olfactory disturbances. From the medulla, the neuropathological inclusions progress to the medulla oblongate and pontine tegmentum, followed the by amygdala and SN. Sleep disturbances and the first motor symptoms appear at this stage termed Braak stages 3 and 4. As Lewy pathology reach and continue to propagate throughout the temporal cortex and neocortex in Braak stages 5 and 6, patients develop the emotional and cognitive disturbances characteristic of the later stages of the disease (Braak et al., 2002) (Figure 5; (Doty, 2012)).

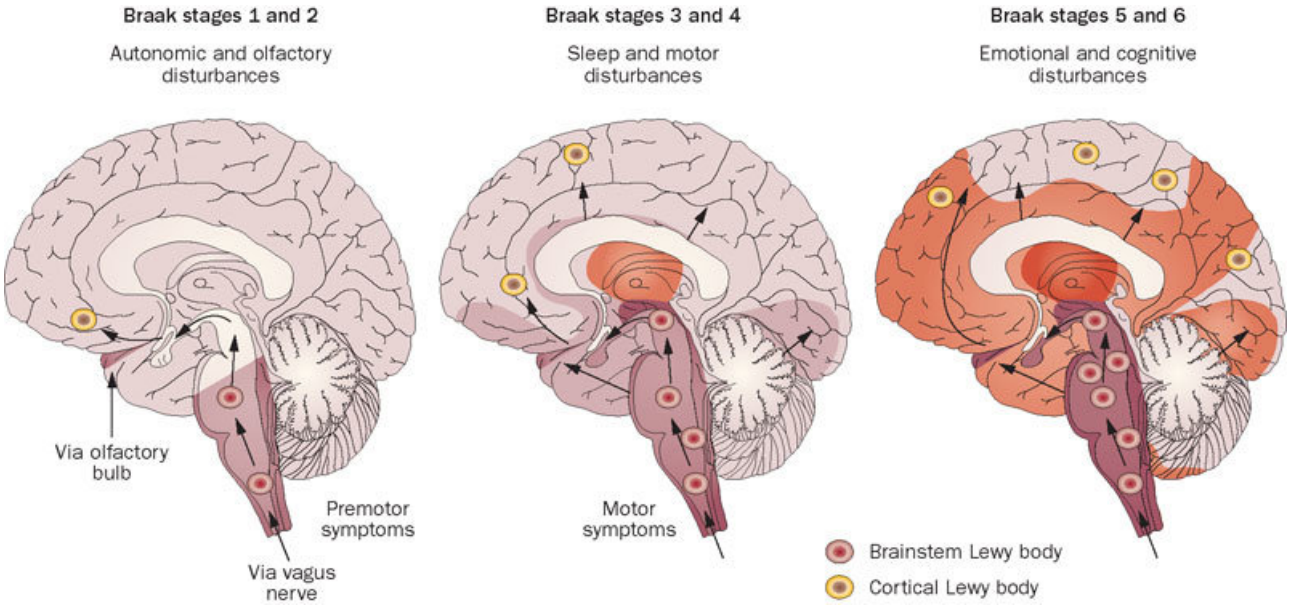

Figure 5. The Braak staging of Lewy Bodies pathology in Parkinson's disease.
Schematic representation of the Braak stages in Parkinson's disease showing the initiation sites in the vagus nerve of the spinal cord and the progression into the medulla and olfactory bulb through to the later infiltration into the substantia nigra and cortical regions. Image adapted from (Doty 2012).

1.5.2 The role of iron in PD pathology

Iron serves as a cofactor in a myriad of metabolic processes throughout the body, and is particularly essential for brain health as it is involved in neurotransmitter synthesis, mitochondrial respiration, myelin synthesis and sulfur-cluster protein synthesis amongst other processes (Ferreira et al., 2019; Ward et al., 2014). Due to the high metabolic activity and reliance on iron for many of these processes it should not be a surprise that this metal accumulates in the brain through age. However, this accumulation is even greater in regions of the brain that happen to be associated with neurodegenerative disorders (Belaidi and Bush, 2016; Haacke et al., 2005). In PD, iron elevation is especially observed in glia and dopaminergic neurons of the SNpc, where levels correlate with disease severity (Dexter et al., 1989a; Hirsch et al., 1991; Pyatigorskaya et al., 2015). In patients, this has been measured by iron-sensitive high-field MRI (Hopes et al., 2016; Pyatigorskaya et al., 2015) and quantitative susceptibility mapping (QSM) analyses (Wang et al., 2017) as well as post-mortem tissue, and is strongly supported in many parkinsonian animal models (Ayton et al., 2013, 2015; Devos et al., 2014; Kaur et al., 2003). In PD, abnormal iron accumulation is most likely due

to an imbalance in the iron homeostatic pathway caused by alterations in iron regulatory proteins (Double et al., 2000; Masaldan et al., 2019). Patients carrying mutations that cause iron-related proteins to be dysfunctional (e.g. transferrin) have an increased risk of developing PD (Borie et al., 2002; Rhodes et al., 2014). Increased levels of Divalent metal transporter 1 (DMT1), reported in the SNpc of PD patients as well as several mouse models of PD, are likely to contribute to an increased cellular iron import (Bi et al., 2020; Salazar et al., 2008). Ferritin levels are also decreased in the SN of post-mortem brains of PD patients (Dexter et al., 1990), and ferroportin (FPN) is decreased in several models of PD including MPTP and 6-OHDA (Song et al., 2010). Such changes in expression may result in a defective iron storage within the cells and an impaired export of iron, further contributing towards iron accumulation in the cytosolic labile iron pool (LIP). Of relevance to impaired neuronal efflux through FPN, rare variants of amyloid precursor protein (APP), which was shown to stabilise FPN at the level of the plasma membrane, with loss of membrane function predispose humans to develop PD (Schulte et al., 2015). In addition, APP expression is decreased in the SN of PD patients, leading to a similar iron-associated phenotype as APP knockout mice (Belaidi et al., 2018; Lei et al., 2012). Furthermore, the ferroxidase activity of CP required to facilitate iron efflux through FPN is decreased in both patients and animal models of PD (Bharucha et al., 2008; Zhao et al., 2018). Further support for iron elevation as a cause of parkinsonian pathology comes from the genetic disorder aceruloplasminemia, in which CP is mutated, often leading to a parkinsonian phenotype including gait difficulties, ataxia, involuntary movements and cognitive decline that correlate with brain iron deposition (Costello et al., 2004; Piperno et al., 2020; Xu et al., 2004). It is likely that an unregulated modulation of iron import and reduced efflux contribute towards the elevation of intracellular iron required for increased vulnerability to free radical formation and oxidative stress.
Based on the extensive evidence supporting the impact of iron on PD pathology, iron chelation has been investigated as a possible therapeutic strategy (Devos et al., 2020; Masaldan et al., 2019; Moreau et al., 2018). Iron chelation in the MPTP mouse model restores iron to physiological levels in correlation with preventing cell toxicity and behavioural deficits (Ayton et al., 2013; Devos et al., 2014). Deferiprone (DFP) is currently used clinically for systemic iron overload disorders such as beta thalassemia and was recently investigated in a double-blind, randomized, placebo-controlled clinical trial of early-stage PD: Over 12 months, patients receiving daily doses of DFP showed a promising decrease in motor handicap progression as well as reduced iron deposition in the SN (Devos et al., 2014).

The potential of DFP as a disease modifying treatment for PD is now being assessed in a phase 3 multicentre clinical trial (FAIRPARK II – NCT01539837). Importantly, similar results have been observed in an independent phase 2 randomised double-blind placebo controlled clinical trial (Martin-Bastida et al., 2017).

1.5.3 The role of oxidative stress in PD pathology

Oxidative stress (OS) is considered a major contributor to the pathophysiology underlying PD (figure 6) and is well reported in patients as well as all PD animal models (Li et al., 1997; Pearce et al., 1997; Trist et al., 2019). Indeed, a number of parkinsonian models induce an OS response that results in a phenotype similar to PD. Cellular damage caused by OS comprises of protein oxidation, leading to protein dysfunction and structural changes, DNA oxidation and cell membrane disruption due to lipid peroxidation. OS is induced by an imbalance in the redox state caused not only by an excessive reactive oxygen species (ROS) production but also by an insufficient antioxidant system response to reduce these reactive species. ROS are defined as highly reactive molecules derived from oxygen and include free radicals such as superoxide (O_2^-) and hydroxyl radicals (·OH) as well as non-radical molecules like H_2O_2 (Kim et al., 2015). ·OH are considered one of the most volatile ROS responsible for the cytotoxicity effect underlying oxidative stress and are predominantly generated from hydrogen peroxide (H_2O_2) and free cytosolic Fe^{2+} through the Fenton Reaction. Mitochondria are one of the main sites of H_2O_2 and ROS production, particularly O_2^-, via the respiratory chain complexes used to transport electrons (Cadenas and Davies, 2000; Lin and Beal, 2006) (figure 6). In the brain, the majority of the O_2^- is produced by Complex I, and it is not a coincidence that this is the primary location from which ROS is generated in various neurodegenerative diseases (Zorov et al., 2014). Indeed, in PD patients a dysfunctional Complex I is present in the SN and frontal cortex as well as fibroblast and platelets from these patients; all of which may lead to increased O_2^- production (Lin and Beal, 2006; Zorov et al., 2014). The deficiency in complex I is related to a CoQ10 deficit, an antioxidant molecule and radical trapper, further contributing to ROS production in mitochondria and lipid peroxidation in membranes. Furthermore, dopamine, which is synthesised in dopaminergic neurons, can rapidly become oxidised in the cytosol and contribute to oxidative damage. It is therefore essential that appropriate dopamine storage in vesicles is achieved to reduce the risk of oxidative stress (Figure 6).

Cells are equipped with an antioxidant system to maintain a balanced redox state, which, if compromised, can result in excessive oxidative stress and subsequent cell death.

The maintenance of glutathione (GSH) is one such antioxidant system heavily used by the brain to remove ROS by directly interacting and removing the highly reactive O_2^- and ·OH radicals (Dringen, 2000; Gandhi and Abramov, 2012). Oxidative stress in PD may in part be due to a reduction in GSH levels that appear to be particularly evident in the SN of PD (Sofic et al., 1992; Sian et al., 1994; Pearce et al., 1997). The Sian *et al* study measured GSH levels in several port-mortem brain regions from PD, progressive supranuclear palsy, multiple-system atrophy and Huntington's disease patients, and the only significant change observed was a specific 40% reduction in the SN from PD patients. The fact that no changes were reported in the other diseases suggests that the alterations in GSH levels were not a general consequence of neurodegeneration, but were specific to PD pathology (Sian et al., 1994). Interestingly, a recent analysis of DNA methylation in 1132 PD cases and 999 controls associated hypermethylation in the promoter region of the SLC7A11 gene (encoding the cysteine-glutamate antiporter XcT-) with risk of PD (Vallerga et al., 2020). This hypermethylation of SLC7A11 results in a downregulation of system XcT- which would lead to a depletion in the intracellular cysteine pool, required for GSH biosynthesis. A similar reduction in GSH level has been shown to trigger the activation of neuronal 12-lipoxygenase (ALOX12) and subsequent accumulation of lipid hydroperoxides (LOOH) (Li et al., 1997). These observations further support the concept that the decrease of GSH in the SN from PD patients is not simply a consequence of neuronal death but a direct indication of oxidative stress. Moreover, as GSH is a natural ligand for Fe^{2+} (Hider and Kong, 2011), its reduction in the SN of PD patients would not only impair the antioxidant capacity of dopaminergic neurons but also increase the LIP, further contributing to the generation of ·OH and other ROS via the Fenton reaction.

DJ-1 is another cellular antioxidant enzyme known to play a key role in regulating oxidative stress, ROS formation and mitochondrial function. As previously mentioned, loss of function mutations in the DJ-1 gene have been linked to autosomal-recessive early onset PD with increased mitochondrial oxidant stress, a drop in basal cellular respiration, oxidized dopamine accumulation and lipid ROS accumulation (Burbulla et al., 2017; Cao et al., 2020).

One would anticipate that such changes to GSH levels and the increase in LOOH would impact upon the expression and activity of key antioxidant enzymes such as GPX4. In post-mortem tissue from PD patients' brains, protein levels of GPX4 are increased compared to control subjects (Blackinton et al., 2009). More recently, GPX4 levels were confirmed to be increased relative to cell density of surviving neurons, despite the apparent reduction when

measuring against total tissue (Bellinger et al., 2011). This implies that only the remaining neurons in the SN of PD patients were able to counter an oxidative environment through an appropriate GPX4 response to prevent cell death. Interestingly, this phenomenon has also been reported in *in vitro* and *in vivo* models of stroke (Alim et al., 2019; Zille et al., 2017).

Recent advances in imaging technology are increasing our capability to measure oxidative stress in living PD patients using positron emission tomography (PET). Copper(II)-diacetyl-bis(4-methylthiosemicarbazonato) (Cu-ATSM) is a PET tracer initially developed for hypoxia imaging but has recently shown potential in reflecting the redox state within the body (Floberg et al., 2020). Interestingly, this brain blood barrier penetrant imaging agent was identified as being neuroprotective in multiple animal models of Parkinson's disease (Hung et al., 2012) and prevent lipid peroxidation without altering the oxidation state of iron. While functional imaging of oxidative stress is currently considered to mainly detect mitochondrial dysfunction, it still appears sensitive enough to show an elevation of striatal oxidative stress in PD patients when compared to controls (Ikawa et al., 2011).

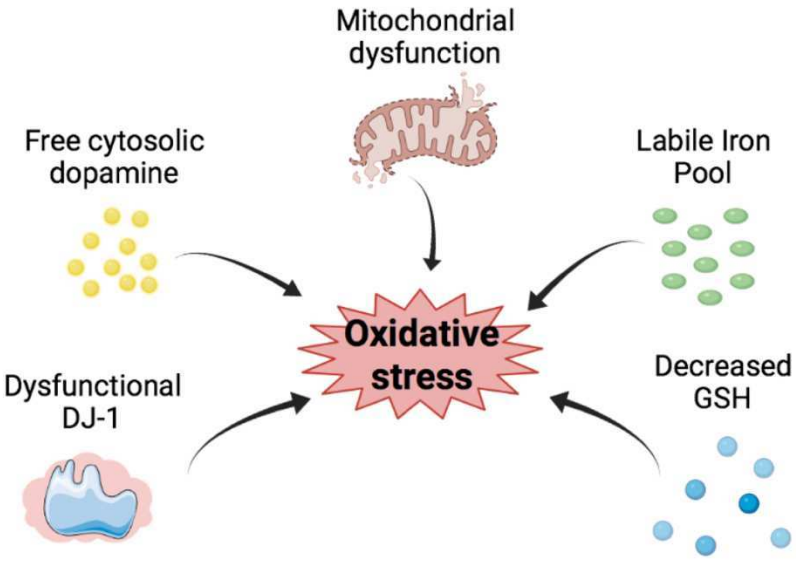

Figure 6. Cellular contributors to oxidative stress in Parkinson's Disease.
The increase generation of ROS caused by a dysfunction of DJ-1, impaired dopamine storage, dysfunctional complex I in mitochondria, an elevation of intracellular iron in the labile iron pool and decreased GSH level all contribute to cellular oxidative stress in PD pathology.

Despite the strong evidence implicating oxidative stress in PD pathology and the neuroprotective properties of antioxidants reported in models of PD, outcomes from clinical trials have remained inconsistent (reviewed in (Kim et al., 2015)). Clinical studies with exogenous antioxidant therapies are mixed with some reporting efficacy (Etminan et al.,

2005; Ross et al., 2016; Spindler et al., 2009) whilst others fail to demonstrate a significant effect (Parkinson Study Group QE3 Investigators et al., 2014). A major component of this disparity could lie with many clinical trials not having the appropriate pharmacokinetic measurements taken, a lack of confirmation in target engagement in the brain, inappropriate treatment duration and/or uncontrolled variances in endogenous antioxidant potential within the patient (Devos et al., 2021).

1.5.4 The role of lipid peroxidation in PD pathology

The brain has the second highest concentration of lipids, after adipose tissue. The proportion of these lipids are largely arachidonic acid (AA) and docosahexaenoic acid (DHA) which contain four and six double bonds respectively (Larrieu and Layé, 2018). The bis-allylic carbons found adjacent to two carbons with double bonds are they key positions within lipids that drive peroxidation as they increase susceptibility to attack from reactive radicals, ALOXs and surrounding lipid peroxides (Yang et al., 2016). Importantly, the high oxygen consumption of the brain and the accumulation of iron with age and disease progression makes it particularly sensitive to lipid peroxidation. Dexter *et al*, were the first to demonstrate the involvement of lipid peroxidation in PD as a cause of nigral cell death (Dexter et al., 1986). Brain post-mortem analyses revealed a reduction in polyunsaturated fatty acids (PUFAs) but not monounsaturated fatty acids (MUFAs) in the SN of PD patients compared to controls (Dexter et al., 1986). Conversely, levels of malondialdehyde (MDA), a toxic by-product of lipid peroxidation, were elevated in the same tissue and LOOH increased in plasma (Sharon et al., 2003). MDA levels were increased both in early and late PD patients whilst LOOH levels were only significantly increased in later stages of the disease. This suggests that while MDA could be a useful biomarker for PD, changes in LOOH levels may correlate better with disease progression (de Farias et al., 2016). Further studies have revealed a correlative increase in another lipid peroxidation metabolite, 4-hydroxy-2-nonenal (4-HNE), as well as HNE-protein adducts, with pathology from Lewy bodies in the SN of PD patients and brainstem of DLB (Di Domenico et al., 2017). Interestingly, in the CSF of PD patients, elevated 4-HNE correlates with an accumulation of iron in the SN (Selley, 1998; Di Domenico et al., 2017).

The mechanism by which lipid peroxidation is involved with PD pathology was expanded upon by Shchepinov *et al* whereby MPTP treated mice were protected against nigrostriatal injury upon supplementation with deuterated-polyunsaturated fatty acids (D-PUFAs) (Shchepinov et al., 2011). D-PUFAs have deuterium in the place of the bis-allylic hydrogens,

which slows radical generation and lipid peroxidation compared to hydrogenate-PUFAs (Shchepinov et al., 2011).

Moreover, the 85-kDa group VI calcium-independent phospholipase A2 beta (PLA2G6) is another key enzyme in the metabolism of lipids associated with neurodegeneration with brain iron accumulation (NBIA). This enzyme hydrolyses the sn-2 acyl chain of glycerophospholipids to release free fatty acids and lysophospholipids. PLA2G6 localizes to the mitochondria and has proposed roles in the remodeling of membrane phospholipids, signal transduction, calcium signaling, cell proliferation and cell death (Kinghorn and Castillo-Quan, 2016). Patients with homozygous PLA2G6 mutations suffer from NBIA, that has neuropathological similarities to both Parkinson's and Alzheimer's disease: as well as iron accumulation, these include widespread Lewy bodies, dystrophic neurites and cortical neuronal neurofibrillary tangles (Gregory et al., 2008). In a recent study, Kinghorn *et al*, showed that knocking-out the *drosophila* homologue of the PLA2G6 gene, iPLA2-VIA, resulted in reduced survival, locomotor deficits, organismal hypersensitivity to oxidative stress (in particular the mitochondria) and a strong association with increased lipid peroxidation levels (Kinghorn et al., 2015). D-PUFA were also shown to rescue the aged-associated locomotor abnormalities and restore mitochondrial membrane potential in this model.

An elevation of iron in combination with high levels of PUFAs within dopaminergic neurons in the brain and reduced GSH levels creates an environment particularly sensitive to oxidative stress and more specifically lipid peroxidation. Therefore, targeting lipid peroxidation with antioxidant or radical trapper molecules in combination with iron chelation therapy therefore represent a potential therapeutic strategy for PD.

1.6 Conclusion

The research contributions of the scientific community over the past two centuries have allowed us to answered several questions around the aetiology and pathology of the PD, leading to a more accurate clinical diagnosis and the generation of effective symptomatic treatments. However, today there remains an unmet need for disease modifying drugs that will slow disease progression and ideally lead to neuroprotection. In order to overcome this demand, it is essential that we fully understand the molecular mechanisms underlying neuronal death in the SNpc and other relevant brain regions affected in the disease. Thanks to more significant *in vitro* neuronal models, several cell death pathways have been discovered and characterised over the past decades and implicated in PD pathogenesis. (reviewed in

(Guiney et al., 2017) This thesis is specifically focused on the novel cell death pathway termed ferroptosis, which was previously implicated in *in vitro* and *in vivo* models of PD in our laboratory (Do Van et al., 2016). The next chapter will provide a detailed overview of the regulatory mechanisms of ferroptosis, and will present the evidence for its implication in synucleinopathies such as PD.

Introduction - Chapter 2:

Ferroptosis - an iron dependent cell death pathway

2.1 Introduction

Cell death is a key process tightly integrated with other biological reactions, critical in shaping an organism's development, homeostasis and disease. It is noteworthy to recognize the distinction between "accidental cell death", caused by severe physical, chemical and mechanical insults and cannot be reversed by molecular mediation, and "regulated cell death", which is under the control of specific intrinsic cellular mechanisms as evident from the fact that it can be modulated pharmacologically and genetically. Furthermore, "programmed cell death" is considered as a subset of regulated cell death that is predetermined to occur during normal physiological contexts such as development (Galluzzi et al., 2015).

Apoptosis was the first regulated and programmed cell death pathway to be characterised at the molecular level, and was soon considered to be the pathological process involved in PD related neuronal death. This was mainly due to the fact that until recently, only a few types of regulated cell death were known, and these were identified predominantly by using oncogenic cell lines (i.e. neuroblastoma). Since then, multiple cell death mechanisms have been studied and implicated in PD pathogenesis (reviewed in (Guiney et al., 2017)), including anoikis (Li et al., 1999; Saha et al., 2000; Gary and Mattson, 2001), autophagy (Chu et al., 2009; Dehay et al., 2010), necroptosis (Mogi et al., 1994; Wu et al., 2015), parthanatos (Mandir et al., 1999; Outeiro et al., 2007) and pyroptosis (Koprich et al., 2008).

More recently, ferroptosis has been established as a regulated cell death morphologically and mechanistically distinct from apoptosis and other known cell death pathways (Dixon et al., 2012). Ferroptotic cell death results from iron induced lipid peroxides that accumulate to toxic levels (Yang and Stockwell, 2016), and interestingly, several PD pathological hallmarks are known key features and/or triggers in the ferroptotic cell death pathway. These include iron overload (Dexter et al., 1987, 1989a; Ayton et al., 2015), elevated lipid peroxidation (Dexter et al., 1986, 1989b; de Farias et al., 2016), reduced GSH levels (Sofic et al., 1992; Sian et al., 1994; Pearce et al., 1997; Li et al., 1997), XcT downregulation (Vallerga et al., 2020), DJ-1 depletion (Bonifati et al., 2003; Cao et al., 2020) and CoenzymeQ10 (CoQ10) reduction (Battino et al., 1996; Mischley et al., 2012). Together,

these well- established diseases features strongly implicate this regulated cell death pathway in the neurodegeneration observed in PD. Furthermore, we have previously shown that ferroptosis is indeed a prevalent mechanism for neuronal cell death in *in vitro* and *in vivo* pro-oxidant models of PD (Do Van et al., 2016), and there is an indication that some familial PD patients carry mutations in proteins important in modulating pathways that alter ferroptosis sensitivity (Cao et al., 2020; Vallerga et al., 2020).

Although the precise metabolic pathways are still currently being elucidated, the past few years of extensive research have deciphered several regulatory mechanisms as well as numerous specific inducer and inhibitor reagents. This chapter will review the current understanding of the regulatory mechanisms of ferroptosis and present the evidence for the involvement of this newly defined cell death in PD neuropathology.

2.2 The biochemical control of ferroptosis

The initiation, execution and inhibition of ferroptosis lies at the intersection of the metabolism of amino acids, lipids and iron, but importantly, the sensitivity to ferroptosis can be modulated by several other pathways and processes (figure 7) (Tang et al., 2021).

2.2.1 Amino acid and glutathione metabolism

Although the termed ferroptosis was coined in 2012, aspects of this cell death pathway were described long before. In the mid-twentieth century, pioneering work conducted by Harry Eagle showed that depriving cell of the amino acid cysteine resulted in cell death (Eagle, 1955), whilst the endogenous synthesis of cysteine made cells resistant to such cell death (Coltorti et al., 1956; Eagle et al., 1961). Today, the relevance of the metabolism of amino acid in controlling ferroptosis is confirmed by the fact that cysteine is required for the biosynthesis of glutathione (GSH), an endogenous antioxidant and the substrate of glutathione peroxidase 4 (GPX4), a key anti-ferroptosis enzyme responsible for reducing lipid hydroperoxides (LOOH) to lipid alcohols (LOH), thus supressing ferroptosis. For the reduction of LOOH to LOH, GPX4 requires reduced GSH as an electron donor, releasing oxidised glutathione (GSSG). GSH is synthesised in the cell from glutamate and cysteine, the latter being the rate-limiting substrate. Cysteine can either be synthesised from methionine via the transsulfuration pathway or taken up in the form of an oxidised cystine dimer via the XcT antiporter before being reduced into the amino acid cysteine. Of relevance to PD pathology, Cao *et al* have recently shown that DJ-1 acts as a ferroptosis inhibitor by preserving the transsulfuration pathway, and thereby the biosynthesis of cysteine and GSH

(Cao et al., 2020). An heterodimer of the XcT unit (encoded by SLC7A11), that forms the Xc^- system, and the 4F2 unit (encoded by SLC3A2) responsible for localizing the Xc^- system to the plasma membrane, is required for intracellular cystine transport (Oestreicher and Morgan, 2019). An impairment of the XcT unit leads to a depletion in the intracellular cysteine pool, with consequential impairment of GSH biosynthesis and GPX4 activity. The subsequent lipid peroxide accumulation results in cell death by ferroptosis. Blocking GSH bioavailability through erastin-induced inhibition of the XcT antiporter or buthionine sulfoximine (BSO) induced inhibition of glutamate-cysteine ligase (GCL); the rate-limiting enzyme in the first step of GHS synthesis, suffices to trigger ferroptosis (Dixon et al., 2012). On the other hand, elevating intracellular GSH levels with cysteine precursors such as n-acetylcysteine (NAC) can protect against ferroptosis (Yang et al., 2014). Of note, the expression or activity of SLC7A11, thus the sensitivity to ferroptosis, is regulated by a variety of factors such as Nrf2 (figure 11) (Chen et al., 2017), p53 (figure 12) (Jiang et al., 2015), BRCA1-associated protein 1 (BAP1) (Zhang et al., 2018b), mucin 1, cell surface-associated (MUC1) (Hasegawa et al., 2016), or BECN1 (Song et al., 2018), which in turn form a complex network to control GSH levels in ferroptosis. As mentioned in the previous chapter, a recent study reported an increased risk of developing PD associated with hypermethylation, thus downregulation of SLC7A11 (Vallerga et al., 2020). These findings suggests that an impaired cystine import and subsequent GSH biosynthesis may contribute towards PD pathogenesis through ferroptosis induction.

Glutamate and glutamine (L-Gln) are also important regulators of ferroptosis (Gao et al., 2015) as glutamate is exchanged for cystine in a 1:1 ratio by the XcT system, meaning that glutamate levels can impact on XcT function, thus GSH levels. Indeed, high extracellular concentrations of glutamate inhibit the XcT system and induce ferroptosis, quite likely explaining the toxic effects of high glutamate concentrations in the nervous system (Dixon et al., 2012). L-Gln is the most abundant amino acid in the body, and through glutaminolysis, cells use L-Gln as a nitrogen source for the biosynthesis of nucleotides, amino acids, and hexamine as a carbon source for the tricarboxylic acid (TCA) cycle (DeBerardinis et al., 2008). Interestingly, glutaminolysis was shown to be essential for ferroptosis cell death as evident from the fact that the absence of L-Gln, or when glutaminolysis is inhibited, cysteine starvation or blockage of cystine import fail to induce the accumulation of lipid peroxidation and ferroptosis (Gao et al., 2015). This finding may be explained by the fact that α-ketoglutarate (αKG), a product of glutaminolysis, is required for ferroptosis (Gao et al.,

2015). Increased αKG promotes ferroptosis through at least two mechanisms. On one hand, αKG-mediated citrate production in mitochondria is used to produce acetyl-CoA in the cytoplasm through ATP citrate lyase (ACL) (Lee et al., 2020). Acetyl-CoA is a precursor of phospholipid biosynthesis by Acetyl-CoA Carboxylase Alpha (ACACA) and fatty acid synthase (FASN). On the other hand, αKG stimulates dihydrolipoamide dehydrogenase (DLD) to generate mitochondrial ROS and increase local iron level during cystine deprivation-induced ferroptosis (Shin et al., 2020). Therefore, αKG is a metabolic intermediate for the induction of ferroptosis by promoting ROS and lipid production.

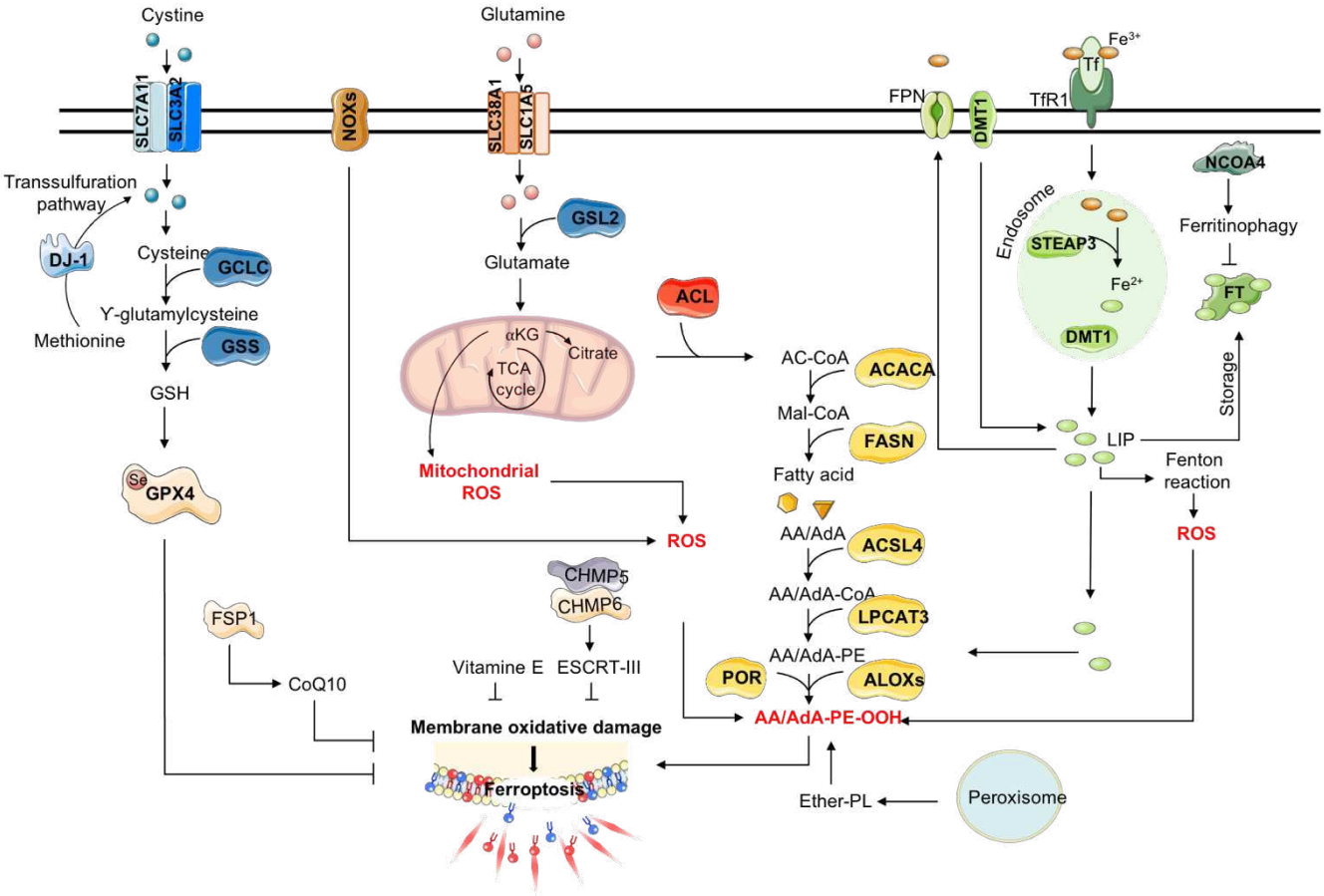

Figure 7. Molecular pathways regulating ferroptosis. Schematic representation of the different molecular pathways involved in ferroptosis induction, in addition to several antioxidant components responsible for preventing membrane oxidative damage, thus ferroptotic cell death. Figure adapted from (Tang et al., 2021).

2.2.2 Lipid metabolism.

2.2.2.a Lipid synthesis

The peroxidation of polyunsaturated fatty acids (PUFAs) in the membrane phospholipids (PL) is a key step in promoting ferroptosis (Yang et al., 2016). Therefore, increased synthesis of PUFAs and their incorporation into membrane PL promotes subsequent lipid peroxidation under oxidative stress conditions. In other words, the lipid composition of the plasma membrane can determine cellular susceptibility to ferroptosis whereby long chain PUFAs increase the risk for lipid peroxidation whilst monounsaturated fatty acids (MUFAs) appear to decrease such risk (Magtanong et al., 2019). For PUFAs to be incorporated into the PL of the plasma membrane, they first need to be conjugated to Coenzyme-A (CoA) by the enzyme acyl-CoA synthetase long-chain family member 4 (ACSL4). PUFA-CoA can then be incorporated into the plasma membrane by lysophosphatidylcholine acyltransferase 3 (LPCAT3). The importance of LPCAT3 in the ferroptosis pathway was initially pointed out by Dixon *et al* (Dixon et al., 2015) but later confirmed by Doll *et al* (Doll et al., 2017) where LPCAT3 deletion mildly protected fibroblast against ferroptosis. ACSL4, but not other members of the ACSL family, is a key player in the ferroptosis pathway as it enriches cellular membranes with long chain omega-6 (ω-6) fatty acids. Inhibiting or genetically depleting ACSL4 prevents ferroptosis-induced lipid peroxidation and subsequent associated cell death (Doll et al., 2017). The selectivity of ACSL4 over the other ACSLs in regulating the ferroptosis pathway is likely due to its substrate preference for arachidonic acid (AA), one of the main PUFAs implicated in ferroptosis (Yan et al., 2015). Indeed, phosphatidylethanolamines (PE) containing AA and adrenic acid (AdA) are the lipids most susceptible to ferroptosis-related peroxidation (Yang and Stockwell, 2016; Kagan et al., 2017). This phenomenon is supported by the fact that human cells enriched with AA show greater sensitivity to ferroptosis (Yang et al., 2016). Of note, dietary supplementation with mixed ω-6 and ω-3 PUFAs restore ferroptosis sensitivity in ACSL4-deficient cells (Doll et al., 2017) and can favour the development of ferroptosis-related inflammatory bowel disease in mice (Mayr et al., 2020), supporting the role of ω-6 and ω-3 PUFAs in ferroptosis.

Recently, another class of phospholipids - ether-linked phospholipids (ether-PL) were reported to be essential for ferroptotic-lipid peroxidation and subsequent cell death, adding to the source of PUFAs that become oxidised during ferroptosis (Zou et al., 2020a; Cui et al., 2021). Unlike ester-linked diacyl phospholipids, ether-PL possess and ether bond at the

glycerol sn-1 position. Ether-PL comprise two subclasses: alkyl-ether phospholipids (ePL) and vinyl-ether phospholipids, also known as plasmalogens (pPL). In the sn-2-position, ether-PL most often contain a PUFA, which is prone to peroxidation. Finally, in the sn-3 position, ether-PL present a polar head group, commonly a phosphoethanolamine and phosphocholine (figure 8).

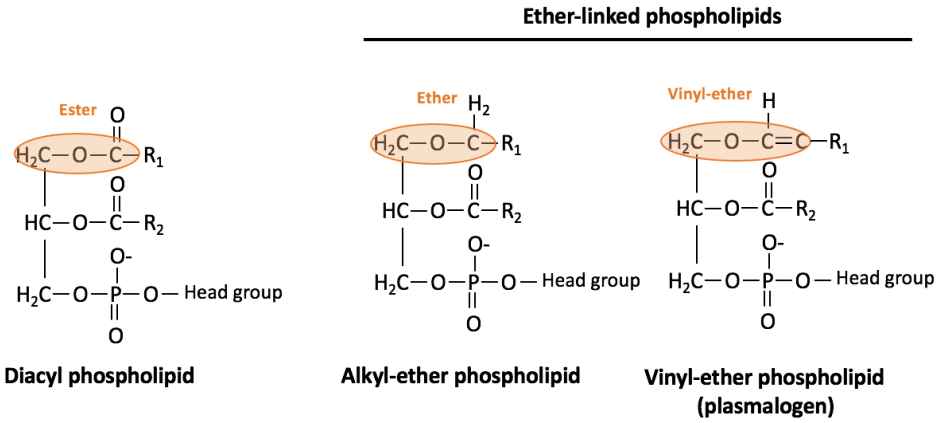

Figure 8. Chemical structure of glycerophospholipids. Schematic representation of the distinct structures of diacyl phospholipids and the two subtypes of ether-linked phospholipids, alkyl-ether phospholipids (ePL) and plasmalogens (pPL).

The biosynthesis of ether-PL commences in the peroxisomes and implicates specific enzymes such as fatty acyl coenzyme A reductase (FAR1), glyceronephosphate O-acyltransferase (GNPAT) and alkylglyceronephosphate (AGPS). First, FAR1 reduces fatty acyls coenzyme A (FA-CoA, mainly palmitoyl and stearoyl CoA) to fatty-alcohols. In the peroxisome, fatty-alcohols are transferred to acyldihydroxyacetone phosphate (acyl-DHAP) by AGPS to yield alkyldihydroxyacetone phosphate (alkyl-DHAP). Acyl-DHAP in the peroxisome is obtained by the acylation of dihydroxyacetone phosphate (DHAP) by GNPAT. Next, alkyl-DHAP is reduced to 1-alkyl-glycerol-3-phosphate (AGP or 1-alkylG3P). The maturation of AGP into ether-PL is completed in the ER where PUFAs are incorporated into the sn-2 position following their conversion to PUFA-CoA by ACSL4. Transmembrane protein 189 (TMEM189) is responsible for converting ePL into pPL. Finally, ether-PL are distributed to the plasma membrane through the Golgi apparatus (Balgoma and Hedeland, 2021). In mammalian cells, pPL are enriched in the inner leaflet of the plasma membrane,

and their excess can inhibit FAR-1 activity, thus the initial step in the synthesis of all ether-PL (Honsho et al., 2017) (figure 9).

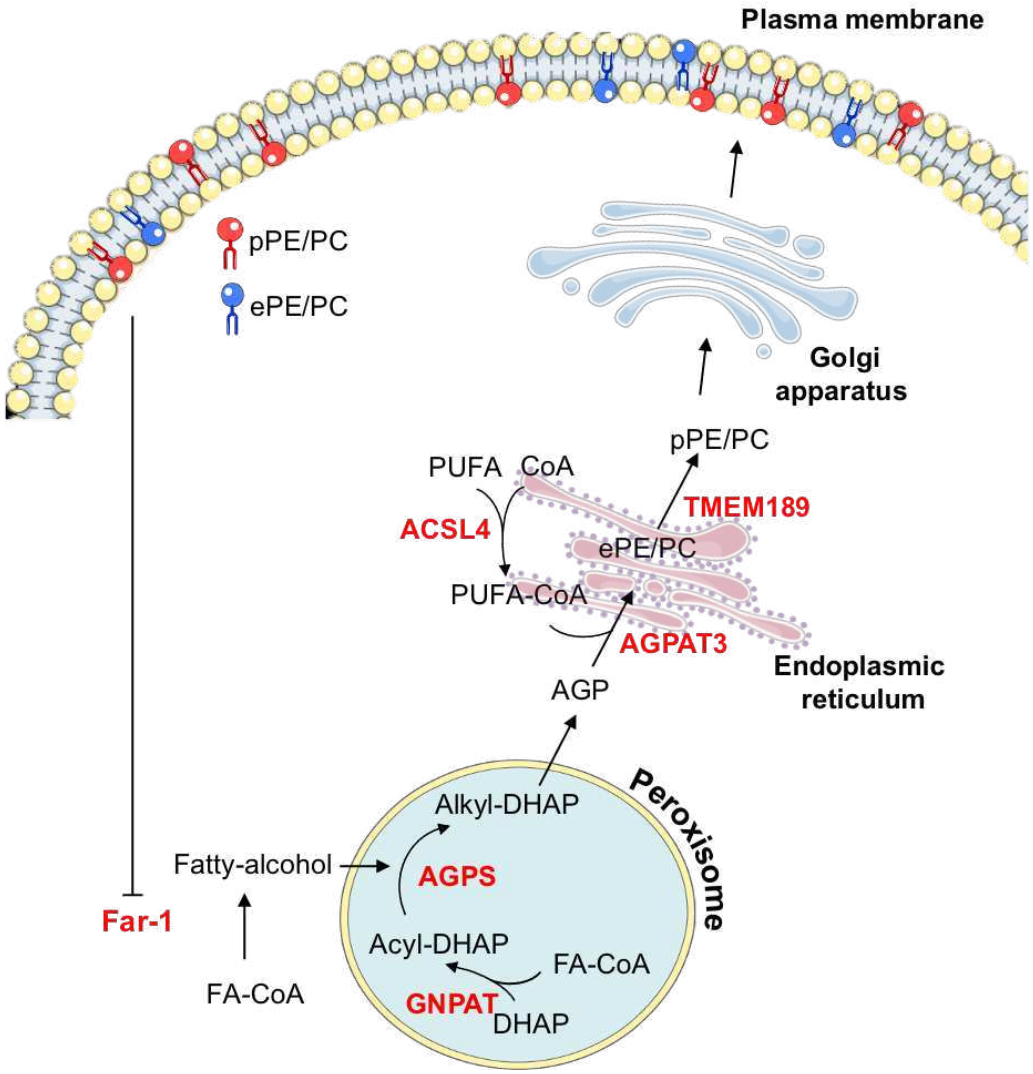

Figure 9. Synthesis of ether-linked phospholipids. Schematic representation of cell biosynthesis, location and regulation of ether-phospholipids. Figure adapted from (Balgoma and Hedeland, 2021).

Cui et al. recently identified FAR1 as a critical factor for saturated fatty acid (SFA)-mediated ferroptosis as FAR1 catalyses the reduction of SFA to fatty alcohols, the first key step in ether-PL synthesis. They also showed that by increasing the synthesis of pPL, thus the amount present in the plasma membrane inner leaflet, TMEM189 abrogates FAR1-ether-PL ferroptosis axis (Cui et al., 2021). Moreover, *Zou et al*. showed in clear-cell renal carcinoma (ccRCC) and ovarian carcinoma cells (OVCAR-8) that impairing ether-PL synthesis by

depleting cells of peroxisomes or FAR1 and AGPS rendered cells resistant to ferroptotic cell death (Zou et al., 2020a). Interestingly, using SH-SY5Y neuroblastoma cells, they reported an acquired sensitivity to ferroptosis in correlation with differentiation-dependent enrichment of ether-PL in the plasma membrane, further strengthening the essential role of ether-PL in ferroptosis lipid peroxidation (Zou et al., 2020a). In another study, *Perez et al*. found contradicting results where inhibiting AGPS sensitised *Caenorhabditis elegans* and HT-1080 cells to dihomogamma-linolenic acid (DGLA)- and RSL3-induced ferroptosis (Perez et al., 2020), thus further research is required to establish the tissue- and context-dependent role of ether-PL in ferroptosis.

2.2.2.b Lipid peroxidation

The oxidation of PUFAs from membrane PL can occur via non-enzymatic and/or enzymatic mechanisms. The free cytosolic Fe^{2+} that constitutes the LIP participates in the Fenton reaction producing highly reactive ·OH from H_2O_2, which in turn mediate the oxidation of PUFAs contained in membrane PL (Dixon and Stockwell, 2014). This process takes place via three steps: initiation, propagation and termination. Firstly, reactive radicals abstract a hydrogen atom from a bis-allylic carbon to form the carbon-centred lipid radical (PL·). Such radicals rapidly react with oxygen forming lipid peroxyl radicals (PLOO·), which can subsequently abstract further hydrogens from neighbouring lipids to propagate the generation of new PLOO· and lipid hydroperoxides (PLOOH) (Girotti, 1998). The lipid peroxidation reaction can be inhibited by the ferroptosis suppressor protein 1 (FSP1)-$CoQ10H_2$ system or when antioxidant enzymes, such as GPX4, donate electrons and reduce the pLOOH to PLOH (figure 10).

In addition to the Fenton reaction, iron can mediate the generation of lipid peroxides by serving as a cofactor to the family of lipoxygenase enzymes (ALOX). The mammalian lipoxygenases (ALOX) family, consisting of six members (ALOXE3, ALOX5, ALOX12, ALOX12B, ALOX15 and ALOX 15B), plays a tissue- or cell-dependent role in mediating PUFAs peroxidation to produce AA/AdA-PE-OOHs, thus leading to ferroptosis (figure 10) (Shah et al., 2018; Shintoku et al., 2017; Yang et al., 2016). For instance, ALOX15 is involved in p53-mediated ferroptosis in H1299 cells whereby p53-target gene spermidine/spermine N1-acetyltransferase 1 (*SAT1*) enhances the expression of ALOX15 (Ou et al., 2016). Moreover, ALOX12 is required for ferroptosis caused by p53-mediated downregulation of SLC7A11 in H1299 cells (Chu et al., 2019). *In vivo*, ALOX12 or

ALOX15 do not seem to be required for GPX4 depletion-induced ferroptotic damage in the kidney (Friedmann Angeli et al., 2014) and T cells (Matsushita et al., 2015). However, ALOX15 was shown to be essential for erastin- or RSL3-induced ferroptotic cell death in airway epithelial cells, kidney epithelial cells and cortical and hippocampal neurons through binding to the partner phosphatidylethanolamine-binding protein 1 (PEBP1), allowing ALOX15 to recognize stearoyl-AA-PE to generate lipid peroxides (Wenzel et al., 2017).

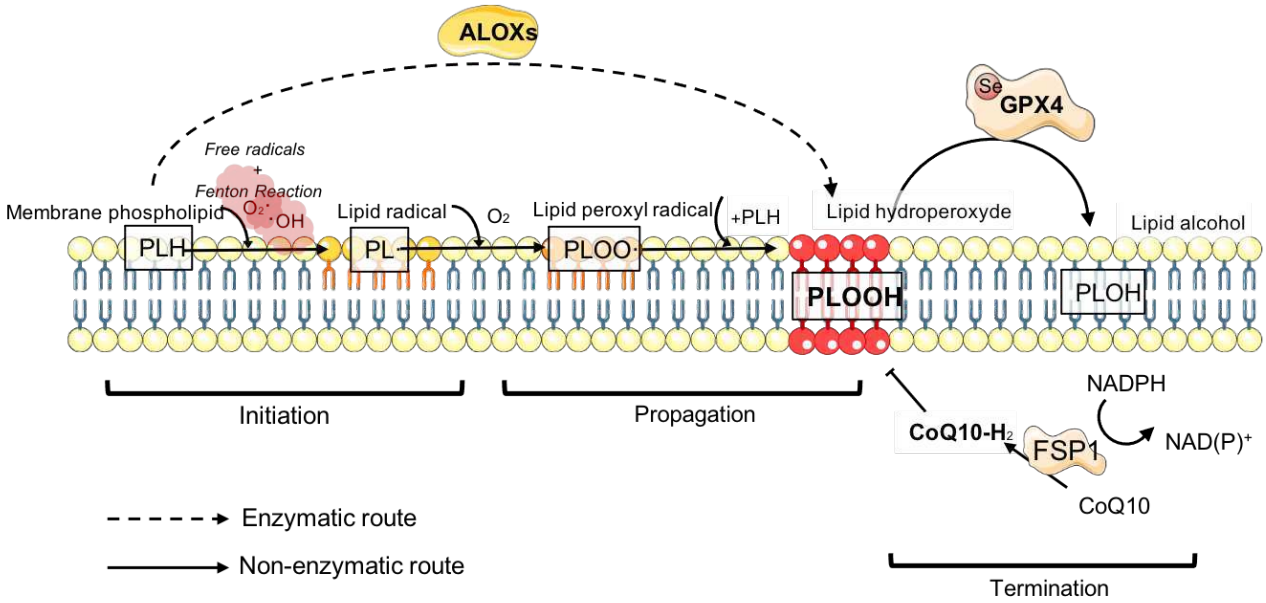

Figure 10. Membrane lipid peroxidation. The oxidation of PL in the plasma membrane can occur through an enzymatic or non-enzymatic route. The initiation can therefore be triggered by hydroxyl radicals (·OH) or ALOXs enzymes attaching the membrane PL. Following the propagation of such oxidative stress, the reduction of PLOOH to PLOH ensured via selenoprotein GPX4. FSP1 can also limit lipid peroxidation through restoration of antioxidant CoQ10-H_2

ALOX are not the only regulators of lipid peroxidation in ferroptosis as evident from the fact that cytochrome p450 oxidoreductase (POR) combines with two cofactors (flavin mononucleotide (FMN) and flavin adenine dinucleotide (FAD)) to directly supply electrons to the P450 enzyme from nicotinamide adenine dinucleotide phosphate (NADPH) thereby promoting PUFA peroxidation in cancer cells in an ALOX-independent manner (Zou et al., 2020b). It remains unknown whether other oxygenases, such as cyclooxygenases (COXs) and peroxygenases, play a similar role in lipid peroxidation. COX2 is usually considered as a biomarker, not a driver of ferroptosis since it doesn't directly oxidize phospholipids, but can oxidize lysophospholipids (Yang et al., 2014). Interestingly, COX2 may mediate ferroptosis in neuronal cells after TBI since miR-212-5p overexpression attenuates ferroptosis while

downregulation of miR-212-5p promoted ferroptotic cell death partially by targeting COX2 in HT-22 and Neuro-2a cells (Xiao et al., 2019).

2.2.2.c Lipid peroxidation detoxification

Keeping LOOH within physiological parameters is a key component in minimizing susceptibility to ferroptosis. Lipophilic antioxidants and lipid peroxide scavengers can block ferroptosis by preventing lipid peroxidation (Friedmann Angeli et al., 2014; Skouta et al., 2014). Under physiological conditions, the cell combats lipid peroxidation with GPX4, an essential selenoprotein that reduces LOOH to LOH. Importantly, GPX4 is the only member of the glutathione peroxidase family capable of reducing LOOH, supporting its central enzymatic role in the ferroptosis pathway (Cozza et al., 2017; Forcina and Dixon, 2019). Direct inactivation of GPX4 by RSL3 is one of the most common strategies to induce ferroptosis experimentally. Deletion of GPX4 in mice is embryonically lethal (Seiler et al., 2008), whilst conditionally knocking out GPX4 in mice leads to acute renal failure, hippocampal and motor neuron neurodegeneration and early death of mice (Friedmann Angeli et al., 2014). In addition, overexpression of GPX4 protects against cell death induced by RSL3 (Yang et al., 2014). For the reduction of LOOH to LOH, GPX4 requires reduced GSH as an electron donor, releasing GSSG. Recently in an attempt to uncover genes able to protect against ferroptosis through glutathione-independent pathways, the flavoprotein "apoptosis inducing factor mitochondria-associated 2" (AIFM2), was identified to rescue cell death caused by GPX4 deletion (Bersuker et al., 2019; Doll et al., 2019). Renamed "ferroptosis suppressor-protein 1" (FSP1), it suppresses ferroptosis by catalysing the regeneration of CoQ10, also known as ubiquinone, to its reduced form CoQ10-H_2 or ubiquinol; a potent mitochondria and lipid peroxyl radical trapping antioxidant. A recent study proposed that FSP1 can abrogate ferroptosis through a CoQ10-independent mechanism by boosting the endosomal sorting complexes required for transport (ESCRT)-III membrane repair system. However, this study failed to identify a direct downstream target of FSP1, and thus, the underlying mechanism remains unclear (Dai et al., 2020a). *Dai et al*. had previously explored the impact of membrane repair mechanisms on ferroptosis and identified that ESCRT-III negatively regulates ferroptosis in cancer cells (PANC1 and HepG2). They found that classical ferroptosis inducers (i.e. erastin and RSL3) triggered the accumulation of ESCRT-III subunits (CHMP5 and CHMP6) in the plasma membrane, likely in an attempt to counter excess lipid peroxidation and cell death. Importantly, knocking-down CHPM5 or CHMP6 rendered human cancer cells more vulnerable to lipid peroxidation-mediated

ferroptosis *in vitro* and *in vivo* (Dai et al., 2020b). Moreover, PLA2G6 was shown to avert ferroptosis by removing from the plasma membrane the ferroptotic 15-hydroperoxy(Hp)-arachidonoyl-phophatidylethanolamine (15-HpETE-PE) death signal (Sun et al., 2021).

2.2.3 Iron metabolism

As the name implies, iron plays a central role in ferroptosis. Co-treatment with several sources of iron sensitizes cells to ferroptosis triggered by erastin or RSL3 (Dixon et al., 2012; Gao et al., 2015) and depletion of iron using drugs such as DFP or genetically silencing transferrin receptor 1 (TfR1) to prevent cellular iron import protects cells against ferroptosis (Do Van et al., 2016; Gao et al., 2015). Indeed, Hemin and ferric ammonium citrate were shown to promote erastin or $FINO_2$-induced ferroptosis in HT-1080 fibroblast cells (Kwon et al., 2015). Iron has two oxidation states: ferrous (Fe^{2+}) or ferric (Fe^{3+}). Although the exact mechanisms through which iron promotes ferroptosis remain unclear, it has been suggested that *i*. ferrous iron directly induces lipid peroxidation (Dixon and Stockwell, 2014), *ii*. iron loads the iron-dependent ALOX12/15 which enzymatically induces lipid peroxidation (Li et al., 1997; Yang et al., 2016; Wenzel et al., 2017), and *iii*. iron loading of the hypoxia inducible factor prolyl-hydroxylase 1 induces ATF4-dependent pro-death gene transcription (Karuppagounder et al., 2016). In biofluids such as cerebrospinal fluid (CSF), iron is predominantly bound to transferrin (Tf). Iron-loaded Tf (holo-Tf) incorporates two ferric (Fe^{3+}) atoms and is internalized into a cell through clathrin-mediated TfR1-dependent endocytosis. Once in the endosome, iron is released from Tf due to its acidic environment and the metalloreductase STEAP3 reduces the bound insoluble Fe^{3+} to its soluble ferrous (Fe^{2+}) form (Knutson, 2007). Iron is then released into the cytosol through DMT1, with Tf and TfR1 being recycled back to the membrane for further use (figure 7). Similar to Tf, lactotransferrin (LTF) also functions as a positive regulator of ferroptosis by increasing iron uptake (Wang et al., 2020). Neuronal import of iron can also occur directly through the DMT1 channel on the plasma membrane, allowing for a less regulated import pathway (Belaidi and Bush, 2016). The appropriate levels of free cytosolic iron in the LIP need to be tightly maintained to avoid the excess generation of free ·OH and other radicals (figure 7). The function of ferritin (FT) is in part to safely store excess iron in the cytosol but neuromelanin also serves as a key iron storage protein specifically in dopaminergic neurons. FT can be degraded by lysosomes in order to increase free iron levels in the cell. This process is termed ferritinophagy, and inhibiting nuclear receptor coactivator 4 (NCOA4)-mediated ferritinophagy, increases iron storage and was shown to limit ferroptosis in cancer cells. On

the other hand, increasing cellular iron availability by enhancing autophagic degradation of FT promotes sensitization to ferroptosis (Gao et al., 2016; Hou et al., 2016). Furthermore, the overexpression of ferritin mitochondrial (FTMT), an iron-storage protein in mitochondria, inhibits erastin-induced ferroptosis in neuroblastoma cells (Wang et al., 2016), supporting the wide anti-ferroptosis role for iron storage proteins. The only known export pathway for iron is through the transmembrane channel FPN in which iron, oxidized to Fe^{3+} by a ferroxidase such as ceruloplasmin, can exit the cell (Hare et al., 2013) (figure 7). The overexpression of FPN inhibits, whilst the knockdown of FPN increases ferroptosis through modulation of iron efflux in breast cancer cells (Ma et al., 2016). In select cells (including neurons) APP is required to facilitate iron efflux by stabilising FPN on the plasma membrane (Lei et al., 2012; McCarthy et al., 2014; Belaidi et al., 2018; Tsatsanis et al., 2019).

As mentioned in the previous chapter, several aspects of the metabolism of iron seem impaired in PD pathology. Indeed, increased iron import via DMT1 upregulation (Salazar et al., 2008) in combination with a defective storage due to FT and neuromelanin decrease (Dexter et al., 1990), and an impaired iron efflux through FPN (Song et al., 2010), result in an abnormal accumulation of iron within neurons, potentially increasing their sensitivity to ferroptosis. Importantly, iron chelation has shown promising results in the MTPT mouse mode, whereby physiological iron levels are restored in correlation with prevention of cell toxicity and behavioural deficits (Ayton et al., 2013; Devos et al., 2014). This therapeutic strategy has also been assessed in several clinical trials showing a promising decrease in motor handicap scores (Devos et al., 2014; Martin-Bastida et al., 2017).

2.2.4 Other metabolic pathways controlling ferroptosis sensitivity

Several other factor have been shown to modulate the sensitivity of cells to ferroptosis. Nuclear factor erythroid-2-related factor 2 (Nrf2), a master transcription factor that coordinates the antioxidant response, is known to protect against ferroptosis (Harvey et al., 2009; Sun et al., 2016; Liu et al., 2020). Upon binding to the antioxidant response element of the target gene promoters, Nrf2 can control the expression of NAD(P)H:quinone oxidoreductase 1 (Kovac et al., 2015), several iron related proteins (i.e. FTH1, FPN and heme oxygenase 1 (HMOX1)) (Kerins and Ooi, 2018), GPX4 (Osburn et al., 2006) and other key ferroptosis regulators involved in GSH biosynthesis (i.e. XcT, GLC and glutathione synthetase (GSS)) (Osburn et al., 2006; Liu et al., 2020) (reviewed in (Song and Long, 2020)). The first evidence of the protective role of Nrf2 against ferroptosis was obtained in hepatocellular carcinoma cells (HCC). Under normal conditions, KEAP1, an adapter protein

of the Cul3 ubiquitin E3 ligase complex responsible for Nrf2 ubiquitination and degradation, maintains low levels of Nfr2, preventing gene transcription and establishing ferroptosis sensitivity (figure 11a). Following a continuous ferroptosis stimulus, p62 mediates the degradation of KEAP1, thus stabilising Nrf2 which initiates a multi-step activation pathway, starting with nuclear translocation, followed by heterodimerization with its partner MAF protein, recruitment of transcription coactivators and binding to the antioxidant response element (ARE) in the promoter of the target genes. (Sun et al., 2016) (figure 11b). Continuous exposure to erastin was later shown to result in Nrf2-dependent upregulation of cystathionine β-synthase (CBS), the enzyme responsible for the biosynthesis of cysteine, in an attempt to counter cell death in ovarian cancer cells (Liu et al., 2020).

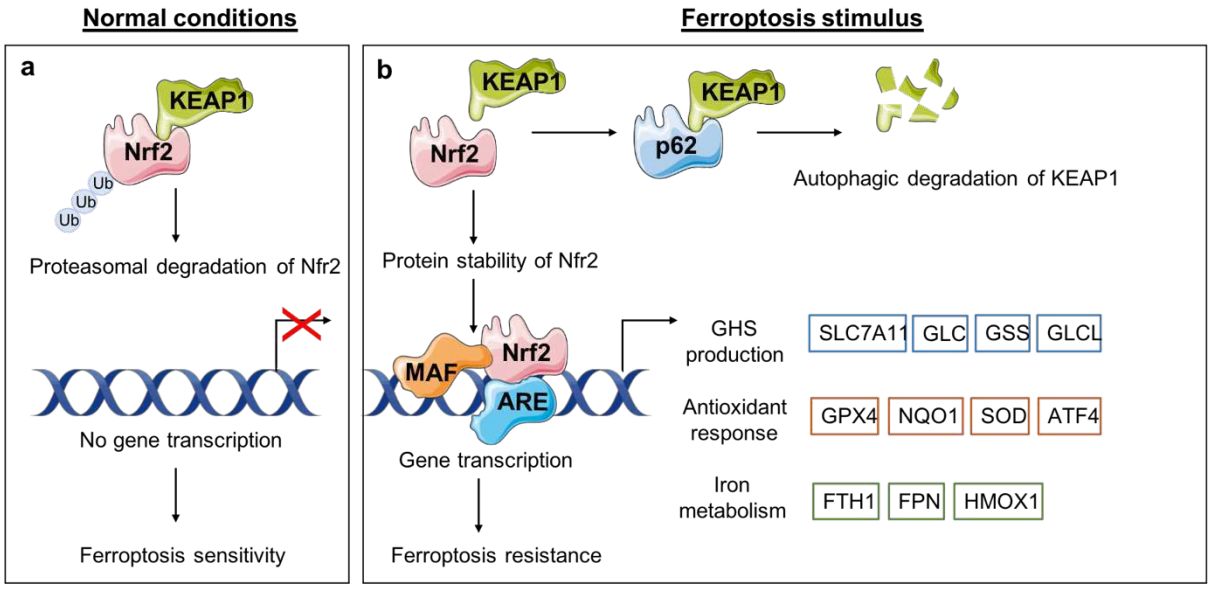

Figure 11. The role of Nrf2 in determining ferroptosis sensitivity. **a.** Under physiological conditions, KEAP1 mediates the degradation of Nfr2, preventing gene transcription, resulting in ferroptosis sensitivity. **b.** Under ferroptosis stimulus, p62 increases Nrf2 stability through the inactivation of KEAP1, allowing for Nfr2-mediated transcription of target genes involved in GSH production, antioxidant response and iron metabolism, all contributing to ferroptosis resistance.

Nrf2 has been extensively studied in the context of PD pathology where and age-related decline in activity leads to reduced GSH levels (Suh et al., 2004; Todorovic et al., 2016). In PD patients, Nrf2 and downstream effectors are highly transcribed in blood leukocytes compared to controls (Petrillo et al., 2020). Interestingly, these Nrf2 transcripts correlate with PD duration, suggesting that Nrf2 plays a role in fighting the intrinsic oxidative stress observed during disease pathology. Furthermore, the cellular localisation of Nrf2 appears to be predominantly nuclei in the SN of PD patients, in contrast to the cytoplasmic location in

affected brain regions from other neurodegenerative diseases such as Alzheimer's disease (AD) or Lewy body variant of AD (Ramsey et al., 2007). Such nuclear translocation in PD indicates a cellular and/or disease dependent recruitment of Nrf2 caused by an intrinsic vulnerability of dopaminergic neurons to oxidative stress. It is worth noting that Nrf2 response to oxidative stress may not be unique to ferroptosis as Nrf2 inhibition has also been implicated in apoptosis cells death (Zhang et al., 2016).

P53 plays a dual role in ferroptosis (figure 12). On one hand, it can promote ferroptosis by transcriptionally inhibiting SLC7A11 expression leading to GSH depletion and subsequent ferroptosis in several cancer cell lines (Jiang et al., 2015). As previously mentioned, p53 can also sensitise cells to ferroptosis through regulating lipid peroxidation via the transcriptional induction of *SAT1 (Ou et al., 2016)*, increasing ALOX15 expression, or glutaminase 2 (GSL2), an enzyme involved in the first step of glutaminolysis (Gao et al., 2015).

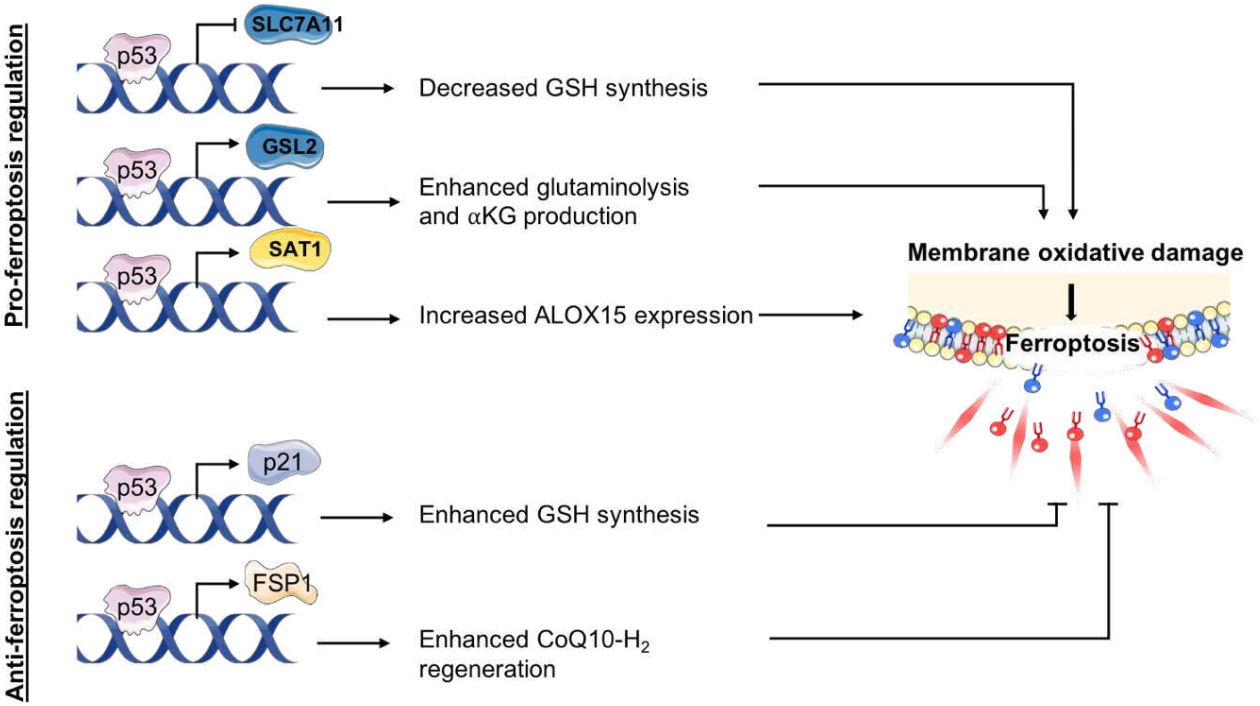

Figure 12. The role of p53 in determining ferroptosis sensitivity. p53 can either enhance or inhibit ferroptosis in a context- and cell-dependent manner. P52 can promote ferroptosis by inhibiting SCL7A11 expression or promoting SAT1 and GLS2 expression. On the contrary, p52 prevents ferroptosis by inducing p21 expression resulting in increased GSH levels.

On the contrary, p53 can prevent ferroptosis by modulating other transcriptional targets, such as FSP1, originally termed p53-responsive gene 3 (PRG3) (Horikoshi et al., 1999). Moreover,

the p53-mediated transcriptional upregulation of cyclin-dependent kinase inhibitor 1A (p21) was shown to inhibit ferroptosis in human fibrosarcoma cells thanks to slowed GSH depletion and reduced accumulation of toxic lipid peroxidation (Tarangelo et al., 2018).

In relation to PD pathology, an increase in p53 levels and activity is observed in selected brain regions from PD patients (Mogi et al., 2007) as well as in PD animal and cellular models (da Costa et al., 2009). Mutations in *parkin* was shown to correlate with an increase in p53 mRNA levels and consequent transcriptional activity in cells and mouse brains, and familial *parkin* missense and deletion mutations enhanced p53 expression in human brains affected my juvenile PD (da Costa et al., 2009). Consistently, p53 gene deletion reduced dopaminergic neuronal loss in the substantia nigra and striatum of the MPTP mouse model (Qi et al., 2016), suggesting a more prominent pro-ferroptosis role of p53 in this particular PD mouse model.

NADPH is an intracellular reductant involved in the elimination of LOOH. Intracellular NADPH levels are considered as a biomarker for ferroptosis sensitivity, but accurate measurement of NADPH level is difficult in patients. Several studies with biofluids from PD patients have demonstrated an altered level of NADPH oxidase (NOX), an enzyme complex which oxidises NADPH to generate oxygen species. The NOX subunits NOX1 and NOX4 are both increased in the SN in several PD mammalian models (Cristóvão et al., 2009; Choi et al., 2012) as well as PD patients (Zawada et al., 2015).

Selenium (Se) is considered a key element in the cellular antioxidant machinery as it is crucial for selenocysteine generation and the synthesis of selenoproteins such as GXP4 (Friedmann Angeli and Conrad, 2018). Se abundance can thus impact upon ferroptosis sensitivity, whereby supplementation promotes ferroptosis resistance and a deficit leads to increased sensitivity, presumably through modulating GPX4 levels and activity (Cardoso et al., 2017). In line with an intrinsically high oxidative environment, the level of Se in the brain is highest in the SN and caudate (Cadet, 1986). Multiple studies report a protective role of Se in several PD models: Se supplementation reduces motor impairments and DNA damage in a rat model of Parkinson induced by Paraquat (Ellwanger et al., 2015), and a single dose of Se was sufficient to reverse the depletion of striatal dopamine and its metabolites in the MPTP mouse model (Khan, 2010). In line with GPX4 expression levels, Selenoprotein P, a peptide with a high content of Se in the form of selenocysteine, was reportedly reduced in PD SN compared to control brains but increased relative to cell density (Bellinger et al., 2012).

Overall, a great number of studies have independently and over the years shown that ferroptosis share common features with the pathological mechanisms associated with PD (Table 1), strengthening our hypothesis that ferroptosis may indeed contribute towards neuronal death in PD. This topic was the subject of a literature review we published in Progress in Neurobiology in 2021 (Figure 13; Annexe 2).

Figure 13. Review article on ferroptosis and its role in Parkinson's Disease.

2.3 Studying ferroptosis experimentally

2.3.1 Ferroptosis induction

Pharmacologically, several compounds have the ability to specifically induce ferroptosis (figure 14). One of the main strategies for triggering ferroptosis in cells is via the inhibition of XcT system thus blocking cystine import. Erastin was the first molecule identified to trigger ferroptosis via inhibiting SLC7A11 in Ras-dependent oncogenic cell lines (Dixon et al., 2012). Since then, other compounds have been developed and identified to block XcT-mediated cystine import and trigger ferroptosis. These include the derivate of erastin, imidazole ketone erastin (IKE), which has a better solubility and high stability, Erastin2 with increased efficiency and potency, and drugs like sorafenib and sulfasalazine.

Features of Parkinson's Disease Pathology consistent with Ferroptosis		
Feature	**Comment**	**Reference**
Decreased GSH	Measured in post mortem brain regions from PD: a reduction in GSH levels in the SN of PD patients	(Pearce et al, 1997; Sian et al, 1994; Sofic et al, 1992)
Decreased XcT expression	Hypermethylation in the SCL7A11 promotor region and subsequent reduction in XcT expression is associated with increased risk of developing PD	(Vallerga et al., 2020)
Depletion of PUFAs	Post-mortem analyses reveal a reduction of PUFAs in the SN of PD patients associated with an nicrease in lipid peroxidation by-products	(Dexter et al, 1989)
Elevated lipid peroxidation by-products	HNE and MDA are elevated in the SN of PD brains and associated with iron accumulation. HNE is equally elevated in the CSF of PD patients	(Dexter et al, 1989; Domenico et al, 2017; de Farias et al, 2016)
Decrease GPX4 in Substantia Nigra	In post mortem analysis: reduced GXP4 levels in the SN in PD brains, but increased relative to cell density of surviving neurons	(Bellinger et al, 2011)
Increased iron in SN	MRI and QSM analyses confirm iron accumulation in the SNpc in PD patients. Iron concentrations correlate with disease severity	(Dexter et al, 1987, 1988; Hirsch et al, 1991; Hopes et al., 2016; Wang et al., 2017)
Clinical benefits of Iron Chelation	A double-blind, randomized, placebo-controlled clinical trial of early-stage PD showed a decresed motor handicap progression and decreased iron deposits in the SN of PD patients taking DFP. An ongoing phase 3 multicentre clinical trial will asses DFP as a disease modifying treatment	(Devos et al, 2014)
Decreased CoQ10 levels	Levels of the antioxidant CoQ10 are reduced in PD animal models and living PD patients	(Battino et al., 1996; Mischley et al., 2012)
DJ-1 depletion	DJ-1 loss of function mutations are associated with early-onset PD. DJ-1 is negative ferroptosis regulator as it maintains the cystein and GSH biosynthesis via the transsulfuration pathway	(Burbulla et al, 2017; Cao et al, 2020)
Nrf2-mediated antioxidant response	Nrf2 translocation to the nucleus and increased downstream effectors in an attempt to compact intrinsic oxidatice stress, and potentially ferroptosis, in PD pathology	(Ramsey el al., 2007; Petrillo et al., 2020)
Enhanced p53 pro-ferroptosis regulation	Increased p53 mRNA levels and transcriptional activity observed in PD patients may lead to decreased GSH syntheiss, enhanced glutaminolysis and ALOXs expression	(Mogi et al., 2007; da Costa et al., 2009)

Table 1. Common features shared between ferroptosis molecular pathways and PD pathology.

Further down the XcT-GSH-GPX4 ferroptosis axis, BSO can induce ferroptosis on its own by inhibiting GCL, the rate-limiting enzyme in GSH biosynthesis, or enhance cellular sensitivity to ferroptosis induction by other agents (Dixon et al., 2012; Sun et al., 2016). Another common strategy to trigger ferroptosis experimentally is via direct or indirect inhibition of GPX4. Small molecules such as RSL3, FIN56, ML210 and $FINO_2$ can therefore efficiently prevent GPX4-mediated detoxification of LOOH resulting in their accumulation and subsequent cell death. In addition to promoting GPX4 degradation, FIN56 also blocks CoQ10 production (Shimada et al., 2016). Furthermore, the activity of FSP1 in ferroptosis can be specifically inhibited by a small-molecule compound called iFSP1, blocking CoQ10-mediated antioxidant defence and resulting in ferroptotic cell death. Iron alone does not suffice to trigger ferroptosis, however, increasing the cytosolic LIP by iron supplementation, increasing ferritinophagy and/or preventing FPN-mediated iron efflux are all successful strategies in increasing cellular sensitivity to ferroptosis induction by other agents (Dixon et al., 2012; Gao et al., 2015; Kwon et al., 2015). Finally, a study conducted in *C. elegans,* and later confirmed in human cancer cells (HT-1080), reported ferroptotic cell death induced by dietary PUFA DGLA, whilst dietary and endogenous MUFAs inhibited ferroptosis (Perez et al., 2020).

2.3.2 Ferroptosis inhibition

Experimentally, inhibition of ferroptosis is mainly achieved through three strategies: *i*. iron depletion by iron chelation treatments including DFP and deferoxamine (DFO), or by reducing iron import by Tfr1 knockdown (Dixon et al., 2012; Gao et al., 2015; Do Van et al., 2016), *ii*. decreasing PUFA-containing phospholipids and their oxidation thanks to ACSL4 inhibitors such as rosiglitazone, troglitazone and pioglitazone (Doll et al., 2017), ALOXs inhibitors including Zileuton, MK886, PD146176 and Balcalein, or deuterated PUFAs (Beaudoin-Chabot et al., 2019), and *iii*. scavenging lipid LOOH with radical trapping agents (RTAs) (figure 14). Of note, several LOX inhibitors were later shown to block ferroptosis via their radical trapping action rather than via a specific inhibition of ALOXs enzymes (Shah et al., 2018). Importantly, genetically depleting cells of ACSL4 or certain ALOXs enzymes will also promote a ferroptosis resistant phenotype *in vitro* and *in vivo* (Doll et al., 2017).

There are three types of RTAs that are widely used as ferroptotic cell death inhibitors: phenolic compounds such as α-tocopherol (α-TOH) and vitamine E (Burton and Ingold, 1986), amines including ferrostatin-1 (fer-1) and liproxstatin-1 (lpx-1) (Shah et al., 2017),

and nitroxides (Krainz et al., 2016; Griesser et al., 2018). Finally, boosting the endogenous antioxidant systems is also effective in preventing ferroptosis, for instance by supplementing with NAC (Yang et al., 2014), Se (Alim et al., 2019), and idebenone (an analogue of CoQ10) (Shimada et al., 2016), or by treatment with allosteric GPX4 activators (Li et al., 2019).

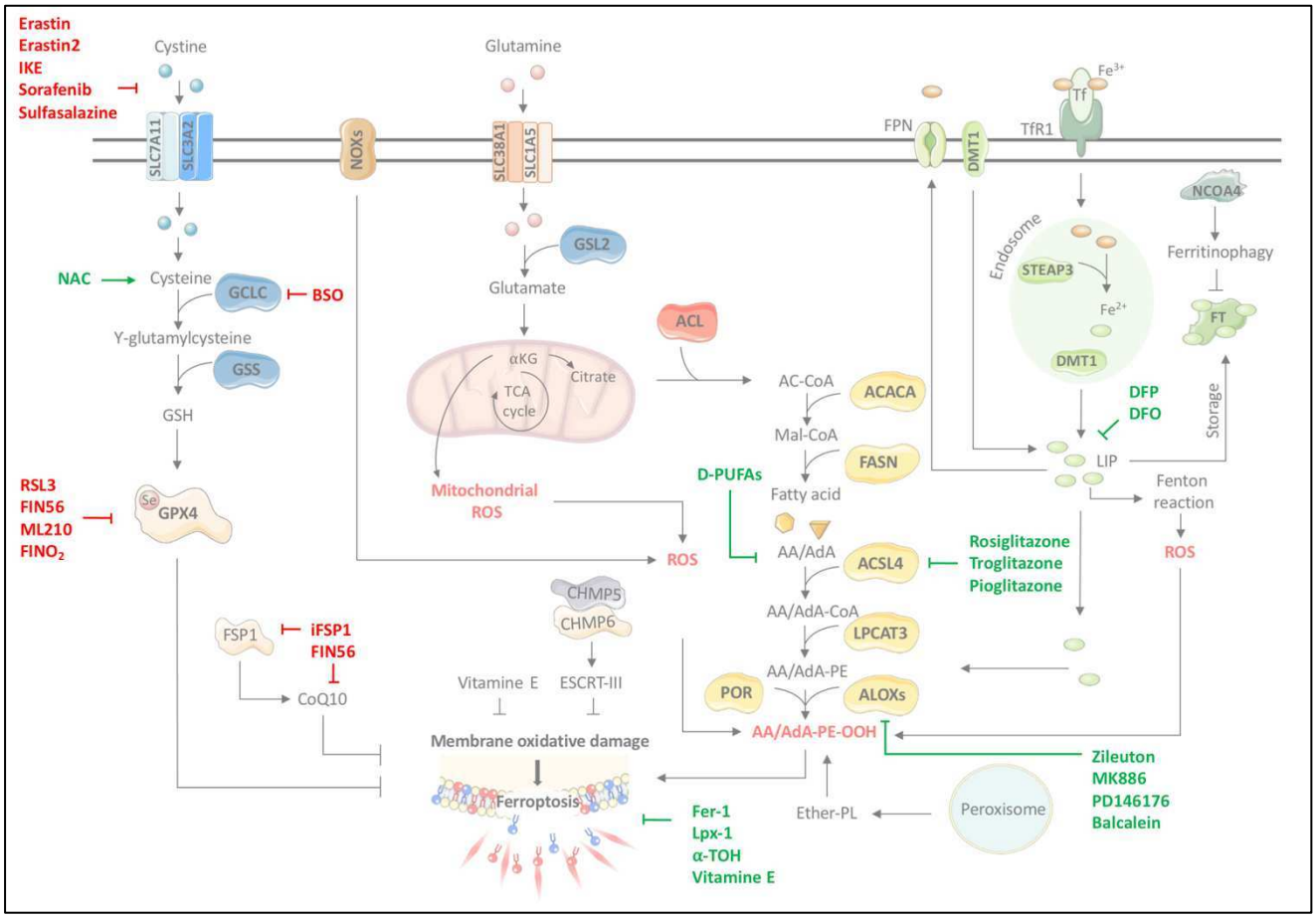

Figure 14. Molecular inducers and inhibitors of ferroptosis. Schematic representation of the different molecular pathways involved in ferroptosis with the molecular inducers in red and inhibitors in green. Figure adapted from (Tang et al., 2021).

2.3.3 Assays for ferroptosis assessment

There are a number of methods available to measure ferroptotic response related to iron and, more importantly, lipid metabolism. Measuring intracellular iron content can allow us to determine ferroptosis susceptibility. This can be accurately measured by inductively-coupled plasma mass spectrometry (ICP-MS) or with the use of fluorescent probes such as Ferrum 430, Ferrum 569 and Ursa520-R although they can only be used to quantify the amount of Fe^{3+} but not the toxic Fe^{2+}. To overcome this limitation, the heavy metal indicator Phen Green

SK can be used to detect the level of Fe^{2+} although it may also react with other metals (Tang et al., 2021).

Regarding lipid peroxidation, several methods exist to detect their presence. These include assays for the direct quantification of LOOHs as well as assays that measure lipid peroxidation end-products or antioxidant molecules like GSH. The most widely used probes for measuring lipid peroxidation during ferroptosis are the fluorometric C11-BODIPY and LiperFluo. They are both lipophilic probes that can interact with peroxyl radicals, although LiperFluo is the only one able to interact with phospho-LOOHs (Kagan et al., 2017). Lipid peroxidation in mitochondria can also be specifically measured with probes like MitoPerOx, MitoPeDPP and MicoCLox, while MitoSOX is more widely used for detecting mitochondrial O_2^- in cells. All the above mentioned fluorescent probes are suitable for either fluorescent microscopy staining or flow cytometry.

Lipid oxidation products can also be identified and quantified in cells and tissue samples via mass spectrometry, in addition to using monoclonal antibodies specific for MDA or 4-HNE in immunohistochemistry staining. Furthermore, the end-products of ALOXs-mediated arachidonic acid peroxidation 15-hydroxyeicosatetraenoic acid (15-HETE) can also be quantified with ELISA kits.

Finally, in order to confirm that ferroptotic cell death is specifically being induced in the experimental models, ferroptosis inhibitors or knocking-down ferroptotic regulators (i.e. ACSL4 or ALOXs) are strategies that should be used in parallel to show a protection in cell viability assays.

2.4 Conclusions and perspectives

Over the past years, there's been an outbreak of ferroptosis research which has led to the publication of over 3500 articles since 2012, with more than 1500 articles being published in 2021 alone. Ferroptosis is now defined as a regulated necrosis, tightly controlled at multiple levels and implicating several metabolic pathways reviewed in this chapter. At the core of the process, we know that PUFA-containing PLs are highly sensitive to oxidation by either an enzymatic (ALOXs and POR) or non-enzymatic (iron-dependent Fenton reaction) route, however the question remains as to what is the final effector of ferroptosis cell death. Iron accumulation and lipid peroxidation can be considered as intermediate events in ferroptosis, but are not the final executors of this novel cell death pathway. This statement is supported by the fact that not all damage caused by lipid peroxidation results in ferroptosis,

and key ferroptosis regulators also play a role in regulating other types of cell death. For example, the activation of SLC7A11 also avoids apoptosis under oxidative stress (Ku et al., 2020), and GPX4 was reported to also inhibit apoptosis (Q et al., 2004), necroptosis (Canli et al., 2016) and pyroptosis (Kang et al., 2018) in response to various tissue injuries. These observations suggest that there might be a crosstalk between the different cell death pathways and thus they may all contribute towards disease pathogenesis. Indeed, different types of cell death usually occur downstream of a common stress response and often share similar initial signals and molecular regulators for example at the level of ER stress, redox stress and mitochondrial dysfunction. Future research on ferroptosis should therefore address this question in order to determine the regulatory pathways that determines the fate of cells.

In regards to the pathological role of ferroptosis in PD, further direct implications between PD pathological markers and ferroptosis are required to strengthen the link between excessive ferroptotic cell death and neurodegeneration. α-syn aggregation has long been considered a key pathological hallmark in PD. Despite the involvement of α-syn in PD pathology, the exact physiological and pathological functions of the protein remain elusive. Establishing a synucleinopathy link to ferroptosis would strengthen the implication of this novel type of cell death in PD. Based on the multiple studies showing a link between α-syn dysfunction and impaired iron and lipid metabolisms, we hypothesised that α-syn may play a role in determining cellular susceptibility to ferroptosis. Interestingly, iron chelators, D-PUFAs and fer-1 all suppress cell death induced by toxic α-syn oligomers (Angelova et al., 2020), meeting the basic criteria set out to define ferroptosis (Yang and Stockwell, 2016; Tang et al., 2021). The next chapter will provide an overview on α-syn and discuss the evidence associating α-syn to iron and lipid metabolism.

Introduction - Chapter 3:

Alpha synuclein – Physiological and pathological implications in Parkinson's disease

3.1 Introduction

The protein alpha-synuclein (α-syn) is a member of the synuclein family along with β- and γ- synuclein. It was first identified in the central nervous system of *Torpedo californica* by Maroteaux in 1988 (Maroteaux et al., 1988) and was named based on its cellular localisation as the protein was initially found both in the synapses and the nuclear envelope, hence the name "synuclein". It was almost a decade after its discovery that α-syn became the focus of intense neurodegenerative research when it was identified as the major component of Lewy bodies and Lewy neurites in 1997, establishing the protein as a major hallmark of synucleinopathies (Spillantini et al., 1997). The different synucleinopathies include Parkinson's disease (PD), dementia with Lewy Bodies (DLB), multiple systems atrophy (MSA) and pure autonomic failure (PAF). PD and DLB share common pathological traits although the clinical manifestations differ significantly. In PD, it is the dopaminergic neurons in the substantia nigra pars compacta (SNpc) that are most affected, resulting in a loss of dopamine neurotransmission and the subsequent motor impairments. Non-motor impairments are also widely observed amongst PD patients preceding the motor symptoms, or latter in the progression of the disease in the form of psychiatric and cognitive alterations (Hely et al., 2008). In DLB, the Lewy body pathology is observed at the level of the cortex and the CA2/3 region of the hippocampus (Dickson et al., 1991), which may explain the Alzheimer's-like symptoms, such as dementia and cognitive decline. DLB patients may also suffer from hallucinations and fluctuation of attention starting as early as 1 year since the onset of motor symptoms (Mayo and Bordelon, 2014; McKeith et al., 2017). In MSA, α-syn accumulates in glial cytoplasmic inclusions mainly in oligodendrocytes. Interestingly, α-syn is poorly expressed in oligodendrocytes, raising the question of how these aggregates are formed. One possible explanation is that these cells are unable to efficiently clear α-syn, resulting in its accumulation. Alternatively, and in line with the prion-like propagation hypothesis, α-syn may be released into the extracellular space by neurons and taken up by oligodendrocytes (Reyes et al., 2014; Steiner et al., 2018). In terms of the clinical manifestation, MSA patients display Parkinson-like symptoms such as bradykinesia, motor weakness, muscular rigidity,

tremor and balance impairments. PAF is a rare sporadic neurodegenerative disorder considered as a synucleinopathy in 2000 when the pathological LBs and LNs were found in the sympathetic ganglia and postganglionic sympathetic axons (Arai et al., 2000). Although the symptoms of the disease are usually related to the periphery with hypoperfusion in the neck area and urinary and sexual dysfunctions, studies have suggested that PAF can progress to PD, DLB or MSA, therefore posing as an intermediate state (Kaufmann et al., 2004; Kaufmann and Goldstein, 2010).

Despite the implication of α-syn in the above mentioned synucleinopathies, and the extensive research around the physiological and pathological functions of α-syn, many questions remain unanswered and a clear direct mechanism linking the protein to the different diseases pathologies is yet to be established. Deciphering such mechanisms, whether they directly or indirectly link the protein to the physiopathology of the disease, will enable the identification of novel therapeutic strategies. This chapter will first provide an overview on the structure of α-syn and its putative physiological functions. Next, the pathological implications of α-syn mutations and overexpression will be described, in addition to the links between the protein and both the metabolisms of iron and lipids which provide evidence for a potential implication of α-syn in the ferroptosis pathway.

3.2 The structure of α-synuclein

α-syn is a small, 140 amino acid (aa) long soluble protein highly expressed in neurons and encoded by the *SNCA* gene located at position 21 in the long arm of chromosome 4 (Shibasaki et al., 1995). It's aa sequence can be divided into three major domains, correlating with both physiological and pathological putative functions (figure 15):

1. **The N-terminal domain** (aa 1 to 60) contains a consensus sequence of aa repeated 7 times (KTKEGV) with alpha-helical propensity. This structure is similar to that of apolipoproteins A2 upon lipid binding (Vamvaca et al., 2009), allowing α-syn to bind and interact with fatty acids and lipids in the plasma and mitochondrial membranes (Vamvaca et al., 2009; Zigoneanu et al., 2012). Of note, this region bares the known mutations responsible for familial PD forms.
2. **The central domain** (aa 61-95) is known as the non-amyloid beta component (NAC). It is highly hydrophobic and prone to aggregation when acquiring beta-sheet structure, as

suggested by the fact that an ablation of this region reduces oligomer and fibril formation (Giasson et al., 2001).

3. **The C-terminal domain** (aa 96-140), is negatively charged and rich in acidic amino acids, providing its natively disordered structure. Thanks to its undefined secondary structure, this region contributes to α-syn solubility, protecting it against aggregation (Eliezer et al., 2001). Several studies have associated the C-terminal domain with the modulation of membrane binding of α-synuclein (Davidson et al., 1998; Eliezer et al., 2001; Perrin et al., 2000), but also multiple protein (Burré et al., 2018) and ion interactions (Bai et al., 2015; Bartels et al., 2019; Lautenschläger et al., 2018).

The exact conformation of α-syn inside the cells remains a matter of debate. Most likely, several conformations of α-syn co-exist in the cytosol depending on the cellular localisation, lipid binding, oligomerization, mutations and posttranslational modifications. Initially, α-syn was reported natively unfolded in solution and monomeric state (Uversky, 2003). However, more recently, several studies reported tetramer conformations enriched in α-helixes, resistant to oligomerization (Bartels et al., 2011; Wang et al., 2011).

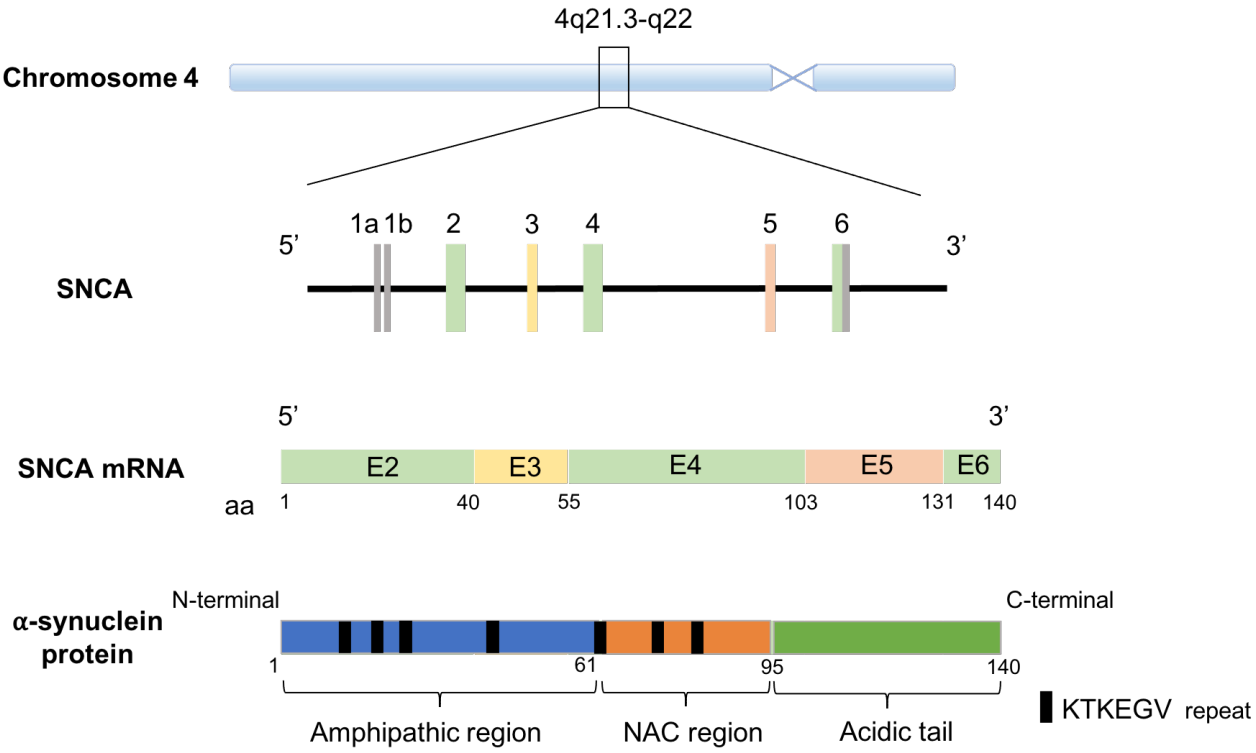

Figure 15. SNCA gene localisation, mRNA and protein structure. The SNCA gene located in chromosome 4 is transcribed into the mRNA containing 6 exons. The 140 amino acid long α-synuclein protein contains three main regions: amphipathic region, NAD region and the acidic tail, with 7 repeats spanning the first two regions.

Upon lipid binding, α-syn adopts either a single elongated α-helix or a broken α-helix depending on the membrane curvature (Bussell and Eliezer, 2003; Chandra et al., 2003). Under pathological conditions, α-syn is reported to adopt a β-sheet conformation contributing the its aggregation and depositions into Lewy bodies (Conway et al., 1998; El-Agnaf et al., 1998; Narhi et al., 1999; Yonetani et al., 2009). These β-sheet conformers have long been considered neurotoxic, despite there been an ongoing debate on the exact nature of the neurotoxic species and the mechanisms leading to such neurotoxicity (figure 16).

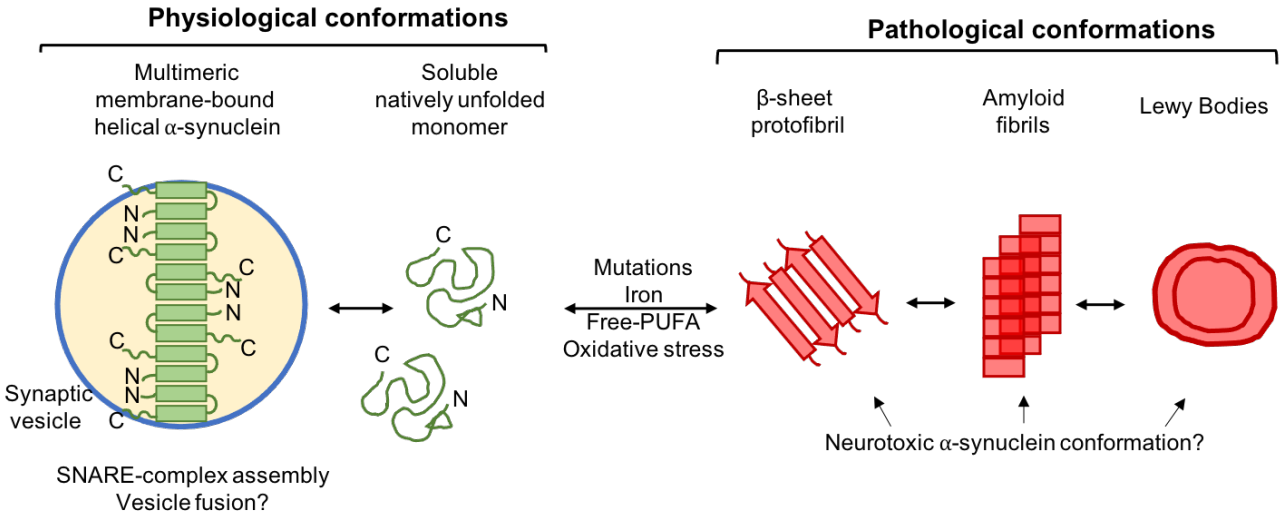

Figure 16. Schematics of α-synuclein conformations associated with its physiological and pathological functions. Under physiological conditions, α-syn is mainly unstructured. Upon binding to curved membranes, such as synaptic vesicles, α-syn undergoes a conformational change and adopts α-helixes. Under pathological conditions, soluble α-syn forms β-sheet-like protofibrils which can convert into larger amyloid fibrils and aggregate into Lewy bodies. Image adapted from (Burré et al., 2018).

During transcription, the *SNCA* gene can undergo alternative splicing, or in-frame splicing, and create different transcripts. In-frame splicing is characterized by the deletion of one or more exons retaining the original reading frame, producing shorter functional proteins (Gámez-Valero and Beyer, 2018). In the case of *SNCA*, the exons 3 and 5 can be alternatively spliced giving rise to at least four transcripts and isoforms (figure 17):

- **α-syn 140** is the main, most abundant and studied isoform originated from a SNCA mRNA containing the full coding sequence (exons 2 to 5), producing the 140-aa long protein.

- **α-syn 126** arises from the translation of the mRNA lacking exon 3. This results in a protein which is 126 amino acids long. This isoform lacks part of the lipid binding domain located in exon 3, and is believed to be less prone to aggregation (Beyer, 2006a; Gámez-Valero and Beyer, 2018).
- **α-syn 112** isoforms lacks exon 5 and results in a protein with a shorter C-terminal region. This variation is thought to increase α-syn aggregation propensity (Beyer, 2006a; Gámez-Valero and Beyer, 2018).
- Finally, when both exon 3 and 5 are alternatively spliced, the isoform **α-syn 98** is generated, characterised by a shortening of the N-terminal (as in α-syn 126) and the interruption of the C-terminal domain (as observed in α-syn 112).

Interestingly, differential expression of α-syn 126 and 112 was reported in the brains of DLB and AD patients when compared to controls (Beyer, 2006a; Beyer et al., 2006). α-syn 126 mRNA were shown to be significantly decreased whilst α-syn 112 mRNA levels were up-regulated in DLB and AD patients' brains when compared to control patients (Beyer et al., 2006). Importantly, α-syn 126 is characterized by its inability to bind cellular membranes due to the interruption and loss of several α-helixes needed for the protein-membrane interactions. Membrane-bound α-syn is thought to be a crucial initial step towards aggregation and provide the seeds for deposition of the less aggregation prone cytosolic forms (Lee et al., 2002). In view of these observations and its markedly reduced expression in DLB and AD patients, it can be suggested that α-syn 126 acts as a protective, aggregation-preventing isoform. On the other hand, the α-syn 112 expression levels were shown to be two-fold increase in DLB patients when compared to controls, suggesting a possible involvement of α-syn 112 in DLB pathogenesis (Beyer, 2006b). Indeed, several studies have reported that C-terminal shortening enhances aggregation of α-syn (Crowther et al., 1998; Murray et al., 2003; Liu et al., 2005).

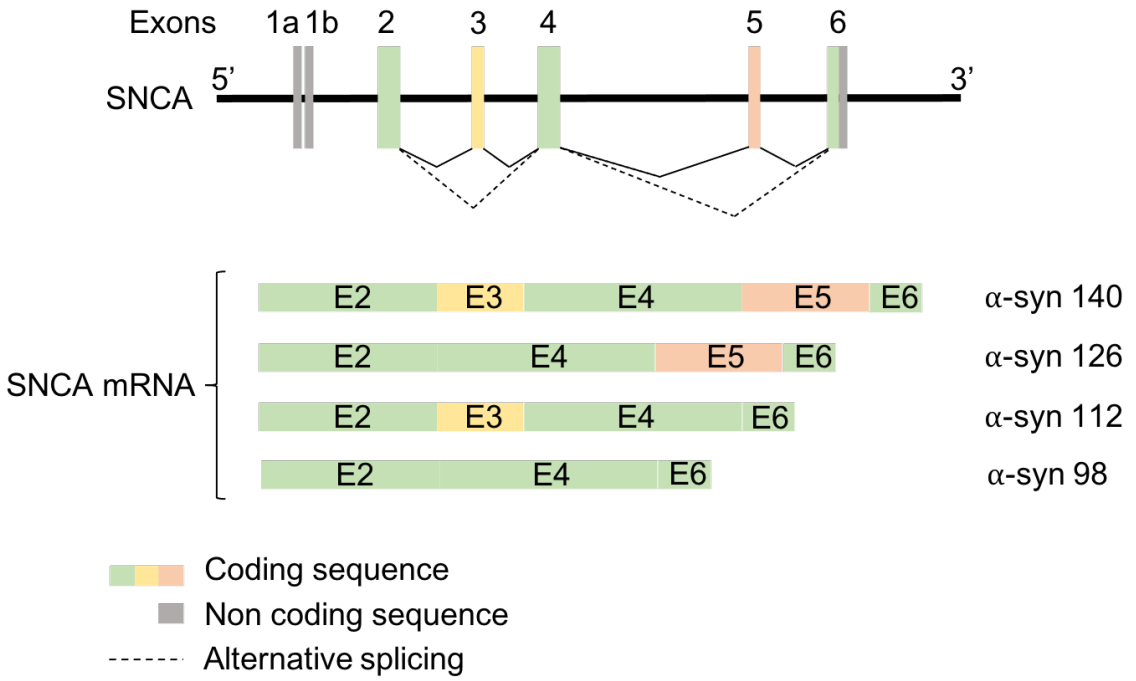

Figure 17. SNCA mRNA variants generated by alternative splicing. Through alternative splicing of exon 3 and 5, four different mRNA transcripts of α-syn can be generated. α-syn 140 is the most studied and predominant isoform whilst the three remaining variants remain poorly studied.

3.3 α-synuclein expression and localisation

Despite the predominant expression of α-syn in the brain, particularly in the neocortex, hippocampus, striatum, thalamus and cerebellum (Nakajo et al., 1990; Jakes et al., 1994; Iwai et al., 1995), α-syn can be detected in the bone marrow, muscle, liver, kidney, lung, heart, cerebrospinal fluid (CSF), blood plasma and red blood cells (where α-syn is believed to be involved in the curvature of the cells) (Hashimoto et al., 1997; Askanas et al., 2000; Shin et al., 2000; Tamo et al., 2002; Ltic et al., 2004; Burré et al., 2018). α-syn protein levels are often mirrored by mRNA levels (Burré et al., 2018), and expression can be altered by several external factors such as herbicide paraquat (Manning-Bog et al., 2002), MPTP (Vila et al., 2000), injury to the brain (Acosta et al., 2015), but also intracellular dopamine and iron levels (Perez et al., 2002; Friedlich et al., 2007), which will be further described in later sections. During development of cultured neurones, α-syn is primarily localised in the cell body of immature neurons and the presynaptic terminal becomes enriched in α-syn once neurons become mature (Withers et al., 1997). The late localisation of α- syn in the presynapse suggest it does not play a role in the synapse development bur rather in proper synaptic

neurotransmission. Moreover, several studies have reported α-syn localisation and binding to mitochondria in tissue from PD patients or from transgenic mouse models (Li et al., 2007; Zhang et al., 2008; Devi et al., 2008). The potential function of α-syn in mitochondria remains unclear due to studies where both overexpression and loss of α-syn expression lead to mitochondrial dysfunction (Ellis et al., 2005). In addition to its localisation to the synapse and mitochondria, α-syn has also been associated with the Golgi apparatus and various secretory and endosomal compartments other than synaptic vesicles (Baksi et al., 2016). Of note, oligomeric α-syn accumulate in the ER in the brains of PD patients and animal models of synucleinpathy (Bellucci et al., 2011; Colla et al., 2012) further implicating the protein in defective endosomal transport in PD pathology.

3.4 Post-translational modifications

In addition to alternative splicing, the structure and functions of α-syn can be vastly altered by post-translational modifications such as phosphorylation, acetylation, nitration, oxidation, ubiquitination and truncation. These PTMs have been associated to physiological and pathological forms of α-syn linked to increased aggregation and oligomerization (Duce et al., 2017).

Among the different PTM, phosphorylation is the most studied. α-syn is constitutively phosphorylated with several phosphorylation sites identified on either tyrosine, threonine or serine residues (e.g. Y39, S87, Y129 and S129) (Okochi et al., 2000; Pronin et al., 2000; Paleologou et al., 2010). S129 is the phosphorylated residue most typically affiliated with pathology since it is identified in almost 90% of aggregated α-syn in the brains of PD and DLB patients, while only 4% is identified in healthy brains (Fujiwara et al., 2002; Nishie et al., 2004; Waxman and Giasson, 2008). Several studies have suggested that phosphorylation of α-syn may regulate the structure, membrane binding and therefore oligomerization and fibril formation propensity of the protein (Waxman and Giasson, 2008; Paleologou et al., 2010). *In vivo* studies have supported the observations from human samples with transgenic mice expressing the mutated A53T α-syn showing phosphorylated S129 in pathological inclusions (Waxman and Giasson, 2008). Additional work conducted on transgenic *Drosophila* show that phosphorylation at S129 is a key mechanism controlling α-syn toxicity, as evident from the fact that replacing S129 with the phosphorylation-incompetent residue alanine completely attenuates α-syn toxicity in both dopaminergic neurons and

retinal cells. Conversely, mutation of S129 to aspartate in order to mimic phosphorylation significantly enhances the aggregation and toxicity of α-syn (Chen and Feany, 2005). Whilst collective studies have elucidated the mechanisms of toxicity related to aggregation, the role of phosphorylation in membrane interaction is becoming apparent. Several studies have shown that phosphorylation at S129, S87 and Y39 may lead to the inability of α-syn to bind membranes (Paleologou et al., 2010; Fiske et al., 2011; Nübling et al., 2014), which may impact the protein's putative physiological function on vesicular transport and uptake (Hara et al., 2013; Duce et al., 2017).

α-syn is natively acetylated in the N-terminal in residues K6 and K10, which contribute to the proper protein folding increasing its resistance to aggregation (Fauvet et al., 2012; Bartels et al., 2014). Indeed, upon deacetylation by Sirtuin 2, the aggregation and cytotoxicity of α-syn increases (Bu et al., 2017). Moreover, several studies have suggested that N-terminal acetylation is required for correct lipid membrane binding, with a higher binding affinity for vesicles containing lower negative charge and higher curvature – properties that relate closely to synaptic vesicles (Maltsev et al., 2012; Dikiy and Eliezer, 2014).

These observations support the hypothesis that a putative physiological role of α-syn is to mediate vesicular transport through synaptic vesicle docking and fusion (Yavich et al., 2004; Lou et al., 2017) and that PTMs like phosphorylation and/or acetylation may therefore modulate the ability of α-syn to control vesicle trafficking.

3.5 Functions of α-synuclein

The vast majority of α-syn research has focused on the pathological functions of its aggregates and their contribution to PD pathology. Less is known about the physiological significance of the putative functions of α-syn and whether its pathological association to PD is due to a loss of function, a gain of toxic function, or both.

α-syn has been reported to interact with a variety of proteins suggesting it may have a number of functions in conjunction with these protein interactions. These include, but are not limited to, binding and inhibiting phospholipase D (Jenco et al., 1998; Ahn et al., 2002; Payton et al., 2004; Gorbatyuk et al., 2010), regulating the interaction of the small GTP-binding protein rab1 and rab3 with synaptic vesicle membranes (Chen et al., 2013), binding to the SNARE protein synaptobrevin-2 and chaperoning SNARE-complex assembly (Burré et al., 2010, 2014), binding to and regulating tyrosine hydroxylase (TH) in part via

modulation of the iron metabolism, binding to DJ-1 (Zondler et al., 2014; Tanudjojo et al., 2021) (Masliah et al., 2000; Perez et al., 2002; Baptista et al., 2003; Wu et al., 2011), and synphilin-1 (Engelender et al., 1999; Ribeiro et al., 2002), regulating microtubule-dependent trafficking by binding to tubulin (Lee et al., 2006), and enhancing tau phosphorylation (Jensen et al., 1999; Haggerty et al., 2011; Siegert et al., 2021).

3.5.1 Vesicle trafficking and neurotransmitter release

Substantial evidence from both *in vitro* and *in vivo* models have reported that α-syn is associated with intracellular vesicle trafficking. Firstly, overexpression of α-syn was shown to inhibits ER-Golgi trafficking in yeast, which could be rescued by overexpressing rab1, the relevant rab GTPase for this function (Cooper et al., 2006). Similar findings were reported in retinal epithelial cells where overexpressing α-syn led to reduced trafficking of hydrolyses from the Golgi to the lysosomes, thus impaired lysosomal activity (Baksi and Singh, 2017). Here again, rab1a overexpression rescued the phenotype. Defects in endosomal trafficking was also reported in mammalian cells with prefibrillar α-syn aggregates (Gosavi et al., 2002), and the A53T PD-mutation appear to inhibit ER to Golgi transport more potently than WT by inhibiting SNARE complex assembly (Thayanidhi et al., 2010). Indeed, physiological WT α-syn has repeatedly been shown to have a role in chaperoning the assembly of SNARE complexes as evident from the fact that α-, β- and γ- synuclein triple KO mice have reduced SNARE-complex assembly, present neuropathological signs and shortened survival (Burré et al., 2010; Greten-Harrison et al., 2010). These studies, in addition to those on PD-linked LRRK2, GBA, VPS35, and DNAJC13 mutations, further strengthen the implication of a defective endolysosomal system, notably the autophagy-lysosomal degradation pathway, in PD pathology.

The presynaptic localization of α-syn (Maroteaux et al., 1988), its interaction with synaptic vesicles and synaptobrevin-2 (Burré et al., 2010) and its SNARE-complex chaperoning activity (Burré et al., 2014; Lou et al., 2017) strongly suggest that α-syn plays a role in neurotransmitter trafficking and release (figure 16). It is understood that the fusion and clustering of SNARE-associated vesicles to the synaptic membrane can be regulated by α-syn associating with the vesicle associated membrane protein 2 (VAMP2/synaptobrevin-2). By keeping VAMP2 in close proximity with the T-SNAREs, α-syn can control stimulated neurotransmitter release (Duce et al., 2017). Furthermore, in the triple synuclein KO mice

model, Greten-Harrison and colleagues, reported a 30% reduction in the excitatory synapse size as well as alterations in synaptic structure and transmission (Greten-Harrison et al., 2010). The effect of α-syn on neurotransmission and synaptic plasticity has been investigated in both KO and in overexpressing models generating conflicting results where α-syn both promotes (Abeliovich et al., 2000; Liu et al., 2004; Gureviciene et al., 2007; Greten-Harrison et al., 2010) and inhibits neurotransmission (Larsen et al., 2006; Senior et al., 2008; Yavich et al., 2006). Interestingly, this functions doesn't seem unique to α-synuclein as β- and γ-synuclein appear to also mediate neurotransmission.

3.5.2 Dopamine synthesis and transport

It is becoming increasingly evident that α-syn plays a physiological role in dopamine homeostasis. Firstly, in both α-syn transgenic mice (Masliah et al., 2000) and α-syn-transfected dopaminergic cells (Perez et al., 2002), the activity of TH was significantly reduced suggesting that α-syn modulates dopamine synthesis by inhibiting the expression and activity of TH. To confirm this, a simpler cell-free system was used to examine whether TH activity could be directly modulated by α-syn. Perez and colleagues found that the activity of isolated TH was inhibited by recombinant human α-syn in a dose-dependent manner (Perez et al., 2002). Furthermore, it is known that only phosphorylated TH is active and this form is thus required for dopamine synthesis (Toska et al., 2002). α-syn has been shown to colocalize and bind to dephosphorylated TH, stabilizing this inactive form of TH (Peng et al., 2005; Perez et al., 2002). Interestingly, both A30P and A53T mutant α-syn have shown similar inhibitory effects on TH (Perez et al., 2002). Another study reported that phosphorylation of α-syn upregulates TH activity and dopamine synthesis in dopaminergic MN9D cells, likely due to the regulation of α-syn's functions due to the different post-translational modifications (Wu et al., 2011). Of note, α-syn can also indirectly mediate cellular dopamine synthesis through the regulation of intracellular iron which serves as a cofactor for TH activity. In parallel, cellular dopamine levels also depend on dopamine reuptake from the synaptic space via the dopamine transporter (DAT), and α-syn has been shown to attenuate DAT activity by reducing the uptake velocity of dopamine (Wersinger and Sidhu, 2003; Sidhu et al., 2004). Interestingly, this regulatory effect on DAT activity has been reported with WT and A30P α-syn, but not the A53T mutant form (Wersinger et al., 2003, 2004). Regarding the A53T mutation, one study reported increased cytosolic dopamine

levels in A53T α-syn expressing mutant dopaminergic neurons, likely due to an impaired activity in dopamine storage into vesicles (Cabin et al., 2002; Lotharius et al., 2002). Indeed, a separate study reported that overexpression of mutant A53T α-syn in differentiated mesencephalic neurons led to a downregulation of the vesicular dopamine transporter (VMAT2), enhancing cytoplasmic dopamine and increasing intracellular superoxide levels (Lotharius and Brundin, 2002). Indeed, excessive cytosolic dopamine due to impaired α-syn functions will facilitate the oxidation of dopamine, contributing to ROS generation and increase oxidative stress. In turn, higher oxidative stress can potentiate the aggregation of α-syn further impairing the functions of the protein thus entering a pathological vicious cycle (Yu et al., 2005).

3.6 The pathological effects of PD-associated mutations and multiplications in α-synuclein.

As previously mentioned, the majority of studies aimed at deciphering the pathological implications of α-syn have focused on the aggregation of the protein. However, some other studies have reported neurotoxic alterations to cellular processes due to α-syn point mutations and/or overexpression which will be described in the following section .

3.6.1 A53T α-synuclein point mutation

The A53T α-syn point mutation was the first disease-linked mutation discovered in 1997 (Polymeropoulos et al., 1997). The PD-associated mutations of α-synuclein have primarily been studied for their effect in enhancing α-syn aggregation and oligomerization (figure 16) (Conway et al., 1998; El-Agnaf et al., 1998; Narhi et al., 1999). However, several studies have also reported alterations to several cellular organelles such as mitochondria, ER and Golgi apparatus: Overexpression of A53T α-syn *in vivo* revealed inhibition of mitochondrial complex I, increased mitochondrial autophagy (mitophagy) and ROS generation (Chinta et al., 2010; Junn and Mouradian, 2002). Other studies have also reported that the A53T point mutation up-regulates mitophagy in primary neurons (Choubey et al., 2011) and overexpression of A53T α-syn in transgenic mice was shown to increase mitochondrial degeneration (Martin et al., 2006). Other than mitochondrial impairments, ER associated stress was observed in a cell culture model of A53T α-syn-induced cell death (Smith et al., 2005). The work of Smith and colleagues reported that the expression of A53T α-synuclein in differentiated PC12 cells caused cell death accompanied by a decrease in

proteasome activity, increased ER stress and intracellular ROS levels, mitochondrial cytochrome C release and elevation of caspase-9 and -3 activities (Smith et al., 2005). The A53T point mutations has also been associated with an increased vulnerability to iron-induced toxicity as evident from the work conducted by Zhu and colleagues where iron treatment caused a more severe motor decline in flies expressing the A53T mutation compared to WT α-syn (Zhu et al., 2016). Furthermore, iron treatment was shown to induce selective dopaminergic neuronal loss in the flies that expressed A53T mutant α-syn, suggesting an increased vulnerability to iron accumulation toxicity in cells expressing mutant α-syn (Zhu et al., 2016).

3.6.2 α-synuclein overexpression

Similarly to α-syn A53T mutation, studies focused on elevated α-syn levels due to SNCA duplication/triplications have primarily focused on the increased aggregation and accumulation of the protein. However, it is important to note that elevated α-syn levels also result in several organelle dysfunction. In multiple cell types, including neurons, α-syn overexpression was shown to promote mitochondrial fission and result in fragmentation of mitochondria. Importantly, the fragmentation involved a direct interaction of α-syn with mitochondrial membranes (Nakamura et al., 2011). Furthermore, α-syn overexpression appears to inhibit complex I (Devi et al., 2008; Nakamura et al., 2008), which is known to contribute to increased mitochondrial ROS production (Hsu et al., 2000; Junn and Mouradian, 2002). Indeed, overexpression of WT or mutant α-syn in SH-SY5Y neuroblastoma cells lead to increased intracellular ROS generation and vulnerability to dopamine-induced cell death (Junn and Mouradian, 2002). Furthermore, transcriptomic analysis conducted on dopaminergic neurons derived from iPSC from PD patients baring SNCA triplication revealed a dysregulation in many mitochondrial genes, a reduction in basal respiration and maximal respiration, changes in mitochondrial morphology, but also increased levels of IRE1α, one of the effectors on the ER stress pathway (Zambon et al., 2019). A separate study also reported that overexpression of α-syn severely delayed ER-Golgi transport in non-neuronal cells by inhibiting ER/Golgi SNARE protein function (Thayanidhi et al., 2010).

3.7 Implications on the role of α-synuclein in ferroptosis

In addition to the already mentioned associations between mutations or overexpression of α-syn and increased intracellular ROS generation, the functions of α-syn with greater relevance to ferroptosis include those modulating the metabolisms of iron (table 2) and lipids (table 3).

3.7.1 α-synuclein and iron metabolism

Over the past two decades, the interactions between α-syn and iron metabolism have been extensively studied and reviewed (e.g. (Duce et al., 2017; Moreau et al., 2018; Chen et al., 2019a)). However, since the emergence of ferroptosis, this relationship should be reassessed and placed in the ferroptosis context. Indeed, both iron deposition and α-syn aggregation are neuropathological hallmarks of PD. As previously described, excessive brain iron accumulation can result in the generation of ROS and subsequent irreversible oxidative damage of lipids, proteins and DNA (Dixon and Stockwell, 2014). Such toxicity is exacerbated in dopaminergic neurons as iron and dopamine are two highly oxidative molecules thus forming a toxic couple reinforcing the prooxidant features of these two molecules (Hare and Double, 2016; Song and Xie, 2018). Of note, iron depositions coexist with α-syn in the core of LB in the remaining dopaminergic neurons of SNpc of PD brains (Castellani et al., 2000), and the SN, cortex and globus pallidus in brains of neurodegeneration with brain iron accumulation (Neumann et al., 2000). This observation suggest a common underlying pathological mechanism leading to iron deposition and formation of α-syn aggregates. This is supported by the fact that both Fe^{2+} and Fe^{3+} strongly bind to α-syn and promote its oligomerization by converting this intrinsically disordered protein into a β-sheet structure (Hashimoto et al., 1999; Ostrerova-Golts et al., 2000; Uversky et al., 2001; Peng et al., 2010). Indeed, iron exposure to neuronal cultures overexpressing α-syn with the familial mutation A53T increases aggregate formation and vulnerability to iron induced toxicity (Ostrerova-Golts et al., 2000). Furthermore, α-syn oligomers interacting with iron in neurons to induce ROS and lipid peroxidation production, reduce GSH levels (Deas et al., 2016), and have subsequently been shown to induce ferroptosis via iron-dependent lipid peroxidation (Angelova et al., 2020). This is particularly poignant with the knowledge that dopaminergic neurons are high in iron and have an intrinsically high oxidative environment due to their dopamine metabolism. Iron chelation has not only been shown to be neuroprotective against PD related neurotoxin insult (i.e MPTP, 6-OHDA and

Paraquat) but can reduced α-syn aggregation *in vitro* and rescue behavioural deficits induced by iron exposure in a mouse model of α-syn aggregation (Carboni et al., 2017).

While iron can modulate the biophysical nature of α-syn, this protein may in turn also have a role in neuronal iron homeostasis. α-Syn contains an iron response element (IRE) within its 5'UTR mRNA region; a binding site involved in regulating the translation of the protein upon modulation of neuronal iron load (Friedlich et al., 2007). As an iron regulated protein, iron depletion causes a decrease in translation of α-syn (Febbraro et al., 2012), whilst overexpression of α-syn in neurons results in higher levels of Fe^{2+} (Ortega et al., 2016).

It is generally accepted that iron promotes the formation of large oligomers of α-syn. However, there is emerging evidence that α-syn in turn plays a role in iron homeostasis. On one hand, it has been suggested that α-syn acts as a ferrireductase reducing Fe^{3+} to Fe^{2+} and increases susceptibility to iron-dependent ROS and LOOH production (Davies et al., 2011). This process, largely dependent on copper as a cofactor and on NADH as an electron donor, was reported in SH-SY5Y neuroblastoma cells where overexpression of α-syn (WT and mutant forms) led to an increase of the proportion of intracellular Fe^{2+} among total iron (Davies et al., 2011). This finding is supported by an *in vivo* study conducted in rats overexpressing human α-syn, where ferrireductase activity is correlated to the expression of α-syn in the SN. However, this was not the case in the SN and striatum of the brains of PD patients, maybe due to the loss of function of aggregated α-syn (McDowall et al., 2017).

More recently, Baksi and colleagues have proposed that α-syn directly mediates iron metabolism by facilitating the uptake of transferrin-bound iron, and colocalizes with TfR1 in the plasma membrane. In retinal epithelial cells, they found that depletion of α-syn results in TfR retention in recycling endosomes and subsequent depletion of cellular iron stores (Baksi et al., 2016), whilst an increase in α-syn seem to affect lysosomal activity by disrupting the trafficking of lysosomal hydrolases thus impairing ferritinophagy (Baksi and Singh, 2017); a process linked to ferroptosis (Hou et al., 2016; Latunde-Dada, 2017; Masaldan et al., 2018).

An alternative mechanism in which α-syn is proposed to modulate cellular iron import is through an ability to upregulate the iron transport protein DMT1. Bi *el al*, showed that α-syn-

induced p38 mitogen-activated protein kinase (MAPK) phosphorylation of parkin, inactivating its E3 ubiquitin ligase activity and reducing DMT1 degradation (Bi et al., 2020).

Implications of α-synuclein in the metabolism of iron		
Feature	**Comment**	**Reference**
Iron promotes α-syn aggregation	Fe2+ and Fe3+ strongly bind to α-syn and promote its oligomerization, and both iron and α-syn co-localize in Lewy Bodies	(Castellani et al., 2000; Hashimoto et al., 1999; Ostrerova-Golts et al., 2000; Peng et al., 2010)
α-syn contains an IRE withing its mRNA	Via an iron response element (IRE), iron depletion causes a decrease in α- syn translation, whilst overexpression of α-syn results in higher levels of Fe2+	(Friedlich et al., 2007; Febbraro et al., 2021; Ortega et al., 2016)
α-syn acts as a ferrireductase	α-syn can reduce Fe3+ to Fe2+, increasing susceptibility to iron-induce ROS	(Davies et al., 2011; McDowall et al., 2017)
α-syn mediates transferrin-bound iron import	α-syn facilitates endocytosis on transferrin-bound iron in retinal epithelial cells	(Baksi et al., 2016)
α-syn regulates ferritinophagy	α-syn overexpression disrupts the trafficking of lysosomal hydrolases and impairs ferritinophagy	(Baksi et al., 2017)
α-syn upregulates DMT1	Via p38-MAPK phosphorylation and inactivation of parkin, α-syn reduces DMT1 degradation	(Bi et al., 2020)

Table 2. Interplay between α-synuclein and the metabolism of iron.

3.7.2 α-synuclein and lipid metabolism

The association of α-syn to membrane and lipids has been widely studied. Of relevance to this PhD project, the evidence linking α-syn with cellular lipid metabolism further implicates α-syn in ferroptosis. First, α-syn has a close association with cellular membrane structures as suggested by the fact that the protein can be isolated from either cytosolic or intracellular membrane fraction (Sharon et al., 2001). Moreover, α-syn has a high degree of sequence homology with apolipoproteins and binds lipids through its N-terminal region. Indeed, the 11-residue repeats located in the N-terminal domain are reminiscent of those in the class A2 apolipoproteins, responsible for carrying lipids, such as membrane phospholipids, by reversibly binding to them (Perrin et al., 2000). Of particularly high binding affinity are the PUFAs α-linolenic acid, DHA and eicosapentaenoic acid (Fecchio et al., 2018; Ugalde et al., 2019), supporting the hypothesis of a role in lipid transport between cytosolic and membranous cellular compartments (Sharon et al., 2001). Interestingly, it seems the PD-associated point mutations A30P and A53T have little or no effect on the ability of α-syn to bind lipids (Perrin et al., 2000; Yu et al., 2005). Furthermore, the interaction between α-syn and PUFAs was shown to affect endocytosis and vesicle recycling

in both neuronal and non-neuronal cells and specifically activate synaptic vesicle recycling after neuronal stimulation by enhancing clathrin-mediated endocytosis (Ben Gedalya et al., 2009). When exposed to free or phospholipid-bound PUFAs, α-syn undergoes structural changes including an increased propensity to oligomerize (Sharon et al., 2001; Broersen et al., 2006; Lücke et al., 2006; De Franceschi et al., 2009), whereas MUFAs have no effect on α-syn aggregation (Fecchio et al., 2018). Lipid peroxidation products from PUFA, such as HNE, can also induce modifications to α-syn and equally promote the formation of toxic oligomers in human neuroblastoma cells (Shamoto-Nagai et al., 2018). Conversely, a role for α-syn in brain lipid metabolism has also been suggested, since fatty acid uptake, incorporation into phospholipids and turnover appear affected in the absence of the protein (Golovko et al., 2005, 2006, 2007). α-syn modulates the metabolism of certain membrane PUFAs including linoleic acid, dihomo-gamma-linoleic acid, AdA and AA, as evident from the fact that both the lipid ratio of these PUFAs in the plasma membrane and the membrane fluidity are increased when α-syn is overexpressed in neuronal cultures as well as in brain tissue from PD and DLB patients (Sharon et al., 2003). In contrast, the cytosolic fatty acid composition is altered and the membrane fluidity reduced in brains of α-syn KO mouse (Golovko et al., 2006). Importantly, Golovko and colleagues reported a reduction in AA-CoA mass and AA incorporation into PLs in the brains of SNCA KO mice, with an opposite effect on DHA incorporation and turnover, suggesting a metabolic compensation for the reduced incorporation of AA (Golovko et al., 2007). Importantly, the reduction in AA-CoA mass and incorporation was due to a reduction in total ACSL activity (Golovko et al., 2006). The ACSL activity was restored upon addition of exogenous α-syn, indicating a role of α-syn in the control of ACSL4 in AA-CoA formation. This is of particular importance to ferroptosis as a modulation in ACSL4 activity by α-syn, thus a remodelling in the plasma membrane PUFAs composition, would directly implicate this protein to a regulatory pathway of ferroptosis. A separate study conducted in mice lacking α-syn reported a 26% reduction in total brain mass of mitochondria-specific phospholipid, cardiolipin, and its acyl side chain showed a 51% increase in saturated fatty acids and a 25% reduction in omega-6 PUFAs (Ellis et al., 2005). These abnormalities in mitochondrial membrane composition were associated with a reduction in complex I/III activity. Finally, another study also suggests that α-syn contributes to membrane remodelling by sensing lipid packing defects and inducing lateral expansion of lipids (Ouberai et al., 2013). These findings strongly indicate that α-syn has a

role in membrane fatty acid compositions, thereby regulating membrane fluidity, vesicle assembly and subsequent synaptic transmission. Indeed, as previously mentioned, α-syn seems to play a crucial role in synaptic vesicle assembly and recycling, a process highly dependent on the plasma membrane composition and in which phospholipase D2 (PLD2) is known to be involved with (Yu et al., 2005). Interestingly, several studies have reported that α-syn interact with PLD2 and inhibits its activity, suggesting another mean by which α-syn may modulate the plasma membrane composition via inhibiting the activity of PLD2 (Jenco et al., 1998; Ahn et al., 2002). Interestingly, two more recent studies conducted in rats showed that the lipase activity of PLD2 was responsible for severe neurodegeneration of dopamine neurons, loss of striatal dopamine and associated motor deficit, all of which were restored upon co-expression of human α-syn (Gorbatyuk et al., 2010; Mendez-Gomez et al., 2018).

Finally, technological advances in transmission electron microscopy in association with light microscopy imaging has enabled a clearer understanding of Lewy Body composition, revealing a high level of membranous content, fragmented organelles and vesicles at the core of α-syn immunoreactivity (Shahmoradian et al., 2019), suggesting that somewhere along the pathological line, a disruption in the role of α-syn in the metabolism of lipids ultimately results in the deposition of membrane fractions and vesicles within α-syn aggregates and LB.

Implications of α-synuclein in the metabolism of lipids		
Feature	**Comment**	**Reference**
α-syn has a high affinity for binding lipids	α-syn has a high degree of sequence homology with apolipoproteins and binds lipids through its N-terminal region	(Sharon el al., 2001; Perrin et al., 2000; Fecchio et al., 2018)
PUFAs or lipid peroxidation byproducts induces α-syn oligomerization	α-syn undergoes structural changes that increase its propensity to oligomerize when exposed to free or phospholipid-bound PUFAs or 4-HNE	(Broersen et al., 2006; Lücke et al., 2006; De Franceschi et al., 2009; Shamoto-Nagai et al., 2018)
α-syn modulates the PUFAs plasma membrane composition	High levels of α-syn increase the proportion of PUFAs in the plasma membrane in neuronal cultures and brains from PD and DLB patients, whilst absence of α-syn reduces PUFAs content in membranes	(Sharon et al., 2003; Golovko et al., 2006)
α-syn regulates the activity of ACSL enzymes	Absense of α-syn reduces the incorporation of arachidonic acid in brain phospholipids due to reduced ACSL activity	(Golovko et al., 2006)
α-syn inhibits phospholipase D2	α-syn interracts wit phospholipase D2 and inhibits its activity	(Jenco et al., 1998; Ahn et al., 2002; Gorbatyuk et al., 2010)

Table 3. Interplay between α-synuclein and the metabolism of lipids

Overall, iron and PUFA dependent studies suggest that α-syn's physiological and/or pathological functions may generate, over time, a pro-ferroptotic environment in dopaminergic neurons. Specifically how α-syn functionally regulates membrane composition remains unclear but Golovko and colleagues have shown *in vivo* that α-syn plays a key role in the metabolism of brain AA (Golovko et al., 2006); the main substrate of ALOX15 and ACSL4, two key enzymes implicated in the ferroptosis pathway. Direct or indirect enrichment of cellular membranes with AA, amongst other PUFAs, by α-syn under the pathological conditions of elevated free labile iron and oxidative stress, may lead to further lipid peroxidation and drive neurons towards ferroptosis. Further research is essential to strengthen this hypothesis and establish whether α-syn's ability to regulate both iron and lipid homeostasis in neurons can be implicated in the ferroptosis pathway.

3.8 Conclusion

One can safely consider α-syn as the most studied protein in synucleinopathy research, such as PD. Today, we have an extensive, hence complex, vision of the putative physiological roles this protein may perform within neurons. These include, but are not limited to, synaptic vesicle assembly, endosomal transport, neurotransmitter release, dopamine synthesis and handling, modulation of iron homeostasis, lipid transport and plasma membrane phospholipid composition. Despite our knowledge on α-syn, it remains unclear how this protein is associated to the pathological features of PD and most specifically its implication in neuronal death. We can imagine that a disruption in α-syn functions may in part result in intracellular free iron accumulation, improper storage of dopamine, thus increased oxidation, elevated PUFAs in the cellular membranes, all of which would facilitate a pro-ferroptotic environment in a subpopulation of neurons known to have an intrinsically high oxidative environment. The recent finding that α-syn oligomers bind the plasma membrane to drive ferroptosis cell death through lipid peroxide generation provide the first direct evidence to support ferroptosis as a pathological mechanism in synucleinopathies (Angelova et al., 2020). We have decided to take this further and assess the potential implication of endogenous α-syn in ferroptosis using two highly relevant human dopaminergic neuronal cell models: Lund human mesencephalic cells (LUMES) and small-molecule derived neuronal precursor cells (smNPC) differentiated into midbrain neurons (mDANs).

Materials and Methods - Chapter 4:

PhD Preface

4.1 Research context and hypothesis

Since the early twentieth century, PD's pathological features were known to include the degeneration of dopamine neurons, alpha synuclein (α-syn) aggregation within Lewy bodies and iron accumulation (Lhermitte et al., 1924) in the SNpc. Today we known that PD is a multifactorial and complex disorder whose aetiology sits in the interplay between epidemiological, genetic and toxicological factors. Several therapeutic strategies have been explored over the past decades and have led to the generation of drugs efficient at treating the motor symptoms of the disease but lack any neuroprotective potential. What is important to understand is that the many pathological features today identified in *in vitro* and *in vivo* models of PD ultimately result in the death of dopaminergic neurons. It is therefore essential to fully understand and characterise the regulation of cell death and how a deregulation may lead to the excessive neuronal death observed in PD in order to generate efficient neuroprotective or disease-modifying therapies. For many years, the pathological process involved in PD related neuronal death was considered to be apoptosis. This was mainly due to the fact that until recently, only a few types of programmed cell death were known, and these were identified predominantly by using oncogenic cell lines (i.e. neuroblastoma). Since then, multiple regulated cell death mechanisms have been identified and studied and implicated in PD pathogenesis (reviewed in (Guiney et al., 2017)), including anoikis (Li et al., 1999; Saha et al., 2000), autophagy (Chu et al., 2009; Dehay et al., 2010), necroptosis (Mogi et al., 1994; Wu et al., 2015), parthanatos (Mandir et al., 1999; Outeiro et al., 2007) and pyroptosis (Koprich et al., 2008).

More recently, ferroptosis has been established as a regulated necrosis that is morphologically and mechanistically distinct from apoptosis and other known cell death pathways (Dixon et al., 2012). Ferroptosis is characterised by iron dependent lipid peroxidation (Stockwell et al., 2017). Interestingly, several PD pathological hallmarks are known key features and/or triggers in the ferroptotic cell death pathway. These include iron overload (Ayton et al., 2015; Dexter et al., 1987, 1989a; Hirsch et al., 1991; Pyatigorskaya et al., 2015), elevated lipid peroxidation (Dexter et al., 1986, 1989b; de Farias et al., 2016), reduced GSH levels (Li et al., 1997; Pearce et al., 1997; Sian et al., 1994; Sofic et al., 1992),

XcT downregulation (Vallerga et al., 2020), DJ-1 depletion (Bonifati et al., 2003; Cao et al., 2020) and CoQ10 reduction (Battino et al., 1996; Mischley et al., 2012; Bersuker et al., 2019; Doll et al., 2019). Together, these well-established diseases features strongly implicate this regulated cell death pathway in the neurodegeneration observed in PD. To this extent, our laboratory was the first to show that ferroptosis is a prevalent cell death pathway in several oxidative stress *in vitro* and *in vivo* models of Parkinsonism (Do Van et al., 2016). The discovery of ferroptosis therefore opens a new therapeutic avenue that can be targeted in the hopes of slowing the disease progression.

In addition to being a major component of Lewy body pathology, α-syn is implicated in PD causality by genome wide association studies of sporadic PD and autosomal dominantly inherited mutations and duplication/triplication in the *SNCA* gene that lead to various clinical phenotypes ranging from typical late-onset to rapid progressive early-onset familial PD (Blauwendraat et al., 2019; Zhang et al., 2018a). Despite the genetic support for the involvement of α-syn in PD pathology, the exact neuropathological mechanisms linking this protein to the death of dopaminergic neurons remain unclear. Interestingly, α-syn has been functionally linked with the metabolism of both iron and lipids, suggesting a possible interplay between dysregulated α-syn and other PD pathological hallmarks related to ferroptosis. We raise the hypothesis that ferroptosis could be the missing part in the relationship between synucleinopathy, iron accumulation, oxidative stress and related cell death in PD. Establishing the implication of ferroptosis in neurodegenerative diseases such as AD, Amyotrophic lateral sclerosis (ALS) and PD, will lead to interest in generating a range of anti-ferroptosis based therapies that could delay onset of disease and slow the progression.

4.2 Thesis Objectives

The aims of this PhD project are to:

- Optimise the CRISPR/Cas9 genome editing technique in LUHMES cells in order to generate *in vitro* synucleinopathy models.
- **Investigate whether α-synuclein is implicated in the ferroptosis pathway in dopaminergic neurons.**
- Characterise the role of α-synuclein in ferroptosis via the interplay between α-syn and the metabolisms lipids.

4.3 Materials and methods

4.3.1 Cell culture

4.3.1.a LUHMES cells

LUHMES cells are neuronal precursor cells, conditionally-immortalized which can be differentiated in 5 days into post-mitotic dopaminergic neurons by shutting-down the v-*myc* transgene. For LUHMES cell culture, Nunclon plastic cell culture flasks and well-plates were pre-coated with 50µg/ml of poly-L-ornithine a 1µg/ml fibronectin. Cells were grown at 37ºC in a humidified 95% air, 5% CO2 atmosphere. Proliferating cells are maintained in advanced DMEM/F12 media supplemented with N2, 2mM L-glutamine and 40ng/ml recombinant basic fibroblast growth factor. For standard differentiation, $2x10^6$ cells were seeded in a T75 flask for 2 days and the proliferative media was replaced by differentiation media (d0) (advanced DMEM/F12, 1x N2 supplement, 2mM L-glutamine, 1mM dibutyryl cAMP, 1µg/ml tetracycline and 2ng/ml recombinant human GDNF). After 2 days of pre-differentiation (d2), cells were harvested with trypsine, centrifuged for 5 minutes at 300g, counted and seeded in appropriate supports in differentiation media. Cells were left to fully differentiate for 3 more days (d5) (Figure 18).

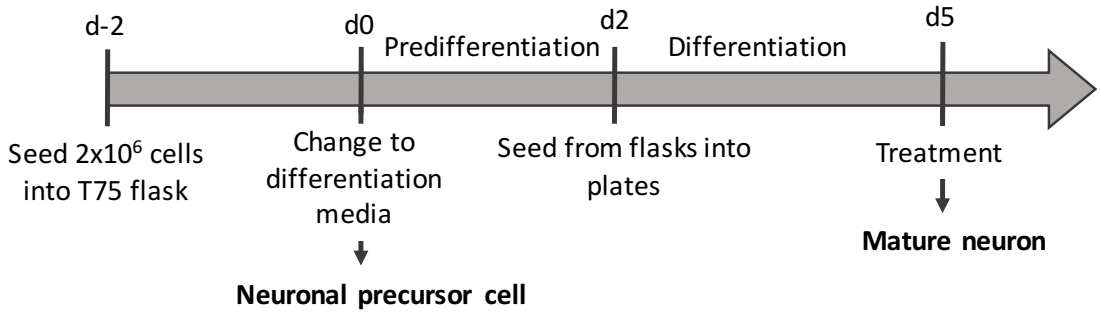

Figure 18. LUHMES maintenance and differentiation timeline.

4.3.1.b Small-molecule derived neuronal precursor cells (smNPC) derived midbrain neurons

Small molecule derived neuronal precursor cells (smNPC) were differentiated from iPSC as described in *(Reinhardt et al., 2013)*. smNPC were culture on Matrigel-coated culture plates and smNPC expansion medium consisted of N2B27 supplemented with CHIR,

PMA and ascorbic acid (AscA), with a medium change every other day. For splitting, cells were digested into single cells with a 15 minutes incubation at 37ºC with prewarmed accutase (PAA). Cells were diluted and collected with DMEM and centrifuged at 200g for 5 mins. The cells pellet was resuspended in fresh smNPC expansion medium and plated on Matrigel-coated culture plates.

For generation of midbrain dopaminergic neurons, smNPC expansion medium was changed to N2B27 with 100ng/ml FGF8, 1µM PMA and 200µM AscA. After 8 days, media was changed to maturation medium: N2B27 with 10ng/ml BDNF, 10ng/ml GDNF, 1ng/ml TGF-b3, 200µM AA and 500µM cAMP. Neuronal maturation and differentiation of smNPC was performed for at least 28 days to generate midbrain-specific dopaminergic neurons.

4.3.1.c smNPC characterization – FACS staining

To determine the efficiency of differentiation into midbrain neurons, cells at day 31 and above were disaggregated and fixed with 4% PFA in suspension. Following permeabilization with saponin and blocking with BSA, cells were intracellularly stained with antibodies against neuronal marker Tuj1 or Map2 and dopaminergic marker TH. Staining was then analysed using a Fortessa X20 FACS in order to determine the % of TH positive neurons relative to the appropriate isotype control.

4.3.2 CRISPR/Cas9 genome editing

The experimental procedure for generating CRISPR/Cas 9 clones on Luhmes cells was adapted from on *Shah et al, 2016*, with some minor alterations., in order to generate stable CRISPR clones which can continue to be differentiated into dopaminergic neurons for experimentations (Figure 19). Chapter 5 will provided a more detailed description of the optimisation process of CRISPR/Cas9 transfection in LUHMES cells.

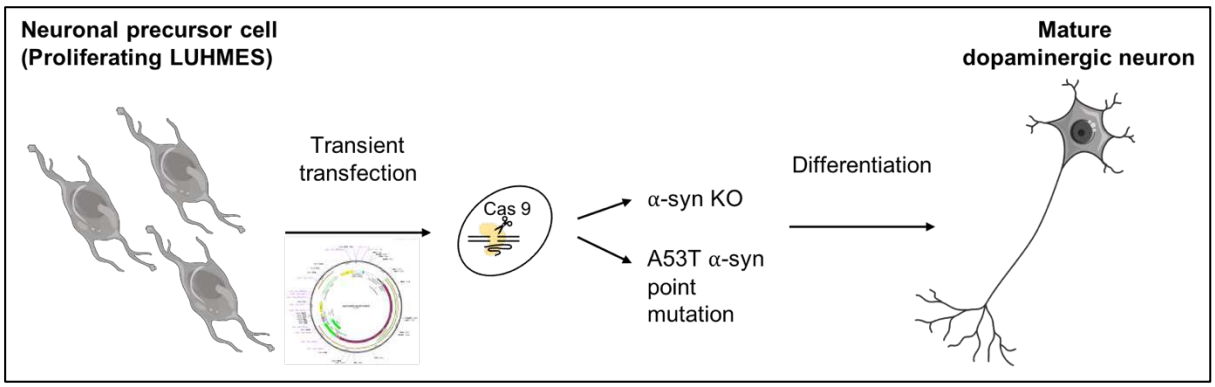

Figure 19. Outline of CRISPR/Cas9 genome editing protocol for stable cell line generation.

4.3.2.a Plasmid and cloning

The CRISPR plasmid px458 was purchased from Addgene and originated from the Zhang lab. The crispor.tefor.net online web tool was used for sgRNA design (Table1) and the 100 base pair long A53T ssODN was ordered from TibMolBio (CTAgATACTTTAAATATCATCTTTggATATAAgCACAATgAAgCTTACCTgTTgTCA CACCATgCACCACTCCCTCCTTggTTTTggAgCCTACAAAAAC). sgRNA ligation with the plasmid was performed overnight and the following day OneShot *E.Coli* bacteria were transformed with the appropriate plasmids. Bacteria were then spread on separate labelled LB agar plates with ampycilin (50µg/ml) and colonies were left to grow overnight at 37ºC. The following day, 25 individual colonies were picked and PCR analyses were conducted using primers spanning the px458 plasmid and the sgRNA fragments. After an initial validation, the remaining bacteria were put back in culture and allowed to grow overnight before extracting the plasmid (according to manufactures protocol), dosing and sequencing for final validation.

sgRNA name	Experiment	Sequence (5'→ 3')
A53Tguide41up	Insertion of A53T point mutation	CACCgTggTgCATggTgTggCAAC
A53Tguide41rev		AAACgTTgCCACACCATgCACCAC
Guide5G1s	α-syn KO by deleting exon 2	CACCgTgAATTCCTTTACACCACAC
Guide5G1as		AAACgTgTggTgTAAAggAATTCAC
Guide3G1s		CACCgCCATggATgTATTCATgAA
Guide3G1as		AAACTTCATgAATACATCCATggC
GuideA5G4s		CACCgTggTgCTTgTTCATgAgTgA
GuideA5G4as		AAACTCACTCATgAACAAgCACCAC
Guide3G4s		CACCgATAATCAATACTCTAAATgC
Guide3G4as		AAACgCATTTAgAgTATTgATTATC

Table 4. sgRNA and their sequences used to generate CRISPR/Cas9 LUHMES sub-clones.

4.3.2.b Transfection method

LUHMES cells were transfected by nucleofection (Lonza) using the Amaxa P3 Primary cell kit (V4XP-3024)) and the 4D Nucleofector device, or the Basic nucleofector kit for primary neurons (VPI-1003) and the Nucleofector II device. Luhmes cells were dissociated with trypsine, centrifuged at 300g for 5 minutes and resuspended in PBS for cell counting. Aliquots of $2x10^6$ cells were pipetted into 15ml falcons and these were centrifuged for 10 minutes at 100g. PBS was removed and cells were resuspended with 82µl of transfection

solution and 18µl of Supplement 1. 3ug of either the GFP positive control or px458+sgRNA plasmid were added to the cell suspension. 10µl of 10µM ssODN was added before transferring cells into a cuvette. Electoporation was conducted with the EM-110 program when using the Nucleofector 4D device and the X-01 program when using the Nucleofector II device. Cells were immediately transferred into 15ml falcons containing pre-warmed proliferation media before seeding into 6 well plates at a density of $1x10^6$ cells per well. Media was changed after a minimum of 6 hours.

4.3.2.c FACS sorting

Efficiently transfected LUHMES cells will express GFP allowing for FACS sorting. 24 hours after the nucleofection, the media from the 6 well plate was collected and filtered using a 0,22µm filter. 50µl of this "conditioned" media was added into the middle 60 wells of a coated 96 well plate, and topped to 100µl with "fresh" proliferation media. Transfected cells were harvested, centrifuged for 5 mins at 300g and resuspended with 1ml PBS. As a negative control, the autofluorescence was determined in non-nucleofected Luhmes cells, and the GFP positive cells were determined with the cells transfected with the GFP control plasmid provided with the kit. CRISPR/Cas 9 transfected cells were then sorted with a FACS Aria machine according to theit GFP expression, one single cell per well. Cells were left to grow at 37ºC and at day 6 post-sorting 100ul of proliferation media was added to 96 well-plate.

4.3.2.d Clones amplification and selection

Approximately 9 days post nucleofection, single cell colonies grown in 96 well plates were transferred into 24 and 6-well plate. As cells continue to proliferate, they are moved to T25 and T75 flask and are left to proliferate until they are confluent enough to freeze several 5 million-cell vials. Genomic DNA is isolated from each surviving clone and sequenced.

4.3.2.e CRISPR/Cas9-mediated SNCA KO in smNPC

Control smNPC line C4 - WT was previously described and characterised in (Boussaad et al., 2020). C4 - SNCA KO iPSC were generated as described in (Barbuti et al., 2020a). The Cas9 plasmid pX330 (Addgene, 42230) containing a sgRNA targeting the human *SNCA* sequence gctgctgagaaaaccaaaca was transfected into C4 -WT cells. Briefly, iPSCs were dissociated to single cells using PAA and plated in iPS media as described in (Barbuti et al., 2020b; Boussaad et al., 2020), plus Rho-Kinase Inhibitor Y-27632 (10µM, Abcam

ab120129). 1 x 10^6 cells were then electroporated using the 2D-Amaxa nucleofector unit (Lonza, Basel, Switzerland) with program B16. After electroporation, 1mL of E8 was added to the cuvette before being placed at 37ºC for 10 minutes. Cells were then plated into 6-well plates and cell selection was achieved using antibiotic resistance to puromycin when small to medium-sized colonies began to appear.

4.3.3 Cell viability assay

Briefly, a stock solution was prepared at a concentration of 10mg/ml by dissolving resazurin dye (7-hydroxy-3H-phenoxazin-3-one 10-oxide) in dH_2O. Approximately $4x10^4$ LUHMES or mDANs were plated on coated 96-well plates in appropriate medium. Cytotoxicity was assayed 24 or 48h post treatment by adding resazurin solution (10% of cell culture volume per well – final concentration 100µg/ml) and cells were left to incubate for 2h at 37ºC. Samples were analysed fluorometrically on a microplate reader (Mithras LB950 or BioTek citation 5 imaging reader, Ex= 540nM, Em= 600nM). Background signals obtained from cell-free wells were subtracted from each sample. Cell viability under treatment conditions were reported as a percentage relative to untreated control cells.

4.3.4 Lipid peroxidation analysis

LUHMES cells were seeded at day 2 of differentiation in 24 well-plates at a density of 300 000 cells per well and left to complete the differentiation until day 5. Following ferroptosis induction (6h, 20-30nM RSL3, or 24h, 20µM Arachidonic acid + 20µM $FeCl_3$:NTA), cells were collected with the addition of 200µl trypsin and 800µl PBS, centrifuged for 5 minutes at 300g and resuspended in 200µl PBS containing the LIVE/DEAD (Thermo Fisher - L23105) probe for cell viability measurements. Following a 15 minutes incubation at 37ºC, an additional 200µl of PBS containing C11-BODIPY (Thermo Fisher - D3861) probe was added to the cells at a final concentration of 1µM. Cells were incubated for another 15 minutes at 37ºC and analysed using the FORTESSA X20 flow cytometer (BD Biosciences). Data were collected from at least 10 000 cells and C11-BODIPY staining was analysed from the living single cell population (Figure 20). Data was analysed using the Kaluza software (figure 20).

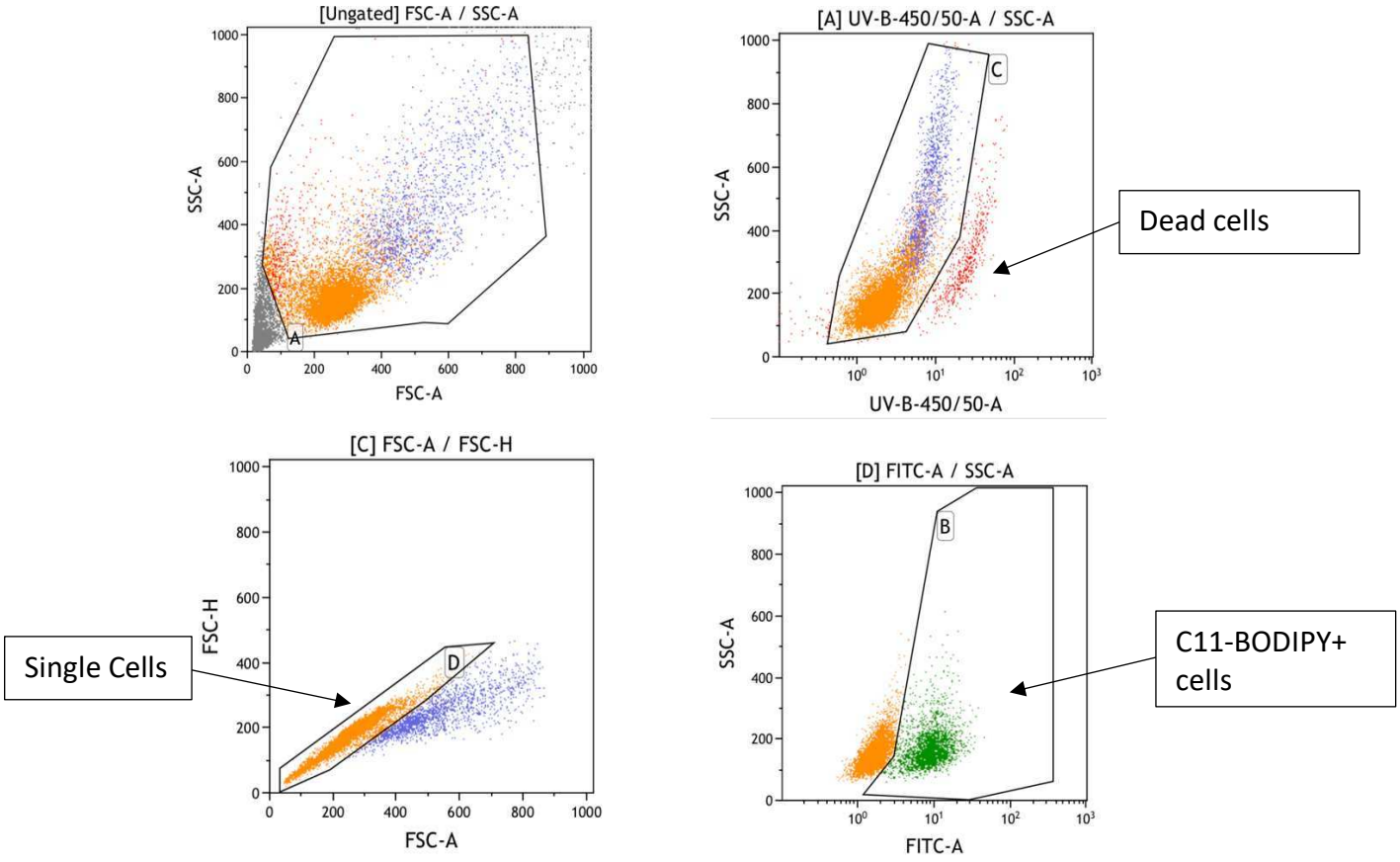

Figure 20. Example of lipid peroxidation analysis using the software Kaluza. Following an initial gating to select the live cells, single cells are gated and the percentage of C11-BODIPY+ cells measured.

For smNPC derived midbrain neurons, lipid peroxidation measurements were conducted as described above with some minor alterations: Following treatment, cells were collected with prewarmed accutase and centrifuged at 500g for 5 minutes. Cells were resuspended in 300µl of PBS containing 2µM C11-BODIPY and incubated for 20 minutes at 37ºC. For staining of viable cells, 17µg/ml DAPI was added to the cells immediately before measurement.

4.3.5 siRNA-mediated knock-down of α-syn and ACSL4

siRNA transfection was performed by preparing solution A - RNAiMAX lipofectamine (ThermoFisher Scientific, 10601435) and OptiMEM (ThermoFisher Scientific, 10149832), and solution B consisting of siRNA (10µM) and OptiMEM. The siRNA control-A (sc-37007), control-B (sc-44230), α-syn (sc-29619) and ACSL4 (sc-60619) were purchased from SantaCruz Biotechnology. After 5 minutes of incubation, both solutions were combined

vol:vol and transferred to wells before seeding day 2 pre-differentiated LUHMES cells. Cells were left to fully differentiate for an additional 3 days before treatments. siRNA-mediated KD efficiency was measured by PCR and western blot 72h post transfection.
For smNPC derived midbrain, the media was removed from seeded cells in 24-well plates and replaced by 400µl maturation media per well. The siRNA mix was prepared as follow: for 1 well, 1,5µl RNAiMAX lipofectamine was carefully mixed with 50µl OptiMEM and separately, 1,5µl of the control or α-syn siRNA were mixed with 50µl OptiMEM. The two solutions were left to incubate at room temperature for 5 minutes before carefully mixing vol:vol. The transfection solution was left to incubate at room temperature for an additional 15 minutes before adding 100µl per well. 6h later, 500µl of maturation was added to each well and cells were left for 72h before conducting any experimentation or extracting the RNA.

4.3.6 Western blot

Cells were lysed in RIPA buffer containing 1% phosphatase and protease inhibitors for 15mins at 4ºC. Cells were fully lysed by sonicating for 15 seconds with 1 second impulses every 0,5s with an amplitude of 20%. Cell debris was removed by centrifugation at 1000g for 10 minutes, 4ºC and protein concentration was determined using a BCA protein assay kit. For western blot analysis, samples were denaturated by heating at 90ºC for 10 minutes in standard loading dye for SDS-Page and loaded on 4-20% SDS gels. Proteins were transferred onto polyvinylidene difluoride (PVDF) or nitrocellulose membranes. For optimal α-syn detection, blots were then fixed with 4%PFA for 30 mins at room temperature before blocking with either 5%BSA TBS-Tween 20 0.1% or 5% NFDM TBS-T 0.05% (non-fat dry milk) for 1 hour at room temperature. The blots were incubated with the indicated primary antibodies diluted in either 5% BSA TBS-T or 5% NFDM TBT-T 0.05%, according to manufacturer's instructions, overnight at 4ºC. The following day, primary antibodies were washed 3x 5mins with TBS-T 0.1% and 3x 5mins with TBS. Membranes were incubated with species-specific secondary antibodies conjugated to horseradish peroxidase which was detected by enhanced chemiluminescence with Amersham ECL detection reagents. Chemiluminescence signals were visualised with Fujifilm LAS (4000), and quantification of the signals was done using ImageJ and protein quantification was normalized to β-actin signals and expressed as ratio.

4.3.7 Quantitative reverse transcription PCR

Total RNA was extracted from differentiated cells in either 6 well-plates or 24 well-plates using the QIAGEN RNAeasy extraction kit according to manufacturer's instructions. Total RNA was dosed with BioSpec-nanodrop and a DNase step was performed on 2µg of total RNA before reverse transcription with Superscript II reverse Transcriptase (ThermoFisher Scientific, 18064022) using random primers (ThermoFisher Scientific, 48190011) in a 40µl reaction. PCR amplification of the cDNA was quantified using the LightCycler FastStart DNA Master SYBR Green I (Roche, 3003230). The housekeeping gene control was TBP. Primers were designed using NCBI primer design and purchased from TibMolBio. Threshold cycles were determined for each gene and expression levels were calculated relative to TBP.

4.3.8 Lipid extraction

Lipids were extracted from cells according to the method of *Folch et al, 1957* (Folch et al., 1957). Briefly, 3 million cells were homogenized with 2mL of NaCl solution in water (0.73%). Lipids were extracted with 10 ml of $CHCl_3$/CH_3OH (2:1, v/v), and vortexed for 1 minute. Mixture was centrifuged at 3000 rpm for 3 minutes. The upper phase was discarded and the lower phase collected through a protein interface using a Pasteur pipette. After evaporation, the lipid extract (lower phase) was re-dissolved in 200μL of $CHCl_3$/CH_3OH (2:1, v/v) and stored, under nitrogen, at -20°C until further analyses.

4.3.9 Analysis of phospholipid molecular species

In the 200µl lipid extract, 10µl of internal standards mixture containing 320µg/ml PC(14:0/14:0) and 160µg/ml PE(14:0/14:0) were added. The process of identification and quantification of phospholipids species was performed on a Thermo UltiMate™ 3000 coupled to an Orbitrap Fusion™ Tribrid Mass Spectrometer equipped with an EASY-MAX NG™ Ion Source (H-ESI) (Thermo Scientific). Separation of phospholipid classes was achieved under HILIC conditions using Kinetex Hilic 100 x 2.1 mm, 1.7μm column (Phenomenex), with a flow of 0.500 $mL.min^{-1}$. The mobile phase consisted of (A) CH_3CN/H_2O (96/4, v/v) containing 10 mM ammonium acetate and (B) CH_3CN/H_2O (50/50, v/v) containing 10 mM ammonium acetate. The injection volume was 10 μL and the column was maintained at 50°C. PL species were detected by high resolution mass spectrometry (HRMS) analysis, and H-ESI source parameters were optimized and set as follows: ion

transfer tube temperature of 285°C, vaporizer temperature of 370°C, sheath gas flow rate of 35 au, sweep gas of 1 au and auxiliary gas flow rate of 25 au. Positive and negative ions were monitored alternatively by switching polarity approach with a static spray voltage at 3500V and 2800V in positive and negative respectively. Mass spectra in full scan mode were obtained using the Orbitrap mass analyzer with the normal mass range and a target resolution of 240,000 (FWHM at m/z 200), on a mass range to charge ratio m/z form 200-1600 using a Quadrupole isolation on a normal mass range. All MS data were recorded using a max injection time of 100 ms, automated gain AGC target (%) at 112.5, RF lens (%) at 50 and one microscan. An Intensity Threshold filter of 1.10^3 counts was applied. For MS/MS analyses, data-dependent mode was used for the characterization of PL species. Precursor isolation was performed in the Quadrupole analyzer with an isolation width of m/z 1.6. Higher-energy Collisional Dissociation was employed for the fragmentation of PL species with optimized stepped collision energy of 27%. The linear ion trap was used to acquire spectra for fragment ions in data-dependent mode. The AGC target was set to 2.10^4 with a max injection time of 50 ms. All MS and MS/MS data were acquired in the profile mode.
The Orbitrap Fusion was controlled by Xcalibur™ 4.1 software. Data of high accuracy and the information collected from fragmentation spectra, with the help of the LipidSearch™ software (Thermo) and the LIPID MAPS® database (https://www.lipidmaps.org/) were used for PL species identification.

The index of peroxidability for PC and PE (PI = (% monoenoic FA × 0.025) + (% dienoic FA × 1) + (% trienoic FA × 2) + (% tetraenoic FA × 4) + (% pentaenoic FA×6) + (% hexaenoic FA × 8)) was calculated according to (Naudí et al., 2017).

4.3.10 Organotypic brain slice cultures

Organotypic brain slice (OBS) cultures were prepared based on a modified protocol by (Gogolla et al., 2006). Briefly, C57Bl6 mice pups (day 8-10) were decapitated and skulls opened along the commissural lines. Brains were separated with a sagittal cut along the brain midline to obtain two separate hemispheres. The resulting brain hemispheres were placed in ice-cold artificial CSF (GBSSK) composed by Gey's Balanced Salt Solution (GBBS, Sigma G9779) supplemented with 33.3mM glucose 45% (Sigma, G8769) and 100mM Kynurenic acid (Sigma, K3375). The brain hemispheres were set in GBSSK containing 2% low-melting-point agarose in order to obtain a solid block which was glued onto the chuck of an ice-cooled vibratome (figure 21). 350µm sagittal slices were cut using

the vibratome Leica VT1200 with low frequency (1.9mm) and speed (0.12mm/s). The slices were collected and transferred into 6-well plates containing ice-cold GBSSK. Slices were then placed on interface-style Millicell® culture inserts, 30 mm, hydrophilic PTFE, 0.4μM (Millipore PICMORG50) in 6 well plates containing 1,1 mL of sterile slice culture medium (25% (v/v) Basal medium eagle (BME) (Ozyme, BE12-105F), 25% (v/v) 2X MEM Eagle EBSS (Ozyme, BE12-668F), 25% (v/v) Heat inactivated Horse serum (ThermoFisher 26050070), 1% (v/v) GlutaMAX (ThermoFisher, 35050061), 1% (v/v) penicillin/streptomycin (ThermoFisher, 15140-122) and 1,375% (v/v) Glucose 45% wt/vol in sterile H2O, adjusted to pH 7,4 and sterile filtered (0.2 μm)). Brain slices were incubated at 37°C, 5% CO2, and the slice culture medium was changed every 2-3 days.

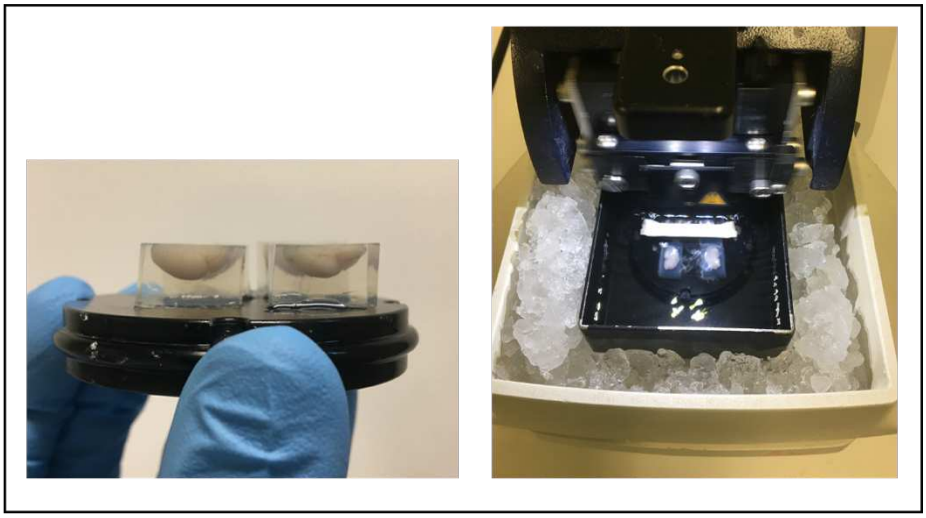

Figure 21: Mice brain hemispheres inclusion in 2% agarose GBSSK and vibratome set-up.

4.3.10.a siRNA-mediated knock-down of α-syn and ACSL4 in OBS

OBSs dedicated for siRNA-mediated KD were prepared and cultured as previously described. Accell siRNA mediated KD protocol was adapted from (Ruigrok et al., 2018). At day 3 of OBS culture, the media was replaced by siRNA culture media which consisted of the previously described media with the exception that it contained 1% (v/v) heat inactivated horse serum and 2% (v/v) B-27 supplement. 1μM of either non-targeting control (Horizon discovery, D-001910), α-syn (Horizon discovery, E-042790) or ACSL4 siRNA (Horizon discovery, E-‘65318) was added to the wells containing the siRNA culture media and slices were returned to the incubator and left for 96h before protein extraction and Western blot analysis

4.3.10.b TH DAB immunohistochemistry staining of OBSs

Slices dedicated for TH DAB immunohistochemistry staining were fixed right after brain slicing for 40 mins with 4% PFA at room temperature followed by 3 washes with PBS. Slices were then transferred into 24-well plates and permeabilized with PBS, 0,1% Triton, 3% H_2O_2 for 20 mins at room temperature followed by blocking in normal goat serum (NGS) diluted 1:10 in 4% BSA, 1% Triton, PBS for 4 hours at room temperature and low agitation. After 3x 5 mins washes with PBS, slices were incubated with primary rabbit antibody anti- mouse TH (abcam, ab152) diluted 1:250 in 5% NGS, 4% BSA, 1% Triton, PBS over night at 4ºC. The following day, primary antibody was washed with 3x 5 mins PBS and slices were incubated with secondary antibody anti-IgG anti rabbit diluted 1:500 in PBS 4% BSA, 1% Triton for 2 hours at room temperature under low agitation- Finally, slices were incubates with VECTASTAIN® Elite ABC-HRP Kit, Peroxidase (Eurobio, PK-6100) for 1 hour. Following 3x 5mins PBS washes, TH staining was performed by addition of 3,3'-Diaminobenzidine (DAB) chromogen diluted 1:50 in PBS, 0.03% H_2O_2 for 30-40 secs. Slices were dehydrated through graded ethanol solutions, cleared in xylene, mounted in DPX (DBH Laboratory Supplies, Poole, UK), and covered with a coverslip for microscopy. Images were acquired using a Zeiss Axio Scan Z.1 slide scanner (20× objective) and Zen software, Blue edition (Zeiss, Oberkochen, Germany).

4.3.10.c TH immunofluorescent staining of OBSs

Slices were fixed, permeabilized, blocked and stained with the primary antibody against TH as previously described. In order to obtain immunofluorescent staining, the slices were incubated with a secondary antibody anti-rabbit Alexa 488 diluted 1:500 in PBS, 1% Triton, 4% BSA 5% NGA for 2h at room temperature. Following 3x 5mins washes with PBS, slices were mounted with HardSet Vectashield onto slides and covered with coverslip. Images were acquired with a Zeiss confocal spinning disk.

4.3.11 Statistical analysis

All statistical analyses were performed using the Prism 9 GraphPad Software. The number of biological replicates for each experiment is indicated in the figure legends. Unless otherwise stated, differences between means were determined using the parametric two-tailed Student's *t*-tests and following data normality verification, and were considered significant at $p < 0.05$.

Results - Chapter 5:

First steps towards investigating the implication of α-synuclein in ferroptosis
§
CRISPR/Cas9-mediated genome editing in LUHMES cells

5.1. Introduction

The technological advances that allow for the introduction of targeted mutations into the genome has dramatically changed the way in which diseases can be modelled and studied. The most recent development in the genome editing field is the clustered regularly interspaced short palindromic repeats (CRISPR) and CRISPR associated 9 (Cas9) system, which has proven to be successful in part due to its ease of use and efficient implementation in a variety of cell lines (Cong et al., 2013; Jinek et al., 2013; Chen et al., 2019b) and model organisms (Friedland et al., 2013; Gratz et al., 2013; Platt et al., 2014; Zhao et al., 2020).

For the study of neurodegenerative diseases *in vitro,* until quite recently, the choice of available cells lines was govern by inducible pluripotent stem cell (iPSC)-derived neurons, and SH-SY5Y cells. Despite both the physiological and pathological relevance of using iPSCs and the optimisation in neuronal differentiation protocols, iPSCs remain a complex, time-consuming and costly culture with some limitations such as genetic variability of clonal iPS cell lines when they are derived, and the robustness and consistency of the epigenome in iPSCs after reprogramming (Kim et al., 2010; Ohi et al., 2011). On the other hand, SH-SY5Y cells are neuroblastoma cells with multiple chromosomal duplications and deletions (Krishna et al., 2014), and of relevance to this PhD project, they lack sensitivity to ferroptotic cell death.

The LUHMES neuronal progenitor cell line is a recent alternative that has been reported as a highly relevant and useful cell line in the neuroscience research field, more specifically, PD research (Lotharius et al., 2002). These human "pre-neuronal" cells originating from mesencephalic cells are kept in a proliferative state by expression of the retroviral element *v-myc* (Hoshimaru et al., 1996). In this system, a tetracycline-controlled transactivator strongly activate transcription from a minimal CMV promotor, which, in turn, drives *v-myc* expression in the absence of tetracycline. The administration of tetracycline into the cell culture media result in a rapid and robust differentiation into a homogeneous

population of post-mitotic, electrically active, mature dopaminergic neurons (Lotharius et al., 2002).

Over the past years, LUHMES cells have been cultured in our laboratory to study the implication of ferroptosis in PD (Do Van et al., 2016). In order to tackle the main objective of this PhD and study the potential implication of α-syn in the ferroptosis pathway, we first needed to generate the appropriate models. To this extent, we decided to modulate endogenous α-syn in LUHMES cells via CRISPR/Cas9 and introduce the PD-linked A53T point mutation. This techniques first needed to be implemented in our laboratory and optimised for LUHMES cells, known to be considerably difficult cells to transfect (Schildknecht et al., 2013; Shah et al., 2016). Indeed, only two articles currently report CRISPR/Cas 9 genome editing in LUHMES cells (Shah et al., 2016; Lalli et al., 2020). For the implementation of CRISPR/Cas9 in this study, we based the protocol on the work previously described by Shah and colleagues (Shah et al., 2016).

This chapter will first describe the optimisation process of the CRISPR/Cas9-mediated genome editing protocol which led to the generation of homozygous A53T α-syn mutant and 140aa α-syn isoform KO subclones, followed by the characterisation of the single-cell clones obtained. Ferroptosis sensitivity will then be studied in these cell lines and provide the first evidence for the implication of endogenous α-syn in this novel cell death pathway.

5.2 Transfection of proliferating LUHMES cells by nucleofection

In order to study the potential implication of α-syn in ferroptosis, we sought to generate stable LUHMES clones by editing the genome in proliferating non-differentiated LUHMES cells in two ways: *i*. by introducing the familiar-PD α-syn point mutation A53T, and *ii*. by disrupting the target gene to generate α-syn KO cell lines. Based on the encouraging nucleofection efficiency reported by (Shah et al., 2016), we decided to start by transfecting LUHMES cells by nucleofection in our laboratory. In order to find the optimal nucleofection condition in our hands, we compared two different nucleofection kits and two nucleofector devices. On one hand, we tested the Basic nucleofector kit for primary neurons (VPI-1003) in the Nucleofector II device, and in parallel, the P3-Amaxa Nucleofector Kit for primary cells (V4XP-3024) was used with the more recent 4D-Nucleofector system. Of note, this first optimization step was conducted with the GFP control plasmid provided in both kits, and different plasmid concentrations (3 or 5 μg) and nucleofection programs (D33, X-01 and EM-110) were compared. Following nucleofection, LUHMES cells were collected and

analysed via FACS in order to measure specific outcomes. These included viability, efficiency of transfection represented by the percentage of GFP positive cells, and fluorescence intensity. Finally, these measures were taken either 24 or 48h post nucleofection in order to find the optimal timepoint in which to detect the efficiently transfected cells (Table x).

First, regarding the viability, we noticed a significant different between cells analysed 24h vs 48h post nucleofection, with higher viability when measured at 48h. This is likely due to the fact that the cells had an extra 24h to adhere to the wells and proliferate. Moreover, transfecting LUHMES cells with 5μg of plasmid instead of 3μg led to reduced viability with the D-33 program but not the others; and among the three different nucleofection programs tested, X-01 reported the lowest viability at 24h post nucleofection whilst the EM-110 program led to the highest viability measure.

	Nucleofector II												Nucleofector 4D					
Program	D-33						X-01						EM-110					
Plasmid [c]	3μg			5μg			3μg			5μg			3μg			5μg		
Measure	% viable	% GFP	Intensity	% viable	% GFP	Intensity	% viable	% GFP	Intensity	% viable	% GFP	Intensity	% viable	% GFP	Intensity	% viable	% GFP	Intensity
24h	24	12,4	1,8	8	16,4	2,3	18	15,9	2,1	18	17,7	2	30	12,4	2,6	33	12,9	2,6
48h	34	0,4	3	15	0,6	3,1	70	0,8	2,5	45	0,6	2,5	61	0,9	2,4	70	0,7	2,3

Table 5. Summary of nucleofection optimisation in LUHMES cells. In order to determine to optimal nucleofection protocol for LUHMES cells, several plasmid concentration, nucleofection protocols, nucleofector devices and time points were assessed. The outcomes measured included viability, GFP expression and fluorescence intensity.

In terms of transfection efficiency, we noticed a difference of % GFP cells between 24h or 48h post nucleofection. Indeed, there was a significant reduction of GFP positive cells when analysed at 48h, instead of 24h post nucleofection. In fact, the percentage of GFP positive cells at 48h post nucleofection was equivalent to that of non-transfected cells. This is likely due to the fact that cells are only transiently transfected, meaning the GFP transgene is not integrated into the cell's genome, and as cells proliferate during those extra 24h, the GFP expression is lost. Furthermore, when cells were transfected with 3μg instead of 5μg, we reported a slight decrease in % GFP cells when analysed at 24h. Regarding the different programs tested, we reported highest GFP positive cells when using the X-01 program

followed by D-33 and EM-110 equally. Finally, there was a slight increase in fluorescent intensity in cells transfected with the Nucleofector II and analysed 48h post nucleofection compared to 24h, although this increase was not found in cells transfected with the 4D device. Regarding the different transfection programs tested during this first optimisation step, the highest intensity was reported in cells nucleofected with the EM-110 program, while the lowest was detected with the D-33 program.

Overall, there were some advantages and limitations to all the programs and conditions tested. However, we found that the best compromise in order to obtain the best viability and transfection efficiency was to transfect LUHMES cells with **3μg** of plasmid using the **X-01**

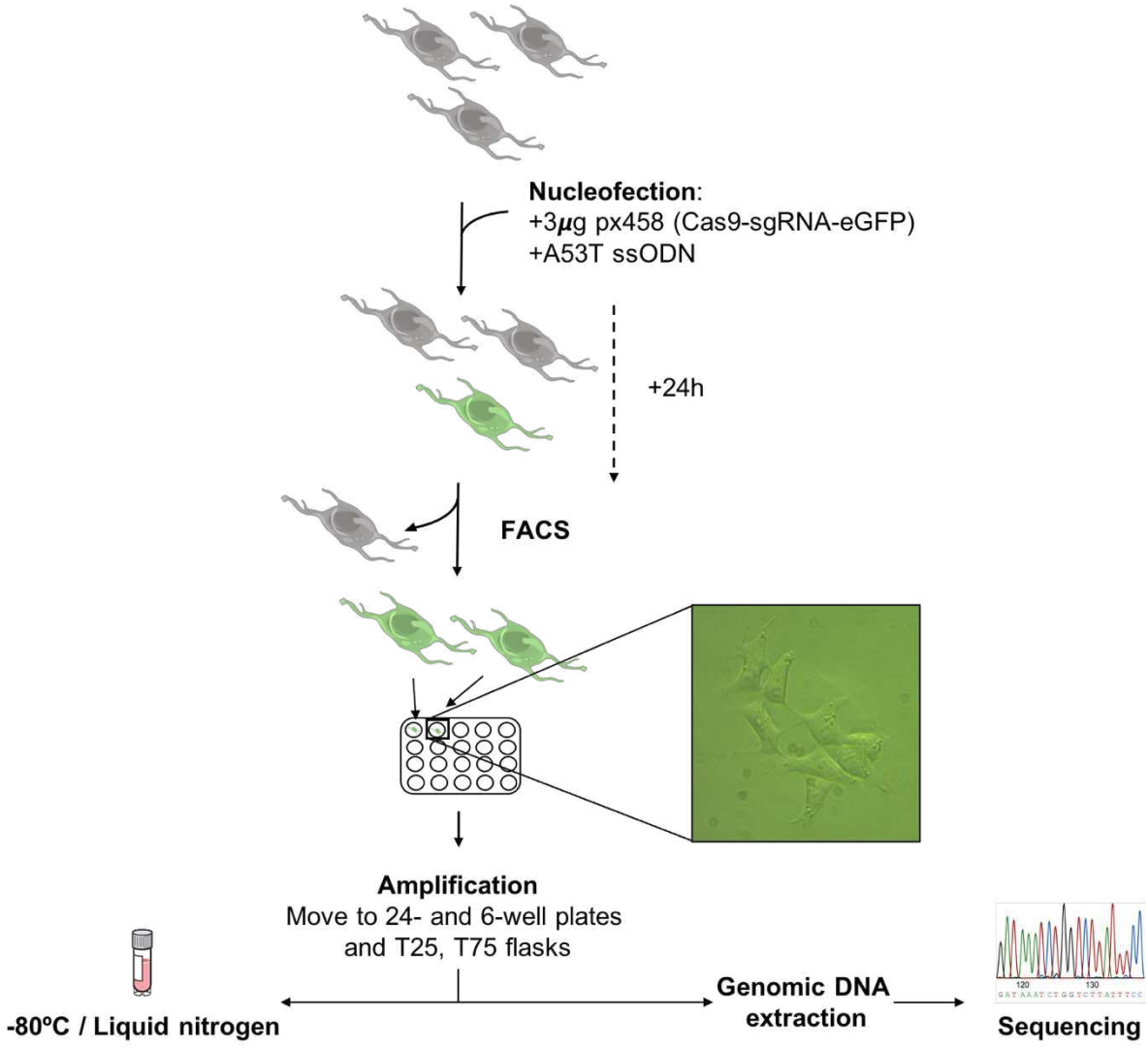

Figure 22. CRISPR/Cas9 protocol for introducing the A53T α-syn point mutation in LUHMES cells. In order to determine to optimal nucleofection protocol for LUHMES cells, several plasmid concentration, nucleofection protocols, nucleofector devices and time points were assessed. The outcomes measured included viability, GFP expression and fluorescence intensity.

and/or **EM-110** program and most importantly, to FACS sort the cells **24h** post nucleofection in order to visualise the maximum number of efficiently transfected cells.
These parameters were therefore implemented in the protocol designed to introduce the A53T point mutation in the *SNCA* gene and/or knock-out α-syn in LUHMES cells (figure 22).

5.3 Generation of A53T α-synuclein LUHMES cell lines.

After having determined the optimal nucleofection protocol to follow, we tested the ability of CRISPR/Cas9 to knock-in the point mutation A53T in the *SNCA* gene. For this, we transfected proliferating LUHMES cells from a low passage number (~p10) with the px458 Addgene CRISPR/Cas9 plasmid containing the 2A-eGFP sequence (supplementary figure 1). The sgRNA was designed against exon 3 of the *SNCA* gene and cloned into the plasmid that also encodes the Cas9 endonuclease responsible for generating a double strand cut a few nucleotides downstream from the protospacer adjacent motif (PAM) sequence (figure 23a). LUHMES cells were co-transfected with a 100bp ssODN fragment containing the A53T mutation (highlighted in red in figure 23a) so that, via homologous recombination (HR), the DNA can be repaired and incorporate the A53T mutation present in the ssODN fragment.

Following transfection, cells were transferred into 6-well plates and left overnight in the cell incubator. 24h post transfection, cells were harvested and the expression of GFP was used to FACS sort the efficiently transfected LUHMES cells into single wells of several 96-well plates containing 100μl proliferation media. We noticed that when FACS sorting and seeding a single cell per well, the survival rate was increased when using a 50:50 mix of the proliferation media collected from the 6-well plate and fresh proliferation media in the 96-well plates. This may due to the cytokines or other factors released by the cells during the previous 24h to FACS sorting. Once in the 96-well plates, single cells were left to proliferate into colonies for 1-2 weeks, frequently changing the media to provide fresh proliferation media, before transferring the colonies into larger wells (24- and 6-well plates).

Once the single-cell colonies had grown and were transferred into flasks, 2-3 vials of each clone were stored at -80ºC until genome sequencing confirmed the introduction of the A53T mutation (figure 23b).

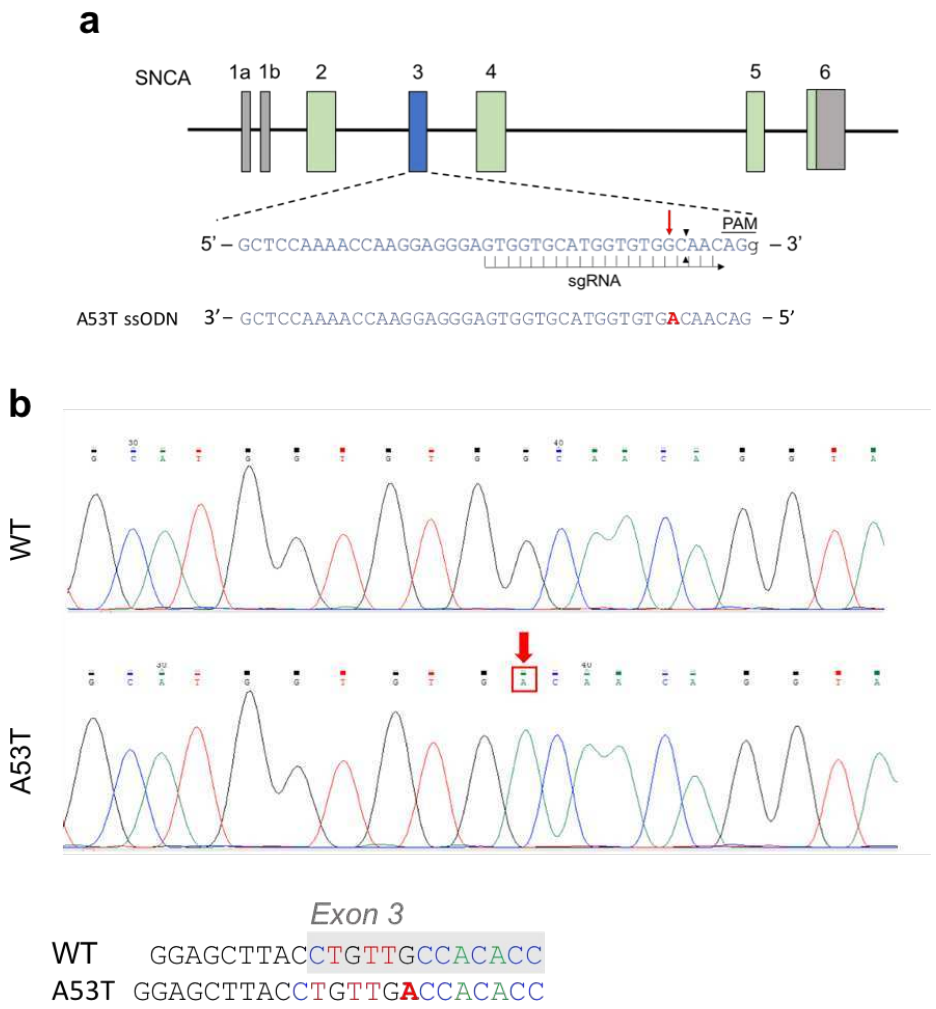

Figure 23. A53T α-syn point mutation in LUHMES cells. **a.** *CRISPR/Cas9 sgRNA target sequence in exon 3 of the SNCA gene depicturing the PAM motif, the site of double strand break by Cas9 (arrow heads) and the location of the single nucleotide mutation (red arroc). The mutation in the ssODN fragment is shown in red.* ***b.*** Genomic sequencing of WT vs A53T CRISPR/Cas9 subclone. The A53T mutation is represented by the change of a guanidine to an adenine (red box).

5.3.1 The A53T α-synuclein point mutation increases the sensitivity of neurons to ferroptosis.

At first, only one A53T CRISPR mutant subclone was obtained (the XC5 – A53T α-syn). To investigate the impact of a PD-linked α-syn mutation on ferroptosis sensitivity, we conducted the first ferroptosis measurements on this clone, whilst generating more independent homozygous mutant cell lines in parallel.

Ferroptosis sensitivity was determined by measuring cell viability in response to two commonly used ferroptosis inducers – Erastin and RSL3. Interestingly, we reported a significant vulnerability against both ferroptosis inducers in the A53T mutant clone when

compared to WT LUHMES cells (Figure 24a). Since ferroptotic cell death ultimately occurs due to a cellular imbalance in elevated lipid peroxides that outweigh the capacity of GPX4 to act as a reductant, lipid peroxidation is considered a classic ferroptosis biomarker. Using the fluorescent probe C-11 BODIPY to measure lipid ROS by flow cytometry, we found that the A53T α-syn point mutation rendered LUHMES cells more vulnerable to RSL3-induced lipid peroxidation, displaying a higher percentage of BOPIDY positive cells when compared to WT cells (figure 24b). These lipid peroxidation measurements are consistent with the viability results, suggesting that the A53T mutation may indeed increases the sensitivity of LUHMES cells to ferropotosis induced lipid peroxidation and cell death. In order to confirm this finding and exclude the possibility that the vulnerability phenotype might be due to unknown changes in the single-cell subclone, it is essential that other A53T mutant clones are analysed. To this extent, two new A53T α-syn CRISPR clones have recently been generated (3F4 and 3D10). Although still preliminary, it seems like the 3F4 – A53T α-syn clone displays a similar vulnerability phenotype against ferroptosis induced lipid peroxidation (figure 24c). These results should be interpreted with caution until the experiments are repeated in order to confirm that the increase in lipid peroxidation observed is indeed due to the A53T mutation. In addition, cell viability measures in response to Erastin and RSL3 in the new 3F4 – A53T α-syn clone are also required.

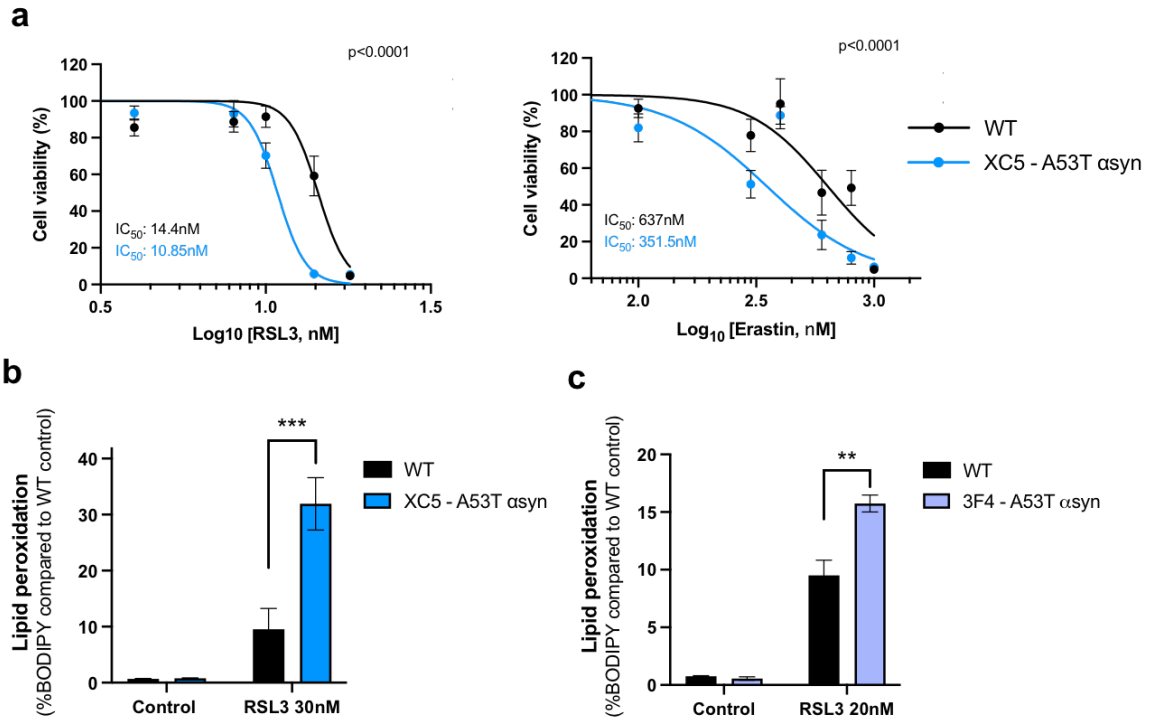

Figure 24. The A53T α-syn point mutation renders LUHMES cells more vulnerable to ferroptosis. **a.** Non-linear regression dose curved for viability in WT and XC5 – A53T α-syn LUHMES cells upon 24h treatment with ferroptosis inducers RSL3 and Erastin.

Curves were fitted to assess whether differences were statistically significant. **b.** Lipid peroxidation analysis of WT vs XC5- A53T α-syn and **c.** 3F4 – A53T α-syn LUHMES cells in response to 6h treatment of RSL3. All data represented ad mean ± SEM of at least three independent experiments (except **c.** where experiment was conducted once in triplicate. Comparisons were made using the two-tailed, unpaired Student's *t-test*; ** p<0.01, *** p<0.001.

5.4 Generation of 140 α-synuclein KO LUHMES cell lines.

CRISPR/cas9 genome editing is known to introduce non-specific modifications to the targeted genome sequence due to the double strand cut and the subsequent DNA repair. Indeed, through non-homologous end joining (NHEJ) repair, un-targeted deletions and insertions may occur adjacent to the site of double strand break. During the first round of nucleofection, such mutations occurred in the exon 3 of the *SNCA* gene, and two clones in particular were brought to our attention (termed F6 and G5). Indeed, through NHEJ repair, one extra guanidine was inserted in the exon 3 of the F6 clone (highlighted with an arrow in figure 25), creating a shift in the reading frame and introducing an early STOP codon.

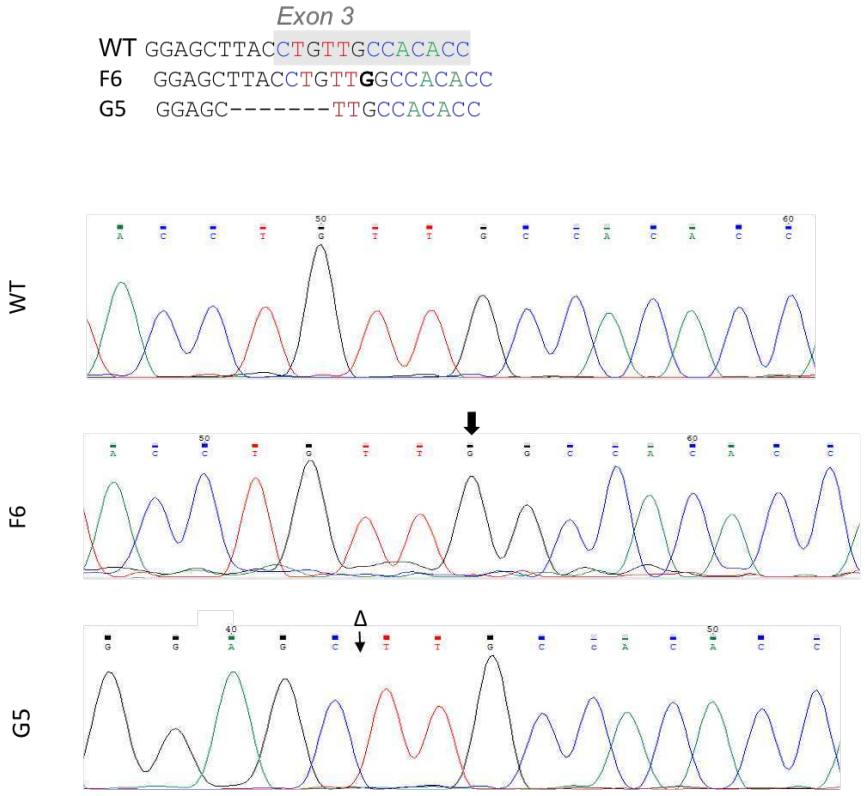

Figure 25. Sequencing of genomic DNA from WT LUHMES cells, F6- and G5-CRISPR/Cas 9 subclones. *Arrow indicates the insertion of a guanidine in exon 3 of the F6 CRISPR clone, whilst delta represents the deletion of seven nucleotides spanning the intron and exon 3 in the G5 clone.*

In the G5 clone, a deletion of 7 nucleotides occurred adjacent to the site of Cas9-mediated double strand break (highlighted with a Δ in figure 25). Of note, this deletion spans the splice site in the intron and the first three nucleotides of exon 3.

Initially, we expected α-syn to be knocked-out in these two CRISPR clones. In order to assess this, the presence of α-syn was studied via WB, qRT-PCR and immunocytochemistry. Firstly, two different α-syn antibodies were tested by WB in order to detect the protein: syn211 (Thermo Fisher, 32-8100) and 4D6 (Bio Legend, 834304). Both antibodies revealed a specific α-syn band of approximately 15KDa in the WT cell lane. Regarding the F6 and G5 CRISPR clones, we noticed that the α-syn band detected had a slightly lower molecular weight (figure 26a), suggesting that a shorter α-syn protein is still present in these cells. This was further confirmed by immunocytochemistry where α-syn staining was still observed in the F6 and G5 clones (figure 26b).

As mentioned in chapter 3 of the introduction, the *SNCA* gene can be alternatively spliced in order to generate 4 different transcripts or isoforms. Of note, it is the exon 3 and/or 5 that can be deleted from the mRNA. Since the "spontaneous" mutations in these two clones were located in the exon 3 of the *SNCA* gene, we hypothesised that the F6 and G5 CRISPR/Cas 9 subclones were unable to express the main, full length 140 aa long α-syn isoform (140 α-syn), however the other less predominant and shorter α-syn isoforms may still be expressed. To investigate this possibility, primers designed to detect exons 1/2, exons 2/3, and the 126 α-syn isoform were used by qRT-PCR (figure 26c&d). As expected, when measuring SNCA mRNA targeting exon 1/2, we detected an amplicon in both F6 and G5 clones, despite a slight reduction in expression levels compared to WT. Importantly, they lacked exon 3 as evident from the fact the primers targeting exon 2/3 were unable to generate an amplicon in the CRISPR clones. Interestingly, when using specific primers to detect the 126 α-syn transcript variant (primers spanning exon 2/4 and exon 6), we noticed that both clones had higher mRNA levels, with a more prominent upregulation in the G5 clone (figure 26c).

Following this characterisation step, we concluded that both CRISPR clones lacked the main 140 α-syn isoform. We therefore termed them F6- and G5-140 α-syn KO.

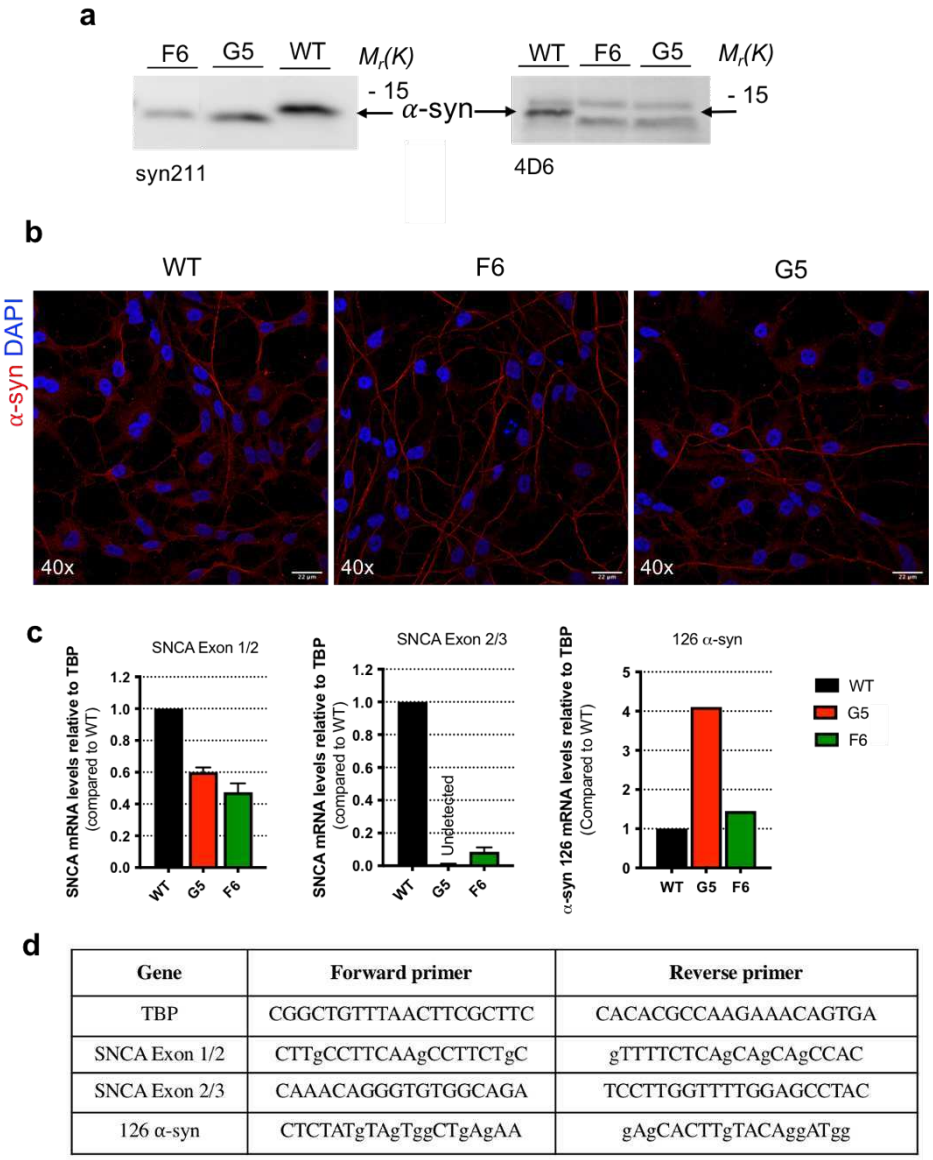

d

Gene	Forward primer	Reverse primer
TBP	CGGCTGTTTAACTTCGCTTC	CACACGCCAAGAAACAGTGA
SNCA Exon 1/2	CTTgCCTTCAAgCCTTCTgC	gTTTTCTCAgCAgCAgCCAC
SNCA Exon 2/3	CAAACAGGGTGTGGCAGA	TCCTTGGTTTTGGAGCCTAC
126 α-syn	CTCTATgTAgTggCTgAgAA	gAgCACTTgTACAggATgg

Figure 26. Characterization of F6 and G5 CRISPR clones. a. *Western blot of α-syn in WT LUHMES and both F6 and G5 CRISPR clones using two antibodies against α-syn: syn211 (left) and 4D6 (right).* ***b.*** *Immunocytochemistry staining for α-syn and DAPI in WT and F6 and G5 clones.* ***c.*** *SNCA mRNA levels detected with primers against exon 1/2 (left), exon 2/3 (middle) or the 126αsyn isoform (right). The relative expression is normalized to TBP and represented as mean ± SEM.* ***d.*** *Table with the primer sequences used to detect SNCA mRNA in WT and F6 and G5 clones*

5.4.1 Absence of full length α-synuclein protects neurons against ferroptosis

To ultimately assess whether α-syn is implicated in ferroptosis, investigating cells lacking the protein of interest represents an optimal strategy. We therefore decided to measure ferroptosis sensitivity in both 140 α-syn KO clones.

In contrast to the A53T α-syn experiments, both 140 α-syn KO CRISPR clones were found to be resistant to ferroptosis induced by RSL3 and Erastin (figure 27a), when compared to WT cells, whilst no difference was observed against STS-induced apoptosis (figure 27b). These findings suggest a ferroptosis specific effect of knocking-out the main, full length α-syn isoform. Consistent with the viability results, both 140 α-syn KO subclones exhibited reduced RSL3-induced lipid peroxidation accumulation compared to the WT parental line (figure 27c).

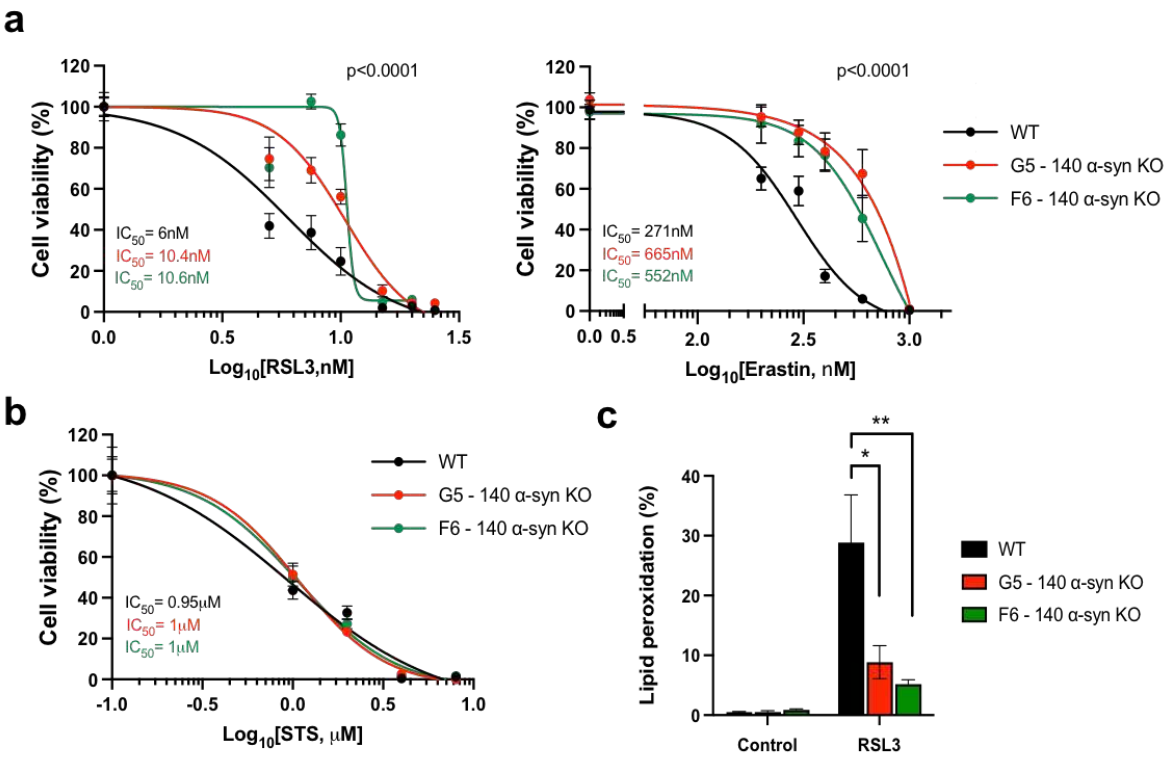

Figure 27. Depletion of full length α-synuclein selectively protects dopaminergic neurons from ferropotosis. a. Non-linear regression dose curves for viability in WT LUHMES, F6- and G5 - 140α-syn KO clones in response to treatments (24h) with RSL3, Erastin and **b.** STS. Curves were fitted to assess whether differences were statistically significant. **c.** Lipid peroxidation analysis in WT and 140 α-syn KO clones after treatment with RSL3 (15nM; 24h). All data is represented as mean ± SEM of three independent experiments. Comparisons were made using the two-tailed, unpaired Student's t-test; * p<0.05, ** p<0.01

These results strongly suggest that α-syn is somehow involved in the ferroptosis pathway and provide the first evidence of a direct link between endogenous α-syn levels and ferroptosis sensitivity in a relevant human dopaminergic cell line.

5.5 Strengths and limitations

When discussing these results, it is important to considerer the fact that single-cell derived subclones were used and compared to the parental WT line. When generating genetically modified CRISPR clones, one must remember we are selecting a clone generated from a single cell and this alone can induce phenotypic variations beyond the intended gene modification. It is it therefore essential to include several independent CRISPR/Cas 9 subclones in the experiments. This was the case for the 140 α-syn KO experiments, where two independent subclones presented the same ferroptosis resistant phenotype, strengthening the finding. On the other hand, one A53T α-syn subclones was initially assessed, and the observed ferroptosis vulnerability phenotype requires further validation in the two additional A53T α-syn subclones generated.

Finally, we briefly studied "CRISPR WT" clones and compared them to the parental WT line in order to determine whether the transfection, single-cell clone selection and difference in passage number may induce modifications and phenotypic variations. We consider a CRISPR WT to be a single cell clone generated during the CRISPR/Cas9-mediated gene modification technique, where the *SNCA* gene has not been modified, allowing for WT α-syn to be expressed. Four "CRISPR WT" clones were therefore randomly selected and studied in comparison to the WT parental line in terms of differentiation efficiency, as measured by TH mRNA levels, and ferroptosis sensitivity. Overall only minor differences in TH levels and Erastin- and RSL3- induced ferroptotic cell death sensitivity were observed between the 4 CRISPR WT clones and the parental WT line (Supplementary figure 2). These results support our findings that the differences in ferroptosis sensitivity observed in the different A53T / 140 α.syn KO CRISPR sub-clones were indeed due to modifications to α-syn.

5.6 Conclusion and perspectives

The first aim of this project was to investigate whether the PD-linked protein α-syn is implicated in the ferroptosis pathway. To begin with, we decided to target endogenous α-syn via a technique that had never been performed in our laboratory: CRISPR/Cas9-mediated genome-editing. Following an optimisation process, we were successful in generating the appropriate cell model in which to study our hypothesis: Homozygous A53T α-syn mutant and the unexpected 140 α-syn KO cell lines.

Previously in the lab, we reported that ferroptosis is a prevalent cell death in several *in vitro, ex vivo* and *in vivo* pro-oxidant models of PD (Do Van et al., 2016). Here we provide the first evidence that ferroptosis may also be implicated in synucleinopathies as evident from the increased vulnerability to ferroptosis observed in the A53T α-syn mutant CRISPR/Cas9 LUHMES clones, despite further experiments required to fully assess ferroptosis sensitivity in otherindependent A53T α-syn clones, in addition to investigating the sensitivity of such clones to other types of regulated cell death. Although the results obtained with the A53T α-syn clones are preliminary, they set the path for a promising research avenue focused on further deciphering the implications of familial-PD α-syn mutations in the neuropathology of PD, with inference to the ferroptosis pathway. Of note, several independent studies have indicated a potential association between the A53T α-syn point mutation and alterations to the metabolism of lipid (Sharon et al., 2003; Golovko et al., 2006; Yakunin et al., 2014; Sánchez Campos et al., 2018), which may potentiate a pro-ferroptosis environment.

In this first part of the PhD, we were also able to demonstrate that depleting LUHMES dopaminergic neurons from the main, full length α-syn isoform renders cells resistant against ferroptosis induced-cell death and lipid peroxidation. Importantly, we were able to report such phenotype in two independent CRISPR clone, strengthening our finding. This observation, in addition to the results obtained with the A53T α-syn clones, suggests that α-syn may indeed be implicated in the ferroptosis pathway. To our knowledge, this is the first evidence directly linking endogenous α-syn levels to ferroptosis sensitivity in dopaminergic neurons.

To strengthen these initial observations, we sought to perform complementary experiments and transiently modulate α-syn levels by small interfering RNA (siRNA) in LUHMES cells and assess ferroptosis sensitivity. The results obtained with this experimental strategy will are detailed in the next chapter.

Results - Chapter 6:

α-synuclein determines ferroptosis sensitivity in dopaminergic neurons via modulation of ether-phospholipid membrane composition
§
siRNA-mediated knock-down in LUHMES cells

6.1 Introduction

As discussed in the previous chapter, CRISPR/Cas 9 has revolutionised the genome editing potential and the way disease can be modelled in fundamental research. This technique however comes with limitations, such as the genetic variability that may arise from single cell clonal selection. In this project, the use of two independent sub-clones showing the same phenotype provides strength to our initial finding that depleting cells of the main 140 α-syn isoform protects them from ferroptosis induced lipid peroxidation and cell death. Unfortunately, the use of one single experimental model often results in poor reproducibility in animal models and clinical studies. One way to overcome this issue is via implementing several complementary *in vitro* models in preclinical studies. Therefore, to consolidate our initial findings, we decided to assess ferroptosis sensitivity in LUHMES cells where we transiently or acutely reduce endogenous α-syn levels via siRNA.

6.2 α-synuclein knock-down in LUHMES cells.

In order to reduce intracellular α-syn levels, LUHMES cells were transfected with either a scramble (ctrl), α-syn or ACSL4 siRNA at day 2 of their differentiation process, and were allowed to fully differentiate until they become mature post-mitotic neurons at day 5. As ACSL4 is a well-established pro-ferroptotic modulator (Doll et al., 2017), all readouts were compared to KD of this enzyme in the same dopaminergic cell line. siRNA-mediated KD efficiently reduced both α-syn and ACSL4 mRNA by approximately 70% and 80% respectively (figure 28a). Ultimately, this resulted in a strong reduction of both α-syn and ACSL4 protein levels when compared to the control KD (Ctl KD) (figure 28b). Importantly, reducing α-syn expression did non modify ACSL4 mRNA or protein levels, and vice versa.

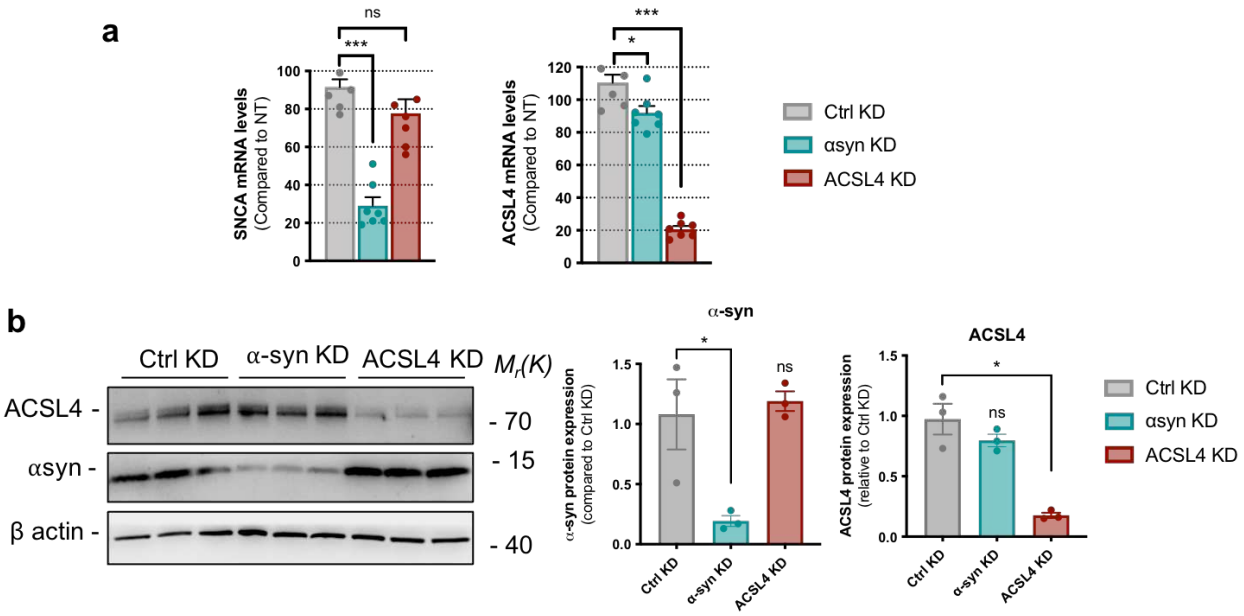

Figure 28. α-syn and ACSL4 siRNA-mediated KD confirmation in LUHMES cells. **a.** mRNA levels of α-syn (left) and ACSL4 (right) in Ctrl, α-syn and ACSL4 KD LUHMES cells as determined by qRT-PCR. The relative expression is normalized to TBP and represented as mean ± SEM. Comparisons were made using the two-tailed, unpaired Student's *t-test*. **b.** Western blot analysis of Ctrl, α-syn and ACSL4 KD LUHMES cells confirming the reduction in protein expression levels. Relative expression is normalized to β-actin levels. Comparisons were made using the one-tailed, unpaired Mann-Whitney test. * p<0.05, ** p<0.01, *** p<0-001, ns. no statistical significance.

6.3 Reducing α-synuclein expression selectively protects dopaminergic neurons against ferroptosis.

To validate the resistance phenotype observed in the 140 α-syn KO LUHMES clones, ferroptosis sensitivity was assessed in α-syn KD cells, comparing the effect to ACSL4 KD. Reducing both α-syn and ACSL4 expression significantly protected neurons against RSL3- and erastin-induced ferroptosis (figure 29a), whilst no difference in sensitivity was observed against STS triggered apoptosis (figure 29b), once again suggesting a ferroptosis specific effect. Of note, since α-syn modulation of ferroptosis sensitivity was still observed when triggering this cell death pathway through a downstream component (e.g. GPX4 inhibition via RSL3), it is likely that the ferroptosis associated mechanism involving α-syn is not upstream of GPX4. Using the fluorescent probe C-11 BODIPY to measure lipid ROS, we found that a depletion of α-syn levels via siRNA mitigated lipid peroxidation induced by RSL3 to a similar levels as ACSL4 KD (figure 29c). These results are consistent with the

initial findings that depleting cells of the main 140 α-syn isoform selectively protects neurons against ferroptosis (figure 27).

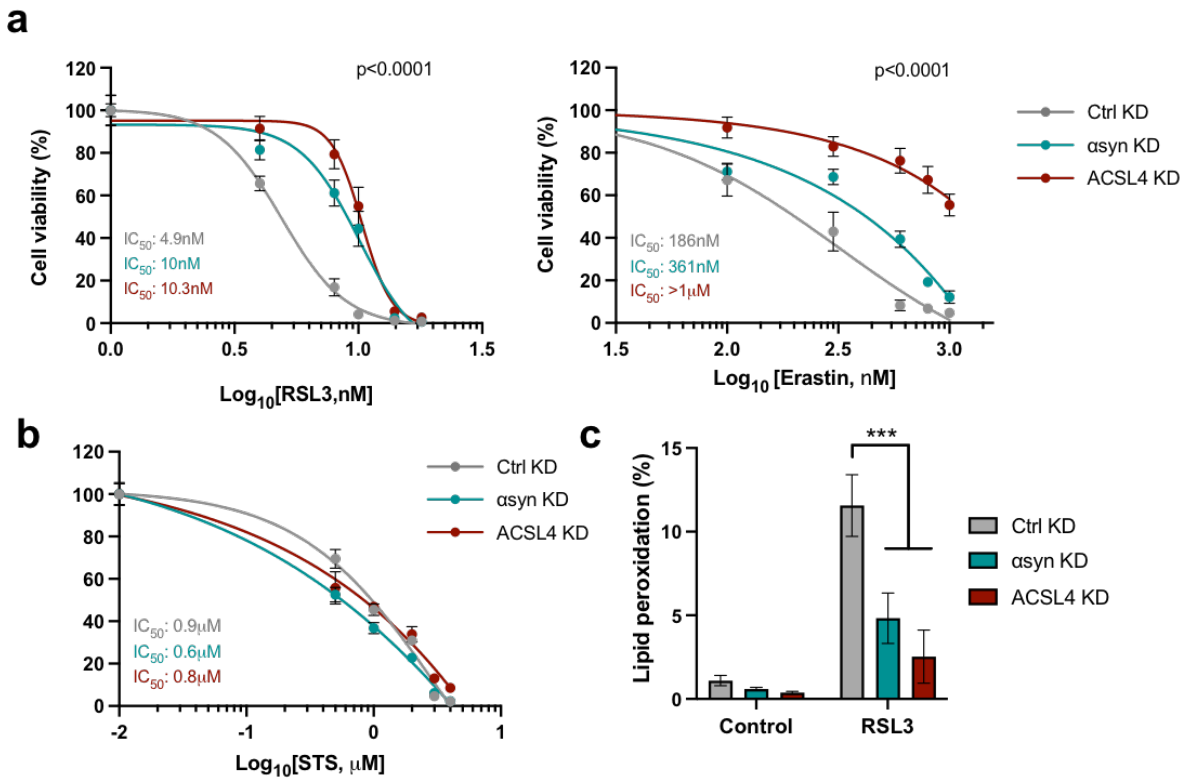

Figure 29. Depletion of α-synuclein selectively protects dopaminergic neurons from ferroptosis comparative to ACSL4. **a.** Non-linear regression dose curves for viability in Ctrl, α-syn and ACLS4 KD LUHMES in response to 24h treatments with RSL3, Erastin and **b.** STS. Curves were fitted to assess whether differences were statistically significant. **c.** Lipid peroxidation analysis in Ctrl, α-syn and ACSL4 KD LUHMES cells after treatment with RSL3 (20nM; 6h). All data is represented as mean ± SEM of three independent experiments. Comparisons were made using the two-tailed, unpaired Student's t-test; * p<0.05, ** p<0.01

6.4 Arachidonic acid and iron induced ferroptosis is mediated by α-synuclein expression

Two key pathological hallmarks of PD include iron overload (Dexter et al., 1987, 1989a; Devos et al., 2014) and elevated lipid peroxidation in the SNpc. Of note, impaired metabolism of fatty acids with higher levels of membrane PUFAs are evident in both PD and DLB post-mortem brain samples (Sharon et al., 2003). In an attempt to model a more physiologically relevant environment to induce ferroptosis that also has relevance to PD, the abundant brain PUFA arachidonic acid (AA) and $FeCl_3$ were studied in combination at doses that were sub-toxic when administered separately (figure 30a). This has been the topic of a

parallel PhD project in the laboratory, which has meticulously characterised the cell death pathway triggered by the co-treatment of AA and Fe. Specific induction of ferroptotic cell death and lipid peroxidation was confirmed using this model as evident from the fact the ferroptosis inhibitors (e.g. deferiprone, ferrostratin-1 (Fer-1) and liproxstatin) as well as genetic depletion of ACSL4 or 15/15BALOX protected neurons against lipid peroxidation and cell death induced by AA + Fe (Bouchaoui et al., in review).

Here, we found that depletion of α-syn in LUHMES neurons co-treated with 20μM AA and 20μM Fe protected against both lipid peroxide (figure 30b) and cell death (figure 30c), similar to that observed with pharmacologically induced ferroptosis (figure 29a). Importantly, the level of protection by α-syn KD were comparable to ACSL4 depletion (figure 30b&c).

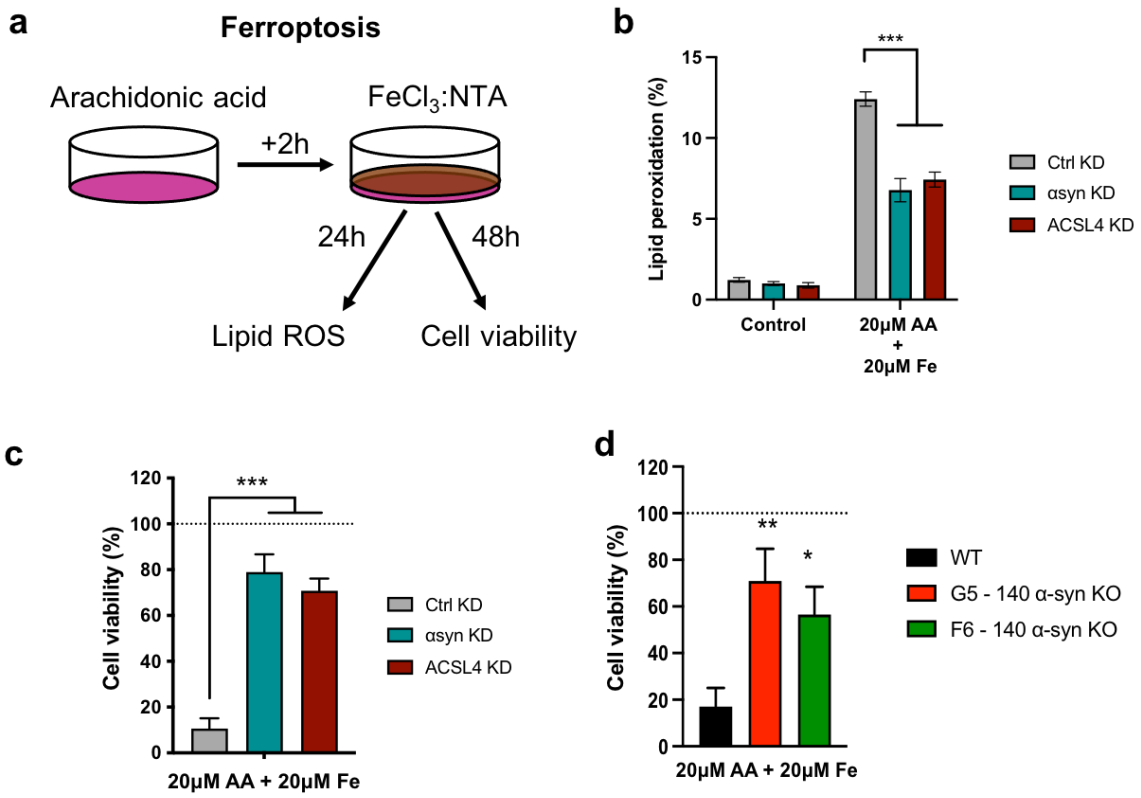

Figure 30. α-synuclein and ACSL4 mediate dopaminergic neuron sensitivity to ferroptosis induced by arachidonic acid and iron. a. Schematic representation of a more physiologically relevant model of ferroptosis in which differentiated LUHMES cells were treated with arachidonic acid (AA) (20µM) followed by FeCl3:NTA (20µM) before measuring lipid peroxidation or cell viability at 24h and 48h respectively. **b&c.** Lipid peroxidation (**b**) and cell viability (**c**) in Ctrl, α-syn or ACSL4 KD LUHMES cells with the AA + Fe model of ferroptosis. **d.** Cell viability for WT and 140 α-syn KO LUHMES clones in response to AA + Fe co-treatment (48h). Results expressed as mean ± SEM of three independent experiments. Statistical comparisons were made using two-tailed, unpaired Student's t-test; * p<0.05, ** p<0.01, *** p< 0.001.

A similar protection against AA and Fe induced ferroptotic cell death was also observed in both 140 α-syn KO CRISPR subclones (figure 30d).

Taken together, these findings, in addition to prior studies, support α-syn having a role in the metabolisms of PUFAs and/or iron (Sharon et al., 2003; Golovko et al., 2006; Barceló-Coblijn et al., 2007; Baksi et al., 2016; Baksi and Singh, 2017), and subsequently indicates that α-syn specifically mediates the sensitivity of dopaminergic neurons to ferroptosis induced by the toxic combination of AA and Fe.

6.5 α-synuclein modulates the composition of ether- linked phospholipids in the plasma membrane.

Prior studies have shown altered fatty acid composition in response to abnormal α-syn levels in both *in vitro* and *in vivo* models as well as human brain (Sharon et al., 2001, 2003; Golovko et al., 2006; Barceló-Coblijn et al., 2007). The overexpression of α-syn increases levels of arachidonic acid, linoleic acid and dihomo- γ -linoleic acid, whist the absence of α-syn reduces PUFA content in brain phospholipids (PLs) (Sharon et al., 2003; Golovko et al., 2006). Based on these findings, we hypothesized that the ferroptosis resistant phenotype observed in α-syn depleted neurons could be due to plasma membrane remodelling, specifically a reduction in PUFA content in PLs.

In search of potential mechanisms that underlie the observed evasion from ferroptosis in the α-syn depleted neurons, PL membrane composition in the α-syn KD neurons was measured by mass spectrometry and compared to the effects caused by a reduction in ACSL4 expression. Similar to previous reports in other cell types (Doll et al., 2017), the percentages of total phosphatidylcholine (PC) and phosphatidylethanolamine (PE) containing PUFAs were reduced in the ACSL4 depleted dopaminergic neurons (Figure 31a). Interestingly, a similar profile was observed when α-syn levels were reduced (figure 31a), indicating that α-syn may mediate the phospholipid PUFA content in dopaminergic neurons through a similar pathway as ACSL4. To elucidate how these changes in PC and PE would impact on the generation of lipid peroxides, a peroxidability index (PI) (Naudí et al., 2017) was calculated for each condition. This index takes into account the number of double bonds present in the PUFAs and determines the risk of PL to oxidize.

Equation 1

$$PI = (\%\, monoenoic\ FA \times 0.025) + (\%\, dienoic\ FA \times 1) + (\&\, trienoic\ FA \times 2) + (\%\, tetraenoic\ FA \times 4) + (\%\, pentaenoic\ FA \times 6) + (\%hexaenoic\ FA \times 8)$$

Consistent with the reduction in PUFA content in the PC and PE, the PI was reduced in LUHMES neurons with either α-syn or ACSL4 depleted by siRNA (figure 31b).

Taking more in-depth lipidomic profiling of the different PC and PE molecular species in both α-syn and ACSL4 depleted neurons revealed a prominent and selective loss of ether-linked phospholipids (ether-PL) (figure 31c). Unlike ester-linked diacyl-PL, ether-PL possess an ether bond at the glycerol sn-1 position. Ether-PL comprise two subclasses: alkyl-ether phospholipids (ePL) and vinyl-ether phospholipids, also known as plasmalogens (pPL). In the sn-2 position, ether-PL most often contain a PUFA, which is prone to peroxidation. Finally, in the sn-3 position, ether-PL present a polar head group commonly a phosphoethanolamine and phosphocholine. Of note, two recent studies have shown that ether-PL are essential for ferroptosis and that a reduction in this class of PL suffices to protect cells against this novel cell death pathway (Cui et al., 2021; Zou et al., 2020a) (refer to chapter 2 for more details). In line with these findings, reduced α-syn or ACSL4 expression in LUHMES cells resulted in a specific downregulation of ether-linked PC (ether-PC) and PE (ether-PE) (figure 31c&d). Upon evaluating specific ether-PLs species previously associated with an increased vulnerability to ferroptosis (PC(16:0e/20:4), PC/PE(16:0p/20:4), PC/PE(18:0p/20:4), PC/PE(18:1p/20:4), PE(18:1p/22:4) and PE(18:1p/22:6)), several were consistently downregulated in LUHMES dopaminergic neurons where α-syn or ACSL4 was depleted (figure 31d). Taken together, these findings indicate that a key factor in α-syn capability to mediate the sensitivity of dopaminergic neurons to ferroptosis-induced lipid peroxidation and cell death is through ether-PL modulation in the plasma membrane.

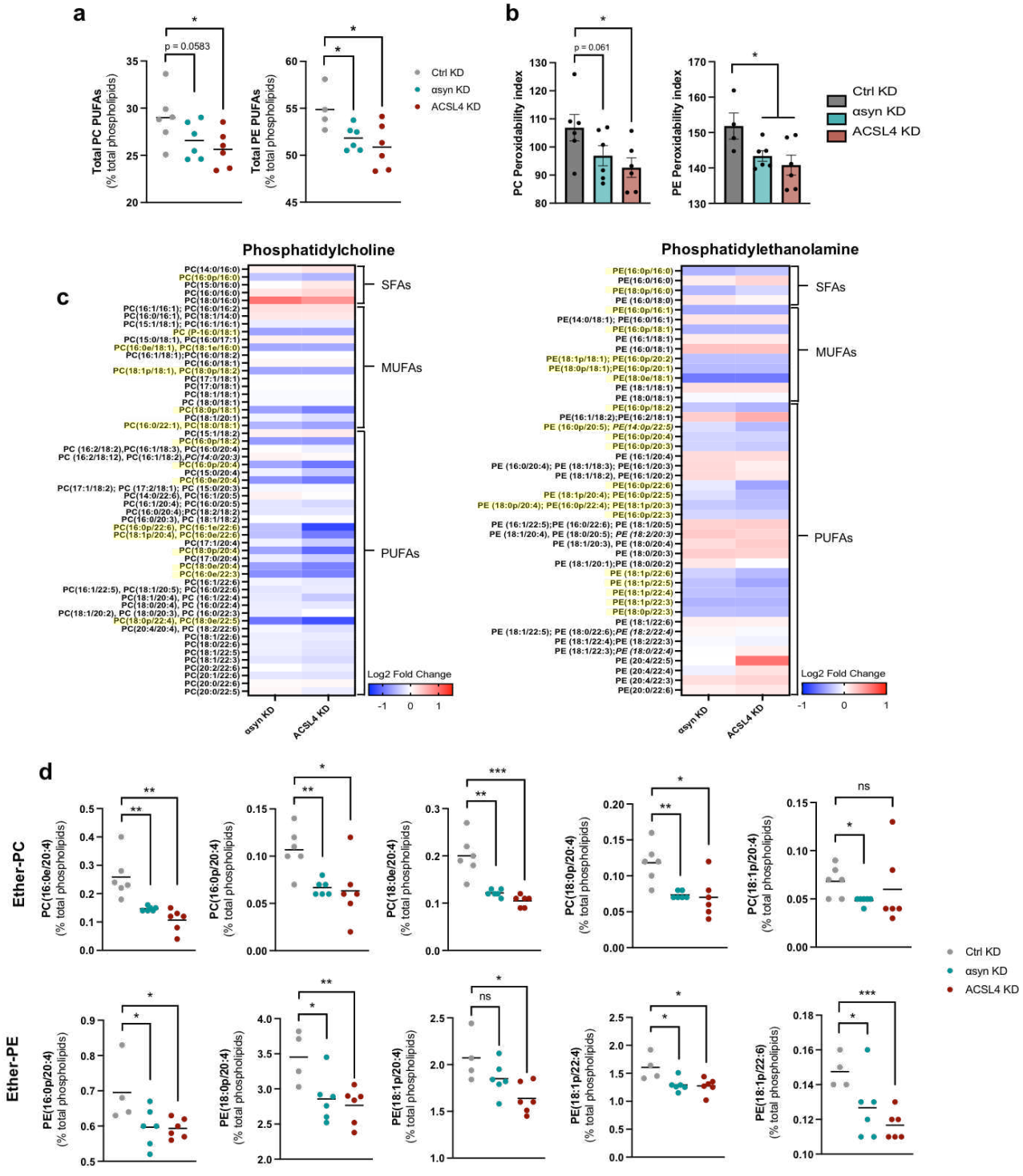

Figure 31. Modulated ether-linked phospholipid composition by α-synuclein and ACSL4 expression in dopaminergic neurons. a&b. Total levels (**a**) and the peroxidability index (**b**) of phosphatidylcholine (PC) and phosphatidylethanolamine (PE) phospholipids containing PUFAs measured in α-syn and ACSL4 KD Luhmes cells. **C.** Heat maps comparing the abundance of the different PC and PE molecular species in α-syn and ACSL4 KD LUHMES cells relative to Ctrl KD. Highlighter in yellow are the ether-linked PL shown to be reduced in both α-syn and ACSL4 KD conditions. **d.** The different ether-PC and PE molecular species previously shown to increase ferroptosis vulnerability (Zou et al., 2020; Cui et al., 2021) in Ctrl, α-syn and ACSL4 KD LUHMES cells. Statistical comparisons were made using two-tailed, unpaired Student's t-test; * p<0.05, ** p<0.01, *** p< 0.001.

6.6 The level of ether-linked phospholipids in α-synuclein depleted neurons is restored upon arachidonic acid supplementation.

A reduction in ether-PL upon α-syn depletion could be explained by: *i*. greater peroxidation of the PUFAs within the ether-PL, *ii*. increased removal from the plasma membrane by the relevant phospholipase, and/or *iii*. impaired biosynthesis. The loss of all molecular species of ether-PL, regardless of fatty acid length or saturation status, to a levels that is comparable to that observed upon ACSL4 depletion (figure 31c) indicates an unlikelihood that reduced α-syn caused a greater peroxidation of the PUFA in the ether-PL and thus this avenue of investigation was not pursued further. The calcium-independent phospholipase A2 (iPLA2) has been implicated in the removal of ether-PL from the plasma membrane (Wolf and Gross, 1985; Ford et al., 1991; Yang et al., 1996; Beckett et al., 2007). However, a lack of change to iPLA2 levels in the α-syn depleted neurons makes increased enzymatic removal of ether-PL from the plasma membrane also an unlikely protective mechanism (figure 32a).

To assess whether the observed downregulation of ether-PLs in the α-syn KD cells might be driven by defective biogenesis at the peroxisome, established peroxisome markers - Peroxisomal biogenesis factor 3 and 14 (PEX3 and PEX14), were assessed along with the enzymes Fatty Acyl-CoA Reductase 1 (FAR1), Glyceronephosphate O-Acyltransferase - (GNPAT), Alkyldihydroxyacetonephosphate synthase, (AGPS) and 1-Acylglycerol-3-Phosphate O-Acyltransferase 3 (AGPAT3) required for the synthesis of the ether-PL precursor 1-*O*-alkyl-glycerol-3-phosphate (AGP) (figure 32c). Again, similar to ACSL4 KD, neither levels of peroxisome markers or the relevant upstream proteins requited for ether-PL biogenesis seemed altered (figure 32a&b), suggesting the initial stages of ether-PL synthesis in the peroxisomes were not impaired.

The role of ACSL4 is essential for the generation and incorporation of PUFA-CoA into the ferroptosis-relevant ether-PL in the ER (figure 32c). Supplementation of AA (20μM), the preferential substrate of ACSL4, restored ether-PLs back to control levels in LUHMES depleted of ACSL4 (figure 32d&e). Similarly, AA supplementation restored the levels of ether-PL upon α-syn depletion (figure 32d&e) despite no observable changes in ACSL4 expression (figure 32a and figure 28), suggesting the reduction in ether-PL may be due to a lack of PUFA-CoA generation required for ether-PL synthesis. One possible explanation for a lack of PUFA-CoA may be an impaired ACSL4 activity in α-syn depleted neurons, which would be restored upon AA supplementation, the preferential substrate of ACSL4.

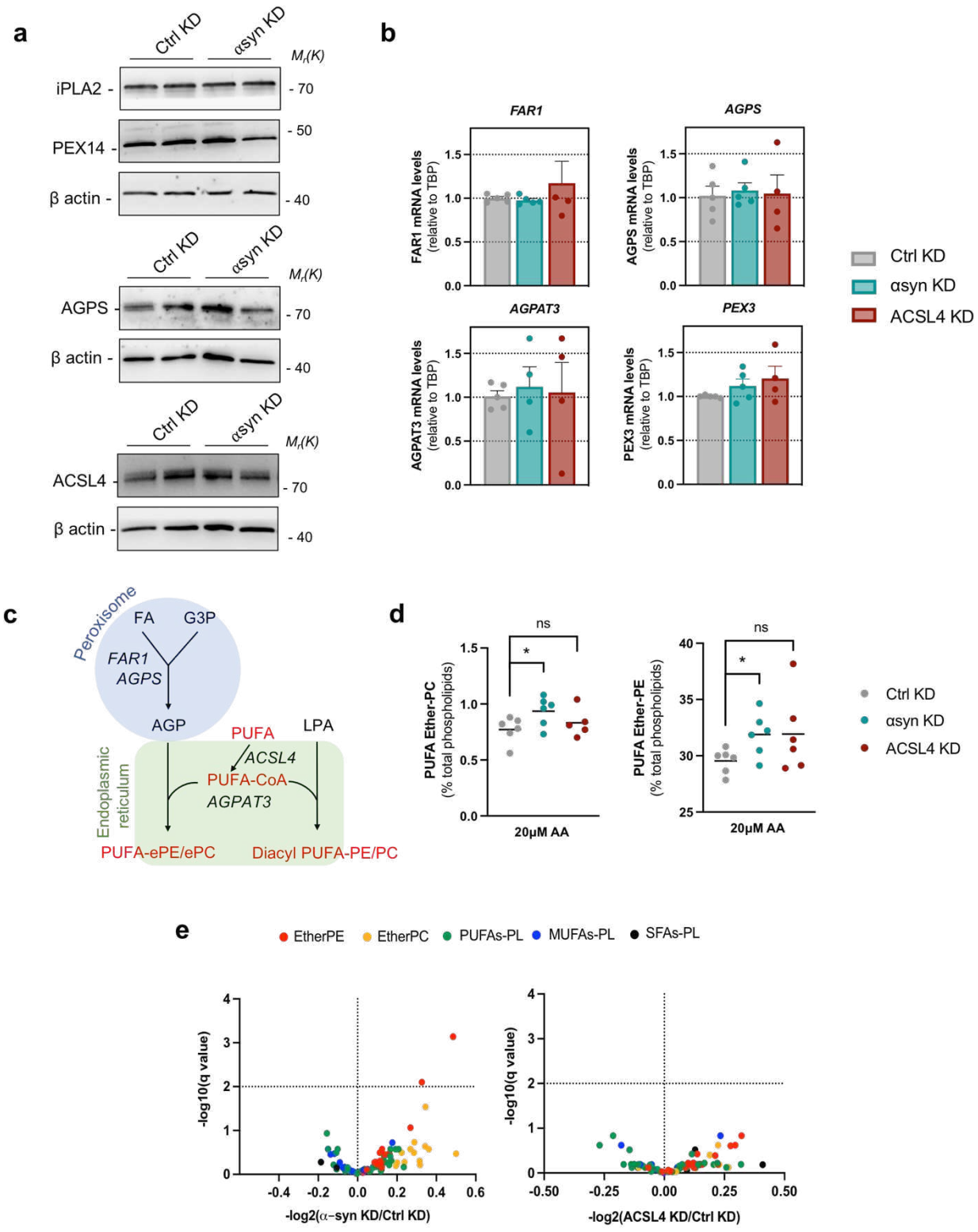

Figure 32. **Arachidonic acid supplementation restores ether-PL levels in neurons that have a depletion in α-syn or ACSL4. a&b.** Protein (**a**) and mRNA (**b**) expression of several key enzymes involved in the ether-PL biosynthesis pathway in α-syn and ACSL4 KD LUHMES. The relative gene expression was normalized to TBP. **c.** Schematic representation of the ether-PL biosynthesis pathway starting at the peroxisomal level through to the ER. **d.** PUFA ether-PC and PUFA ether-PE proportion measured in α-syn and ACSL4 after AA (20μM; 24h) supplementation. **e** Volcano plots illustrating changes in the neuronal PE and PC phospholipid composition upon KD of α-syn or ACSL4 KD and treatment with AA (20μM;24h). Statistical comparisons were made using two-tailed, unpaired Student's t-test; * p<0.05

6.7 Conclusion

The previous work conducted in the laboratory in addition to the results obtained throughout this PhD clearly demonstrates that dopaminergic neurons are highly sensitive to ferroptosis. This can partly be explained by the high oxidative environment created by their high oxygen consumption, and the metabolisms of dopamine and iron, essential for proper neurotransmitter synthesis and transmission. Furthermore, the brain has the highest proportion of lipids in the body, following the adipose tissue, with a particular abundance in PUFAs such as AA, adrenic acid (AdA) and docosahexaenoic acid (DHA) (Crawford et al., 1976; Brenna and Diau, 2007), fatty acids associated with ferroptosis-dependent lipid peroxidation (Kagan et al., 2017). Is it therefore essential that ferroptosis sensitivity is tightly regulated in dopaminergic neurons. Whilst the immense majority of studies that have contributed towards deciphering the biochemical regulatory pathways of ferroptosis were conducted in cancer cells, less is known about ferroptosis regulation in neurons. In this second part of the PhD, we have confirmed our initial findings observed in the 140 α-syn KO LUHMES cells whereby a depletion of α-syn protects dopaminergic neurons against ferroptosis to a similar extent as knocking-down the pro-ferroptotic modulator, ACSL4. In addition to reporting a protection against pharmacological ferroptosis induction, we report that α-syn depletion protects dopaminergic neurons from ferroptosis induced by the toxic combination of AA and Fe, similarly to ACSL4 KD.

After confirming the implication of α-syn in ferroptosis sensitivity, we proceeded towards unravelling the potential mechanism underlying the protection observed against ferroptosis when α-syn is depleted in LUHMES cells. Based on the several studies reporting α-syn dependent alterations in PUFA content in the plasma membrane (Sharon et al., 2003; Golovko et al., 2005, 2006; Barceló-Coblijn et al., 2007, 2007), we hypothesised that depleting α-syn in LUHMES dopaminergic neurons may have resulted in lower PUFAs in the plasma membrane, thus reducing the risk of ferroptosis-dependent peroxidation and cell death. Consistent with previous studies (Sharon et al., 2003; Golovko et al., 2006; Barceló-Coblijn et al., 2007; Doll et al., 2017), we observed a reduction in total PUFA content in either PC- and PE-PL and a subsequent lower PI. By investigating specific PL molecular species, we revealed a more prominent reduction in ether-PL in the plasma membrane. Importantly, two recent studies have identified peroxisome-derived ether-PL as essential for ferroptosis unfolding, as evident from the fact that blocking ether-PL synthesis by either depleting cells of peroxisomes or specific ether-PL synthesis enzymes, lead to ferroptosis

evasion. Our lipidomic analysis in LUHMES cells provides the first steps towards unravelling the molecular mechanism by which α-syn determines ferroptosis sensitivity in neurons: by enriching cellular membranes with ether-PL.

Here, we report that, similar to ACSL4 KD, α-syn depletion result in a ether-PL downregulation despite no observable changes in mRNA or protein levels of several peroxisome markers and enzymes involved in the biosynthesis of ether-PLs. Enzymatic removal of ether-PL from the plasma membrane by the plasmalogen selective iPLA2 (Ford et al., 1991; Beckett et al., 2007; Hayashi et al., 2022) seemed unlikely since the protein levels remained unchanged. However, an increase in the enzymatic activity cannot be excluded, in addition to the involvement of other phospholipase enzymes not studied in this project. Overall, our results suggest that the function of α-syn in modulating ether-PL is not related to the upstream enzymes involved with the early stages of biosynthesis. The restoration of ether-PL levels by AA supplementation in neurons depleted of α-syn paralleled that observed with ACSL4 depletion, and suggests an impaired activity of ACSL4 in dopaminergic neurons lacking α-syn. This hypothesis is strengthen by Golovko and colleagues who reported a reduction in AA-CoA mass and AA incorporation into PLs in the brains of SNCA KO mice due to a reduction in total ACSL activity (Golovko et al., 2006).

Results - Chapter 7:

Confirming the role of α-synuclein in modulating ferroptosis sensitivity in other disease models
§
smNPC-derived midbrain neurons and brain organotypic slices

7.1 Introduction

So far, we have shown that α-syn is involved in determining ferroptosis sensitivity in LUHMES dopaminergic neurons using two different genome editing approaches – CRISPR/Cas9 and siRNA-mediated KD. Next, in order to strengthen our results, we sought to confirm our findings in other disease models and investigate the effects of α-syn overexpression in ferroptosis sensitivity. Whilst attending the International Parkinson and Movement Disorder Society's International Congress on September 2019 in Nice, I became acquainted and established a new collaboration with Prof. Rejko Krüger from Luxemburg Centre for Systems Biomedicine and his PhD student Dr. Zoe Hanns who had conducted her research on iPSCs and small molecule-derived neuronal precursor cells (smNPC) which can be further differentiated into midbrain dopaminergic neurons (mDANs). Importantly, they had smNPCs where α-syn had been knocked-out by CRISPR/Cas9 (SNCA KO), and smNPC from PD patients baring a triplication of *SNCA* (SNCA Trip). Despite a delay caused by the COVID-19 global pandemic, I was able to visit Prof. Krüger's laboratory in May and November 2021 and perform ferroptosis sensitivity assays on SNCA KO and SNCA Trip smNPC-derived midbrain neurons.

Furthermore, a fellow PhD colleague, Hind Bouchaoui, and I established in our laboratory the culture of mice organotypic brain slices (OBSs) in order to asses ferroptosis in an *ex vivo* model. The aim was to optimize the culture of sagittal slices containing the nigrostriatal pathway and knock-down α-syn and ACSL4 expression by siRNA in order to reproduce the results obtained in the α-syn and ACSL4 depleted LUHMES cells.

This chapter will first describe the work conducted on smNPC-derived midbrain neurons, followed by the optimization of OBSs containing the nigrostriatal pathway and the initial KD results obtained in the OBSs.

7.2 α-synuclein levels determine ferroptosis sensitivity in patient derived midbrain neurons.

To determine that observations in LUHMES dopaminergic neurons were not due to a cell specific phenotype, a second *in vitro* human cell model was studied. Three independent differentiations were used to generate mDANs differentiated from smNPC where α-syn had been knocked-out by CRISPR/Cas9 (SNCA KO). Following a characterisation step, we concluded that both SNCA KO and the parental WT cell lines had efficiently differentiated into mature, post-mitotic neurons as evident from the expression of neuronal markers Tuj1 (Figure 33 a&b), despite the relatively low percentage of double stained TH and Tuj1 dopaminergic neurons (fugure 33b).

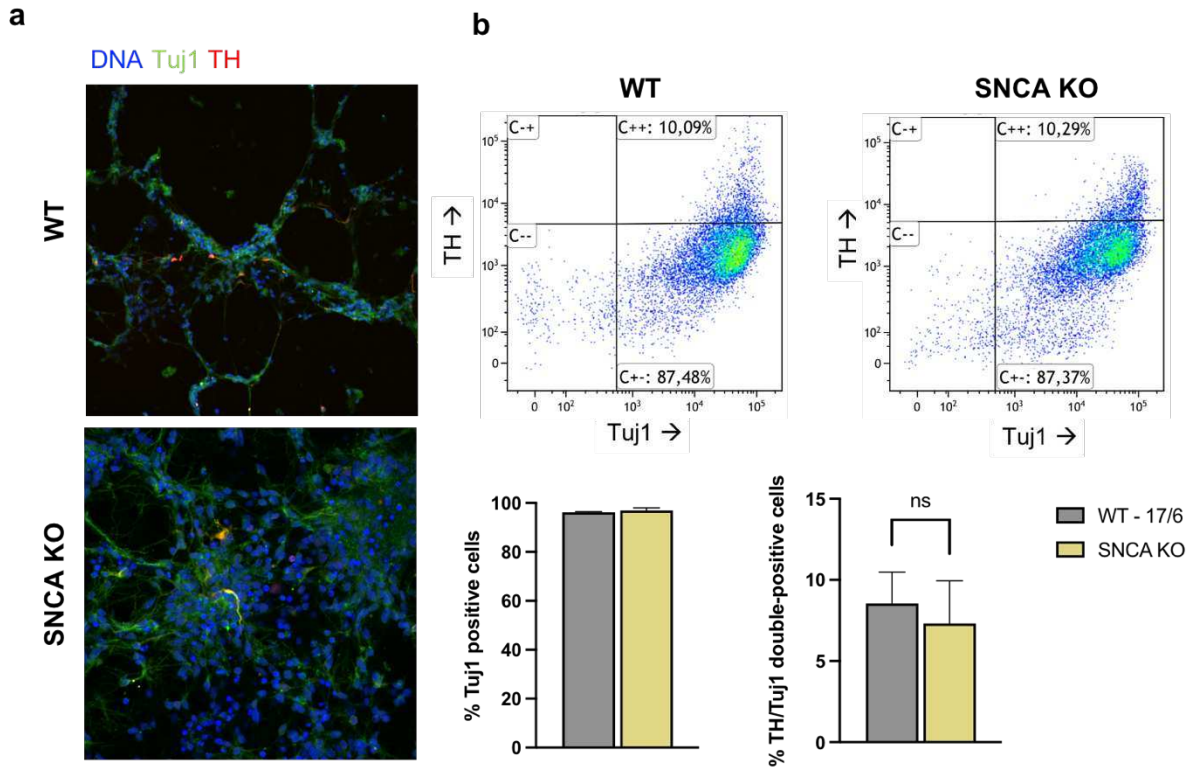

Figure 33. Neuronal characterisation of WT and SNCA KO smNPC-derived midbrain neurons. **a.** Immunocytochemistry staining for Tuj1 and TH in WT and SNCA KO mDANs. **b.** FACS quantification of mDANs double stained with Tuj1 and TH antibodies. Data is represented as mean ± SEM of three independent experiments. Comparisons were made using the two-tailed, unpaired Student's t-test

Comparing WT and SNCA KO mDANs confirmed that the absence of α-syn protects neurons against RSL3-induced ferroptosis but has no effect on apoptosis sensitivity as assessed by STS sensitivity (figure 34b). Paralleling the selective changes to ferroptotic cell

death, lipid peroxidation levels in response to ferroptosis induction were lower in the SNCA KO mDANs when compared to the parental WT cell line (figure 34c).

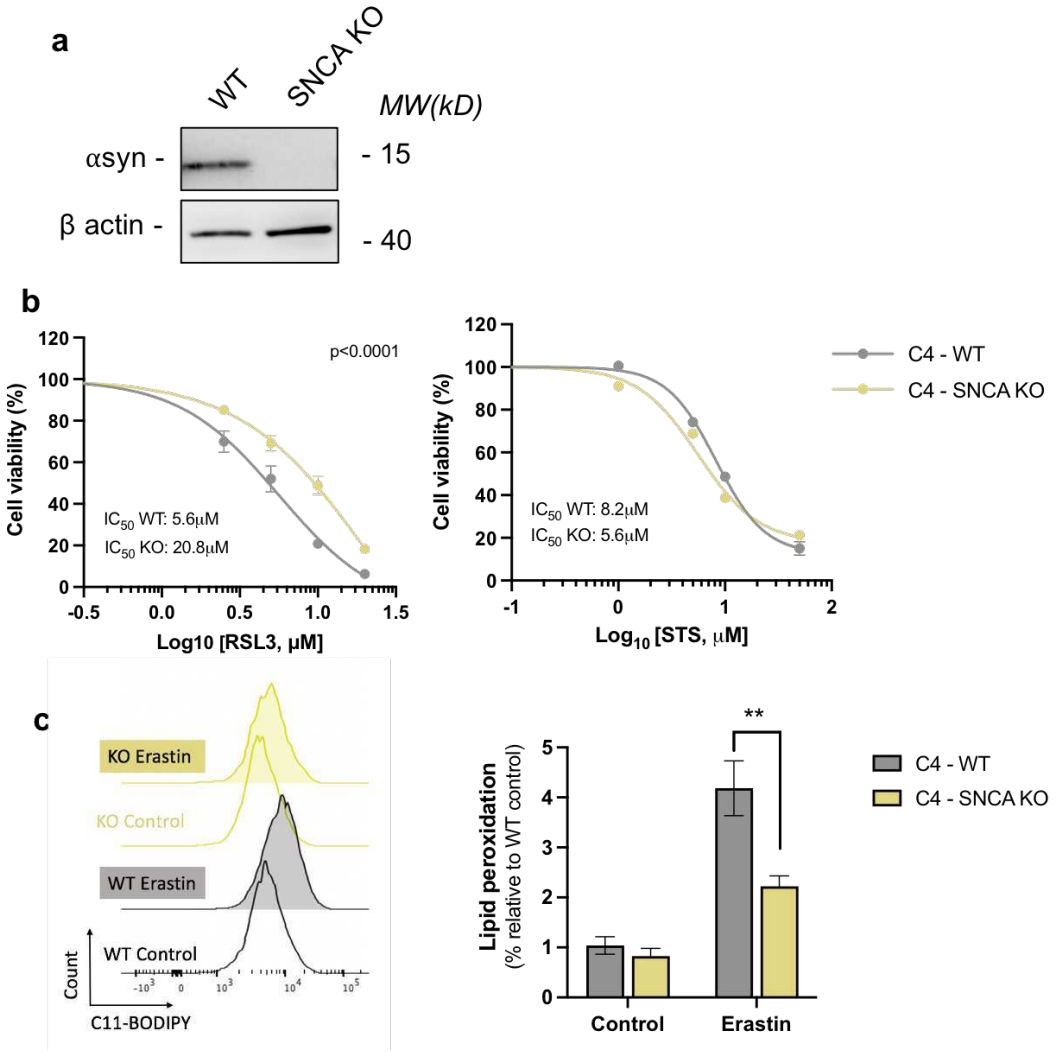

Figure 34. Absence of α-synuclein protects smNPC-derived midbrain neurons from ferroptosis. **a.** Western blot of α-synuclein in WT and SNCA KO smNPC derived mDANs. **b.** Non-linear regression dose curves for viability in WT and SNCA KO smNPC derived mDANs. following RSL3 and STS treatments (24h). Curves were fitted to assess whether differences were statistically significant. **c.** Lipid peroxidation analysis after Erastin (80μM, 6h) treatment. All data is represented as mean ± SEM of three independent experiments. Comparisons were made using the two-tailed, unpaired Student's *t*-test; **p <0.01

Next, we sought to investigate whether an elevation of α-syn would lead to the opposite phenotype, resulting in ferroptosis vulnerability. To this extent, SNCA Trip smNPC derived midbrain neurons were studied and compared to the gene corrected isogenic control (Iso WT). Similarly to the characterisation step performed for the SNCA KO and the parental WT

cell lines, SNCA Trip and its Iso WT smNPCs were differentiated into mDANs and characterised by double staining with Tuj1 and TH antibodies (Figure 35 a&b). Throughout six independent differentiation, we obtained an homogenous population of Tuj1 positive cells for both SNCA Trip and Iso WT, and a slightly more efficient differentiation of SNCA Trip smNPCs into mDANs, as evident from the double Tuj1 and TH staining in figure 35b.

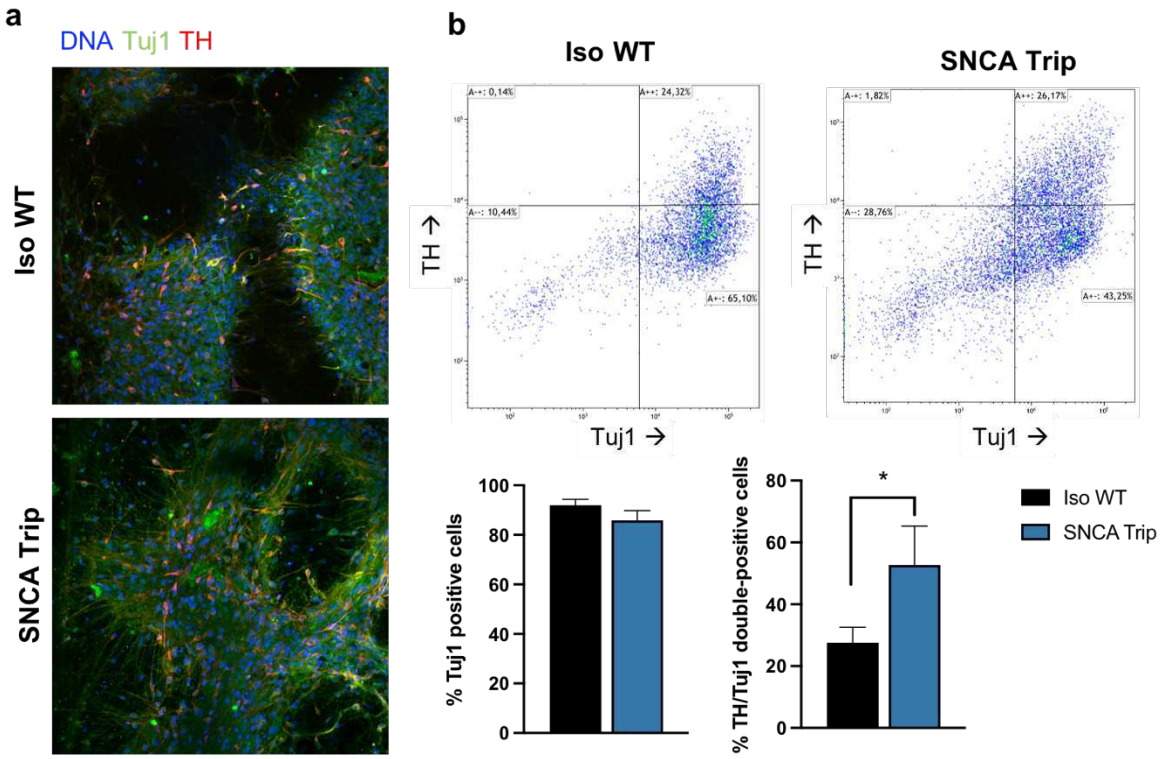

Figure 35. Neuronal characterisation of SNCA Trip and Iso WT smNPC-derived midbrain neurons. **a.** Immunocytochemistry staining for Tuj1 and Iso WT and SNCA Trip mDANs. **b.** FACS quantification of mDANs double stained with Tuj1 and TH antibodies. Data is represented as mean ± SEM of six independent experiments. Comparisons were made using the two-tailed, unpaired Student's t-test; * p <0.05.

In contrast to the results obtained with the SNCA KO neurons, mDANs carrying SNCA triplication were more vulnerable to RSL3 toxicity when compared to their isogenic control despite having no observable differences in theirt response to STS-triggered apoptosis (Figure 36b). Regarding lipid peroxidation, SNCA Trip mDANS had higher levels of ferroptosis-induced lipid peroxidation compared to the Iso WT cells (figure 36c). Importantly, the triplication of SNCA alone sufficed to trigger lipid peroxidation under basal control conditions, indicating that an increase in α-syn levels could prime the cells to be more sensitive to ferroptosis. To further confirm that the observed changes to lipid peroxidation in

the SNCA Trip neurons were specifically due to an elevation of α-syn, we performed siRNA to reduce α-syn expression back to similar levels observed in the isogenic control (supplementary figure 5). As expected, KD of α-syn in the SNCA Trip neurons significantly reduced the levels of ferroptosis induced lipid peroxidation (figure 36d).

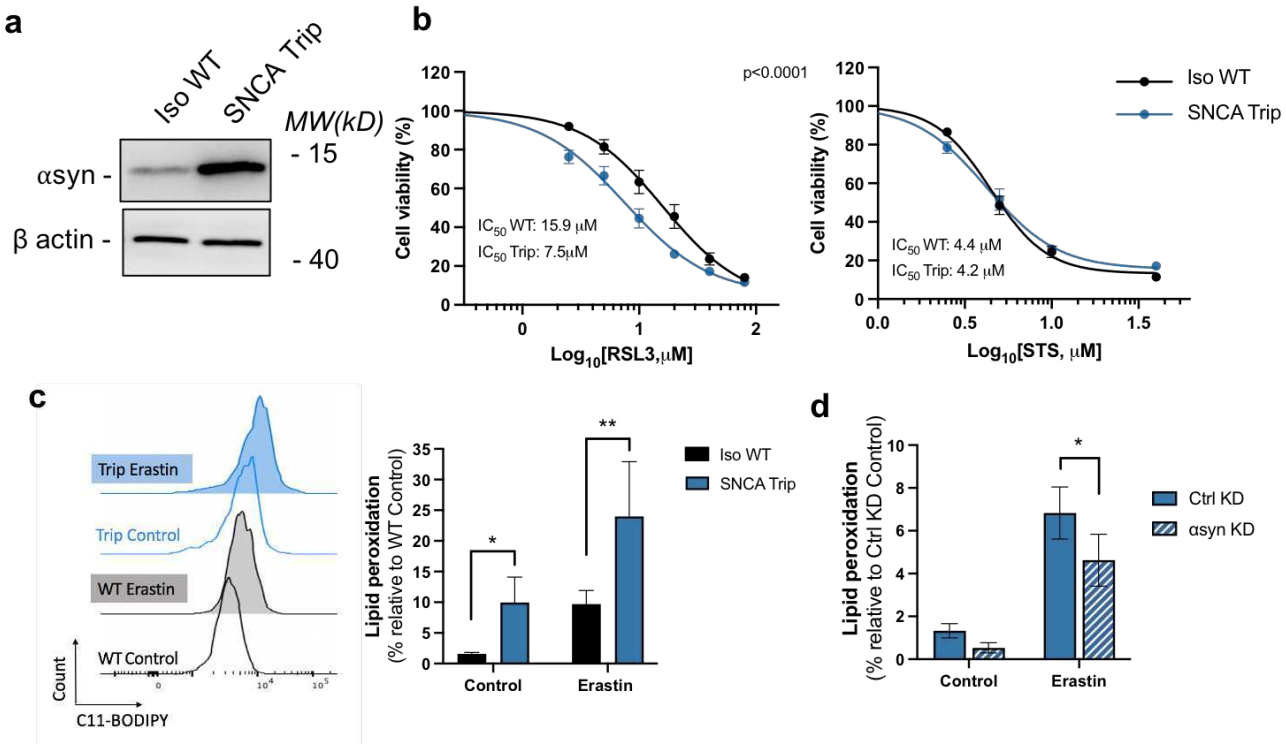

Figure 36. Elevated α-synuclein levels render smNPC-derived midbrain neurons more vulnerable to ferroptosis. **a.** Western blot of α-synuclein in Iso WT and SNCA Trip smNPC derived mDANs. **b.** Non-linear regression dose curves for viability in Iso WT and SNCA Trip smNPC derived mDANs following RSL3 and STS treatments (24h). Curves were fitted to assess whether differences were statistically significant. **c.** Lipid peroxidation analysis after Erastin (80μM, 6h) treatment. **d.** Lipid peroxidation in SNCA Trip mDANS transfected with α-syn siRNA in response to eratin (80μM, 6h) relative to Ctrl KD SCA Trip mDANs. All data is represented as mean ± SEM of three independent experiments. Comparisons were made using the one-tailed, unpaired Student's *t*-test; * p<0.05, **p <0.01

Taken together, the findings obtained with patient's smNPC derived mDANs further support α-syn as a positive modulator of ferroptosis and provide the first direct evidence that ferroptosis may indeed be a key pathological mechanism underlying the dopaminergic neurodegeneration in synucleinopathies associated with α-syn elevation.

7.3 Mice organotypic brain slices to study ferroptosis in the nigrostriatal pathway

Functional and reliable *in vitro* models of PD are valuable for studying mechanisms associated to dopaminergic degeneration. In part due to a greater effectiveness and reduced cost and time required for genetic modulation in *in vitro* models, cellular models represent an optimal tool for performing exploratory studies and decipher molecular pathways. However, the value of 2D neuronal monocultures to model a brain disease remains limited, and studies often require other more complex models to support their working hypothesis. In contrast, organotypic slice cultures from different regions of the central nervous system (CNS) have been successfully used to study neurodegeneration associated with different brain diseases (Gogolla et al., 2006; Cavaliere et al., 2006, 2010; Wu et al., 2020). The culture of OBSs preserve the structural integrity of a brain region and the complexity of neuronal interactions with glial cells. Culture of OBSs therefore represent a useful *ex vivo* intermediate model before conducting *in vivo* experiments to study physiological and pathological features of brain tissue.

Here, we have developed a sagittal OBS culture model that includes all the areas involved in the nigrostriatal pathway – substantia nigra, medial forebrain bundle (MFB) and striatum. The brains of C57Bl6 mice pups aged 8-9 days were dissected and cut along the medial longitudinal fissure to separate the two brain hemisphere (figure 37a). After analysing the morphology of several 350 μm sagittal OBSs and performed TH immunohistochemistry staining, we concluded that slices 3 to 6 contained the entire nigrostriatal pathway (figure 37b). Following brain dissection and sagittal cutting, the OBSs were placed in semipermeable membranes in contact with culture media and were placed in an incubator at 37ºC and 5% CO_2. OBSs were kept in culture for up to 8 days (figure 37a) with culture media changed every two days.

Culturing conditions remarkable affect OBSs viability and this was in fact the biggest struggle we faced when establishing this technique. Using propidium iodide, the viability of neurons within specific brain regions of the OBS was assessed. We often reported an increased dryness and mortality in the centre of the slices, where the thalamus is located, (supplementary figure 6) which we believe it partly due to the size of the slices (~1cm long), meaning the middle region had reduced access to culture media and gas exchange. In order to overcome this issue, we tested several approaches such as increasing the volume of culture media per well and adding PBS in the plate surrounding the wells to increase the humidity

and reduce media evaporation. Unfortunately, these approaches were unsuccessful in reducing OBSs mortality, which remained an unresolved issue.

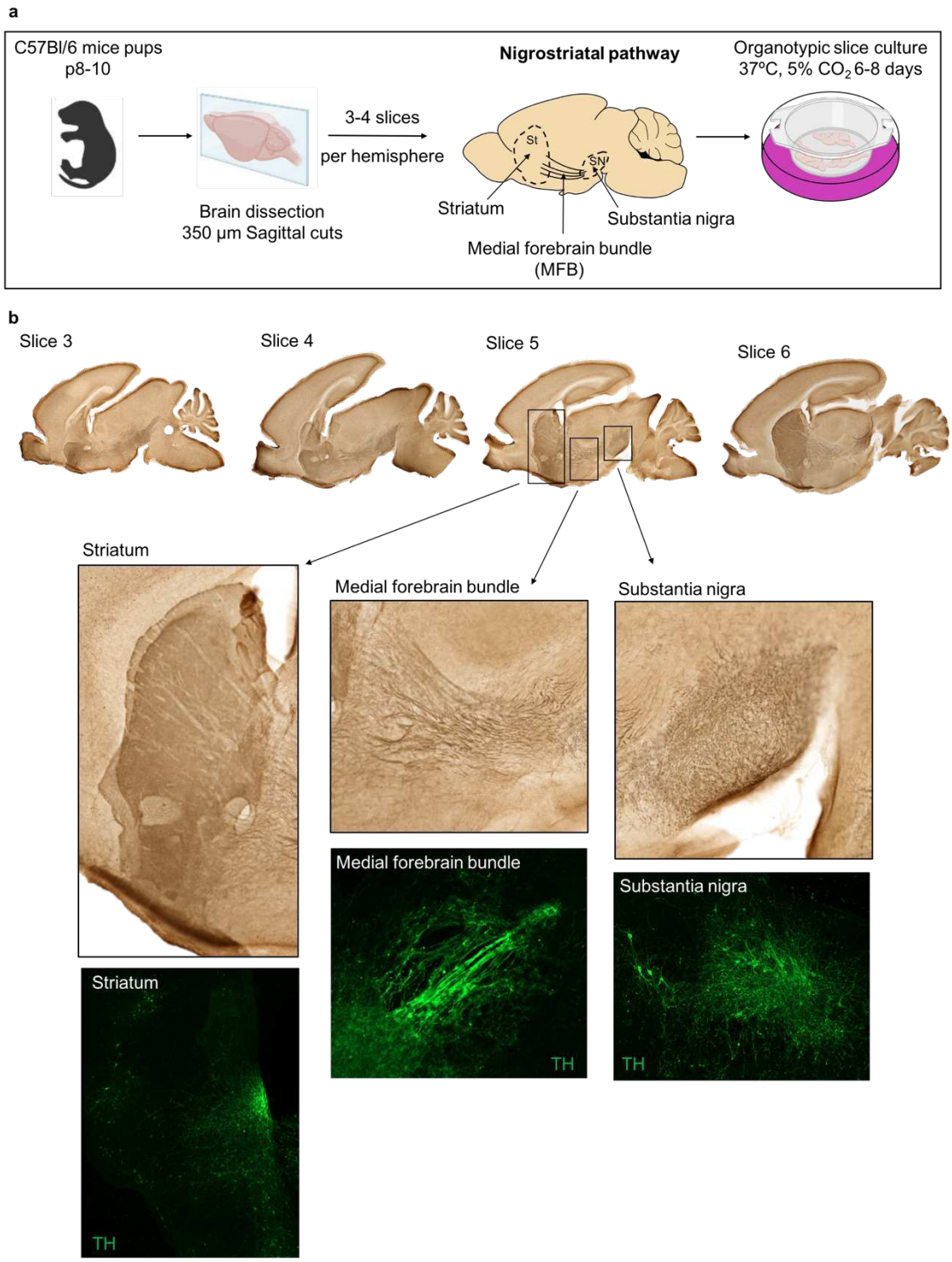

Figure 37. Mouse organotypic brain slice preparation containing the nigrostriatal pathway. **a.** Schematic representation of the procedure to obtain mice OBSs containing the nigrostriatal pathway (striatum, MFB and SN). **b.** TH 3,3'-diaminobenzidine (DAB) and fluorescent immunohistochemistry staining of the nigrostriatal pathway in sagittal OBSs 3 to 6. MFB, medial forebrain bundle; SN, substantia nigra

7.3.1 siRNA-mediated protein knockdown in organotypic brain slices

Once we had optimised the dissection protocol and determined the location of the slices containing the nigrostriatal pathway, we sought to knock-down α-syn and ACSL4 in OBSs by self-deliverable siRNA (Accell siRNA) in order to further characterise the implication of α-syn in ferroptosis sensitivity in dopaminergic neurons. This siRNA-mediated KD approach had previously been reported to efficiently reduce mRNA and protein levels of several target genes in mouse lung and kidney slices (Ruigrok et al., 2017, 2018). Therefore, the siRNA-mediated KD protocol in OBSs was adapted from (Ruigrok et al., 2018).

Accell self-delivery siRNA allow the delivery of siRNA into OBSs independent of transfection reagents. However, serum present in the media can interfere with the penetration of siRNA into neurons, therefore, the culture media had to be adapted to siRNA culture media containing 1% heat inactivated horse serum, instead of 25%, and 2% B-27 serum to partly compensate for the removal of serum. First, we tried incubating slices with no siRNA (non-transfected, NT), non-targeting siRNA (Ctrl), or gene-targeting siRNA against α-syn and ACSL4 from day 0, right after slicing the brains. We tested two different siRNA concentrations (0,5μM and 1 μM) before deciding to use 1μM (protocol 1, supplementary figure 7). Unfortunately, due to the high mortality of OBSs during the first days of culture, we often lost the majority of transfected slices independent of the transfection. In order to overcome the loss of siRNA slices, we decided to slightly adapt the protocol and incubate OBSs with siRNA at day 3 of culture, once we were able to determine the slices that had survived the critical first days of culture (protocol 2, figure 38a). The non-targeting, α-syn and ACSL4 Accell siRNAs were left for 96h before the slices were homogenized and proteins extracted for WB analysis (figure 38a). Overall, we obtained heterogenous results with some transfections reporting KD of our target genes, whilst others showed no effect. Encouragingly, in two independent experiments, we were able to obtain a significant KD of α-syn in OBS incubated with α-syn siRNA from day 3 to day 7 (figure 38b&c). On the other hand, a reduction of ACSL4 protein levels was only observed in one transfection experiment (figure 38b&c), meaning further experiments are required to confirm the ACSL4 KD efficiency. Unfortunately, by the time we started to obtain encouraging siRNA-mediated KD results in OBSs, we ceased experimental work in order to prepare the research article for submission and write this PhD manuscript.

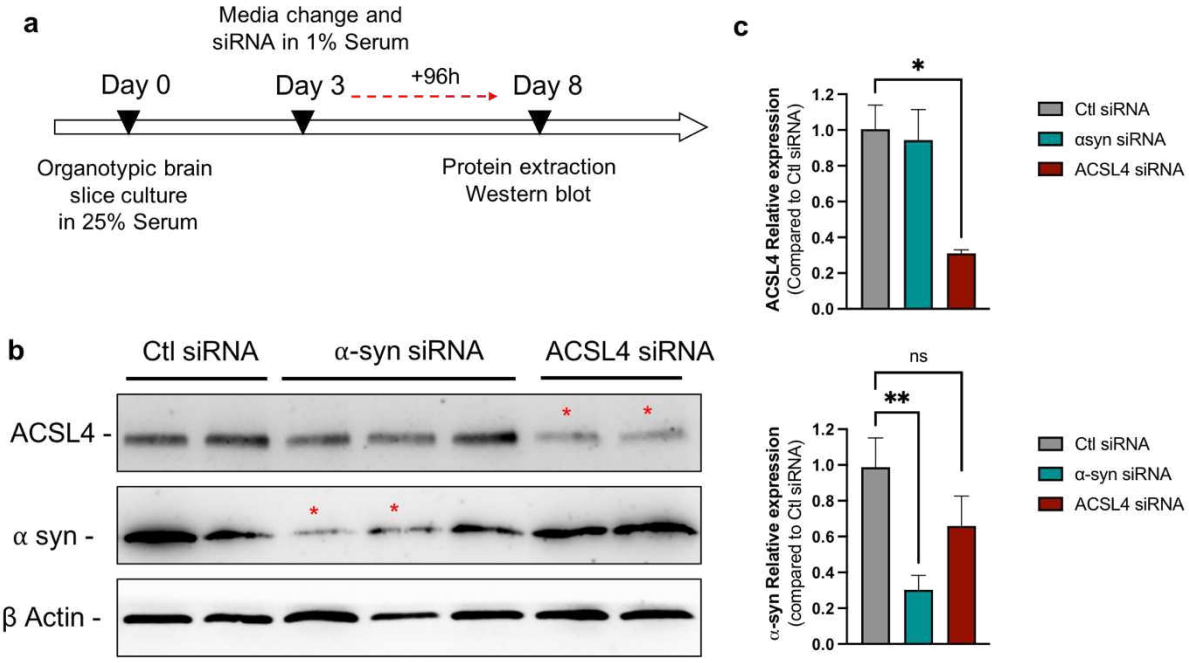

Figure 38. siRNA-mediated KD of α-syn and ACSL4 in mouse organotypic brain slices. **a.** Timeline of the Accell siRNA protocol in OBSs. **b.** Representative WB of one successful KD experiment against α-syn and ACSL4. **c.** ACSL4 and α-syn relative protein expression in Ctrl, α-syn and ACSL4 KD OBSs. ACSL4 expression data represents the mean of one experiment, whilst α-syn expression data represents the mean of two independent experiments. Comparisons were made using the two-tailed Student's *t*-test; * $p<0.05$, ** $p<0.01$, ns. non-significant

7.4 Conclusion

With the use of a second *in vitro* neuronal model, we confirm that the ferroptosis resistant phenotype observed in α-syn depleted LUHMES cells is not cell dependent and represents a robust and novel finding. Indeed, smNPC-derived midbrain neurons lacking α-syn were shown to be protected against RSL3 induced ferroptotic cell death but showed no difference in STS-triggered apoptosis, mirroring the results obtained with the 140 α-syn KO CRISPR/Cas9 and α-syn KD LUHMES cells. The ferroptosis resistance phenotype was also evident when measuring ferroptosis induced lipid peroxidation. Of note, during my first stay at the LCSB, we were only able to optimise the experimental conditions for lipid ROS following Erastin treatment, but not RSL3, hence the use of Erastin in figures 34c and 36c&d.

By the time we had confirmed via three independent approaches (CRISPR/Cas9 KO, siRNA KD in LUHMES cells and CRISPR/Cas9 KO in mDANs), that reducing α-syn in neurons lead to ferroptosis evasion, we were eager to study the effect of α-syn overexpression on ferroptosis sensitivity. During the course of this PhD, this was assessed on smNPC derived mDANs from a PD patient baring the triplication of SNCA which showed increased basal lipid ROS levels and vulnerability to RSL3 induced ferroptotic cell death when compared to the isogenic WT control. Interestingly, SNCA Trip mDANs showed similar apoptosis sensitivity as the isogenic WT cells, suggesting the elevation on α-syn levels primes the cells to be more sensitive to ferroptosis. To our knowledge, ours is the first study to report an increased vulnerability to ferroptosis, as assessed with the use of specific ferroptosis inducers, in patient mDANs baring SNCA triplication.

Towards the end of this PhD, we sought to establish an *ex vivo* model of mice nigrostriatal OBS and perform α-syn and ACSL4 KD via siRNA in the hope of reproducing the results obtained in LUHMES and smNPC derived mDANs. This technique had never been established in our laboratory apart from some rat sagittal OBSs cultures performed at the University of Angers by a previous PhD student. Establishing this technique in our laboratory was proven more difficult than anticipated for several reasons, including the fact that the vibratome used was located in a separate building, which delayed the critical time it took for us to put the slices in culture. In addition, we were confronted with difficulties during the culture which caused a substantial number of slices to die during the first couple days of the culture. We based our culture protocol from (Gogolla et al., 2006) which was described for the culture of hippocampal slices. This study addresses the importance of serum in the media, which constitutes 25% of the media. However, two studies report a deleterious effect of serum and report increased viability of OBSs when switching to serum-free media 3 days after the initiation of the cultures (Kim et al., 2013; Daviaud et al., 2014). Further optimisation of the media composition is required to address the mortality of OBSs in our laboratory. Despite the difficulties confronted, we were able to establish a siRNA-mediated KD protocol which significantly reduced α-syn expression in mice OBSs containing the nigrostriatal pathway. This represents a valuable strategy to further address the implication of ferroptosis in brain neurodegenerative diseases and more specifically the role of α-syn in ferroptosis sensitivity in neurons.

Conclusion and Discussion - Chapter 8:

General conclusions and discussion
§
The role of Ferroptosis in the avenue of Parkinson's Disease research

8.1 Summary of PhD results and discussion

Over the past four years, we have worked towards answering the simple question: "*Does α-synuclein play a role in Ferroptosis?*". The direct association of α-syn with ferroptosis had never been made when this project started in 2018. Today, only one study reports a potential link between the lipid peroxidation induced by α-syn oligomers and ferroptosis (Angelova et al., 2020). Over the course of this PhD project, we have provided some direct proof that α-syn levels in dopaminergic neurons can indeed determine neuronal sensitivity to ferroptosis.

In our laboratory, we have been working with LUHMES cells, a human precursor dopaminergic neuronal line, for almost a decade. These cells represent an optimal *in vitro* model for studying PD-associated mechanisms in part thanks to their rapid and robust differentiation into mature dopaminergic neurons (Scholz et al., 2011; Zhang et al., 2014). To answer our question and tackle the main objective of this project, we first needed to create LUHMES cell lines with stable modifications to the endogenous α-syn. As CRISPR/Cas9 genome editing was becoming more accessible to research laboratories, we decided to implement this technique in our hands for this and future projects to come. Following an optimisation period, we were able to successfully generate three independent homozygous A53T α-syn, two 140 α-syn KO and four full α-syn KO LUHMES sub-clones (Table 6). Using the A53T α-syn subclones, we found that the PD-associated *SNCA* mutation increased the sensitivity of dopaminergic neurons to ferroptosis induced lipid peroxidation and cell death (chapter 5). To our knowledge, this is the first study to ever report a direct association between a PD-linked α-syn mutation and an increased vulnerability to this unique cell death pathway. Interestingly, a study conducted by Sánchez Campos et al., reported an increase in the activity of Acyl-CoA synthetase (ACS), as measured by the generation of [^{3}H]oleoyl-CoA, in N27 dopaminergic neurons overexpressing A53T α-syn (Sánchez Campos et al.,

2018). Although this study did not assess the activity of the other members of the ACS family, in particular the Acyl-CoA synthetase long chain (ACSL) enzymes, this would be interesting to measure in our A53T α-syn dopaminergic neuronal model, since an increase in ACSL4 activity would explain the vulnerability reported against ferroptosis. It is, however, important to consider the findings of Golovko and colleagues who showed that the reduced activity of ACSL enzymes reported in brain of SNCA KO mice, was only restored upon administration of WT α-syn but not the mutant forms (A30P, E46K and A53T) (Golovko et al., 2006). Another study reported higher levels of plasmalogens, a class of phospholipids recently implicated in ferroptosis (refer to chapter 2 for more information) in brains of A53T α-syn mice (Yakunin et al., 2014), further implicating the familial A53T α-syn PD mutation with greater ferroptosis sensitivity. Furthermore, mesencephalic neurons overexpressing the A53T α-syn mutant form were found to accumulate PUFAs, such as arachidonic acid (AA), adrenic acid (AdrA) and docosahexaenoic acid (DHA), at the level of the plasma membrane when compared to WT cells (Sharon et al., 2003). As previously mentioned in chapter 2, the PUFAs composition of the plasma membrane can determine ferroptosis sensitivity whereby an increase in PUFAs results in greater ferroptosis vulnerability.

Via CRISPR/Cas9 genome editing in LUHMES cells, we accidently obtained 140 α-syn KO clones which lacked the main α-syn isoform. Interestingly, the 140 α-syn KO cell lines were protected against both ferroptosis-induced lipid peroxidation and cell death, but showed no difference in apoptosis sensitivity, providing the first direct link between endogenous α-syn levels and ferroptosis sensitivity in a neuronal cell line. By this point, it remains unclear whether the protective phenotype observed is a result of the absence of the full length 140 α-syn isoform, an increase in the 126 α-syn isoform or both. Indeed, as described in the chapter 3, a reduction in 126 α-syn levels has been reported in the brains of DLB and AD patients (Beyer et al., 2006). Importantly, the shorter 126 α-syn isoforms lacks its lipid binding affinity and has been suggested to act as a protective, less prone to aggregation isoform (Beyer, 2006a; Gámez-Valero and Beyer, 2018). These observations suggests that it may be the ability of α-syn to bind lipids that is involved in ferroptosis modulation. Moreover, several studies conducted on α-syn KO or KD cell and animal models have shown impairments in the metabolism of iron (impaired ferritinophagy (Baksi and Singh, 2017) or TfR-mediated iron import (Baksi et al., 2016)) and the metabolism of lipids (altered plasma membrane composition (Sharon et al., 2003) or ACSL activity (Golovko et

al., 2006)) which support our hypothesis and initial findings that endogenous α-syn can modulate ferroptosis sensitivity. In order to further investigate the association between α-syn levels and ferroptosis sensitivity, we have generated 4 independent full α-syn KO CRISPR/Cas9 sub-clones (Table 6), by targeting and deleting exon 2 of the *SNCA* gene, where the START codon is located (supplementary figure 3). This approach was recently reported by Chen et al., to successfully KO α-syn from human embryonic stem cells and iPSCs (Chen et al., 2019b). Throughout this PhD, these cell lines have not been fully characterised nor ferroptosis sensitivity properly assessed in them, thus representing experiments for the future of this research project.

CRISPR/Cas9 mediated α-syn modification	Clone name	Details
A53T α-syn	XC5 3D10 3F4	LUHMES subclone with an homozygous A53T α-syn mutation in exon 3
140 α-syn KO	F6 G5	LUHMES subclones lacking the main full length α-syn isoform
α-syn KO	1F7 3D9 3F5 4C4	Full α-syn KO LUHMES subclones generated by targeting exon 2

Table 6. List of CRISPR/Cas9 LUHMES sub-clones generated throughout the PhD project.

In parallel to using CRISPR/Cas9 sub-clones, we were determined to confirm our initial results using a different genome editing technique which would support our novel discovery by providing a complementary approach and limiting the potential variations induced by single cell clonal selection. To this extent, we were able to reproduce the ferroptosis resistance phenotype in α-syn KD LUHMES cells as evident from reduced ferroptosis-induced lipid peroxidation and cell death. As ACSL4 is a well-established pro-ferroptosis regulator, we compared the effects of knocking-down α-syn to those of ACSL4 depletion, in order to confirm that ferroptosis was induced in all experimental designs. Furthermore, a parallel PhD project in our laboratory reported ferroptosis induction in LUHMES cells with a co-treatment of AA and Fe. This findings shows that this unique cell death pathway can be induced by means other than drugs, and represent an experimental design more relevant to PD pathology as both iron and lipid metabolism alterations and conspicuous features of PD neuropathology (Dexter et al., 1989b, 1994; Yoritaka et al., 1996; Sharon et al., 2003; Hopes et al., 2016; Fais et al., 2021). Interestingly, we were able to show

that α-syn levels here again can determine the sensitivity of neurons to ferroptosis induced by AA and Fe to a similar extent as ACSL4. Of note, a study conducted by Perez and colleagues showed that dietary dihomogamma-linoleic acid (DGLA; 20:3) can also trigger ferroptotic cell death of germ cells, sperm and oocytes in *C. elegans* and human cancer cells (Watts and Browse, 2006; Deline et al., 2013; Perez et al., 2020). Using HT-1080 and HEK cells, they confirmed ferroptosis induction since Fer-1 rescued cell death and lipid peroxidation following DGLA treatment. It is interesting to note that ferroptosis in human cancer cells was induced only with high doses of DGLA (500μM), whilst a lower dose (250μM) was not lethal to HT-1080 (Perez et al., 2020). In comparison, we used significantly lower doses of AA (20μM) in combination with low sub-toxic doses of Fe (20μM) in order to trigger ferroptosis. We believe this approach to be more relevant, despite the uncertainty around the exact concentration of AA in human brains.

As we confirmed that α-syn is indeed implicated in determining ferroptosis sensitivity in neurons, we sought the study the cellular mechanisms which could have led to such a protection against ferroptosis when α-syn levels are reduced. Based on the extensive literature showing an interplay between α-syn and plasma membrane fatty acid content, were decided to measure the PL composition in LUHMES cells depleted of α-syn or ACSL4. To our surprise, we reported a selective and prominent reduction in ether-PL, a predominant class of phospholipids in the brain. Such a α-syn-dependent modulation of ether-PL had never been reported before, a part from one study previously mentioned showing increased plasmalogens in the brain of A53T mice (Yakunin et al., 2014). Importantly, two recent studies have elegantly shown that ether-PL are essential in driving ferroptosis. Indeed, both (Zou et al., 2020a) and (Cui et al., 2021) confirmed that depletion of the ether-PL biosynthesis enzymes (GNPAT, FAR1, AGPS and AGPAT3) markedly promoted ferroptosis resistance in diverse cancer cells. The work conducted by Zou et al., further showed that depletion of these genes results in decreased levels of PUFA containing ether-PL (PUFA-ether-PL), and supplementation of PUFA-ether-PL in cells with deficiency in ether-PL synthesis resensitized these cells to ferroptosis (Zou et al., 2020a). Interestingly Zou and colleagues showed that supplementing cells with either PUFA-ether-PL or their non-ether-linked PL counterparts have similar sensitizing effect on ferroptosis (Zou et al., 2020a). These results suggest that PUFA-ether-PL are not intrinsically more sensitive to ferroptosis-induced peroxidation than other PUFA-PLs. However, ether-PL are essential in driving ferroptosis perhaps because they represent an abundant pool of PUFA-PLs that are available

for peroxidation during ferroptosis. This statement is supported by the fact that SH-SY5Y neuroblastoma cells acquire sensitivity to ferroptosis as the levels of ether-PL increase during differentiation. Of note, the brain has the highest proportion of ether-PL, more specifically ether-PE. In line with this, LUHMES dopaminergic neurons have a greater proportion of PUFA-ether-PE compared to PUFA-diacyl-PE: 30 ± 0.95% vs 21.89 ± 0.65%, respectively (supplementary figure 4), suggesting that ferroptosis in neurons may be governed by peroxidation of ether-PL.

It is worth discussing that the double bond in plasmalogens is believed to provide them with some antioxidant properties against the propagation of lipid peroxidation (Shi et al., 2016; Dean and Lodhi, 2018). Indeed, the role of ether-PL as pro-ferroptotic molecular species is opposed by the work of Perez and colleagues who report that inhibiting AGPS, the rate limiting enzyme in ether-PL synthesis, sensitized HT-1080 cells to cell death induced by DGLA and RSL3 (Perez et al., 2020). However, the data from pharmacologic inhibition of AGPS in this study differs from the results from Zou et al., showing that genetic ablation of AGPS supressed ferroptosis (Zou et al., 2020a). This discrepancy may lie in the different cell lines used in these two studies and the different approaches used (pharmacological vs genetic) to study the implication of AGPS dependent ether-PL in ferroptosis.

Here, we report that depleting LUHMES cells of α-syn or ACSL4 caused a reduction in ether-PL despite no observable changes in mRNA and protein levels of peroxisome markers and enzymes involved in the synthesis of ether-PL. Among the different proteins studied, we found no changes in the plasmalogen selective iPLA2 protein levels, suggesting that enzymatic removal of ether-PL from the plasma membrane is unlikely. However, an increase in enzymatic activity cannot be excluded, not the implication of other phospholipases enzymes. Indeed, some studies have suggested that phospholipase D (PLD) may play a role in plasmalogen removal from the plasma membrane (Van Iderstine et al., 1997; Tsuboi et al., 2011). Interestingly, α-syn was reported to inhibit phospholipase D2 (PLD2) (Jenco et al., 1998; Ahn et al., 2002), suggesting another mean by which α-syn may modulate the plasma membrane composition. A more in-depth analysis of the different phospholipases including their enzymatic activity in the different α-syn conditions would allow us to further explore this possibility.

One possible mechanism by which α-syn depletion leads to reduced PUFA and more specifically ether-PLs content in the plasma membrane is that α-syn somehow mediates ACSL (or even ACSL4) activity. This hypothesis is supported by the work conducted by

Golovko and colleagues (Golovko et al., 2006). In the study, the authors report a reduced activity of ACSL enzymes in the brain microsome fraction SNCA KO mice. Of note, they used AA, the preferential substrate of ACSL4, as the PUFA for measuring the activity of ACSL, suggesting the observed reduction in ACSL activity may actually represent an impaired ACSL4 activity in the brains of SNCA KO mice. Importantly, this ACSL activity was restored upon addition of exogenous α-syn, indicating a role of α-syn in the control of ACSL4 in AA-CoA formation, and subsequent incorporation into plasma membrane phospholipids. In order to assess the hypothesis that downregulating α-syn in LUHMES neurons lead to a reduction in ACSL4 activity, thus PUFA content in the plasma membrane, the activity of ACSL4 needs to be directly assessed in our different synuclein *in vitro* models. In order to achieve this, some initial optimisation work including radioactive ^{3}H-AA handling and liquid scintillation measurements of ^{3}H-AA-CoA was conducted, in parallel to a biochemical assay designed to measure the by-product of fatty acyl-CoA generation, pyrophosphate (PPi). Whilst some promising measures were obtained with this later assay using palmitic acid as the substrate, we were unable to detect a signal with AA. In addition, we were unable to separate the contributions of the several ACSL enzymes present in the cells. To overcome this limitation, we have planned on measuring the activity of recombinant ACSL4 incubated with recombinant monomeric α-syn, in the hope of simplifying the model. These experiments were planned and anticipated should the reviewers of the research article demand them.

Another possible mechanism by which α-syn depletion causes ether-PL deficiency in the plasma membrane might be via an impaired transport and fusion of vesicles containing the ether-PL precursors and mature ether-PL along the peroxisome-ER-plasma membrane route. Indeed, as previously described in the introduction, α-syn has been extensively linked to vesicular transport and fusion with the plasma membrane (Cabin et al., 2002; Vargas et al., 2014; Lou et al., 2017; Lautenschläger et al., 2018). In order to assess this hypothesis, proximity ligation or fluorescence resonance energy transfer (FRET) assays could be performed to determine whether α-syn colocalizes or interacts with peroxisomes. Furthermore, by labelling ether-PL precursors with a fluorescent tag, it might be possible to determine whether α-syn is implicated in the maturation and incorporation of ether-PL into the plasma membrane.

Finally, is it important to discuss the roles of ether-PL and plasmalogens in health and disease. As previously mentioned, plasmalogens represent the major constituent of the

glycerophosphoethanolamine fraction of the human brain, comprising over 50% of this fraction. Due to their abundance in cellular membranes, they are believed to play a role in membrane dynamics including synaptic transmission (Paul et al., 2019). Indeed, PE plasmalogens (pPE) we shown to facilitate a more rapid membrane fusion of synaptic vesicles, with a faster rate in vesicles containing PE plasmalogens with arachidonic acid (Glaser and Gross, 1994), which may in part explain the need for abundant AA in the brain. Moreover, plasmalogens have long been studied for their anti-oxidant potential. The characteristics of plasmalogens that makes them anti-oxidants include the enhanced electron density of the vinyl ether bond that is thought to make it more susceptible to ROS attack than diacyl-PLs (Lessig and Fuchs, 2009), and the suggested slow propagation of the plasmalogen hydroperoxyl radicals (Murphy, 2001). Indeed, the oxidation of PUFA within diacyl-PLs was shown to be delayed in the presence of plasmalogens (Reiss et al., 1997). This suggests that ether-PLs are preferentially oxidised over diacyl-PLs under certain oxidative environment, suggesting they may indeed play a predominant role in ferroptosis in PD. The involvement of plasmalogens in neurodegenerative diseases has mostly been studied in the context of Alzheimer's disease, whilst their potential implication in PD remains largely unknown. One study reported lower plasma plasmalogens levels in PD patients (Dragonas et al., 2009), whilst another observed the same phenomenon in the frontal cortex from PD patients (Fabelo et al., 2011). This reduction in plasmalogen levels can partly be explained by the overall increased oxidative stress observed in PD patients. As ferroptosis is becoming increasingly implicated in PD pathology, the potential role of plasmalogens in the disease may be revisited in future research, along with this newly described function of α-syn in modulating ether-PL plasma membrane composition.

Via a newly established collaboration with the Luxembourg Centre for Systems Biomedicine (LCSB), we were able to confirm the implication of α-syn in determining ferroptosis sensitivity in a second highly relevant *in vitro* model: Patient's smNPC-derived midbrain neurons (mDANs) with SNCA KO. In line with the results obtained in LUHMES cells, we showed that SNCA KO mDANs were significantly more resistant to RSL3-induced cell death and Erastin-induced lipid peroxidation when compared to WT cells. Importantly, I was also able to study ferroptosis sensitivity in mDANs from a PD patient baring a SNCA triplication. The elevation of α-syn alone led to increased levels of lipid peroxidation under basal condition, a findings supported by a previous report in SNCA Trip iPSC derived cortical neurons which also present elevated basal lipid peroxidation (Angelova et al., 2020).

Increased susceptibility to oxidative stress in SNCA Trip iPSC derived mDANs has also been reported in another study conducted by (Byers et al., 2011) which showed elevation in certain oxidative stress related genes and increased cell death in response to hydrogen peroxide treatments. However, ours is the first study showing a specific increased vulnerability to ferroptosis induced cell death and lipid peroxidation, implicating ferroptosis in synucleinopathy conditions. These results further strengthen our novel finding that endogenous α-syn can determine the fate of neurons regarding ferroptosis induction.

Finally, towards the end of this PhD, we decided to investigate our *in vitro* findings in an *ex vivo* OBS model of the nigrostriatal pathway. A considerable amount of time and effort was put towards implementing this technique in our laboratory and establish a siRNA-mediated KD of α-syn and ACSL4 protocol in OBSs. Unfortunately, due to a lack of time, I was not able to study ferroptosis sensitivity in OBSs where α-syn levels had been reduced by siRNA.

Overall, this PhD project has successfully answered our initial question and clearly shown that α-syn does indeed play a role in determining ferroptosis sensitivity in neurons by modulating the plasma membrane ether-PL composition.

8.2 Perspectives

Having reached the end of this PhD program and being able to look back at the work conducted over the past four years, I cannot help but think of additional experiments which would allow to further understand how α-syn modulates the plasma membrane composition of neurons, thus determining their sensitivity to ferroptosis. First of all, the CRISPR/Cas9 cell lines generated represent an optimal model in which to further assess the implication of α-syn in ferroptosis (table 6). A more in-depth analysis of ferroptosis sensitivity in our A53T α-syn cell lines would provide some definite evidence for the implication of PD-linked α-syn mutation to ferroptosis. This could include analysing other ferroptosis biomarkers such as 4-hydroxynonenal (4-HNE), 15-hydroxyeicosatetraenoic acid (15-HETE) and isoprostanoids (all end-products of enzymatic and non-enzymatic lipid peroxidation), and investigating whether the increased vulnerability of the A53T α-syn neurons to ferroptosis could be rescued by genetically or pharmacologically blocking pro-ferroptotic enzymes such as ACSL4 and ALOX15/15B. In addition, a lipidomic analysis would also be of interest in our A53T α-syn dopaminergic neuronal model in order to investigate the potential alterations to the metabolism of lipids. Another obvious next step is to study ferroptosis sensitivity in the

four full α-syn KO clones and measure their plasma membrane PL composition. It would also be relevant to measure the other members of the synuclein family in case β or γ-synuclein are upregulated upon α-syn depletion.

Moreover, further experiments would allow a more in-depth characterisation of the implication of α-syn in the metabolism of ether-PL and the subsequent role of ether-PL in ferroptosis sensitivity in LUHMES cells. For example, LUHMES cells could be supplemented with ether-PL precursors, such as Bathyl alcohol (alkyl DHAP; C18:1o) or 1-O-1'-(Z)-octadecenyl-sn-glycerol (C18plasm), in order to boost the synthesis of ether-PL and determine whether this results in an increased sensitivity to ferroptosis. Furthermore, the supplementation with ether-PL precursors could be conducted on α-syn and ACSL4 KD LUHMES cells and the plasma composition analysed by LC-HRMS in order to assess whether genetic modulation of α-syn and ACSL4 can directly impair the maturation of alkyl DHAP or C18plasm into ether-PL. Finally, genetic modulation of ether-PL biosynthesis enzymes (i.e., AGPS, GNPAT or AGPAT3 KD/KO) and ferroptosis assessment would further contribute towards deciphering the role of this class of PL in the sensitivity of dopaminergic neurons to ferroptosis. As previously mentioned, it would be interesting the measure the plasma membrane composition in the A53T α-syn CRISPR clones in order to investigate whether the point mutation may induce changes to the levels of ether-PL, thus explaining the increased ferroptosis vulnerability. The plasma membrane composition could also be analysed in the 140 α-syn KO and full α-syn KO CRISPR clones in order to confirm that α-syn regulation of ferroptosis is indeed dependent on its ability to modulate ether-PLs. On the other hand, the plasma membrane composition of the SNCA KO and SNCA Trip smNPC derived mDANs would allow to further determine the role of α-syn in modulating the ether-PL plasma membrane composition in neurons.

Based on the encouraging results obtained with the SNCA Trip smNPC derived mDANs, we sought to establish an α-syn overexpression model in LUHMES cells in our laboratory. At first, we thought on designing a CRISPR activation (CRISPRa) plasmid in order to increase transcription of endogenous SNCA. This technology utilizes nuclease-deactivated Cas9 (dCas9) that binds to the target genomic region (particularly within the promotor region), but cannot generate DBS and instead results in transcriptional control. CRISPRa employs dCas9 fused to transcriptional activation domains which can be directed to promoter regions by guide RNA resulting in transcriptional activation and increased

expression of the target gene. Some initial work was performed in order to generate and amplify several dCas9 plasmids, both to activate and suppress SNCA transcription (supplementary table x), however, we were unable to proceed with the transfection of LUHMES cells and generation stable dCas9 subclones due to lack of time. The validity of such plasmids was confirmed by sequencing and therefore they remain available for future experiments. On the other hand, a new collaboration with Dr. Solange Desagher has enabled us to obtain a LUHMES cell line overexpressing α-syn obtained by lentiviral stable transduction. The characterisation of such cell line (and its transduction control cell line) is currently the topic of a Master's project in our laboratory. Once we've validated the cell lines, ferroptosis sensitivity measures and membrane PL composition analysis could be conducted in order to determine whether the elevation of α-syn expression may lead to changes in membrane PUFAs content, as previously reported in other cell types and patients brain tissue (Sharon et al., 2003), and increase ferroptosis sensitivity in LUHMES cells.

Finally, the role of ether-PL in PD pathology deserved further elucidations as little is known on the topic. With the use of transgenic mice models overexpressing WT or mutant α-syn, we would be able to determine whether correlations exist between degeneration of dopaminergic neurons, cognitive or motor impairments and ether- PL levels in the brain or biofluids.

8.3 Future research avenues in Parkinson's Disease and Ferroptosis research

New disease modifying therapies and novel therapeutic strategies are in high demand for PD patients. Ultimately, the greatest achievement would be to slow the progression of the disease enough for patients to live with minimal disabilities until a late age. Therefore, in order to efficiently design molecules that will slow the progression of the disease, it is required that *i*. we fully decipher and characterise the pathological mechanisms that cause the death of dopaminergic neurons, allowing for targeted molecules, and *ii*. we discover biomarkers characteristic of the prodromal phase of the disease, thus enabling early therapeutic interventions. Moreover, it is important to consider that there is no "one Parkinson's Disease", and that in fact, several initial triggers and effectors may lead to the emergence of the disease via different pathological pathways. As research advances and new pathological mechanisms are associated with the neurodegeneration in PD, one might consider a combined treatment which would target several pathological pathways simultaneously.

Importantly, an emerging knowledge on ferroptosis is shedding a different perspective on several physiological and pathophysiological conditions, including neurodegenerative diseases. Indeed, for decades, researchers have been heavily characterising several aspects of PD pathology as independent components, which now may be linked in conferring susceptibility to ferroptosis. These include elevated lipid peroxidation (Dexter et al., 1994, 1989b), glutathione depletion (Sofic et al., 1992; Sian et al., 1994), DJ-1 (Bonifati et al., 2003; Blackinton et al., 2009) and CoQ10 deficiency (Mischley et al., 2012), GPX4 reduction (Bellinger et al., 2011), mitochondriopathy (Cadenas and Davies, 2000; Lin and Beal, 2006), iron accumulation (Dexter et al., 1987, 1989a; Devos et al., 2014) and α-synuclein aggregation (Spillantini et al., 1997; Shahmoradian et al., 2019). Based on this information it is hard to believe that the extensive similarities between PD neuropathology and aspects of the ferroptosis cell death pathway are due to a mere coincidence. We therefore propose ferroptosis as a key contributor to PD progression with broader implications in synucleinopathies. Deciphering the role of α-synuclein in the iron and/or lipid components of the ferroptotic pathway now represents an area of increased research focus that is hoped to not only provide a greater understanding to the physiological function of the protein but also elucidate one of its neuropathological features in PD.

The fact that iron chelation, an established anti-ferroptotic strategy, has shown the first clinical benefits in two independent clinical trials on early-PD (Devos et al., 2014; Martin-Bastida et al., 2017) should encourage further progress in targeting ferroptosis. Ultimately, the role of ferroptosis in neurodegenerative disorders will only be confirmed when additional anti-ferroptotic therapies advance successfully to clinical trial.

References

Abbas, N., Lücking, C.B., Ricard, S., Dürr, A., Bonifati, V., De Michele, G., Bouley, S., Vaughan, J.R., Gasser, T., Marconi, R., et al. (1999). A wide variety of mutations in the parkin gene are responsible for autosomal recessive parkinsonism in Europe. French Parkinson's Disease Genetics Study Group and the European Consortium on Genetic Susceptibility in Parkinson's Disease. Hum. Mol. Genet. *8*, 567–574. https://doi.org/10.1093/hmg/8.4.567.

Abeliovich, A., Schmitz, Y., Fariñas, I., Choi-Lundberg, D., Ho, W.H., Castillo, P.E., Shinsky, N., Verdugo, J.M., Armanini, M., Ryan, A., et al. (2000). Mice lacking alpha-synuclein display functional deficits in the nigrostriatal dopamine system. Neuron *25*, 239–252. https://doi.org/10.1016/s0896-6273(00)80886-7.

Acosta, S.A., Tajiri, N., de la Pena, I., Bastawrous, M., Sanberg, P.R., Kaneko, Y., and Borlongan, C.V. (2015). Alpha-synuclein as a pathological link between chronic traumatic brain injury and Parkinson's disease. J. Cell. Physiol. *230*, 1024–1032. https://doi.org/10.1002/jcp.24830.

Agid, Y., Chase, T., and Marsden, D. (1998). Adverse reactions to levodopa: drug toxicity or progression of disease? The Lancet *351*, 851–852. https://doi.org/10.1016/S0140-6736(05)70285-3.

Agid, Y., Olanow, C., and Mizuno, Y. (2002). Levodopa: why the controversy? The Lancet *360*, 575. https://doi.org/10.1016/S0140-6736(02)09733-7.

Ahn, B.-H., Rhim, H., Kim, S.Y., Sung, Y.-M., Lee, M.-Y., Choi, J.-Y., Wolozin, B., Chang, J.-S., Lee, Y.H., Kwon, T.K., et al. (2002). alpha-Synuclein interacts with phospholipase D isozymes and inhibits pervanadate-induced phospholipase D activation in human embryonic kidney-293 cells. J. Biol. Chem. *277*, 12334–12342. https://doi.org/10.1074/jbc.M110414200.

Alim, I., Caulfield, J.T., Chen, Y., Swarup, V., Geschwind, D.H., Ivanova, E., Seravalli, J., Ai, Y., Sansing, L.H., Ste Marie, E.J., et al. (2019). Selenium Drives a Transcriptional Adaptive Program to Block Ferroptosis and Treat Stroke. Cell *177*, 1262-1279.e25. https://doi.org/10.1016/j.cell.2019.03.032.

Angelova, P.R., Choi, M.L., Berezhnov, A.V., Horrocks, M.H., Hughes, C.D., De, S., Rodrigues, M., Yapom, R., Little, D., Dolt, K.S., et al. (2020). Alpha synuclein aggregation drives ferroptosis: an interplay of iron, calcium and lipid peroxidation. Cell Death Differ. 1–16. https://doi.org/10.1038/s41418-020-0542-z.

Appel-Cresswell, S., Vilarino-Guell, C., Encarnacion, M., Sherman, H., Yu, I., Shah, B., Weir, D., Thompson, C., Szu-Tu, C., Trinh, J., et al. (2013). Alpha-synuclein p.H50Q, a novel pathogenic mutation for Parkinson's disease. Mov. Disord. Off. J. Mov. Disord. Soc. *28*, 811–813. https://doi.org/10.1002/mds.25421.

Arai, K., Kato, N., Kashiwado, K., and Hattori, T. (2000). Pure autonomic failure in association with human alpha-synucleinopathy. Neurosci. Lett. *296*, 171–173. https://doi.org/10.1016/s0304-3940(00)01623-2.

Ascherio, A., and Schwarzschild, M.A. (2016). The epidemiology of Parkinson's disease: risk factors and prevention. Lancet Neurol. *15*, 1257–1272. https://doi.org/10.1016/S1474-4422(16)30230-7.

Ascherio, A., Chen, H., Weisskopf, M.G., O'Reilly, E., McCullough, M.L., Calle, E.E., Schwarzschild, M.A., and Thun, M.J. (2006). Pesticide exposure and risk for Parkinson's disease. Ann. Neurol. *60*, 197–203. https://doi.org/10.1002/ana.20904.

Askanas, V., Engel, W.K., Alvarez, R.B., McFerrin, J., and Broccolini, A. (2000). Novel immunolocalization of alpha-synuclein in human muscle of inclusion-body myositis, regenerating and necrotic muscle fibers, and at neuromuscular junctions. J. Neuropathol. Exp. Neurol. *59*, 592–598. https://doi.org/10.1093/jnen/59.7.592.

Ayton, S., Lei, P., Duce, J.A., Wong, B.X.W., Sedjahtera, A., Adlard, P.A., Bush, A.I., and Finkelstein, D.I. (2013). Ceruloplasmin dysfunction and therapeutic potential for Parkinson disease. Ann. Neurol. *73*, 554–559. https://doi.org/10.1002/ana.23817.

Ayton, S., Lei, P., Hare, D.J., Duce, J.A., George, J.L., Adlard, P.A., McLean, C., Rogers, J.T., Cherny, R.A., Finkelstein, D.I., et al. (2015). Parkinson's disease iron deposition caused by nitric oxide-induced loss of β-amyloid precursor protein. J. Neurosci. Off. J. Soc. Neurosci. *35*, 3591–3597. https://doi.org/10.1523/JNEUROSCI.3439-14.2015.

Bai, J., Zhang, Z., Liu, M., and Li, C. (2015). α-synuclein-lanthanide metal ions interaction: binding sites, conformation and fibrillation. BMC Biophys. *9*, 1. https://doi.org/10.1186/s13628-016-0026-1.

Baksi, S., and Singh, N. (2017). α-Synuclein impairs ferritinophagy in the retinal pigment epithelium: Implications for retinal iron dyshomeostasis in Parkinson's disease. Sci. Rep. *7*, 12843. https://doi.org/10.1038/s41598-017-12862-x.

Baksi, S., Tripathi, A.K., and Singh, N. (2016). Alpha-synuclein modulates retinal iron homeostasis by facilitating the uptake of transferrin-bound iron: Implications for visual manifestations of Parkinson's disease. Free Radic. Biol. Med. *97*, 292–306. https://doi.org/10.1016/j.freeradbiomed.2016.06.025.

Baldi, I., Cantagrel, A., Lebailly, P., Tison, F., Dubroca, B., Chrysostome, V., Dartigues, J.-F., and Brochard, P. (2003). Association between Parkinson's disease and exposure to pesticides in southwestern France. Neuroepidemiology *22*, 305–310. https://doi.org/10.1159/000071194.

Balgoma, D., and Hedeland, M. (2021). Etherglycerophospholipids and ferroptosis: structure, regulation, and location. Trends Endocrinol. Metab. TEM *32*, 960–962. https://doi.org/10.1016/j.tem.2021.08.005.

Baptista, M.J., O'Farrell, C., Daya, S., Ahmad, R., Miller, D.W., Hardy, J., Farrer, M.J., and Cookson, M.R. (2003). Co-ordinate transcriptional regulation of dopamine synthesis genes by alpha-synuclein in human neuroblastoma cell lines. J. Neurochem. *85*, 957–968. https://doi.org/10.1046/j.1471-4159.2003.01742.x.

Barbuti, P., Antony, P., Santos, B., Massart, F., Cruciani, G., Dording, C., Arias, J., Schwamborn, J., and Krüger, R. (2020a). Using High-Content Screening to Generate Single-

Cell Gene-Corrected Patient-Derived iPS Clones Reveals Excess Alpha-Synuclein with Familial Parkinson's Disease Point Mutation A30P. Cells *9*, 2065. https://doi.org/10.3390/cells9092065.

Barbuti, P.A., Santos, B.F.R., Dording, C.M., Cruciani, G., Massart, F., Hummel, A., and Krüger, R. (2020b). Generation of two iPS cell lines (HIHDNDi001-A and HIHDNDi001-B) from a Parkinson's disease patient carrying the heterozygous p.A30P mutation in SNCA. Stem Cell Res. *48*, 101951. https://doi.org/10.1016/j.scr.2020.101951.

Barceló-Coblijn, G., Golovko, M.Y., Weinhofer, I., Berger, J., and Murphy, E.J. (2007). Brain neutral lipids mass is increased in alpha-synuclein gene-ablated mice. J. Neurochem. *101*, 132–141. https://doi.org/10.1111/j.1471-4159.2006.04348.x.

Bartels, M., Weckbecker, D., Kuhn, P.-H., Ryazanov, S., Leonov, A., Griesinger, C., Lichtenthaler, S.F., Bötzel, K., and Giese, A. (2019). Iron-mediated aggregation and toxicity in a novel neuronal cell culture model with inducible alpha-synuclein expression. Sci. Rep. *9*, 9100. https://doi.org/10.1038/s41598-019-45298-6.

Bartels, T., Choi, J.G., and Selkoe, D.J. (2011). α-Synuclein occurs physiologically as a helically folded tetramer that resists aggregation. Nature *477*, 107–110. https://doi.org/10.1038/nature10324.

Bartels, T., Kim, N.C., Luth, E.S., and Selkoe, D.J. (2014). N-alpha-acetylation of α-synuclein increases its helical folding propensity, GM1 binding specificity and resistance to aggregation. PloS One *9*, e103727. https://doi.org/10.1371/journal.pone.0103727.

Battino, M., Littarru, G.P., Gorini, A., and Villa, R.F. (1996). Coenzyme Q, peroxidation and cytochrome oxidase features after parkinson's-like disease by MPTP toxicity in intra-synaptic and non-synaptic mitochondria from Macaca fascicularis cerebral cortex and hippocampus: action of dihydroergocriptine. Neurochem. Res. *21*, 1505–1514. https://doi.org/10.1007/BF02533098.

Beaudoin-Chabot, C., Wang, L., Smarun, A.V., Vidović, D., Shchepinov, M.S., and Thibault, G. (2019). Deuterated Polyunsaturated Fatty Acids Reduce Oxidative Stress and Extend the Lifespan of C. elegans. Front. Physiol. *10*. https://doi.org/10.3389/fphys.2019.00641.

Beckett, C.S., Kell, P.J., Creer, M.H., and McHowat, J. (2007). Phospholipase A2-catalyzed hydrolysis of plasmalogen phospholipids in thrombin-stimulated human platelets. Thromb. Res. *120*, 259–268. https://doi.org/10.1016/j.thromres.2006.09.005.

Belaidi, A.A., and Bush, A.I. (2016). Iron neurochemistry in Alzheimer's disease and Parkinson's disease: targets for therapeutics. J. Neurochem. *139*, 179–197. https://doi.org/10.1111/jnc.13425.

Belaidi, A.A., Gunn, A.P., Wong, B.X., Ayton, S., Appukuttan, A.T., Roberts, B.R., Duce, J.A., and Bush, A.I. (2018). Marked Age-Related Changes in Brain Iron Homeostasis in Amyloid Protein Precursor Knockout Mice. Neurother. J. Am. Soc. Exp. Neurother. *15*, 1055–1062. https://doi.org/10.1007/s13311-018-0656-x.

Bellinger, F.P., Bellinger, M.T., Seale, L.A., Takemoto, A.S., Raman, A.V., Miki, T., Manning-Boğ, A.B., Berry, M.J., White, L.R., and Ross, G.W. (2011). Glutathione

Peroxidase 4 is associated with Neuromelanin in Substantia Nigra and Dystrophic Axons in Putamen of Parkinson's brain. Mol. Neurodegener. *6*, 8. https://doi.org/10.1186/1750-1326-6-8.

Bellinger, F.P., Raman, A.V., Rueli, R.H., Bellinger, M.T., Dewing, A.S., Seale, L.A., Andres, M.A., Uyehara-Lock, J.H., White, L.R., Ross, G.W., et al. (2012). Changes in selenoprotein P in substantia nigra and putamen in Parkinson's disease. J. Park. Dis. *2*, 115–126. https://doi.org/10.3233/JPD-2012-11052.

Bellucci, A., Navarria, L., Zaltieri, M., Falarti, E., Bodei, S., Sigala, S., Battistin, L., Spillantini, M., Missale, C., and Spano, P. (2011). Induction of the unfolded protein response by α-synuclein in experimental models of Parkinson's disease. J. Neurochem. *116*, 588–605. https://doi.org/10.1111/j.1471-4159.2010.07143.x.

Ben Gedalya, T., Loeb, V., Israeli, E., Altschuler, Y., Selkoe, D.J., and Sharon, R. (2009). α–Synuclein and PolyUnsaturated Fatty Acids Promote Clathrin Mediated Endocytosis and Synaptic Vesicle Recycling. Traffic Cph. Den. *10*, 218–234. https://doi.org/10.1111/j.1600-0854.2008.00853.x.

Bersuker, K., Hendricks, J.M., Li, Z., Magtanong, L., Ford, B., Tang, P.H., Roberts, M.A., Tong, B., Maimone, T.J., Zoncu, R., et al. (2019). The CoQ oxidoreductase FSP1 acts parallel to GPX4 to inhibit ferroptosis. Nature *575*, 688–692. https://doi.org/10.1038/s41586-019-1705-2.

Bertoncini, C.W., Fernandez, C.O., Griesinger, C., Jovin, T.M., and Zweckstetter, M. (2005). Familial mutants of alpha-synuclein with increased neurotoxicity have a destabilized conformation. J. Biol. Chem. *280*, 30649–30652. https://doi.org/10.1074/jbc.C500288200.

Beyer, K. (2006a). Alpha-synuclein structure, posttranslational modification and alternative splicing as aggregation enhancers. Acta Neuropathol. (Berl.) *112*, 237–251. https://doi.org/10.1007/s00401-006-0104-6.

Beyer, K. (2006b). α-Synuclein structure, posttranslational modification and alternative splicing as aggregation enhancers. Acta Neuropathol. (Berl.) *112*, 237–251. https://doi.org/10.1007/s00401-006-0104-6.

Beyer, K., Humbert, J., Ferrer, A., Lao, J.I., Carrato, C., López, D., Ferrer, I., and Ariza, A. (2006). Low alpha-synuclein 126 mRNA levels in dementia with Lewy bodies and Alzheimer disease. Neuroreport *17*, 1327–1330. https://doi.org/10.1097/01.wnr.0000224773.66904.e7.

Bharucha, K.J., Friedman, J.K., Vincent, A.S., and Ross, E.D. (2008). Lower serum ceruloplasmin levels correlate with younger age of onset in Parkinson's disease. J. Neurol. *255*, 1957–1962. https://doi.org/10.1007/s00415-009-0063-7.

Bi, M., Du, X., Jiao, Q., Liu, Z., and Jiang, H. (2020). α-Synuclein regulates iron homeostasis via preventing parkin-mediated DMT1 ubiquitylation in Parkinson's disease models. ACS Chem. Neurosci. https://doi.org/10.1021/acschemneuro.0c00196.

Blackinton, J., Kumaran, R., van der Brug, M.P., Ahmad, R., Olson, L., Galter, D., Lees, A., Bandopadhyay, R., and Cookson, M.R. (2009). Post-transcriptional regulation of mRNA

associated with DJ-1 in sporadic Parkinson disease. Neurosci. Lett. *452*, 8–11. https://doi.org/10.1016/j.neulet.2008.12.053.

Blauwendraat, C., Heilbron, K., Vallerga, C.L., Bandres-Ciga, S., von Coelln, R., Pihlstrøm, L., Simón-Sánchez, J., Schulte, C., Sharma, M., Krohn, L., et al. (2019). Parkinson's disease age at onset genome-wide association study: Defining heritability, genetic loci, and α-synuclein mechanisms. Mov. Disord. Off. J. Mov. Disord. Soc. *34*, 866–875. https://doi.org/10.1002/mds.27659.

Bonifati, V., Rizzu, P., van Baren, M.J., Schaap, O., Breedveld, G.J., Krieger, E., Dekker, M.C.J., Squitieri, F., Ibanez, P., Joosse, M., et al. (2003). Mutations in the DJ-1 gene associated with autosomal recessive early-onset parkinsonism. Science *299*, 256–259. https://doi.org/10.1126/science.1077209.

Borie, C., Gasparini, F., Verpillat, P., Bonnet, A.-M., Agid, Y., Hetet, G., Brice, A., Dürr, A., Grandchamp, B., and French Parkinson's disease genetic study group (2002). Association study between iron-related genes polymorphisms and Parkinson's disease. J. Neurol. *249*, 801–804. https://doi.org/10.1007/s00415-002-0704-6.

Boussaad, I., Obermaier, C.D., Hanss, Z., Bobbili, D.R., Bolognin, S., Glaab, E., Wołyńska, K., Weisschuh, N., Conti, L.D., May, C., et al. (2020). A patient-based model of RNA mis-splicing uncovers treatment targets in Parkinson's disease. Sci. Transl. Med. https://doi.org/10.1126/scitranslmed.aau3960.

Braak, H., Del Tredici, K., Bratzke, H., Hamm-Clement, J., Sandmann-Keil, D., and Rüb, U. (2002). Staging of the intracerebral inclusion body pathology associated with idiopathic Parkinson's disease (preclinical and clinical stages). J. Neurol. *249 Suppl 3*, III/1-5. https://doi.org/10.1007/s00415-002-1301-4.

Braak, H., Del Tredici, K., Rüb, U., de Vos, R.A.I., Jansen Steur, E.N.H., and Braak, E. (2003). Staging of brain pathology related to sporadic Parkinson's disease. Neurobiol. Aging *24*, 197–211. https://doi.org/10.1016/s0197-4580(02)00065-9.

Brenna, J.T., and Diau, G.-Y. (2007). The influence of dietary docosahexaenoic acid and arachidonic acid on central nervous system polyunsaturated fatty acid composition. Prostaglandins Leukot. Essent. Fatty Acids *77*, 247–250. https://doi.org/10.1016/j.plefa.2007.10.016.

Brice, A. (2005). Genetics of Parkinson's disease: LRRK2 on the rise. Brain J. Neurol. *128*, 2760–2762. https://doi.org/10.1093/brain/awh676.

Brites, P., Waterham, H.R., and Wanders, R.J.A. (2004). Functions and biosynthesis of plasmalogens in health and disease. Biochim. Biophys. Acta BBA - Mol. Cell Biol. Lipids *1636*, 219–231. https://doi.org/10.1016/j.bbalip.2003.12.010.

Broersen, K., van den Brink, D., Fraser, G., Goedert, M., and Davletov, B. (2006). Alpha-synuclein adopts an alpha-helical conformation in the presence of polyunsaturated fatty acids to hinder micelle formation. Biochemistry *45*, 15610–15616. https://doi.org/10.1021/bi061743l.

van der Brug, M.P., Singleton, A., Gasser, T., and Lewis, P.A. (2015). Parkinson's disease: From human genetics to clinical trials. Sci. Transl. Med. *7*, 205ps20. https://doi.org/10.1126/scitranslmed.aaa8280.

Bu, B., Tong, X., Li, D., Hu, Y., He, W., Zhao, C., Hu, R., Li, X., Shao, Y., Liu, C., et al. (2017). N-Terminal Acetylation Preserves α-Synuclein from Oligomerization by Blocking Intermolecular Hydrogen Bonds. ACS Chem. Neurosci. *8*, 2145–2151. https://doi.org/10.1021/acschemneuro.7b00250.

Burbulla, L.F., Song, P., Mazzulli, J.R., Zampese, E., Wong, Y.C., Jeon, S., Santos, D.P., Blanz, J., Obermaier, C.D., Strojny, C., et al. (2017). Dopamine oxidation mediates mitochondrial and lysosomal dysfunction in Parkinson's disease. Science *357*, 1255–1261. https://doi.org/10.1126/science.aam9080.

Burré, J., Sharma, M., Tsetsenis, T., Buchman, V., Etherton, M.R., and Südhof, T.C. (2010). Alpha-synuclein promotes SNARE-complex assembly in vivo and in vitro. Science *329*, 1663–1667. https://doi.org/10.1126/science.1195227.

Burré, J., Sharma, M., and Südhof, T.C. (2014). α-Synuclein assembles into higher-order multimers upon membrane binding to promote SNARE complex formation. Proc. Natl. Acad. Sci. U. S. A. *111*, E4274-4283. https://doi.org/10.1073/pnas.1416598111.

Burré, J., Sharma, M., and Südhof, T.C. (2018). Cell Biology and Pathophysiology of α-Synuclein. Cold Spring Harb. Perspect. Med. *8*, a024091. https://doi.org/10.1101/cshperspect.a024091.

Burton, G.W., and Ingold, K.U. (1986). Vitamin E: application of the principles of physical organic chemistry to the exploration of its structure and function. Acc. Chem. Res. *19*, 194–201. https://doi.org/10.1021/ar00127a001.

Bussell, R., and Eliezer, D. (2003). A structural and functional role for 11-mer repeats in alpha-synuclein and other exchangeable lipid binding proteins. J. Mol. Biol. *329*, 763–778. https://doi.org/10.1016/s0022-2836(03)00520-5.

Byers, B., Cord, B., Nguyen, H.N., Schüle, B., Fenno, L., Lee, P.C., Deisseroth, K., Langston, J.W., Pera, R.R., and Palmer, T.D. (2011). SNCA triplication Parkinson's patient's iPSC-derived DA neurons accumulate α-synuclein and are susceptible to oxidative stress. PloS One *6*, e26159. https://doi.org/10.1371/journal.pone.0026159.

Cabin, D.E., Shimazu, K., Murphy, D., Cole, N.B., Gottschalk, W., McIlwain, K.L., Orrison, B., Chen, A., Ellis, C.E., Paylor, R., et al. (2002). Synaptic vesicle depletion correlates with attenuated synaptic responses to prolonged repetitive stimulation in mice lacking alpha-synuclein. J. Neurosci. Off. J. Soc. Neurosci. *22*, 8797–8807. .

Cadenas, E., and Davies, K.J. (2000). Mitochondrial free radical generation, oxidative stress, and aging. Free Radic. Biol. Med. *29*, 222–230. https://doi.org/10.1016/s0891-5849(00)00317-8.

Cadet, J.L. (1986). The potential use of vitamin E and selenium in Parkinsonism. Med. Hypotheses *20*, 87–94. https://doi.org/10.1016/0306-9877(86)90089-7.

Canet-Avilés, R.M., Wilson, M.A., Miller, D.W., Ahmad, R., McLendon, C., Bandyopadhyay, S., Baptista, M.J., Ringe, D., Petsko, G.A., and Cookson, M.R. (2004). The Parkinson's disease protein DJ-1 is neuroprotective due to cysteine-sulfinic acid-driven mitochondrial localization. Proc. Natl. Acad. Sci. U. S. A. *101*, 9103–9108. https://doi.org/10.1073/pnas.0402959101.

Canli, Ö., Alankuş, Y.B., Grootjans, S., Vegi, N., Hültner, L., Hoppe, P.S., Schroeder, T., Vandenabeele, P., Bornkamm, G.W., and Greten, F.R. (2016). Glutathione peroxidase 4 prevents necroptosis in mouse erythroid precursors. Blood *127*, 139–148. https://doi.org/10.1182/blood-2015-06-654194.

Cao, J., Chen, X., Jiang, L., Lu, B., Yuan, M., Zhu, D., Zhu, H., He, Q., Yang, B., and Ying, M. (2020). DJ-1 suppresses ferroptosis through preserving the activity of S-adenosyl homocysteine hydrolase. Nat. Commun. *11*, 1251. https://doi.org/10.1038/s41467-020-15109-y.

Carboni, E., Tatenhorst, L., Tönges, L., Barski, E., Dambeck, V., Bähr, M., and Lingor, P. (2017). Deferiprone Rescues Behavioral Deficits Induced by Mild Iron Exposure in a Mouse Model of Alpha-Synuclein Aggregation. Neuromolecular Med. *19*, 309–321. https://doi.org/10.1007/s12017-017-8447-9.

Cardoso, B.R., Hare, D.J., Bush, A.I., and Roberts, B.R. (2017). Glutathione peroxidase 4: a new player in neurodegeneration? Mol. Psychiatry *22*, 328–335. https://doi.org/10.1038/mp.2016.196.

Carmona-Torre, F., Martinez-Urbistondo, D., and Del Pozo, J.L. (2013). Neurostimulation for Parkinson's disease with early motor complications. N. Engl. J. Med. *368*, 2037. https://doi.org/10.1056/NEJMc1303485.

Castellani, R.J., Siedlak, S.L., Perry, G., and Smith, M.A. (2000). Sequestration of iron by Lewy bodies in Parkinson's disease. Acta Neuropathol. (Berl.) *100*, 111–114. https://doi.org/10.1007/s004010050001.

Cavaliere, F., Dinkel, K., and Reymann, K. (2006). The subventricular zone releases factors which can be protective in oxygen/glucose deprivation-induced cortical damage: an organotypic study. Exp. Neurol. *201*, 66–74. https://doi.org/10.1016/j.expneurol.2006.03.020.

Cavaliere, F., Vicente, E.S., and Matute, C. (2010). An organotypic culture model to study nigro-striatal degeneration. J. Neurosci. Methods *188*, 205–212. https://doi.org/10.1016/j.jneumeth.2010.02.008.

Chandra, S., Chen, X., Rizo, J., Jahn, R., and Südhof, T.C. (2003). A broken alpha -helix in folded alpha -Synuclein. J. Biol. Chem. *278*, 15313–15318. https://doi.org/10.1074/jbc.M213128200.

Charcot, J.M. (1886). Lecons sur, les maladies du système nerveux (Lecrosnier et Babé).

Chen, L., and Feany, M.B. (2005). Alpha-synuclein phosphorylation controls neurotoxicity and inclusion formation in a Drosophila model of Parkinson disease. Nat. Neurosci. *8*, 657–663. https://doi.org/10.1038/nn1443.

Chen, B., Wen, X., Jiang, H., Wang, J., Song, N., and Xie, J. (2019a). Interactions between iron and α-synuclein pathology in Parkinson's disease. Free Radic. Biol. Med. *141*, 253–260. https://doi.org/10.1016/j.freeradbiomed.2019.06.024.

Chen, D., Tavana, O., Chu, B., Erber, L., Chen, Y., Baer, R., and Gu, W. (2017). NRF2 Is a Major Target of ARF in p53-Independent Tumor Suppression. Mol. Cell *68*, 224-232.e4. https://doi.org/10.1016/j.molcel.2017.09.009.

Chen, R.H.C., Wislet-Gendebien, S., Samuel, F., Visanji, N.P., Zhang, G., Marsilio, D., Langman, T., Fraser, P.E., and Tandon, A. (2013). α-Synuclein Membrane Association Is Regulated by the Rab3a Recycling Machinery and Presynaptic Activity♦. J. Biol. Chem. *288*, 7438–7449. https://doi.org/10.1074/jbc.M112.439497.

Chen, Y., Dolt, K.S., Kriek, M., Baker, T., Downey, P., Drummond, N.J., Canham, M.A., Natalwala, A., Rosser, S., and Kunath, T. (2019b). Engineering synucleinopathy-resistant human dopaminergic neurons by CRISPR -mediated deletion of the *SNCA* gene. Eur. J. Neurosci. *49*, 510–524. https://doi.org/10.1111/ejn.14286.

Chinta, S.J., Mallajosyula, J.K., Rane, A., and Andersen, J.K. (2010). Mitochondrial α-synuclein accumulation impairs complex I function in dopaminergic neurons and results in increased mitophagy in vivo. Neurosci. Lett. *486*, 235–239. https://doi.org/10.1016/j.neulet.2010.09.061.

Choi, D.-H., Cristóvão, A.C., Guhathakurta, S., Lee, J., Joh, T.H., Beal, M.F., and Kim, Y.-S. (2012). NADPH oxidase 1-mediated oxidative stress leads to dopamine neuron death in Parkinson's disease. Antioxid. Redox Signal. *16*, 1033–1045. https://doi.org/10.1089/ars.2011.3960.

Choubey, V., Safiulina, D., Vaarmann, A., Cagalinec, M., Wareski, P., Kuum, M., Zharkovsky, A., and Kaasik, A. (2011). Mutant A53T alpha-synuclein induces neuronal death by increasing mitochondrial autophagy. J. Biol. Chem. *286*, 10814–10824. https://doi.org/10.1074/jbc.M110.132514.

Chu, B., Kon, N., Chen, D., Li, T., Liu, T., Jiang, L., Song, S., Tavana, O., and Gu, W. (2019). ALOX12 is required for p53-mediated tumour suppression through a distinct ferroptosis pathway. Nat. Cell Biol. *21*, 579–591. https://doi.org/10.1038/s41556-019-0305-6.

Chu, Y., Dodiya, H., Aebischer, P., Olanow, C.W., and Kordower, J.H. (2009). Alterations in lysosomal and proteasomal markers in Parkinson's disease: relationship to alpha-synuclein inclusions. Neurobiol. Dis. *35*, 385–398. https://doi.org/10.1016/j.nbd.2009.05.023.

Coelho, M., and Ferreira, J.J. (2012). Late-stage Parkinson disease. Nat. Rev. Neurol. *8*, 435–442. https://doi.org/10.1038/nrneurol.2012.126.

Colla, E., Jensen, P.H., Pletnikova, O., Troncoso, J.C., Glabe, C., and Lee, M.K. (2012). Accumulation of toxic α-synuclein oligomer within endoplasmic reticulum occurs in α-synucleinopathy in vivo. J. Neurosci. Off. J. Soc. Neurosci. *32*, 3301–3305. https://doi.org/10.1523/JNEUROSCI.5368-11.2012.

Coltorti, M., De Ritis, F., and Giusti, G. (1956). [Enzymatic mechanisms of transsulfuration in biology and clinical practice]. G. Clin. Med. *37*, 285–323. .

Cong, L., Ran, F.A., Cox, D., Lin, S., Barretto, R., Habib, N., Hsu, P.D., Wu, X., Jiang, W., Marraffini, L.A., et al. (2013). Multiplex genome engineering using CRISPR/Cas systems. Science *339*, 819–823. https://doi.org/10.1126/science.1231143.

Connolly, B.S., and Lang, A.E. (2014). Pharmacological treatment of Parkinson disease: a review. JAMA *311*, 1670–1683. https://doi.org/10.1001/jama.2014.3654.

Conway, K.A., Harper, J.D., and Lansbury, P.T. (1998). Accelerated in vitro fibril formation by a mutant alpha-synuclein linked to early-onset Parkinson disease. Nat. Med. *4*, 1318–1320. https://doi.org/10.1038/3311.

Cooper, A.A., Gitler, A.D., Cashikar, A., Haynes, C.M., Hill, K.J., Bhullar, B., Liu, K., Xu, K., Strathearn, K.E., Liu, F., et al. (2006). Alpha-synuclein blocks ER-Golgi traffic and Rab1 rescues neuron loss in Parkinson's models. Science *313*, 324–328. https://doi.org/10.1126/science.1129462.

da Costa, C.A., Sunyach, C., Giaime, E., West, A., Corti, O., Brice, A., Safe, S., Abou-Sleiman, P.M., Wood, N.W., Takahashi, H., et al. (2009). Transcriptional repression of p53 by parkin and impairment by mutations associated with autosomal recessive juvenile Parkinson's disease. Nat. Cell Biol. *11*, 1370–1375. https://doi.org/10.1038/ncb1981.

Costello, D.J., Walsh, S.L., Harrington, H.J., and Walsh, C.H. (2004). Concurrent hereditary haemochromatosis and idiopathic Parkinson's disease: a case report series. J. Neurol. Neurosurg. Psychiatry *75*, 631–633. https://doi.org/10.1136/jnnp.2003.027441.

Cozza, G., Rossetto, M., Bosello-Travain, V., Maiorino, M., Roveri, A., Toppo, S., Zaccarin, M., Zennaro, L., and Ursini, F. (2017). Glutathione peroxidase 4-catalyzed reduction of lipid hydroperoxides in membranes: The polar head of membrane phospholipids binds the enzyme and addresses the fatty acid hydroperoxide group toward the redox center. Free Radic. Biol. Med. *112*, 1–11. https://doi.org/10.1016/j.freeradbiomed.2017.07.010.

Crawford, M.A., Hassam, A.G., and Williams, G. (1976). Essential fatty acids and fetal brain growth. Lancet Lond. Engl. *1*, 452–453. https://doi.org/10.1016/s0140-6736(76)91476-8.

Cristóvão, A.C., Choi, D.-H., Baltazar, G., Beal, M.F., and Kim, Y.-S. (2009). The role of NADPH oxidase 1-derived reactive oxygen species in paraquat-mediated dopaminergic cell death. Antioxid. Redox Signal. *11*, 2105–2118. https://doi.org/10.1089/ARS.2009.2459.

Crowther, R.A., Jakes, R., Spillantini, M.G., and Goedert, M. (1998). Synthetic filaments assembled from C-terminally truncated alpha-synuclein. FEBS Lett. *436*, 309–312. https://doi.org/10.1016/s0014-5793(98)01146-6.

Cui, W., Liu, D., Gu, W., and Chu, B. (2021). Peroxisome-driven ether-linked phospholipids biosynthesis is essential for ferroptosis. Cell Death Differ. *28*, 2536–2551. https://doi.org/10.1038/s41418-021-00769-0.

Dai, E., Zhang, W., Cong, D., Kang, R., Wang, J., and Tang, D. (2020a). AIFM2 blocks ferroptosis independent of ubiquinol metabolism. Biochem. Biophys. Res. Commun. *523*, 966–971. https://doi.org/10.1016/j.bbrc.2020.01.066.

Dai, E., Meng, L., Kang, R., Wang, X., and Tang, D. (2020b). ESCRT-III-dependent membrane repair blocks ferroptosis. Biochem. Biophys. Res. Commun. *522*, 415–421. https://doi.org/10.1016/j.bbrc.2019.11.110.

Daviaud, N., Garbayo, E., Lautram, N., Franconi, F., Lemaire, L., Perez-Pinzon, M., and Montero-Menei, C.N. (2014). Modeling nigrostriatal degeneration in organotypic cultures, a new ex vivo model of Parkinson's disease. Neuroscience *256*, 10–22. https://doi.org/10.1016/j.neuroscience.2013.10.021.

Davidson, W.S., Jonas, A., Clayton, D.F., and George, J.M. (1998). Stabilization of alpha-synuclein secondary structure upon binding to synthetic membranes. J. Biol. Chem. *273*, 9443–9449. https://doi.org/10.1074/jbc.273.16.9443.

Davies, P., Moualla, D., and Brown, D.R. (2011). Alpha-synuclein is a cellular ferrireductase. PloS One *6*, e15814. https://doi.org/10.1371/journal.pone.0015814.

Davis, G.C., Williams, A.C., Markey, S.P., Ebert, M.H., Caine, E.D., Reichert, C.M., and Kopin, I.J. (1979). Chronic Parkinsonism secondary to intravenous injection of meperidine analogues. Psychiatry Res. *1*, 249–254. https://doi.org/10.1016/0165-1781(79)90006-4.

De Franceschi, G., Frare, E., Bubacco, L., Mammi, S., Fontana, A., and de Laureto, P.P. (2009). Molecular insights into the interaction between alpha-synuclein and docosahexaenoic acid. J. Mol. Biol. *394*, 94–107. https://doi.org/10.1016/j.jmb.2009.09.008.

Dean, J.M., and Lodhi, I.J. (2018). Structural and functional roles of ether lipids. Protein Cell *9*, 196–206. https://doi.org/10.1007/s13238-017-0423-5.

Deas, E., Cremades, N., Angelova, P.R., Ludtmann, M.H.R., Yao, Z., Chen, S., Horrocks, M.H., Banushi, B., Little, D., Devine, M.J., et al. (2016). Alpha-Synuclein Oligomers Interact with Metal Ions to Induce Oxidative Stress and Neuronal Death in Parkinson's Disease. Antioxid. Redox Signal. *24*, 376–391. https://doi.org/10.1089/ars.2015.6343.

DeBerardinis, R.J., Lum, J.J., Hatzivassiliou, G., and Thompson, C.B. (2008). The biology of cancer: metabolic reprogramming fuels cell growth and proliferation. Cell Metab. *7*, 11–20. https://doi.org/10.1016/j.cmet.2007.10.002.

Dehay, B., Bové, J., Rodríguez-Muela, N., Perier, C., Recasens, A., Boya, P., and Vila, M. (2010). Pathogenic lysosomal depletion in Parkinson's disease. J. Neurosci. Off. J. Soc. Neurosci. *30*, 12535–12544. https://doi.org/10.1523/JNEUROSCI.1920-10.2010.

Deline, M.L., Vrablik, T.L., and Watts, J.L. (2013). Dietary supplementation of polyunsaturated fatty acids in Caenorhabditis elegans. J. Vis. Exp. JoVE https://doi.org/10.3791/50879.

Deng, H., Wu, Y., and Jankovic, J. (2015). The EIF4G1 gene and Parkinson's disease. Acta Neurol. Scand. *132*, 73–78. https://doi.org/10.1111/ane.12397.

Devi, L., Raghavendran, V., Prabhu, B.M., Avadhani, N.G., and Anandatheerthavarada, H.K. (2008). Mitochondrial import and accumulation of alpha-synuclein impair complex I in human dopaminergic neuronal cultures and Parkinson disease brain. J. Biol. Chem. *283*, 9089–9100. https://doi.org/10.1074/jbc.M710012200.

Devos, D., Moreau, C., Devedjian, J.C., Kluza, J., Petrault, M., Laloux, C., Jonneaux, A., Ryckewaert, G., Garçon, G., Rouaix, N., et al. (2014). Targeting chelatable iron as a therapeutic modality in Parkinson's disease. Antioxid. Redox Signal. *21*, 195–210. https://doi.org/10.1089/ars.2013.5593.

Devos, D., Moreau, C., Kyheng, M., Garçon, G., Rolland, A.S., Blasco, H., Gelé, P., Timothée Lenglet, T., Veyrat-Durebex, C., Corcia, P., et al. (2019). A ferroptosis–based panel of prognostic biomarkers for Amyotrophic Lateral Sclerosis. Sci. Rep. *9*, 1–6. https://doi.org/10.1038/s41598-019-39739-5.

Devos, D., Cabantchik, Z.I., Moreau, C., Danel, V., Mahoney-Sanchez, L., Bouchaoui, H., Gouel, F., Rolland, A.-S., Duce, J.A., Devedjian, J.-C., et al. (2020). Conservative iron chelation for neurodegenerative diseases such as Parkinson's disease and amyotrophic lateral sclerosis. J. Neural Transm. https://doi.org/10.1007/s00702-019-02138-1.

Devos, D., Hirsch, E., and Wyse, R. (2021). Seven Solutions for Neuroprotection in Parkinson's Disease. Mov. Disord. Off. J. Mov. Disord. Soc. *36*, 306–316. https://doi.org/10.1002/mds.28379.

Dexter, D., Carter, C., Agid, F., Agid, Y., Lees, A.J., Jenner, P., and Marsden, C.D. (1986). Lipid peroxidation as cause of nigral cell death in Parkinson's disease. Lancet Lond. Engl. *2*, 639–640. https://doi.org/10.1016/s0140-6736(86)92471-2.

Dexter, D.T., Wells, F.R., Agid, F., Agid, Y., Lees, A.J., Jenner, P., and Marsden, C.D. (1987). Increased nigral iron content in postmortem parkinsonian brain. Lancet Lond. Engl. *2*, 1219–1220. https://doi.org/10.1016/s0140-6736(87)91361-4.

Dexter, D.T., Wells, F.R., Lees, A.J., Agid, F., Agid, Y., Jenner, P., and Marsden, C.D. (1989a). Increased nigral iron content and alterations in other metal ions occurring in brain in Parkinson's disease. J. Neurochem. *52*, 1830–1836. https://doi.org/10.1111/j.1471-4159.1989.tb07264.x.

Dexter, D.T., Carter, C.J., Wells, F.R., Javoy-Agid, F., Agid, Y., Lees, A., Jenner, P., and Marsden, C.D. (1989b). Basal lipid peroxidation in substantia nigra is increased in Parkinson's disease. J. Neurochem. *52*, 381–389. https://doi.org/10.1111/j.1471-4159.1989.tb09133.x.

Dexter, D.T., Carayon, A., Vidailhet, M., Ruberg, M., Agid, F., Agid, Y., Lees, A.J., Wells, F.R., Jenner, P., and Marsden, C.D. (1990). Decreased ferritin levels in brain in Parkinson's disease. J. Neurochem. *55*, 16–20. https://doi.org/10.1111/j.1471-4159.1990.tb08814.x.

Dexter, D.T., Holley, A.E., Flitter, W.D., Slater, T.F., Wells, F.R., Daniel, S.E., Lees, A.J., Jenner, P., and Marsden, C.D. (1994). Increased levels of lipid hydroperoxides in the parkinsonian substantia nigra: an HPLC and ESR study. Mov. Disord. Off. J. Mov. Disord. Soc. *9*, 92–97. https://doi.org/10.1002/mds.870090115.

Di Domenico, F., Tramutola, A., and Butterfield, D.A. (2017). Role of 4-hydroxy-2-nonenal (HNE) in the pathogenesis of alzheimer disease and other selected age-related neurodegenerative disorders. Free Radic. Biol. Med. *111*, 253–261. https://doi.org/10.1016/j.freeradbiomed.2016.10.490.

Dickson, D.W., Ruan, D., Crystal, H., Mark, M.H., Davies, P., Kress, Y., and Yen, S.H. (1991). Hippocampal degeneration differentiates diffuse Lewy body disease (DLBD) from Alzheimer's disease: light and electron microscopic immunocytochemistry of CA2-3 neurites specific to DLBD. Neurology *41*, 1402–1409. https://doi.org/10.1212/wnl.41.9.1402.

Dikiy, I., and Eliezer, D. (2014). N-terminal acetylation stabilizes N-terminal helicity in lipid- and micelle-bound α-synuclein and increases its affinity for physiological membranes. J. Biol. Chem. *289*, 3652–3665. https://doi.org/10.1074/jbc.M113.512459.

Dixon, S.J., and Stockwell, B.R. (2014). The role of iron and reactive oxygen species in cell death. Nat. Chem. Biol. *10*, 9–17. https://doi.org/10.1038/nchembio.1416.

Dixon, S.J., Lemberg, K.M., Lamprecht, M.R., Skouta, R., Zaitsev, E.M., Gleason, C.E., Patel, D.N., Bauer, A.J., Cantley, A.M., Yang, W.S., et al. (2012). Ferroptosis: an iron-dependent form of nonapoptotic cell death. Cell *149*, 1060–1072. https://doi.org/10.1016/j.cell.2012.03.042.

Dixon, S.J., Winter, G.E., Musavi, L.S., Lee, E.D., Snijder, B., Rebsamen, M., Superti-Furga, G., and Stockwell, B.R. (2015). Human Haploid Cell Genetics Reveals Roles for Lipid Metabolism Genes in Nonapoptotic Cell Death. ACS Chem. Biol. *10*, 1604–1609. https://doi.org/10.1021/acschembio.5b00245.

Do Van, B., Gouel, F., Jonneaux, A., Timmerman, K., Gelé, P., Pétrault, M., Bastide, M., Laloux, C., Moreau, C., Bordet, R., et al. (2016). Ferroptosis, a newly characterized form of cell death in Parkinson's disease that is regulated by PKC. Neurobiol. Dis. *94*, 169–178. https://doi.org/10.1016/j.nbd.2016.05.011.

Doll, S., Proneth, B., Tyurina, Y.Y., Panzilius, E., Kobayashi, S., Ingold, I., Irmler, M., Beckers, J., Aichler, M., Walch, A., et al. (2017). ACSL4 dictates ferroptosis sensitivity by shaping cellular lipid composition. Nat. Chem. Biol. *13*, 91–98. https://doi.org/10.1038/nchembio.2239.

Doll, S., Freitas, F.P., Shah, R., Aldrovandi, M., Silva, M.C. da, Ingold, I., Grocin, A.G., Silva, T.N.X. da, Panzilius, E., Scheel, C.H., et al. (2019). FSP1 is a glutathione-independent ferroptosis suppressor. Nature *575*, 693–698. https://doi.org/10.1038/s41586-019-1707-0.

Doty, R.L. (2012). Olfactory dysfunction in Parkinson disease. Nat. Rev. Neurol. *8*, 329–339. https://doi.org/10.1038/nrneurol.2012.80.

Double, K.L., Gerlach, M., Youdim, M.B., and Riederer, P. (2000). Impaired iron homeostasis in Parkinson's disease. J. Neural Transm. Suppl. 37–58. https://doi.org/10.1007/978-3-7091-6301-6_3.

Dragonas, C., Bertsch, T., Sieber, C.C., and Brosche, T. (2009). Plasmalogens as a marker of elevated systemic oxidative stress in Parkinson's disease. Clin. Chem. Lab. Med. *47*, 894–897. https://doi.org/10.1515/CCLM.2009.205.

Dringen, R. (2000). Metabolism and functions of glutathione in brain. Prog. Neurobiol. *62*, 649–671. https://doi.org/10.1016/s0301-0082(99)00060-x.

Driver, J.A., Logroscino, G., Gaziano, J.M., and Kurth, T. (2009). Incidence and remaining lifetime risk of Parkinson disease in advanced age. Neurology *72*, 432–438. https://doi.org/10.1212/01.wnl.0000341769.50075.bb.

Duce, J.A., Wong, B.X., Durham, H., Devedjian, J.-C., Smith, D.P., and Devos, D. (2017). Post translational changes to α-synuclein control iron and dopamine trafficking; a concept for neuron vulnerability in Parkinson's disease. Mol. Neurodegener. *12*, 45. https://doi.org/10.1186/s13024-017-0186-8.

Eagle, H. (1955). Nutrition needs of mammalian cells in tissue culture. Science *122*, 501–514. https://doi.org/10.1126/science.122.3168.501.

Eagle, H., Piez, K.A., and Oyama, V.I. (1961). The biosynthesis of cystine in human cell cultures. J. Biol. Chem. *236*, 1425–1428. .

Eichmann, C., Kumari, P., and Riek, R. (2017). High-density lipoprotein-like particle formation of Synuclein variants. FEBS Lett. *591*, 304–311. https://doi.org/10.1002/1873-3468.12543.

El-Agnaf, O.M., Jakes, R., Curran, M.D., and Wallace, A. (1998). Effects of the mutations Ala30 to Pro and Ala53 to Thr on the physical and morphological properties of alpha-synuclein protein implicated in Parkinson's disease. FEBS Lett. *440*, 67–70. https://doi.org/10.1016/s0014-5793(98)01419-7.

Eliezer, D., Kutluay, E., Bussell, R., and Browne, G. (2001). Conformational properties of alpha-synuclein in its free and lipid-associated states. J. Mol. Biol. *307*, 1061–1073. https://doi.org/10.1006/jmbi.2001.4538.

Ellis, C.E., Murphy, E.J., Mitchell, D.C., Golovko, M.Y., Scaglia, F., Barceló-Coblijn, G.C., and Nussbaum, R.L. (2005). Mitochondrial lipid abnormality and electron transport chain impairment in mice lacking alpha-synuclein. Mol. Cell. Biol. *25*, 10190–10201. https://doi.org/10.1128/MCB.25.22.10190-10201.2005.

Ellwanger, J.H., Molz, P., Dallemole, D.R., Pereira dos Santos, A., Müller, T.E., Cappelletti, L., Gonçalves da Silva, M., Franke, S.I.R., Prá, D., and Pêgas Henriques, J.A. (2015). Selenium reduces bradykinesia and DNA damage in a rat model of Parkinson's disease. Nutr. Burbank Los Angel. Cty. Calif *31*, 359–365. https://doi.org/10.1016/j.nut.2014.07.004.

Engelender, S., Kaminsky, Z., Guo, X., Sharp, A.H., Amaravi, R.K., Kleiderlein, J.J., Margolis, R.L., Troncoso, J.C., Lanahan, A.A., Worley, P.F., et al. (1999). Synphilin-1 associates with alpha-synuclein and promotes the formation of cytosolic inclusions. Nat. Genet. *22*, 110–114. https://doi.org/10.1038/8820.

Etminan, M., Gill, S.S., and Samii, A. (2005). Intake of vitamin E, vitamin C, and carotenoids and the risk of Parkinson's disease: a meta-analysis. Lancet Neurol. *4*, 362–365. https://doi.org/10.1016/S1474-4422(05)70097-1.

Fabelo, N., Martín, V., Santpere, G., Marín, R., Torrent, L., Ferrer, I., and Díaz, M. (2011). Severe Alterations in Lipid Composition of Frontal Cortex Lipid Rafts from Parkinson's Disease and Incidental Parkinson's Disease. Mol. Med. *17*, 1107–1118. https://doi.org/10.2119/molmed.2011.00119.

Fahn, S. and Parkinson Study Group (2005). Does levodopa slow or hasten the rate of progression of Parkinson's disease? J. Neurol. *252 Suppl 4*, IV37–IV42. https://doi.org/10.1007/s00415-005-4008-5.

Fahn, S., Oakes, D., Shoulson, I., Kieburtz, K., Rudolph, A., Lang, A., Olanow, C.W., Tanner, C., Marek, K., and Parkinson Study Group (2004). Levodopa and the progression of Parkinson's disease. N. Engl. J. Med. *351*, 2498–2508. https://doi.org/10.1056/NEJMoa033447.

Fais, M., Dore, A., Galioto, M., Galleri, G., Crosio, C., and Iaccarino, C. (2021). Parkinson's Disease-Related Genes and Lipid Alteration. Int. J. Mol. Sci. *22*, 7630. https://doi.org/10.3390/ijms22147630.

Fang, F., Chen, H., Feldman, A.L., Kamel, F., Ye, W., and Wirdefeldt, K. (2012). Head injury and Parkinson's disease: a population-based study. Mov. Disord. Off. J. Mov. Disord. Soc. *27*, 1632–1635. https://doi.org/10.1002/mds.25143.

de Farias, C.C., Maes, M., Bonifácio, K.L., Bortolasci, C.C., de Souza Nogueira, A., Brinholi, F.F., Matsumoto, A.K., do Nascimento, M.A., de Melo, L.B., Nixdorf, S.L., et al. (2016). Highly specific changes in antioxidant levels and lipid peroxidation in Parkinson's disease and its progression: Disease and staging biomarkers and new drug targets. Neurosci. Lett. *617*, 66–71. https://doi.org/10.1016/j.neulet.2016.02.011.

Fauvet, B., Mbefo, M.K., Fares, M.-B., Desobry, C., Michael, S., Ardah, M.T., Tsika, E., Coune, P., Prudent, M., Lion, N., et al. (2012). α-Synuclein in central nervous system and from erythrocytes, mammalian cells, and Escherichia coli exists predominantly as disordered monomer. J. Biol. Chem. *287*, 15345–15364. https://doi.org/10.1074/jbc.M111.318949.

Fearnley, J.M., and Lees, A.J. (1991). Ageing and Parkinson's disease: substantia nigra regional selectivity. Brain J. Neurol. *114 (Pt 5)*, 2283–2301. https://doi.org/10.1093/brain/114.5.2283.

Febbraro, F., Giorgi, M., Caldarola, S., Loreni, F., and Romero-Ramos, M. (2012). α-Synuclein expression is modulated at the translational level by iron. Neuroreport *23*, 576–580. https://doi.org/10.1097/WNR.0b013e328354a1f0.

Fecchio, C., Palazzi, L., and de Laureto, P.P. (2018). α-Synuclein and Polyunsaturated Fatty Acids: Molecular Basis of the Interaction and Implication in Neurodegeneration. Mol. Basel Switz. *23*. https://doi.org/10.3390/molecules23071531.

Ferreira, A., Neves, P., and Gozzelino, R. (2019). Multilevel Impacts of Iron in the Brain: The Cross Talk between Neurophysiological Mechanisms, Cognition, and Social Behavior. Pharm. Basel Switz. *12*. https://doi.org/10.3390/ph12030126.

Fischer, T.D., Hylin, M.J., Zhao, J., Moore, A.N., Waxham, M.N., and Dash, P.K. (2016). Altered Mitochondrial Dynamics and TBI Pathophysiology. Front. Syst. Neurosci. *10*, 29. https://doi.org/10.3389/fnsys.2016.00029.

Fiske, M., Valtierra, S., Solvang, K., Zorniak, M., White, M., Herrera, S., Konnikova, A., Brezinsky, R., and Debburman, S. (2011). Contribution of Alanine-76 and Serine

Phosphorylation in α-Synuclein Membrane Association and Aggregation in Yeasts. Park. Dis. *2011*, 392180. https://doi.org/10.4061/2011/392180.

Floberg, J.M., Wang, L., Bandara, N., Rashmi, R., Mpoy, C., Garbow, J.R., Rogers, B.E., Patti, G.J., and Schwarz, J.K. (2020). Alteration of Cellular Reduction Potential Will Change 64Cu-ATSM Signal With or Without Hypoxia. J. Nucl. Med. Off. Publ. Soc. Nucl. Med. *61*, 427–432. https://doi.org/10.2967/jnumed.119.230805.

Folch, J., Lees, M., and Sloane Stanley, G.H. (1957). A simple method for the isolation and purification of total lipides from animal tissues. J. Biol. Chem. *226*, 497–509. .

Forcina, G.C., and Dixon, S.J. (2019). GPX4 at the Crossroads of Lipid Homeostasis and Ferroptosis. PROTEOMICS *19*, 1800311. https://doi.org/10.1002/pmic.201800311.

Ford, D.A., Hazen, S.L., Saffitz, J.E., and Gross, R.W. (1991). The rapid and reversible activation of a calcium-independent plasmalogen-selective phospholipase A2 during myocardial ischemia. J. Clin. Invest. *88*, 331–335. https://doi.org/10.1172/JCI115296.

Friedland, A.E., Tzur, Y.B., Esvelt, K.M., Colaiácovo, M.P., Church, G.M., and Calarco, J.A. (2013). Heritable genome editing in C. elegans via a CRISPR-Cas9 system. Nat. Methods *10*, 741–743. https://doi.org/10.1038/nmeth.2532.

Friedlich, A.L., Tanzi, R.E., and Rogers, J.T. (2007). The 5'-untranslated region of Parkinson's disease alpha-synuclein messengerRNA contains a predicted iron responsive element. Mol. Psychiatry *12*, 222–223. https://doi.org/10.1038/sj.mp.4001937.

Friedmann Angeli, J.P., and Conrad, M. (2018). Selenium and GPX4, a vital symbiosis. Free Radic. Biol. Med. *127*, 153–159. https://doi.org/10.1016/j.freeradbiomed.2018.03.001.

Friedmann Angeli, J.P., Schneider, M., Proneth, B., Tyurina, Y.Y., Tyurin, V.A., Hammond, V.J., Herbach, N., Aichler, M., Walch, A., Eggenhofer, E., et al. (2014). Inactivation of the ferroptosis regulator Gpx4 triggers acute renal failure in mice. Nat. Cell Biol. *16*, 1180–1191. https://doi.org/10.1038/ncb3064.

Fuchs, J., Nilsson, C., Kachergus, J., Munz, M., Larsson, E.-M., Schüle, B., Langston, J.W., Middleton, F.A., Ross, O.A., Hulihan, M., et al. (2007). Phenotypic variation in a large Swedish pedigree due to SNCA duplication and triplication. Neurology *68*, 916–922. https://doi.org/10.1212/01.wnl.0000254458.17630.c5.

Fujiwara, H., Hasegawa, M., Dohmae, N., Kawashima, A., Masliah, E., Goldberg, M.S., Shen, J., Takio, K., and Iwatsubo, T. (2002). alpha-Synuclein is phosphorylated in synucleinopathy lesions. Nat. Cell Biol. *4*, 160–164. https://doi.org/10.1038/ncb748.

Galluzzi, L., Bravo-San Pedro, J.M., Vitale, I., Aaronson, S.A., Abrams, J.M., Adam, D., Alnemri, E.S., Altucci, L., Andrews, D., Annicchiarico-Petruzzelli, M., et al. (2015). Essential versus accessory aspects of cell death: recommendations of the NCCD 2015. Cell Death Differ. *22*, 58–73. https://doi.org/10.1038/cdd.2014.137.

Galluzzi, L., Vitale, I., Aaronson, S.A., Abrams, J.M., Adam, D., Agostinis, P., Alnemri, E.S., Altucci, L., Amelio, I., Andrews, D.W., et al. (2018). Molecular mechanisms of cell

death: recommendations of the Nomenclature Committee on Cell Death 2018. Cell Death Differ. *25*, 486–541. https://doi.org/10.1038/s41418-017-0012-4.

Gámez-Valero, A., and Beyer, K. (2018). Alternative Splicing of Alpha- and Beta-Synuclein Genes Plays Differential Roles in Synucleinopathies. Genes *9*. https://doi.org/10.3390/genes9020063.

Gandhi, S., and Abramov, A.Y. (2012). Mechanism of oxidative stress in neurodegeneration. Oxid. Med. Cell. Longev. *2012*, 428010. https://doi.org/10.1155/2012/428010.

Gao, M., Monian, P., Quadri, N., Ramasamy, R., and Jiang, X. (2015). Glutaminolysis and Transferrin Regulate Ferroptosis. Mol. Cell *59*, 298–308. https://doi.org/10.1016/j.molcel.2015.06.011.

Gao, M., Monian, P., Pan, Q., Zhang, W., Xiang, J., and Jiang, X. (2016). Ferroptosis is an autophagic cell death process. Cell Res. *26*, 1021–1032. https://doi.org/10.1038/cr.2016.95.

Gary, D.S., and Mattson, M.P. (2001). Integrin signaling via the PI3-kinase-Akt pathway increases neuronal resistance to glutamate-induced apoptosis. J. Neurochem. *76*, 1485–1496. https://doi.org/10.1046/j.1471-4159.2001.00173.x.

Giasson, B.I., Murray, I.V., Trojanowski, J.Q., and Lee, V.M. (2001). A hydrophobic stretch of 12 amino acid residues in the middle of alpha-synuclein is essential for filament assembly. J. Biol. Chem. *276*, 2380–2386. https://doi.org/10.1074/jbc.M008919200.

Girotti, A.W. (1998). Lipid hydroperoxide generation, turnover, and effector action in biological systems. J. Lipid Res. *39*, 1529–1542. .

Glaser, P.E., and Gross, R.W. (1994). Plasmenylethanolamine Facilitates Rapid Membrane Fusion: A Stopped-Flow Kinetic Investigation Correlating the Propensity of a Major Plasma Membrane Constituent to Adopt an HII Phase with Its Ability to Promote Membrane Fusion. Biochemistry *33*, 5805–5812. https://doi.org/10.1021/bi00185a019.

Gogolla, N., Galimberti, I., DePaola, V., and Caroni, P. (2006). Preparation of organotypic hippocampal slice cultures for long-term live imaging. Nat. Protoc. *1*, 1165–1171. https://doi.org/10.1038/nprot.2006.168.

Golovko, M.Y., Faergeman, N.J., Cole, N.B., Castagnet, P.I., Nussbaum, R.L., and Murphy, E.J. (2005). Alpha-synuclein gene deletion decreases brain palmitate uptake and alters the palmitate metabolism in the absence of alpha-synuclein palmitate binding. Biochemistry *44*, 8251–8259. https://doi.org/10.1021/bi0502137.

Golovko, M.Y., Rosenberger, T.A., Faergeman, N.J., Feddersen, S., Cole, N.B., Pribill, I., Berger, J., Nussbaum, R.L., and Murphy, E.J. (2006). Acyl-CoA synthetase activity links wild-type but not mutant alpha-synuclein to brain arachidonate metabolism. Biochemistry *45*, 6956–6966. https://doi.org/10.1021/bi0600289.

Golovko, M.Y., Rosenberger, T.A., Feddersen, S., Faergeman, N.J., and Murphy, E.J. (2007). Alpha-synuclein gene ablation increases docosahexaenoic acid incorporation and turnover in brain phospholipids. J. Neurochem. *101*, 201–211. https://doi.org/10.1111/j.1471-4159.2006.04357.x.

Gorbatyuk, O.S., Li, S., Nguyen, F.N., Manfredsson, F.P., Kondrikova, G., Sullivan, L.F., Meyers, C., Chen, W., Mandel, R.J., and Muzyczka, N. (2010). α-Synuclein expression in rat substantia nigra suppresses phospholipase D2 toxicity and nigral neurodegeneration. Mol. Ther. J. Am. Soc. Gene Ther. *18*, 1758–1768. https://doi.org/10.1038/mt.2010.137.

Gosavi, N., Lee, H.-J., Lee, J.S., Patel, S., and Lee, S.-J. (2002). Golgi fragmentation occurs in the cells with prefibrillar alpha-synuclein aggregates and precedes the formation of fibrillar inclusion. J. Biol. Chem. *277*, 48984–48992. https://doi.org/10.1074/jbc.M208194200.

Gratz, S.J., Cummings, A.M., Nguyen, J.N., Hamm, D.C., Donohue, L.K., Harrison, M.M., Wildonger, J., and O'Connor-Giles, K.M. (2013). Genome engineering of Drosophila with the CRISPR RNA-guided Cas9 nuclease. Genetics *194*, 1029–1035. https://doi.org/10.1534/genetics.113.152710.

Gregory, A., Westaway, S.K., Holm, I.E., Kotzbauer, P.T., Hogarth, P., Sonek, S., Coryell, J.C., Nguyen, T.M., Nardocci, N., Zorzi, G., et al. (2008). Neurodegeneration associated with genetic defects in phospholipase A2. Neurology *71*, 1402–1409. https://doi.org/10.1212/01.wnl.0000327094.67726.28.

Greten-Harrison, B., Polydoro, M., Morimoto-Tomita, M., Diao, L., Williams, A.M., Nie, E.H., Makani, S., Tian, N., Castillo, P.E., Buchman, V.L., et al. (2010). αβγ-Synuclein triple knockout mice reveal age-dependent neuronal dysfunction. Proc. Natl. Acad. Sci. U. S. A. *107*, 19573–19578. https://doi.org/10.1073/pnas.1005005107.

Griesser, M., Shah, R., Van Kessel, A.T., Zilka, O., Haidasz, E.A., and Pratt, D.A. (2018). The Catalytic Reaction of Nitroxides with Peroxyl Radicals and Its Relevance to Their Cytoprotective Properties. J. Am. Chem. Soc. *140*, 3798–3808. https://doi.org/10.1021/jacs.8b00998.

Guiney, S.J., Adlard, P.A., Bush, A.I., Finkelstein, D.I., and Ayton, S. (2017). Ferroptosis and cell death mechanisms in Parkinson's disease. Neurochem. Int. *104*, 34–48. https://doi.org/10.1016/j.neuint.2017.01.004.

Gureviciene, I., Gurevicius, K., and Tanila, H. (2007). Role of alpha-synuclein in synaptic glutamate release. Neurobiol. Dis. *28*, 83–89. https://doi.org/10.1016/j.nbd.2007.06.016.

Haacke, E.M., Cheng, N.Y.C., House, M.J., Liu, Q., Neelavalli, J., Ogg, R.J., Khan, A., Ayaz, M., Kirsch, W., and Obenaus, A. (2005). Imaging iron stores in the brain using magnetic resonance imaging. Magn. Reson. Imaging *23*, 1–25. https://doi.org/10.1016/j.mri.2004.10.001.

Haggerty, T., Credle, J., Rodriguez, O., Wills, J., Oaks, A.W., Masliah, E., and Sidhu, A. (2011). Hyperphosphorylated Tau in an α-synuclein-overexpressing transgenic model of Parkinson's disease. Eur. J. Neurosci. *33*, 1598–1610. https://doi.org/10.1111/j.1460-9568.2011.07660.x.

Hara, S., Arawaka, S., Sato, H., Machiya, Y., Cui, C., Sasaki, A., Koyama, S., and Kato, T. (2013). Serine 129 phosphorylation of membrane-associated α-synuclein modulates dopamine transporter function in a G protein-coupled receptor kinase-dependent manner. Mol. Biol. Cell *24*, 1649–1660, S1-3. https://doi.org/10.1091/mbc.E12-12-0903.

Hare, D.J., and Double, K.L. (2016). Iron and dopamine: a toxic couple. Brain *139*, 1026–1035. https://doi.org/10.1093/brain/aww022.

Hare, D., Ayton, S., Bush, A., and Lei, P. (2013). A delicate balance: Iron metabolism and diseases of the brain. Front. Aging Neurosci. *5*, 34. https://doi.org/10.3389/fnagi.2013.00034.

Harvey, C.J., Thimmulappa, R.K., Singh, A., Blake, D.J., Ling, G., Wakabayashi, N., Fujii, J., Myers, A., and Biswal, S. (2009). Nrf2-regulated glutathione recycling independent of biosynthesis is critical for cell survival during oxidative stress. Free Radic. Biol. Med. *46*, 443–453. https://doi.org/10.1016/j.freeradbiomed.2008.10.040.

Hasegawa, M., Takahashi, H., Rajabi, H., Alam, M., Suzuki, Y., Yin, L., Tagde, A., Maeda, T., Hiraki, M., Sukhatme, V.P., et al. (2016). Functional interactions of the cystine/glutamate antiporter, CD44v and MUC1-C oncoprotein in triple-negative breast cancer cells. Oncotarget *7*, 11756–11769. https://doi.org/10.18632/oncotarget.7598.

Hashimoto, M., Yoshimoto, M., Sisk, A., Hsu, L.J., Sundsmo, M., Kittel, A., Saitoh, T., Miller, A., and Masliah, E. (1997). NACP, a synaptic protein involved in Alzheimer's disease, is differentially regulated during megakaryocyte differentiation. Biochem. Biophys. Res. Commun. *237*, 611–616. https://doi.org/10.1006/bbrc.1997.6978.

Hashimoto, M., Hsu, L.J., Xia, Y., Takeda, A., Sisk, A., Sundsmo, M., and Masliah, E. (1999). Oxidative stress induces amyloid-like aggregate formation of NACP/alpha-synuclein in vitro. Neuroreport *10*, 717–721. https://doi.org/10.1097/00001756-199903170-00011.

Hayashi, D., Mouchlis, V.D., and Dennis, E.A. (2022). Each phospholipase A2 type exhibits distinct selectivity toward sn-1 ester, alkyl ether, and vinyl ether phospholipids. Biochim. Biophys. Acta Mol. Cell Biol. Lipids *1867*, 159067. https://doi.org/10.1016/j.bbalip.2021.159067.

Healy, D.G., Abou-Sleiman, P.M., Gibson, J.M., Ross, O.A., Jain, S., Gandhi, S., Gosal, D., Muqit, M.M.K., Wood, N.W., and Lynch, T. (2004). PINK1 (PARK6) associated Parkinson disease in Ireland. Neurology *63*, 1486–1488. https://doi.org/10.1212/01.wnl.0000142089.38301.8e.

Hely, M.A., Morris, J.G.L., Reid, W.G.J., and Trafficante, R. (2005). Sydney Multicenter Study of Parkinson's disease: non-L-dopa-responsive problems dominate at 15 years. Mov. Disord. Off. J. Mov. Disord. Soc. *20*, 190–199. https://doi.org/10.1002/mds.20324.

Hely, M.A., Reid, W.G.J., Adena, M.A., Halliday, G.M., and Morris, J.G.L. (2008). The Sydney multicenter study of Parkinson's disease: the inevitability of dementia at 20 years. Mov. Disord. Off. J. Mov. Disord. Soc. *23*, 837–844. https://doi.org/10.1002/mds.21956.

Hider, R.C., and Kong, X.L. (2011). Glutathione: a key component of the cytoplasmic labile iron pool. Biometals Int. J. Role Met. Ions Biol. Biochem. Med. *24*, 1179–1187. https://doi.org/10.1007/s10534-011-9476-8.

Hirsch, E.C., Brandel, J.P., Galle, P., Javoy-Agid, F., and Agid, Y. (1991). Iron and aluminum increase in the substantia nigra of patients with Parkinson's disease: an X-ray microanalysis. J. Neurochem. *56*, 446–451. https://doi.org/10.1111/j.1471-4159.1991.tb08170.x.

Honsho, M., Abe, Y., and Fujiki, Y. (2017). Plasmalogen biosynthesis is spatiotemporally regulated by sensing plasmalogens in the inner leaflet of plasma membranes. Sci. Rep. *7*, 43936. https://doi.org/10.1038/srep43936.

Hopes, L., Grolez, G., Moreau, C., Lopes, R., Ryckewaert, G., Carrière, N., Auger, F., Laloux, C., Petrault, M., Devedjian, J.-C., et al. (2016). Magnetic Resonance Imaging Features of the Nigrostriatal System: Biomarkers of Parkinson's Disease Stages? PloS One *11*, e0147947. https://doi.org/10.1371/journal.pone.0147947.

Horikoshi, N., Cong, J., Kley, N., and Shenk, T. (1999). Isolation of differentially expressed cDNAs from p53-dependent apoptotic cells: activation of the human homologue of the Drosophila peroxidasin gene. Biochem. Biophys. Res. Commun. *261*, 864–869. https://doi.org/10.1006/bbrc.1999.1123.

Hoshimaru, M., Ray, J., Sah, D.W., and Gage, F.H. (1996). Differentiation of the immortalized adult neuronal progenitor cell line HC2S2 into neurons by regulatable suppression of the v-myc oncogene. Proc. Natl. Acad. Sci. U. S. A. *93*, 1518–1523. https://doi.org/10.1073/pnas.93.4.1518.

Hou, W., Xie, Y., Song, X., Sun, X., Lotze, M.T., Zeh, H.J., Kang, R., and Tang, D. (2016). Autophagy promotes ferroptosis by degradation of ferritin. Autophagy *12*, 1425–1428. https://doi.org/10.1080/15548627.2016.1187366.

Hruska, K.S., LaMarca, M.E., Scott, C.R., and Sidransky, E. (2008). Gaucher disease: mutation and polymorphism spectrum in the glucocerebrosidase gene (GBA). Hum. Mutat. *29*, 567–583. https://doi.org/10.1002/humu.20676.

Hsu, L.J., Sagara, Y., Arroyo, A., Rockenstein, E., Sisk, A., Mallory, M., Wong, J., Takenouchi, T., Hashimoto, M., and Masliah, E. (2000). alpha-synuclein promotes mitochondrial deficit and oxidative stress. Am. J. Pathol. *157*, 401–410. https://doi.org/10.1016/s0002-9440(10)64553-1.

Hung, L.W., Villemagne, V.L., Cheng, L., Sherratt, N.A., Ayton, S., White, A.R., Crouch, P.J., Lim, S., Leong, S.L., Wilkins, S., et al. (2012). The hypoxia imaging agent CuII(atsm) is neuroprotective and improves motor and cognitive functions in multiple animal models of Parkinson's disease. J. Exp. Med. *209*, 837–854. https://doi.org/10.1084/jem.20112285.

Hunn, B.H.M., Cragg, S.J., Bolam, J.P., Spillantini, M.-G., and Wade-Martins, R. (2015). Impaired intracellular trafficking defines early Parkinson's disease. Trends Neurosci. *38*, 178–188. https://doi.org/10.1016/j.tins.2014.12.009.

Ikawa, M., Okazawa, H., Kudo, T., Kuriyama, M., Fujibayashi, Y., and Yoneda, M. (2011). Evaluation of striatal oxidative stress in patients with Parkinson's disease using [62Cu]ATSM PET. Nucl. Med. Biol. *38*, 945–951. https://doi.org/10.1016/j.nucmedbio.2011.02.016.

Iwai, A., Masliah, E., Yoshimoto, M., Ge, N., Flanagan, L., de Silva, H.A., Kittel, A., and Saitoh, T. (1995). The precursor protein of non-A beta component of Alzheimer's disease amyloid is a presynaptic protein of the central nervous system. Neuron *14*, 467–475. https://doi.org/10.1016/0896-6273(95)90302-x.

Jakes, R., Spillantini, M.G., and Goedert, M. (1994). Identification of two distinct synucleins from human brain. FEBS Lett. *345*, 27–32. https://doi.org/10.1016/0014-5793(94)00395-5.

Jankovic, J. (2008). Parkinson's disease: clinical features and diagnosis. J. Neurol. Neurosurg. Psychiatry *79*, 368–376. https://doi.org/10.1136/jnnp.2007.131045.

Jankovic, J., McDermott, M., Carter, J., Gauthier, S., Goetz, C., Golbe, L., Huber, S., Koller, W., Olanow, C., and Shoulson, I. (1990). Variable expression of Parkinson's disease: a baseline analysis of the DATATOP cohort. The Parkinson Study Group. Neurology *40*, 1529–1534. https://doi.org/10.1212/wnl.40.10.1529.

Jenco, J.M., Rawlingson, A., Daniels, B., and Morris, A.J. (1998). Regulation of phospholipase D2: selective inhibition of mammalian phospholipase D isoenzymes by alpha- and beta-synucleins. Biochemistry *37*, 4901–4909. https://doi.org/10.1021/bi972776r.

Jensen, P.H., Hager, H., Nielsen, M.S., Hojrup, P., Gliemann, J., and Jakes, R. (1999). alpha-synuclein binds to Tau and stimulates the protein kinase A-catalyzed tau phosphorylation of serine residues 262 and 356. J. Biol. Chem. *274*, 25481–25489. https://doi.org/10.1074/jbc.274.36.25481.

Jiang, L., Kon, N., Li, T., Wang, S.-J., Su, T., Hibshoosh, H., Baer, R., and Gu, W. (2015). Ferroptosis as a p53-mediated activity during tumour suppression. Nature *520*, 57–62. https://doi.org/10.1038/nature14344.

Jinek, M., East, A., Cheng, A., Lin, S., Ma, E., and Doudna, J. (2013). RNA-programmed genome editing in human cells. ELife *2*, e00471. https://doi.org/10.7554/eLife.00471.

Johnson, J., Hague, S.M., Hanson, M., Gibson, A., Wilson, K.E., Evans, E.W., Singleton, A.A., McInerney-Leo, A., Nussbaum, R.L., Hernandez, D.G., et al. (2004). SNCA multiplication is not a common cause of Parkinson disease or dementia with Lewy bodies. Neurology *63*, 554–556. https://doi.org/10.1212/01.WNL.0000133401.09043.44.

Junn, E., and Mouradian, M.M. (2002). Human alpha-synuclein over-expression increases intracellular reactive oxygen species levels and susceptibility to dopamine. Neurosci. Lett. *320*, 146–150. https://doi.org/10.1016/s0304-3940(02)00016-2.

Kagan, V.E., Mao, G., Qu, F., Angeli, J.P.F., Doll, S., Croix, C.S., Dar, H.H., Liu, B., Tyurin, V.A., Ritov, V.B., et al. (2017). Oxidized arachidonic and adrenic PEs navigate cells to ferroptosis. Nat. Chem. Biol. *13*, 81–90. https://doi.org/10.1038/nchembio.2238.

Kalia, L.V., and Lang, A.E. (2015). Parkinson's disease. The Lancet *386*, 896–912. https://doi.org/10.1016/S0140-6736(14)61393-3.

Kang, R., Zeng, L., Zhu, S., Xie, Y., Liu, J., Wen, Q., Cao, L., Xie, M., Ran, Q., Kroemer, G., et al. (2018). Lipid Peroxidation Drives Gasdermin D-Mediated Pyroptosis in Lethal Polymicrobial Sepsis. Cell Host Microbe *24*, 97-108.e4. https://doi.org/10.1016/j.chom.2018.05.009.

Karuppagounder, S.S., Alim, I., Khim, S.J., Bourassa, M.W., Sleiman, S.F., John, R., Thinnes, C.C., Yeh, T.-L., Demetriades, M., Neitemeier, S., et al. (2016). Therapeutic targeting of oxygen-sensing prolyl hydroxylases abrogates ATF4-dependent neuronal death

and improves outcomes after brain hemorrhage in several rodent models. Sci. Transl. Med. *8*, 328ra29. https://doi.org/10.1126/scitranslmed.aac6008.

Karuppagounder, S.S., Alin, L., Chen, Y., Brand, D., Bourassa, M.W., Dietrich, K., Wilkinson, C.M., Nadeau, C.A., Kumar, A., Perry, S., et al. (2018). N-acetylcysteine targets 5 lipoxygenase-derived, toxic lipids and can synergize with prostaglandin E2 to inhibit ferroptosis and improve outcomes following hemorrhagic stroke in mice. Ann. Neurol. *84*, 854–872. https://doi.org/10.1002/ana.25356.

Kaufmann, H., and Goldstein, D.S. (2010). Pure autonomic failure: a restricted Lewy body synucleinopathy or early Parkinson disease? Neurology *74*, 536–537. https://doi.org/10.1212/WNL.0b013e3181d26982.

Kaufmann, H., Nahm, K., Purohit, D., and Wolfe, D. (2004). Autonomic failure as the initial presentation of Parkinson disease and dementia with Lewy bodies. Neurology *63*, 1093–1095. https://doi.org/10.1212/01.wnl.0000138500.73671.dc.

Kaur, D., Yantiri, F., Rajagopalan, S., Kumar, J., Mo, J.Q., Boonplueang, R., Viswanath, V., Jacobs, R., Yang, L., Beal, M.F., et al. (2003). Genetic or pharmacological iron chelation prevents MPTP-induced neurotoxicity in vivo: a novel therapy for Parkinson's disease. Neuron *37*, 899–909. https://doi.org/10.1016/s0896-6273(03)00126-0.

Kerins, M.J., and Ooi, A. (2018). The Roles of NRF2 in Modulating Cellular Iron Homeostasis. Antioxid. Redox Signal. *29*, 1756–1773. https://doi.org/10.1089/ars.2017.7176.

Khan, H.A. (2010). Selenium partially reverses the depletion of striatal dopamine and its metabolites in MPTP-treated C57BL mice. Neurochem. Int. *57*, 489–491. https://doi.org/10.1016/j.neuint.2010.06.020.

Kim, G.H., Kim, J.E., Rhie, S.J., and Yoon, S. (2015). The Role of Oxidative Stress in Neurodegenerative Diseases. Exp. Neurobiol. *24*, 325–340. https://doi.org/10.5607/en.2015.24.4.325.

Kim, H., Kim, E., Park, M., Lee, E., and Namkoong, K. (2013). Organotypic hippocampal slice culture from the adult mouse brain: a versatile tool for translational neuropsychopharmacology. Prog. Neuropsychopharmacol. Biol. Psychiatry *41*, 36–43. https://doi.org/10.1016/j.pnpbp.2012.11.004.

Kim, K., Doi, A., Wen, B., Ng, K., Zhao, R., Cahan, P., Kim, J., Aryee, M.J., Ji, H., Ehrlich, L.I.R., et al. (2010). Epigenetic memory in induced pluripotent stem cells. Nature *467*, 285–290. https://doi.org/10.1038/nature09342.

Kinghorn, K.J., and Castillo-Quan, J.I. (2016). Mitochondrial dysfunction and defects in lipid homeostasis as therapeutic targets in neurodegeneration with brain iron accumulation. Rare Dis. *4*. https://doi.org/10.1080/21675511.2015.1128616.

Kinghorn, K.J., Castillo-Quan, J.I., Bartolome, F., Angelova, P.R., Li, L., Pope, S., Cochemé, H.M., Khan, S., Asghari, S., Bhatia, K.P., et al. (2015). Loss of PLA2G6 leads to elevated mitochondrial lipid peroxidation and mitochondrial dysfunction. Brain J. Neurol. *138*, 1801–1816. https://doi.org/10.1093/brain/awv132.

Klein, C., and Westenberger, A. (2012). Genetics of Parkinson's disease. Cold Spring Harb. Perspect. Med. *2*, a008888. https://doi.org/10.1101/cshperspect.a008888.

Klein, C., Grünewald, A., and Hedrich, K. (2006). Early-onset parkinsonism associated with PINK1 mutations: frequency, genotypes, and phenotypes. Neurology *66*, 1129–1130; author reply 1129-1130. https://doi.org/10.1212/01.wnl.0000220157.81513.85.

Kleiner-Fisman, G., Herzog, J., Fisman, D.N., Tamma, F., Lyons, K.E., Pahwa, R., Lang, A.E., and Deuschl, G. (2006). Subthalamic nucleus deep brain stimulation: summary and meta-analysis of outcomes. Mov. Disord. Off. J. Mov. Disord. Soc. *21 Suppl 14*, S290-304. https://doi.org/10.1002/mds.20962.

Knutson, M.D. (2007). Steap Proteins: Implications for Iron and Copper Metabolism. Nutr. Rev. *65*, 335–340. https://doi.org/10.1111/j.1753-4887.2007.tb00311.x.

Koprich, J.B., Reske-Nielsen, C., Mithal, P., and Isacson, O. (2008). Neuroinflammation mediated by IL-1beta increases susceptibility of dopamine neurons to degeneration in an animal model of Parkinson's disease. J. Neuroinflammation *5*, 8. https://doi.org/10.1186/1742-2094-5-8.

Kovac, S., Angelova, P.R., Holmström, K.M., Zhang, Y., Dinkova-Kostova, A.T., and Abramov, A.Y. (2015). Nrf2 regulates ROS production by mitochondria and NADPH oxidase. Biochim. Biophys. Acta *1850*, 794–801. https://doi.org/10.1016/j.bbagen.2014.11.021.

Kovacs, G.G., Wagner, U., Dumont, B., Pikkarainen, M., Osman, A.A., Streichenberger, N., Leisser, I., Verchère, J., Baron, T., Alafuzoff, I., et al. (2012). An antibody with high reactivity for disease-associated α-synuclein reveals extensive brain pathology. Acta Neuropathol. (Berl.) *124*, 37–50. https://doi.org/10.1007/s00401-012-0964-x.

Krack, P., Batir, A., Van Blercom, N., Chabardes, S., Fraix, V., Ardouin, C., Koudsie, A., Limousin, P.D., Benazzouz, A., LeBas, J.F., et al. (2003). Five-year follow-up of bilateral stimulation of the subthalamic nucleus in advanced Parkinson's disease. N. Engl. J. Med. *349*, 1925–1934. https://doi.org/10.1056/NEJMoa035275.

Krainz, T., Gaschler, M.M., Lim, C., Sacher, J.R., Stockwell, B.R., and Wipf, P. (2016). A Mitochondrial-Targeted Nitroxide Is a Potent Inhibitor of Ferroptosis. ACS Cent. Sci. *2*, 653–659. https://doi.org/10.1021/acscentsci.6b00199.

Krishna, A., Biryukov, M., Trefois, C., Antony, P.M.A., Hussong, R., Lin, J., Heinäniemi, M., Glusman, G., Köglsberger, S., Boyd, O., et al. (2014). Systems genomics evaluation of the SH-SY5Y neuroblastoma cell line as a model for Parkinson's disease. BMC Genomics *15*, 1154. https://doi.org/10.1186/1471-2164-15-1154.

Krüger, R., Kuhn, W., Müller, T., Woitalla, D., Graeber, M., Kösel, S., Przuntek, H., Epplen, J.T., Schöls, L., and Riess, O. (1998). Ala30Pro mutation in the gene encoding alpha-synuclein in Parkinson's disease. Nat. Genet. *18*, 106–108. https://doi.org/10.1038/ng0298-106.

Ku, C.-C., Wuputra, K., Kato, K., Lin, W.-H., Pan, J.-B., Tsai, S.-C., Kuo, C.-J., Lee, K.-H., Lee, Y.-L., Lin, Y.-C., et al. (2020). Jdp2-deficient granule cell progenitors in the cerebellum

are resistant to ROS-mediated apoptosis through xCT/Slc7a11 activation. Sci. Rep. *10*, 4933. https://doi.org/10.1038/s41598-020-61692-x.

Kuusisto, E., Parkkinen, L., and Alafuzoff, I. (2003). Morphogenesis of Lewy bodies: dissimilar incorporation of alpha-synuclein, ubiquitin, and p62. J. Neuropathol. Exp. Neurol. *62*, 1241–1253. https://doi.org/10.1093/jnen/62.12.1241.

Kwon, M.-Y., Park, E., Lee, S.-J., and Chung, S.W. (2015). Heme oxygenase-1 accelerates erastin-induced ferroptotic cell death. Oncotarget *6*, 24393–24403. https://doi.org/10.18632/oncotarget.5162.

Lalli, M.A., Avey, D., Dougherty, J.D., Milbrandt, J., and Mitra, R.D. (2020). High-throughput single-cell functional elucidation of neurodevelopmental disease-associated genes reveals convergent mechanisms altering neuronal differentiation. Genome Res. *30*, 1317–1331. https://doi.org/10.1101/gr.262295.120.

Laloux, C., Gouel, F., Lachaud, C., Timmerman, K., Do Van, B., Jonneaux, A., Petrault, M., Garcon, G., Rouaix, N., Moreau, C., et al. (2017). Continuous cerebroventricular administration of dopamine: A new treatment for severe dyskinesia in Parkinson's disease? Neurobiol. Dis. *103*, 24–31. https://doi.org/10.1016/j.nbd.2017.03.013.

Langston, J.W., Ballard, P., Tetrud, J.W., and Irwin, I. (1983). Chronic Parkinsonism in humans due to a product of meperidine-analog synthesis. Science *219*, 979–980. https://doi.org/10.1126/science.6823561.

Larrieu, T., and Layé, S. (2018). Food for Mood: Relevance of Nutritional Omega-3 Fatty Acids for Depression and Anxiety. Front. Physiol. *9*, 1047. https://doi.org/10.3389/fphys.2018.01047.

Larsen, K.E., Schmitz, Y., Troyer, M.D., Mosharov, E., Dietrich, P., Quazi, A.Z., Savalle, M., Nemani, V., Chaudhry, F.A., Edwards, R.H., et al. (2006). Alpha-synuclein overexpression in PC12 and chromaffin cells impairs catecholamine release by interfering with a late step in exocytosis. J. Neurosci. Off. J. Soc. Neurosci. *26*, 11915–11922. https://doi.org/10.1523/JNEUROSCI.3821-06.2006.

Latunde-Dada, G.O. (2017). Ferroptosis: Role of lipid peroxidation, iron and ferritinophagy. Biochim. Biophys. Acta Gen. Subj. *1861*, 1893–1900. https://doi.org/10.1016/j.bbagen.2017.05.019.

de Lau, L.M.L., and Breteler, M.M.B. (2006). Epidemiology of Parkinson's disease. Lancet Neurol. *5*, 525–535. https://doi.org/10.1016/S1474-4422(06)70471-9.

Lautenschläger, J., Stephens, A.D., Fusco, G., Ströhl, F., Curry, N., Zacharopoulou, M., Michel, C.H., Laine, R., Nespovitaya, N., Fantham, M., et al. (2018). C-terminal calcium binding of α-synuclein modulates synaptic vesicle interaction. Nat. Commun. *9*, 712. https://doi.org/10.1038/s41467-018-03111-4.

Lee, H., Zandkarimi, F., Zhang, Y., Meena, J.K., Kim, J., Zhuang, L., Tyagi, S., Ma, L., Westbrook, T.F., Steinberg, G.R., et al. (2020). Energy-stress-mediated AMPK activation inhibits ferroptosis. Nat. Cell Biol. *22*, 225–234. https://doi.org/10.1038/s41556-020-0461-8.

Lee, H.-J., Choi, C., and Lee, S.-J. (2002). Membrane-bound alpha-synuclein has a high aggregation propensity and the ability to seed the aggregation of the cytosolic form. J. Biol. Chem. *277*, 671–678. https://doi.org/10.1074/jbc.M107045200.

Lee, H.-J., Khoshaghideh, F., Lee, S., and Lee, S.-J. (2006). Impairment of microtubule-dependent trafficking by overexpression of alpha-synuclein. Eur. J. Neurosci. *24*, 3153–3162. https://doi.org/10.1111/j.1460-9568.2006.05210.x.

Lei, P., Ayton, S., Finkelstein, D.I., Spoerri, L., Ciccotosto, G.D., Wright, D.K., Wong, B.X.W., Adlard, P.A., Cherny, R.A., Lam, L.Q., et al. (2012). Tau deficiency induces parkinsonism with dementia by impairing APP-mediated iron export. Nat. Med. *18*, 291–295. https://doi.org/10.1038/nm.2613.

Lesage, S., Dürr, A., Tazir, M., Lohmann, E., Leutenegger, A.-L., Janin, S., Pollak, P., Brice, A., and French Parkinson's Disease Genetics Study Group (2006). LRRK2 G2019S as a cause of Parkinson's disease in North African Arabs. N. Engl. J. Med. *354*, 422–423. https://doi.org/10.1056/NEJMc055540.

Lesage, S., Anheim, M., Letournel, F., Bousset, L., Honoré, A., Rozas, N., Pieri, L., Madiona, K., Dürr, A., Melki, R., et al. (2013). G51D α-synuclein mutation causes a novel parkinsonian-pyramidal syndrome. Ann. Neurol. *73*, 459–471. https://doi.org/10.1002/ana.23894.

Lessig, J., and Fuchs, B. (2009). Plasmalogens in biological systems: their role in oxidative processes in biological membranes, their contribution to pathological processes and aging and plasmalogen analysis. Curr. Med. Chem. *16*, 2021–2041. https://doi.org/10.2174/092986709788682164.

Lhermitte, J., Kraus, W.M., and McAlpine, D. (1924). Original Papers: ON THE OCCURRENCE OF ABNORMAL DEPOSITS OF IRON IN THE BRAIN IN PARKINSONISM WITH SPECIAL REFERENCE TO ITS LOCALISATION. J. Neurol. Psychopathol. *5*, 195–208. https://doi.org/10.1136/jnnp.s1-5.19.195.

Li, A.E., Ito, H., Rovira, I.I., Kim, K.S., Takeda, K., Yu, Z.Y., Ferrans, V.J., and Finkel, T. (1999). A role for reactive oxygen species in endothelial cell anoikis. Circ. Res. *85*, 304–310. https://doi.org/10.1161/01.res.85.4.304.

Li, C., Deng, X., Zhang, W., Xie, X., Conrad, M., Liu, Y., Angeli, J.P.F., and Lai, L. (2019). Novel Allosteric Activators for Ferroptosis Regulator Glutathione Peroxidase 4. J. Med. Chem. *62*, 266–275. https://doi.org/10.1021/acs.jmedchem.8b00315.

Li, W.-W., Yang, R., Guo, J.-C., Ren, H.-M., Zha, X.-L., Cheng, J.-S., and Cai, D.-F. (2007). Localization of alpha-synuclein to mitochondria within midbrain of mice. Neuroreport *18*, 1543–1546. https://doi.org/10.1097/WNR.0b013e3282f03db4.

Li, Y., Maher, P., and Schubert, D. (1997). A role for 12-lipoxygenase in nerve cell death caused by glutathione depletion. Neuron *19*, 453–463. https://doi.org/10.1016/s0896-6273(00)80953-8.

Lin, M.T., and Beal, M.F. (2006). Mitochondrial dysfunction and oxidative stress in neurodegenerative diseases. Nature *443*, 787–795. https://doi.org/10.1038/nature05292.

Linkermann, A., Skouta, R., Himmerkus, N., Mulay, S.R., Dewitz, C., De Zen, F., Prokai, A., Zuchtriegel, G., Krombach, F., Welz, P.-S., et al. (2014). Synchronized renal tubular cell death involves ferroptosis. Proc. Natl. Acad. Sci. U. S. A. *111*, 16836–16841. https://doi.org/10.1073/pnas.1415518111.

Liu, C.-W., Giasson, B.I., Lewis, K.A., Lee, V.M., Demartino, G.N., and Thomas, P.J. (2005). A precipitating role for truncated alpha-synuclein and the proteasome in alpha-synuclein aggregation: implications for pathogenesis of Parkinson disease. J. Biol. Chem. *280*, 22670–22678. https://doi.org/10.1074/jbc.M501508200.

Liu, N., Lin, X., and Huang, C. (2020). Activation of the reverse transsulfuration pathway through NRF2/CBS confers erastin-induced ferroptosis resistance. Br. J. Cancer *122*, 279–292. https://doi.org/10.1038/s41416-019-0660-x.

Liu, S., Ninan, I., Antonova, I., Battaglia, F., Trinchese, F., Narasanna, A., Kolodilov, N., Dauer, W., Hawkins, R.D., and Arancio, O. (2004). alpha-Synuclein produces a long-lasting increase in neurotransmitter release. EMBO J. *23*, 4506–4516. https://doi.org/10.1038/sj.emboj.7600451.

Lotharius, J., and Brundin, P. (2002). Impaired dopamine storage resulting from alpha-synuclein mutations may contribute to the pathogenesis of Parkinson's disease. Hum. Mol. Genet. *11*, 2395–2407. https://doi.org/10.1093/hmg/11.20.2395.

Lotharius, J., Barg, S., Wiekop, P., Lundberg, C., Raymon, H.K., and Brundin, P. (2002). Effect of mutant alpha-synuclein on dopamine homeostasis in a new human mesencephalic cell line. J. Biol. Chem. *277*, 38884–38894. https://doi.org/10.1074/jbc.M205518200.

Lou, X., Kim, J., Hawk, B.J., and Shin, Y.-K. (2017). α-Synuclein may cross-bridge v-SNARE and acidic phospholipids to facilitate SNARE-dependent vesicle docking. Biochem. J. *474*, 2039–2049. https://doi.org/10.1042/BCJ20170200.

Ltic, S., Perovic, M., Mladenovic, A., Raicevic, N., Ruzdijic, S., Rakic, L., and Kanazir, S. (2004). Alpha-synuclein is expressed in different tissues during human fetal development. J. Mol. Neurosci. MN *22*, 199–204. https://doi.org/10.1385/jmn:22:3:199.

Lücke, C., Gantz, D.L., Klimtchuk, E., and Hamilton, J.A. (2006). Interactions between fatty acids and alpha-synuclein. J. Lipid Res. *47*, 1714–1724. https://doi.org/10.1194/jlr.M600003-JLR200.

Lücking, C.B., Dürr, A., Bonifati, V., Vaughan, J., De Michele, G., Gasser, T., Harhangi, B.S., Meco, G., Denèfle, P., Wood, N.W., et al. (2000). Association between early-onset Parkinson's disease and mutations in the parkin gene. N. Engl. J. Med. *342*, 1560–1567. https://doi.org/10.1056/NEJM200005253422103.

Ma, S., Henson, E.S., Chen, Y., and Gibson, S.B. (2016). Ferroptosis is induced following siramesine and lapatinib treatment of breast cancer cells. Cell Death Dis. *7*, e2307. https://doi.org/10.1038/cddis.2016.208.

Macedo, M.G., Anar, B., Bronner, I.F., Cannella, M., Squitieri, F., Bonifati, V., Hoogeveen, A., Heutink, P., and Rizzu, P. (2003). The DJ-1L166P mutant protein associated with early

onset Parkinson's disease is unstable and forms higher-order protein complexes. Hum. Mol. Genet. *12*, 2807–2816. https://doi.org/10.1093/hmg/ddg304.

Magtanong, L., Ko, P.-J., To, M., Cao, J.Y., Forcina, G.C., Tarangelo, A., Ward, C.C., Cho, K., Patti, G.J., Nomura, D.K., et al. (2019). Exogenous Monounsaturated Fatty Acids Promote a Ferroptosis-Resistant Cell State. Cell Chem. Biol. *26*, 420-432.e9. https://doi.org/10.1016/j.chembiol.2018.11.016.

Mahoney-Sánchez, L., Bouchaoui, H., Ayton, S., Devos, D., Duce, J.A., and Devedjian, J.-C. (2020). Ferroptosis and its potential role in the physiopathology of Parkinson's Disease. Prog. Neurobiol. 101890. https://doi.org/10.1016/j.pneurobio.2020.101890.

Maltsev, A.S., Ying, J., and Bax, A. (2012). Impact of N-terminal acetylation of α-synuclein on its random coil and lipid binding properties. Biochemistry *51*, 5004–5013. https://doi.org/10.1021/bi300642h.

Mandir, A.S., Przedborski, S., Jackson-Lewis, V., Wang, Z.Q., Simbulan-Rosenthal, C.M., Smulson, M.E., Hoffman, B.E., Guastella, D.B., Dawson, V.L., and Dawson, T.M. (1999). Poly(ADP-ribose) polymerase activation mediates 1-methyl-4-phenyl-1, 2,3,6-tetrahydropyridine (MPTP)-induced parkinsonism. Proc. Natl. Acad. Sci. U. S. A. *96*, 5774–5779. https://doi.org/10.1073/pnas.96.10.5774.

Manning-Bog, A.B., McCormack, A.L., Li, J., Uversky, V.N., Fink, A.L., and Di Monte, D.A. (2002). The herbicide paraquat causes up-regulation and aggregation of alpha-synuclein in mice: paraquat and alpha-synuclein. J. Biol. Chem. *277*, 1641–1644. https://doi.org/10.1074/jbc.C100560200.

Maroteaux, L., Campanelli, J.T., and Scheller, R.H. (1988). Synuclein: a neuron-specific protein localized to the nucleus and presynaptic nerve terminal. J. Neurosci. Off. J. Soc. Neurosci. *8*, 2804–2815. .

Marras, C., and Lang, A. (2013). Parkinson's disease subtypes: lost in translation? J. Neurol. Neurosurg. Psychiatry *84*, 409–415. https://doi.org/10.1136/jnnp-2012-303455.

Marras, C., Hincapié, C.A., Kristman, V.L., Cancelliere, C., Soklaridis, S., Li, A., Borg, J., af Geijerstam, J.-L., and Cassidy, J.D. (2014). Systematic review of the risk of Parkinson's disease after mild traumatic brain injury: results of the International Collaboration on Mild Traumatic Brain Injury Prognosis. Arch. Phys. Med. Rehabil. *95*, S238-244. https://doi.org/10.1016/j.apmr.2013.08.298.

Martin, L.J., Pan, Y., Price, A.C., Sterling, W., Copeland, N.G., Jenkins, N.A., Price, D.L., and Lee, M.K. (2006). Parkinson's disease alpha-synuclein transgenic mice develop neuronal mitochondrial degeneration and cell death. J. Neurosci. Off. J. Soc. Neurosci. *26*, 41–50. https://doi.org/10.1523/JNEUROSCI.4308-05.2006.

Martin-Bastida, A., Ward, R.J., Newbould, R., Piccini, P., Sharp, D., Kabba, C., Patel, M.C., Spino, M., Connelly, J., Tricta, F., et al. (2017). Brain iron chelation by deferiprone in a phase 2 randomised double-blinded placebo controlled clinical trial in Parkinson's disease. Sci. Rep. *7*, 1398. https://doi.org/10.1038/s41598-017-01402-2.

Martin-Sanchez, D., Ruiz-Andres, O., Poveda, J., Carrasco, S., Cannata-Ortiz, P., Sanchez-Niño, M.D., Ruiz Ortega, M., Egido, J., Linkermann, A., Ortiz, A., et al. (2017). Ferroptosis, but Not Necroptosis, Is Important in Nephrotoxic Folic Acid-Induced AKI. J. Am. Soc. Nephrol. JASN *28*, 218–229. https://doi.org/10.1681/ASN.2015121376.

Masaldan, S., Clatworthy, S.A.S., Gamell, C., Meggyesy, P.M., Rigopoulos, A.-T., Haupt, S., Haupt, Y., Denoyer, D., Adlard, P.A., Bush, A.I., et al. (2018). Iron accumulation in senescent cells is coupled with impaired ferritinophagy and inhibition of ferroptosis. Redox Biol. *14*, 100–115. https://doi.org/10.1016/j.redox.2017.08.015.

Masaldan, S., Bush, A.I., Devos, D., Rolland, A.S., and Moreau, C. (2019). Striking while the iron is hot: Iron metabolism and ferroptosis in neurodegeneration. Free Radic. Biol. Med. *133*, 221–233. https://doi.org/10.1016/j.freeradbiomed.2018.09.033.

Masliah, E., Rockenstein, E., Veinbergs, I., Mallory, M., Hashimoto, M., Takeda, A., Sagara, Y., Sisk, A., and Mucke, L. (2000). Dopaminergic loss and inclusion body formation in alpha-synuclein mice: implications for neurodegenerative disorders. Science *287*, 1265–1269. https://doi.org/10.1126/science.287.5456.1265.

Matsushita, M., Freigang, S., Schneider, C., Conrad, M., Bornkamm, G.W., and Kopf, M. (2015). T cell lipid peroxidation induces ferroptosis and prevents immunity to infection. J. Exp. Med. *212*, 555–568. https://doi.org/10.1084/jem.20140857.

Mayo, M., and Bordelon, Y. (2014). Dementia with Lewy Bodies. Semin. Neurol. *34*, 182–188. https://doi.org/10.1055/s-0034-1381741.

Mayr, L., Grabherr, F., Schwärzler, J., Reitmeier, I., Sommer, F., Gehmacher, T., Niederreiter, L., He, G.-W., Ruder, B., Kunz, K.T.R., et al. (2020). Dietary lipids fuel GPX4-restricted enteritis resembling Crohn's disease. Nat. Commun. *11*, 1775. https://doi.org/10.1038/s41467-020-15646-6.

McCarthy, R.C., Park, Y.-H., and Kosman, D.J. (2014). sAPP modulates iron efflux from brain microvascular endothelial cells by stabilizing the ferrous iron exporter ferroportin. EMBO Rep. *15*, 809–815. https://doi.org/10.15252/embr.201338064.

McDowall, J.S., Ntai, I., Honeychurch, K.C., Hart, J.P., Colin, P., Schneider, B.L., and Brown, D.R. (2017). Alpha-synuclein ferrireductase activity is detectible in vivo, is altered in Parkinson's disease and increases the neurotoxicity of DOPAL. Mol. Cell. Neurosci. *85*, 1–11. https://doi.org/10.1016/j.mcn.2017.08.001.

McGeer, P.L., Itagaki, S., Boyes, B.E., and McGeer, E.G. (1988). Reactive microglia are positive for HLA-DR in the substantia nigra of Parkinson's and Alzheimer's disease brains. Neurology *38*, 1285–1291. https://doi.org/10.1212/wnl.38.8.1285.

McKeith, I.G., Boeve, B.F., Dickson, D.W., Halliday, G., Taylor, J.-P., Weintraub, D., Aarsland, D., Galvin, J., Attems, J., Ballard, C.G., et al. (2017). Diagnosis and management of dementia with Lewy bodies: Fourth consensus report of the DLB Consortium. Neurology *89*, 88–100. https://doi.org/10.1212/WNL.0000000000004058.

Mendez-Gomez, H.R., Singh, J., Meyers, C., Chen, W., Gorbatyuk, O.S., and Muzyczka, N. (2018). The Lipase Activity of Phospholipase D2 is Responsible for Nigral

Neurodegeneration in a Rat Model of Parkinson's Disease. Neuroscience *377*, 174–183. https://doi.org/10.1016/j.neuroscience.2018.02.047.

Mischley, L.K., Allen, J., and Bradley, R. (2012). Coenzyme Q10 Deficiency in Patients with Parkinson's Disease. J. Neurol. Sci. *318*, 72–75. https://doi.org/10.1016/j.jns.2012.03.023.

Mogi, M., Harada, M., Riederer, P., Narabayashi, H., Fujita, K., and Nagatsu, T. (1994). Tumor necrosis factor-alpha (TNF-alpha) increases both in the brain and in the cerebrospinal fluid from parkinsonian patients. Neurosci. Lett. *165*, 208–210. https://doi.org/10.1016/0304-3940(94)90746-3.

Mogi, M., Kondo, T., Mizuno, Y., and Nagatsu, T. (2007). p53 protein, interferon-gamma, and NF-kappaB levels are elevated in the parkinsonian brain. Neurosci. Lett. *414*, 94–97. https://doi.org/10.1016/j.neulet.2006.12.003.

Mohamed, N.-V., Sirois, J., Ramamurthy, J., Mathur, M., Lépine, P., Deneault, E., Maussion, G., Nicouleau, M., Chen, C.X.-Q., Abdian, N., et al. (2021). Midbrain organoids with an SNCA gene triplication model key feature of synucleinopathy. Brain Commun. *3*, fcab223. https://doi.org/10.1093/braincomms/fcab223.

Moisan, F., Spinosi, J., Delabre, L., Gourlet, V., Mazurie, J.-L., Bénatru, I., Goldberg, M., Weisskopf, M.G., Imbernon, E., Tzourio, C., et al. (2015). Association of Parkinson's Disease and Its Subtypes with Agricultural Pesticide Exposures in Men: A Case-Control Study in France. Environ. Health Perspect. *123*, 1123–1129. https://doi.org/10.1289/ehp.1307970.

Moreau, C., Duce, J.A., Rascol, O., Devedjian, J.-C., Berg, D., Dexter, D., Cabantchik, Z.I., Bush, A.I., and Devos, D. (2018). Iron as a therapeutic target for Parkinson's disease. Mov. Disord. *33*, 568–574. https://doi.org/10.1002/mds.27275.

Murphy, R.C. (2001). Free-radical-induced oxidation of arachidonoyl plasmalogen phospholipids: antioxidant mechanism and precursor pathway for bioactive eicosanoids. Chem. Res. Toxicol. *14*, 463–472. https://doi.org/10.1021/tx000250t.

Murray, I.V.J., Giasson, B.I., Quinn, S.M., Koppaka, V., Axelsen, P.H., Ischiropoulos, H., Trojanowski, J.Q., and Lee, V.M.-Y. (2003). Role of alpha-synuclein carboxy-terminus on fibril formation in vitro. Biochemistry *42*, 8530–8540. https://doi.org/10.1021/bi027363r.

Nagatsua, T., and Sawadab, M. (2009). L-dopa therapy for Parkinson's disease: past, present, and future. Parkinsonism Relat. Disord. *15 Suppl 1*, S3-8. https://doi.org/10.1016/S1353-8020(09)70004-5.

Nakajo, S., Omata, K., Aiuchi, T., Shibayama, T., Okahashi, I., Ochiai, H., Nakai, Y., Nakaya, K., and Nakamura, Y. (1990). Purification and characterization of a novel brain-specific 14-kDa protein. J. Neurochem. *55*, 2031–2038. https://doi.org/10.1111/j.1471-4159.1990.tb05792.x.

Nakamura, K., Nemani, V.M., Wallender, E.K., Kaehlcke, K., Ott, M., and Edwards, R.H. (2008). Optical reporters for the conformation of alpha-synuclein reveal a specific interaction with mitochondria. J. Neurosci. Off. J. Soc. Neurosci. *28*, 12305–12317. https://doi.org/10.1523/JNEUROSCI.3088-08.2008.

Nakamura, K., Nemani, V.M., Azarbal, F., Skibinski, G., Levy, J.M., Egami, K., Munishkina, L., Zhang, J., Gardner, B., Wakabayashi, J., et al. (2011). Direct membrane association drives mitochondrial fission by the Parkinson disease-associated protein alpha-synuclein. J. Biol. Chem. *286*, 20710–20726. https://doi.org/10.1074/jbc.M110.213538.

Narhi, L., Wood, S.J., Steavenson, S., Jiang, Y., Wu, G.M., Anafi, D., Kaufman, S.A., Martin, F., Sitney, K., Denis, P., et al. (1999). Both familial Parkinson's disease mutations accelerate alpha-synuclein aggregation. J. Biol. Chem. *274*, 9843–9846. https://doi.org/10.1074/jbc.274.14.9843.

Naudí, A., Cabré, R., Dominguez-Gonzalez, M., Ayala, V., Jové, M., Mota-Martorell, N., Piñol-Ripoll, G., Gil-Villar, M.P., Rué, M., Portero-Otín, M., et al. (2017). Region-specific vulnerability to lipid peroxidation and evidence of neuronal mechanisms for polyunsaturated fatty acid biosynthesis in the healthy adult human central nervous system. Biochim. Biophys. Acta Mol. Cell Biol. Lipids *1862*, 485–495. https://doi.org/10.1016/j.bbalip.2017.02.001.

Neumann, M., Adler, S., Schlüter, O., Kremmer, E., Benecke, R., and Kretzschmar, H.A. (2000). Alpha-synuclein accumulation in a case of neurodegeneration with brain iron accumulation type 1 (NBIA-1, formerly Hallervorden-Spatz syndrome) with widespread cortical and brainstem-type Lewy bodies. Acta Neuropathol. (Berl.) *100*, 568–574. https://doi.org/10.1007/s004010000224.

Nishie, M., Mori, F., Fujiwara, H., Hasegawa, M., Yoshimoto, M., Iwatsubo, T., Takahashi, H., and Wakabayashi, K. (2004). Accumulation of phosphorylated alpha-synuclein in the brain and peripheral ganglia of patients with multiple system atrophy. Acta Neuropathol. (Berl.) *107*, 292–298. https://doi.org/10.1007/s00401-003-0811-1.

Noyce, A.J., Bestwick, J.P., Silveira-Moriyama, L., Hawkes, C.H., Giovannoni, G., Lees, A.J., and Schrag, A. (2012). Meta-analysis of early nonmotor features and risk factors for Parkinson disease. Ann. Neurol. *72*, 893–901. https://doi.org/10.1002/ana.23687.

Nübling, G.S., Levin, J., Bader, B., Lorenzl, S., Hillmer, A., Högen, T., Kamp, F., and Giese, A. (2014). Modelling Ser129 phosphorylation inhibits membrane binding of pore-forming alpha-synuclein oligomers. PloS One *9*, e98906. https://doi.org/10.1371/journal.pone.0098906.

Oestreicher, J., and Morgan, B. (2019). Glutathione: subcellular distribution and membrane transport 1. Biochem. Cell Biol. Biochim. Biol. Cell. *97*, 270–289. https://doi.org/10.1139/bcb-2018-0189.

Ohi, Y., Qin, H., Hong, C., Blouin, L., Polo, J.M., Guo, T., Qi, Z., Downey, S.L., Manos, P.D., Rossi, D.J., et al. (2011). Incomplete DNA methylation underlies a transcriptional memory of somatic cells in human iPS cells. Nat. Cell Biol. *13*, 541–549. https://doi.org/10.1038/ncb2239.

Okochi, M., Walter, J., Koyama, A., Nakajo, S., Baba, M., Iwatsubo, T., Meijer, L., Kahle, P.J., and Haass, C. (2000). Constitutive phosphorylation of the Parkinson's disease associated alpha-synuclein. J. Biol. Chem. *275*, 390–397. https://doi.org/10.1074/jbc.275.1.390.

Olanow, C.W., Kieburtz, K., Odin, P., Espay, A.J., Standaert, D.G., Fernandez, H.H., Vanagunas, A., Othman, A.A., Widnell, K.L., Robieson, W.Z., et al. (2014). Continuous

intrajejunal infusion of levodopa-carbidopa intestinal gel for patients with advanced Parkinson's disease: a randomised, controlled, double-blind, double-dummy study. Lancet Neurol. *13*, 141–149. https://doi.org/10.1016/S1474-4422(13)70293-X.

Ortega, R., Carmona, A., Roudeau, S., Perrin, L., Dučić, T., Carboni, E., Bohic, S., Cloetens, P., and Lingor, P. (2016). α-Synuclein Over-Expression Induces Increased Iron Accumulation and Redistribution in Iron-Exposed Neurons. Mol. Neurobiol. *53*, 1925–1934. https://doi.org/10.1007/s12035-015-9146-x.

Osburn, W.O., Wakabayashi, N., Misra, V., Nilles, T., Biswal, S., Trush, M.A., and Kensler, T.W. (2006). Nrf2 Regulates an Adaptive Response Protecting Against Oxidative Damage Following Diquat-Mediated Formation of Superoxide Anion. Arch. Biochem. Biophys. *454*, 7–15. https://doi.org/10.1016/j.abb.2006.08.005.

Ostrerova-Golts, N., Petrucelli, L., Hardy, J., Lee, J.M., Farer, M., and Wolozin, B. (2000). The A53T alpha-synuclein mutation increases iron-dependent aggregation and toxicity. J. Neurosci. Off. J. Soc. Neurosci. *20*, 6048–6054. .

Ou, Y., Wang, S.-J., Li, D., Chu, B., and Gu, W. (2016). Activation of SAT1 engages polyamine metabolism with p53-mediated ferroptotic responses. Proc. Natl. Acad. Sci. U. S. A. *113*, E6806–E6812. https://doi.org/10.1073/pnas.1607152113.

Ouberai, M.M., Wang, J., Swann, M.J., Galvagnion, C., Guilliams, T., Dobson, C.M., and Welland, M.E. (2013). α-Synuclein senses lipid packing defects and induces lateral expansion of lipids leading to membrane remodeling. J. Biol. Chem. *288*, 20883–20895. https://doi.org/10.1074/jbc.M113.478297.

Outeiro, T.F., Grammatopoulos, T.N., Altmann, S., Amore, A., Standaert, D.G., Hyman, B.T., and Kazantsev, A.G. (2007). Pharmacological inhibition of PARP-1 reduces alpha-synuclein- and MPP+-induced cytotoxicity in Parkinson's disease in vitro models. Biochem. Biophys. Res. Commun. *357*, 596–602. https://doi.org/10.1016/j.bbrc.2007.03.163.

Ozelius, L.J., Senthil, G., Saunders-Pullman, R., Ohmann, E., Deligtisch, A., Tagliati, M., Hunt, A.L., Klein, C., Henick, B., Hailpern, S.M., et al. (2006). LRRK2 G2019S as a cause of Parkinson's disease in Ashkenazi Jews. N. Engl. J. Med. *354*, 424–425. https://doi.org/10.1056/NEJMc055509.

Paleologou, K.E., Oueslati, A., Shakked, G., Rospigliosi, C.C., Kim, H.-Y., Lamberto, G.R., Fernandez, C.O., Schmid, A., Chegini, F., Gai, W.P., et al. (2010). Phosphorylation at S87 is enhanced in synucleinopathies, inhibits alpha-synuclein oligomerization, and influences synuclein-membrane interactions. J. Neurosci. Off. J. Soc. Neurosci. *30*, 3184–3198. https://doi.org/10.1523/JNEUROSCI.5922-09.2010.

Pankratz, N., Pauciulo, M.W., Elsaesser, V.E., Marek, D.K., Halter, C.A., Wojcieszek, J., Rudolph, A., Shults, C.W., Foroud, T., Nichols, W.C., et al. (2006). Mutations in DJ-1 are rare in familial Parkinson disease. Neurosci. Lett. *408*, 209–213. https://doi.org/10.1016/j.neulet.2006.09.003.

Parkinson Study Group QE3 Investigators, Beal, M.F., Oakes, D., Shoulson, I., Henchcliffe, C., Galpern, W.R., Haas, R., Juncos, J.L., Nutt, J.G., Voss, T.S., et al. (2014). A randomized

clinical trial of high-dosage coenzyme Q10 in early Parkinson disease: no evidence of benefit. JAMA Neurol. *71*, 543–552. https://doi.org/10.1001/jamaneurol.2014.131.

Paul, S., Lancaster, G.I., and Meikle, P.J. (2019). Plasmalogens: A potential therapeutic target for neurodegenerative and cardiometabolic disease. Prog. Lipid Res. *74*, 186–195. https://doi.org/10.1016/j.plipres.2019.04.003.

Payton, J.E., Perrin, R.J., Woods, W.S., and George, J.M. (2004). Structural determinants of PLD2 inhibition by alpha-synuclein. J. Mol. Biol. *337*, 1001–1009. https://doi.org/10.1016/j.jmb.2004.02.014.

PD Med Collaborative Group, Gray, R., Ives, N., Rick, C., Patel, S., Gray, A., Jenkinson, C., McIntosh, E., Wheatley, K., Williams, A., et al. (2014). Long-term effectiveness of dopamine agonists and monoamine oxidase B inhibitors compared with levodopa as initial treatment for Parkinson's disease (PD MED): a large, open-label, pragmatic randomised trial. Lancet Lond. Engl. *384*, 1196–1205. https://doi.org/10.1016/S0140-6736(14)60683-8.

Pearce, R.K., Owen, A., Daniel, S., Jenner, P., and Marsden, C.D. (1997). Alterations in the distribution of glutathione in the substantia nigra in Parkinson's disease. J. Neural Transm. Vienna Austria 1996 *104*, 661–677. https://doi.org/10.1007/BF01291884.

Peng, X., Peng, X.M., Tehranian, R., Dietrich, P., Stefanis, L., and Perez, R.G. (2005). Alpha-synuclein activation of protein phosphatase 2A reduces tyrosine hydroxylase phosphorylation in dopaminergic cells. J. Cell Sci. *118*, 3523–3530. https://doi.org/10.1242/jcs.02481.

Peng, Y., Wang, C., Xu, H.H., Liu, Y.-N., and Zhou, F. (2010). Binding of alpha-synuclein with Fe(III) and with Fe(II) and biological implications of the resultant complexes. J. Inorg. Biochem. *104*, 365–370. https://doi.org/10.1016/j.jinorgbio.2009.11.005.

Perez, M.A., Magtanong, L., Dixon, S.J., and Watts, J.L. (2020). Dietary Lipids Induce Ferroptosis in Caenorhabditiselegans and Human Cancer Cells. Dev. Cell *54*, 447-454.e4. https://doi.org/10.1016/j.devcel.2020.06.019.

Perez, R.G., Waymire, J.C., Lin, E., Liu, J.J., Guo, F., and Zigmond, M.J. (2002). A role for alpha-synuclein in the regulation of dopamine biosynthesis. J. Neurosci. Off. J. Soc. Neurosci. *22*, 3090–3099. https://doi.org/20026307.

Periquet, M., Latouche, M., Lohmann, E., Rawal, N., De Michele, G., Ricard, S., Teive, H., Fraix, V., Vidailhet, M., Nicholl, D., et al. (2003). Parkin mutations are frequent in patients with isolated early-onset parkinsonism. Brain J. Neurol. *126*, 1271–1278. https://doi.org/10.1093/brain/awg136.

Perrin, R.J., Woods, W.S., Clayton, D.F., and George, J.M. (2000). Interaction of human alpha-Synuclein and Parkinson's disease variants with phospholipids. Structural analysis using site-directed mutagenesis. J. Biol. Chem. *275*, 34393–34398. https://doi.org/10.1074/jbc.M004851200.

Petrillo, S., Schirinzi, T., Lazzaro, G.D., D'Amico, J., Colona, V.L., Bertini, E., Pierantozzi, M., Mari, L., Mercuri, N.B., Piemonte, F., et al. (2020). Systemic Activation of Nrf2 Pathway in Parkinson's Disease. Mov. Disord. *35*, 180–184. https://doi.org/10.1002/mds.27878.

Petrovitch, H., Ross, G.W., Abbott, R.D., Sanderson, W.T., Sharp, D.S., Tanner, C.M., Masaki, K.H., Blanchette, P.L., Popper, J.S., Foley, D., et al. (2002). Plantation work and risk of Parkinson disease in a population-based longitudinal study. Arch. Neurol. *59*, 1787–1792. https://doi.org/10.1001/archneur.59.11.1787.

Pickrell, A.M., and Youle, R.J. (2015). The roles of PINK1, parkin, and mitochondrial fidelity in Parkinson's disease. Neuron *85*, 257–273. https://doi.org/10.1016/j.neuron.2014.12.007.

Piperno, A., Pelucchi, S., and Mariani, R. (2020). Inherited iron overload disorders. Transl. Gastroenterol. Hepatol. *5*, 25. https://doi.org/10.21037/tgh.2019.11.15.

Platt, R.J., Chen, S., Zhou, Y., Yim, M.J., Swiech, L., Kempton, H.R., Dahlman, J.E., Parnas, O., Eisenhaure, T.M., Jovanovic, M., et al. (2014). CRISPR-Cas9 knockin mice for genome editing and cancer modeling. Cell *159*, 440–455. https://doi.org/10.1016/j.cell.2014.09.014.

Polymeropoulos, M.H., Lavedan, C., Leroy, E., Ide, S.E., Dehejia, A., Dutra, A., Pike, B., Root, H., Rubenstein, J., Boyer, R., et al. (1997). Mutation in the alpha-synuclein gene identified in families with Parkinson's disease. Science *276*, 2045–2047. https://doi.org/10.1126/science.276.5321.2045.

Postuma, R.B., Aarsland, D., Barone, P., Burn, D.J., Hawkes, C.H., Oertel, W., and Ziemssen, T. (2012). Identifying prodromal Parkinson's disease: pre-motor disorders in Parkinson's disease. Mov. Disord. Off. J. Mov. Disord. Soc. *27*, 617–626. https://doi.org/10.1002/mds.24996.

Pringsheim, T., Jette, N., Frolkis, A., and Steeves, T.D.L. (2014). The prevalence of Parkinson's disease: a systematic review and meta-analysis. Mov. Disord. Off. J. Mov. Disord. Soc. *29*, 1583–1590. https://doi.org/10.1002/mds.25945.

Pronin, A.N., Morris, A.J., Surguchov, A., and Benovic, J.L. (2000). Synucleins are a novel class of substrates for G protein-coupled receptor kinases. J. Biol. Chem. *275*, 26515–26522. https://doi.org/10.1074/jbc.M003542200.

Pyatigorskaya, N., Sharman, M., Corvol, J.-C., Valabregue, R., Yahia-Cherif, L., Poupon, F., Cormier-Dequaire, F., Siebner, H., Klebe, S., Vidailhet, M., et al. (2015). High nigral iron deposition in LRRK2 and Parkin mutation carriers using R2* relaxometry. Mov. Disord. Off. J. Mov. Disord. Soc. *30*, 1077–1084. https://doi.org/10.1002/mds.26218.

Q, R., H, L., M, G., W, Q., Ca, W., Lj, R., B, H., A, R., and H, V.R. (2004). Transgenic mice overexpressing glutathione peroxidase 4 are protected against oxidative stress-induced apoptosis. J. Biol. Chem. *279*. https://doi.org/10.1074/jbc.M410387200.

Qi, X., Davis, B., Chiang, Y.-H., Filichia, E., Barnett, A., Greig, N.H., Hoffer, B., and Luo, Y. (2016). Dopaminergic neuron-specific deletion of p53 gene is neuroprotective in an experimental Parkinson's disease model. J. Neurochem. *138*, 746–757. https://doi.org/10.1111/jnc.13706.

Ramsey, C.P., Glass, C.A., Montgomery, M.B., Lindl, K.A., Ritson, G.P., Chia, L.A., Hamilton, R.L., Chu, C.T., and Jordan-Sciutto, K.L. (2007). Expression of Nrf2 in

Neurodegenerative Diseases. J. Neuropathol. Exp. Neurol. *66*, 75–85. https://doi.org/10.1097/nen.0b013e31802d6da9.

Reinhardt, P., Glatza, M., Hemmer, K., Tsytsyura, Y., Thiel, C.S., Höing, S., Moritz, S., Parga, J.A., Wagner, L., Bruder, J.M., et al. (2013). Derivation and Expansion Using Only Small Molecules of Human Neural Progenitors for Neurodegenerative Disease Modeling. PLOS ONE *8*, e59252. https://doi.org/10.1371/journal.pone.0059252.

Reiss, D., Beyer, K., and Engelmann, B. (1997). Delayed oxidative degradation of polyunsaturated diacyl phospholipids in the presence of plasmalogen phospholipids in vitro. Biochem. J. *323 (Pt 3)*, 807–814. https://doi.org/10.1042/bj3230807.

Reyes, J.F., Rey, N.L., Bousset, L., Melki, R., Brundin, P., and Angot, E. (2014). Alpha-synuclein transfers from neurons to oligodendrocytes. Glia *62*, 387–398. https://doi.org/10.1002/glia.22611.

Rhodes, S.L., Buchanan, D.D., Ahmed, I., Taylor, K.D., Loriot, M.-A., Sinsheimer, J.S., Bronstein, J.M., Elbaz, A., Mellick, G.D., Rotter, J.I., et al. (2014). Pooled analysis of iron-related genes in Parkinson's disease: association with transferrin. Neurobiol. Dis. *62*, 172–178. https://doi.org/10.1016/j.nbd.2013.09.019.

Ribeiro, C.S., Carneiro, K., Ross, C.A., Menezes, J.R.L., and Engelender, S. (2002). Synphilin-1 is developmentally localized to synaptic terminals, and its association with synaptic vesicles is modulated by alpha-synuclein. J. Biol. Chem. *277*, 23927–23933. https://doi.org/10.1074/jbc.M201115200.

Rogaeva, E., Johnson, J., Lang, A.E., Gulick, C., Gwinn-Hardy, K., Kawarai, T., Sato, C., Morgan, A., Werner, J., Nussbaum, R., et al. (2004). Analysis of the PINK1 gene in a large cohort of cases with Parkinson disease. Arch. Neurol. *61*, 1898–1904. https://doi.org/10.1001/archneur.61.12.1898.

Ross, G.W., Petrovitch, H., and Abbott, R.D. (2016). Serum vitamin D and risk of Parkinson's disease. Mov. Disord. Off. J. Mov. Disord. Soc. *31*, 993–935. https://doi.org/10.1002/mds.26639.

Ross, O.A., Braithwaite, A.T., Skipper, L.M., Kachergus, J., Hulihan, M.M., Middleton, F.A., Nishioka, K., Fuchs, J., Gasser, T., Maraganore, D.M., et al. (2008). Genomic investigation of alpha-synuclein multiplication and parkinsonism. Ann. Neurol. *63*, 743–750. https://doi.org/10.1002/ana.21380.

Rugbjerg, K., Ritz, B., Korbo, L., Martinussen, N., and Olsen, J.H. (2008). Risk of Parkinson's disease after hospital contact for head injury: population-based case-control study. BMJ *337*, a2494. https://doi.org/10.1136/bmj.a2494.

Ruigrok, M.J.R., Maggan, N., Willaert, D., Frijlink, H.W., Melgert, B.N., Olinga, P., and Hinrichs, W.L.J. (2017). siRNA-Mediated RNA Interference in Precision-Cut Tissue Slices Prepared from Mouse Lung and Kidney. AAPS J. *19*, 1855–1863. https://doi.org/10.1208/s12248-017-0136-y.

Ruigrok, M.J.R., Xian, J.-L., Frijlink, H.W., Melgert, B.N., Hinrichs, W.L.J., and Olinga, P. (2018). siRNA-mediated protein knockdown in precision-cut lung slices. Eur. J. Pharm.

Biopharm. Off. J. Arbeitsgemeinschaft Pharm. Verfahrenstechnik EV *133*, 339–348. https://doi.org/10.1016/j.ejpb.2018.11.005.

Saha, A.R., Ninkina, N.N., Hanger, D.P., Anderton, B.H., Davies, A.M., and Buchman, V.L. (2000). Induction of neuronal death by alpha-synuclein. Eur. J. Neurosci. *12*, 3073–3077. https://doi.org/10.1046/j.1460-9568.2000.00210.x.

Salazar, J., Mena, N., Hunot, S., Prigent, A., Alvarez-Fischer, D., Arredondo, M., Duyckaerts, C., Sazdovitch, V., Zhao, L., Garrick, L.M., et al. (2008). Divalent metal transporter 1 (DMT1) contributes to neurodegeneration in animal models of Parkinson's disease. Proc. Natl. Acad. Sci. U. S. A. *105*, 18578–18583. https://doi.org/10.1073/pnas.0804373105.

Sánchez Campos, S., Alza, N.P., and Salvador, G.A. (2018). Lipid metabolism alterations in the neuronal response to A53T α-synuclein and Fe-induced injury. Arch. Biochem. Biophys. *655*, 43–54. https://doi.org/10.1016/j.abb.2018.08.007.

Schildknecht, S., Karreman, C., Pöltl, D., Efrémova, L., Kullmann, C., Gutbier, S., Krug, A., Scholz, D., Gerding, H.R., and Leist, M. (2013). Generation of genetically-modified human differentiated cells for toxicological tests and the study of neurodegenerative diseases. ALTEX *30*, 427–444. https://doi.org/10.14573/altex.2013.4.427.

Schneider, S.A., and Obeso, J.A. (2015). Clinical and pathological features of Parkinson's disease. Curr. Top. Behav. Neurosci. *22*, 205–220. https://doi.org/10.1007/7854_2014_317.

Scholz, D., Pöltl, D., Genewsky, A., Weng, M., Waldmann, T., Schildknecht, S., and Leist, M. (2011). Rapid, complete and large-scale generation of post-mitotic neurons from the human LUHMES cell line. J. Neurochem. *119*, 957–971. https://doi.org/10.1111/j.1471-4159.2011.07255.x.

Schuepbach, W.M.M., Rau, J., Knudsen, K., Volkmann, J., Krack, P., Timmermann, L., Hälbig, T.D., Hesekamp, H., Navarro, S.M., Meier, N., et al. (2013). Neurostimulation for Parkinson's disease with early motor complications. N. Engl. J. Med. *368*, 610–622. https://doi.org/10.1056/NEJMoa1205158.

Schulte, E.C., Fukumori, A., Mollenhauer, B., Hor, H., Arzberger, T., Perneczky, R., Kurz, A., Diehl-Schmid, J., Hüll, M., Lichtner, P., et al. (2015). Rare variants in β-Amyloid precursor protein (APP) and Parkinson's disease. Eur. J. Hum. Genet. EJHG *23*, 1328–1333. https://doi.org/10.1038/ejhg.2014.300.

Seiler, A., Schneider, M., Förster, H., Roth, S., Wirth, E.K., Culmsee, C., Plesnila, N., Kremmer, E., Rådmark, O., Wurst, W., et al. (2008). Glutathione peroxidase 4 senses and translates oxidative stress into 12/15-lipoxygenase dependent- and AIF-mediated cell death. Cell Metab. *8*, 237–248. https://doi.org/10.1016/j.cmet.2008.07.005.

Selley, M.L. (1998). (E)-4-hydroxy-2-nonenal may be involved in the pathogenesis of Parkinson's disease. Free Radic. Biol. Med. *25*, 169–174. https://doi.org/10.1016/s0891-5849(98)00021-5.

Senior, S.L., Ninkina, N., Deacon, R., Bannerman, D., Buchman, V.L., Cragg, S.J., and Wade-Martins, R. (2008). Increased striatal dopamine release and hyperdopaminergic-like

behaviour in mice lacking both alpha-synuclein and gamma-synuclein. Eur. J. Neurosci. *27*, 947–957. https://doi.org/10.1111/j.1460-9568.2008.06055.x.

Shah, R., Margison, K., and Pratt, D.A. (2017). The Potency of Diarylamine Radical-Trapping Antioxidants as Inhibitors of Ferroptosis Underscores the Role of Autoxidation in the Mechanism of Cell Death. ACS Chem. Biol. *12*, 2538–2545. https://doi.org/10.1021/acschembio.7b00730.

Shah, R., Shchepinov, M.S., and Pratt, D.A. (2018). Resolving the Role of Lipoxygenases in the Initiation and Execution of Ferroptosis. ACS Cent. Sci. *4*, 387–396. https://doi.org/10.1021/acscentsci.7b00589.

Shah, R.R., Cholewa-Waclaw, J., Davies, F.C.J., Paton, K.M., Chaligne, R., Heard, E., Abbott, C.M., and Bird, A.P. (2016). Efficient and versatile CRISPR engineering of human neurons in culture to model neurological disorders. Wellcome Open Res. *1*, 13. https://doi.org/10.12688/wellcomeopenres.10011.1.

Shahmoradian, S.H., Lewis, A.J., Genoud, C., Hench, J., Moors, T.E., Navarro, P.P., Castaño-Díez, D., Schweighauser, G., Graff-Meyer, A., Goldie, K.N., et al. (2019). Lewy pathology in Parkinson's disease consists of crowded organelles and lipid membranes. Nat. Neurosci. *22*, 1099–1109. https://doi.org/10.1038/s41593-019-0423-2.

Shamoto-Nagai, M., Hisaka, S., Naoi, M., and Maruyama, W. (2018). Modification of α-synuclein by lipid peroxidation products derived from polyunsaturated fatty acids promotes toxic oligomerization: its relevance to Parkinson disease. J. Clin. Biochem. Nutr. *62*, 207–212. https://doi.org/10.3164/jcbn.18-25.

Sharon, R., Goldberg, M.S., Bar-Josef, I., Betensky, R.A., Shen, J., and Selkoe, D.J. (2001). alpha-Synuclein occurs in lipid-rich high molecular weight complexes, binds fatty acids, and shows homology to the fatty acid-binding proteins. Proc. Natl. Acad. Sci. U. S. A. *98*, 9110–9115. https://doi.org/10.1073/pnas.171300598.

Sharon, R., Bar-Joseph, I., Mirick, G.E., Serhan, C.N., and Selkoe, D.J. (2003). Altered fatty acid composition of dopaminergic neurons expressing alpha-synuclein and human brains with alpha-synucleinopathies. J. Biol. Chem. *278*, 49874–49881. https://doi.org/10.1074/jbc.M309127200.

Shchepinov, M.S., Chou, V.P., Pollock, E., Langston, J.W., Cantor, C.R., Molinari, R.J., and Manning-Boğ, A.B. (2011). Isotopic reinforcement of essential polyunsaturated fatty acids diminishes nigrostriatal degeneration in a mouse model of Parkinson's disease. Toxicol. Lett. *207*, 97–103. https://doi.org/10.1016/j.toxlet.2011.07.020.

Shi, X., Tarazona, P., Brock, T.J., Browse, J., Feussner, I., and Watts, J.L. (2016). A Caenorhabditis elegans model for ether lipid biosynthesis and function. J. Lipid Res. *57*, 265–275. https://doi.org/10.1194/jlr.M064808.

Shibasaki, Y., Baillie, D.A., St Clair, D., and Brookes, A.J. (1995). High-resolution mapping of SNCA encoding alpha-synuclein, the non-A beta component of Alzheimer's disease amyloid precursor, to human chromosome 4q21.3-->q22 by fluorescence in situ hybridization. Cytogenet. Cell Genet. *71*, 54–55. https://doi.org/10.1159/000134061.

Shimada, K., Skouta, R., Kaplan, A., Yang, W.S., Hayano, M., Dixon, S.J., Brown, L.M., Valenzuela, C.A., Wolpaw, A.J., and Stockwell, B.R. (2016). Global survey of cell death mechanisms reveals metabolic regulation of ferroptosis. Nat. Chem. Biol. *12*, 497–503. https://doi.org/10.1038/nchembio.2079.

Shin, D., Lee, J., You, J.H., Kim, D., and Roh, J.-L. (2020). Dihydrolipoamide dehydrogenase regulates cystine deprivation-induced ferroptosis in head and neck cancer. Redox Biol. *30*, 101418. https://doi.org/10.1016/j.redox.2019.101418.

Shin, E.C., Cho, S.E., Lee, D.K., Hur, M.W., Paik, S.R., Park, J.H., and Kim, J. (2000). Expression patterns of alpha-synuclein in human hematopoietic cells and in Drosophila at different developmental stages. Mol. Cells *10*, 65–70. https://doi.org/10.1007/s10059-000-0065-x.

Shintoku, R., Takigawa, Y., Yamada, K., Kubota, C., Yoshimoto, Y., Takeuchi, T., Koshiishi, I., and Torii, S. (2017). Lipoxygenase-mediated generation of lipid peroxides enhances ferroptosis induced by erastin and RSL3. Cancer Sci. *108*, 2187–2194. https://doi.org/10.1111/cas.13380.

Sian, J., Dexter, D.T., Lees, A.J., Daniel, S., Agid, Y., Javoy-Agid, F., Jenner, P., and Marsden, C.D. (1994). Alterations in glutathione levels in Parkinson's disease and other neurodegenerative disorders affecting basal ganglia. Ann. Neurol. *36*, 348–355. https://doi.org/10.1002/ana.410360305.

Sidhu, A., Wersinger, C., and Vernier, P. (2004). alpha-Synuclein regulation of the dopaminergic transporter: a possible role in the pathogenesis of Parkinson's disease. FEBS Lett. *565*, 1–5. https://doi.org/10.1016/j.febslet.2004.03.063.

Sidransky, E., Nalls, M.A., Aasly, J.O., Aharon-Peretz, J., Annesi, G., Barbosa, E.R., Bar-Shira, A., Berg, D., Bras, J., Brice, A., et al. (2009). Multicenter analysis of glucocerebrosidase mutations in Parkinson's disease. N. Engl. J. Med. *361*, 1651–1661. https://doi.org/10.1056/NEJMoa0901281.

Siegert, A., Rankovic, M., Favretto, F., Ukmar-Godec, T., Strohäker, T., Becker, S., and Zweckstetter, M. (2021). Interplay between tau and α-synuclein liquid-liquid phase separation. Protein Sci. Publ. Protein Soc. *30*, 1326–1336. https://doi.org/10.1002/pro.4025.

Skouta, R., Dixon, S.J., Wang, J., Dunn, D.E., Orman, M., Shimada, K., Rosenberg, P.A., Lo, D.C., Weinberg, J.M., Linkermann, A., et al. (2014). Ferrostatins inhibit oxidative lipid damage and cell death in diverse disease models. J. Am. Chem. Soc. *136*, 4551–4556. https://doi.org/10.1021/ja411006a.

Smith, W.W., Jiang, H., Pei, Z., Tanaka, Y., Morita, H., Sawa, A., Dawson, V.L., Dawson, T.M., and Ross, C.A. (2005). Endoplasmic reticulum stress and mitochondrial cell death pathways mediate A53T mutant alpha-synuclein-induced toxicity. Hum. Mol. Genet. *14*, 3801–3811. https://doi.org/10.1093/hmg/ddi396.

Sofic, E., Lange, K.W., Jellinger, K., and Riederer, P. (1992). Reduced and oxidized glutathione in the substantia nigra of patients with Parkinson's disease. Neurosci. Lett. *142*, 128–130. https://doi.org/10.1016/0304-3940(92)90355-b.

Song, N., and Xie, J. (2018). Iron, Dopamine, and α-Synuclein Interactions in at-Risk Dopaminergic Neurons in Parkinson's Disease. Neurosci. Bull. *34*, 382–384. https://doi.org/10.1007/s12264-018-0209-7.

Song, X., and Long, D. (2020). Nrf2 and Ferroptosis: A New Research Direction for Neurodegenerative Diseases. Front. Neurosci. *14*. https://doi.org/10.3389/fnins.2020.00267.

Song, N., Wang, J., Jiang, H., and Xie, J. (2010). Ferroportin 1 but not hephaestin contributes to iron accumulation in a cell model of Parkinson's disease. Free Radic. Biol. Med. *48*, 332–341. https://doi.org/10.1016/j.freeradbiomed.2009.11.004.

Song, X., Zhu, S., Chen, P., Hou, W., Wen, Q., Liu, J., Xie, Y., Liu, J., Klionsky, D.J., Kroemer, G., et al. (2018). AMPK-Mediated BECN1 Phosphorylation Promotes Ferroptosis by Directly Blocking System Xc- Activity. Curr. Biol. CB *28*, 2388-2399.e5. https://doi.org/10.1016/j.cub.2018.05.094.

Spillantini, M.G., Schmidt, M.L., Lee, V.M., Trojanowski, J.Q., Jakes, R., and Goedert, M. (1997). Alpha-synuclein in Lewy bodies. Nature *388*, 839–840. https://doi.org/10.1038/42166.

Spillantini, M.G., Crowther, R.A., Jakes, R., Hasegawa, M., and Goedert, M. (1998). alpha-Synuclein in filamentous inclusions of Lewy bodies from Parkinson's disease and dementia with lewy bodies. Proc. Natl. Acad. Sci. U. S. A. *95*, 6469–6473. https://doi.org/10.1073/pnas.95.11.6469.

Spindler, M., Beal, M.F., and Henchcliffe, C. (2009). Coenzyme Q10 effects in neurodegenerative disease. Neuropsychiatr. Dis. Treat. *5*, 597–610. https://doi.org/10.2147/ndt.s5212.

Steiner, J.A., Quansah, E., and Brundin, P. (2018). The concept of alpha-synuclein as a prion-like protein: ten years after. Cell Tissue Res. *373*, 161–173. https://doi.org/10.1007/s00441-018-2814-1.

Stockwell, B.R., Friedmann Angeli, J.P., Bayir, H., Bush, A.I., Conrad, M., Dixon, S.J., Fulda, S., Gascón, S., Hatzios, S.K., Kagan, V.E., et al. (2017). Ferroptosis: A Regulated Cell Death Nexus Linking Metabolism, Redox Biology, and Disease. Cell *171*, 273–285. https://doi.org/10.1016/j.cell.2017.09.021.

Suh, J.H., Shenvi, S.V., Dixon, B.M., Liu, H., Jaiswal, A.K., Liu, R.-M., and Hagen, T.M. (2004). Decline in transcriptional activity of Nrf2 causes age-related loss of glutathione synthesis, which is reversible with lipoic acid. Proc. Natl. Acad. Sci. *101*, 3381–3386. https://doi.org/10.1073/pnas.0400282101.

Sun, W.-Y., Tyurin, V.A., Mikulska-Ruminska, K., Shrivastava, I.H., Anthonymuthu, T.S., Zhai, Y.-J., Pan, M.-H., Gong, H.-B., Lu, D.-H., Sun, J., et al. (2021). Phospholipase iPLA2β averts ferroptosis by eliminating a redox lipid death signal. Nat. Chem. Biol. *17*, 465–476. https://doi.org/10.1038/s41589-020-00734-x.

Sun, X., Ou, Z., Chen, R., Niu, X., Chen, D., Kang, R., and Tang, D. (2016). Activation of the p62-Keap1-NRF2 pathway protects against ferroptosis in hepatocellular carcinoma cells. Hepatol. Baltim. Md *63*, 173–184. https://doi.org/10.1002/hep.28251.

Takahashi-Niki, K., Niki, T., Taira, T., Iguchi-Ariga, S.M.M., and Ariga, H. (2004). Reduced anti-oxidative stress activities of DJ-1 mutants found in Parkinson's disease patients. Biochem. Biophys. Res. Commun. *320*, 389–397. https://doi.org/10.1016/j.bbrc.2004.05.187.

Tamo, W., Imaizumi, T., Tanji, K., Yoshida, H., Mori, F., Yoshimoto, M., Takahashi, H., Fukuda, I., Wakabayashi, K., and Satoh, K. (2002). Expression of alpha-synuclein, the precursor of non-amyloid beta component of Alzheimer's disease amyloid, in human cerebral blood vessels. Neurosci. Lett. *326*, 5–8. https://doi.org/10.1016/s0304-3940(02)00297-5.

Tang, D., Chen, X., Kang, R., and Kroemer, G. (2021). Ferroptosis: molecular mechanisms and health implications. Cell Res. *31*, 107–125. https://doi.org/10.1038/s41422-020-00441-1.

Tanner, C.M., Kamel, F., Ross, G.W., Hoppin, J.A., Goldman, S.M., Korell, M., Marras, C., Bhudhikanok, G.S., Kasten, M., Chade, A.R., et al. (2011). Rotenone, paraquat, and Parkinson's disease. Environ. Health Perspect. *119*, 866–872. https://doi.org/10.1289/ehp.1002839.

Tanudjojo, B., Shaikh, S.S., Fenyi, A., Bousset, L., Agarwal, D., Marsh, J., Zois, C., Heman-Ackah, S., Fischer, R., Sims, D., et al. (2021). Phenotypic manifestation of α-synuclein strains derived from Parkinson's disease and multiple system atrophy in human dopaminergic neurons. Nat. Commun. *12*, 3817. https://doi.org/10.1038/s41467-021-23682-z.

Tarangelo, A., Magtanong, L., Bieging-Rolett, K.T., Li, Y., Ye, J., Attardi, L.D., and Dixon, S.J. (2018). p53 Suppresses Metabolic Stress-Induced Ferroptosis in Cancer Cells. Cell Rep. *22*, 569–575. https://doi.org/10.1016/j.celrep.2017.12.077.

Thayanidhi, N., Helm, J.R., Nycz, D.C., Bentley, M., Liang, Y., and Hay, J.C. (2010). Alpha-synuclein delays endoplasmic reticulum (ER)-to-Golgi transport in mammalian cells by antagonizing ER/Golgi SNAREs. Mol. Biol. Cell *21*, 1850–1863. https://doi.org/10.1091/mbc.e09-09-0801.

Todorovic, M., Wood, S.A., and Mellick, G.D. (2016). Nrf2: a modulator of Parkinson's disease? J. Neural Transm. Vienna Austria 1996 *123*, 611–619. https://doi.org/10.1007/s00702-016-1563-0.

Toska, K., Kleppe, R., Armstrong, C.G., Morrice, N.A., Cohen, P., and Haavik, J. (2002). Regulation of tyrosine hydroxylase by stress-activated protein kinases. J. Neurochem. *83*, 775–783. https://doi.org/10.1046/j.1471-4159.2002.01172.x.

Tran, T.N., Vo, T.N.N., Frei, K., and Truong, D.D. (2018). Levodopa-induced dyskinesia: clinical features, incidence, and risk factors. J. Neural Transm. Vienna Austria 1996 *125*, 1109–1117. https://doi.org/10.1007/s00702-018-1900-6.

Trist, B.G., Hare, D.J., and Double, K.L. (2019). Oxidative stress in the aging substantia nigra and the etiology of Parkinson's disease. Aging Cell *18*, e13031. https://doi.org/10.1111/acel.13031.

Tsatsanis, A., Dickens, S., Kwok, J.C.F., Wong, B.X., and Duce, J.A. (2019). Post Translational Modulation of β-Amyloid Precursor Protein Trafficking to the Cell Surface Alters Neuronal Iron Homeostasis. Neurochem. Res. *44*, 1367–1374. https://doi.org/10.1007/s11064-019-02747-y.

Tsuboi, K., Okamoto, Y., Ikematsu, N., Inoue, M., Shimizu, Y., Uyama, T., Wang, J., Deutsch, D.G., Burns, M.P., Ulloa, N.M., et al. (2011). Enzymatic formation of N-acylethanolamines from N-acylethanolamine plasmalogen through N-acylphosphatidylethanolamine-hydrolyzing phospholipase D-dependent and -independent pathways. Biochim. Biophys. Acta *1811*, 565–577. https://doi.org/10.1016/j.bbalip.2011.07.009.

Ugalde, C.L., Lawson, V.A., Finkelstein, D.I., and Hill, A.F. (2019). The role of lipids in α-synuclein misfolding and neurotoxicity. J. Biol. Chem. *294*, 9016–9028. https://doi.org/10.1074/jbc.REV119.007500.

Uryu, K., Giasson, B.I., Longhi, L., Martinez, D., Murray, I., Conte, V., Nakamura, M., Saatman, K., Talbot, K., Horiguchi, T., et al. (2003). Age-dependent synuclein pathology following traumatic brain injury in mice. Exp. Neurol. *184*, 214–224. https://doi.org/10.1016/s0014-4886(03)00245-0.

Uversky, V.N. (2003). A protein-chameleon: conformational plasticity of alpha-synuclein, a disordered protein involved in neurodegenerative disorders. J. Biomol. Struct. Dyn. *21*, 211–234. https://doi.org/10.1080/07391102.2003.10506918.

Uversky, V.N., Li, J., and Fink, A.L. (2001). Metal-triggered structural transformations, aggregation, and fibrillation of human alpha-synuclein. A possible molecular NK between Parkinson's disease and heavy metal exposure. J. Biol. Chem. *276*, 44284–44296. https://doi.org/10.1074/jbc.M105343200.

Valente, E.M., Salvi, S., Ialongo, T., Marongiu, R., Elia, A.E., Caputo, V., Romito, L., Albanese, A., Dallapiccola, B., and Bentivoglio, A.R. (2004). PINK1 mutations are associated with sporadic early-onset parkinsonism. Ann. Neurol. *56*, 336–341. https://doi.org/10.1002/ana.20256.

Vallerga, C.L., Zhang, F., Fowdar, J., McRae, A.F., Qi, T., Nabais, M.F., Zhang, Q., Kassam, I., Henders, A.K., Wallace, L., et al. (2020). Analysis of DNA methylation associates the cystine–glutamate antiporter SLC7A11 with risk of Parkinson's disease. Nat. Commun. *11*, 1238. https://doi.org/10.1038/s41467-020-15065-7.

Vamvaca, K., Volles, M.J., and Lansbury, P.T. (2009). The first N-terminal amino acids of alpha-synuclein are essential for alpha-helical structure formation in vitro and membrane binding in yeast. J. Mol. Biol. *389*, 413–424. https://doi.org/10.1016/j.jmb.2009.03.021.

Van Den Eeden, S.K., Tanner, C.M., Bernstein, A.L., Fross, R.D., Leimpeter, A., Bloch, D.A., and Nelson, L.M. (2003). Incidence of Parkinson's disease: variation by age, gender, and race/ethnicity. Am. J. Epidemiol. *157*, 1015–1022. https://doi.org/10.1093/aje/kwg068.

Van Iderstine, S.C., Byers, D.M., Ridgway, N.D., and Cook, H.W. (1997). Phospholipase D hydrolysis of plasmalogen and diacyl ethanolamine phosphoglycerides by protein kinase C dependent and independent mechanisms. J. Lipid Mediat. Cell Signal. *15*, 175–192. https://doi.org/10.1016/s0929-7855(96)00552-4.

Vargas, K.J., Makani, S., Davis, T., Westphal, C.H., Castillo, P.E., and Chandra, S.S. (2014). Synucleins regulate the kinetics of synaptic vesicle endocytosis. J. Neurosci. Off. J. Soc. Neurosci. *34*, 9364–9376. https://doi.org/10.1523/JNEUROSCI.4787-13.2014.

Verschuur, C.V.M., Suwijn, S.R., Boel, J.A., Post, B., Bloem, B.R., van Hilten, J.J., van Laar, T., Tissingh, G., Munts, A.G., Deuschl, G., et al. (2019). Randomized Delayed-Start Trial of Levodopa in Parkinson's Disease. N. Engl. J. Med. *380*, 315–324. https://doi.org/10.1056/NEJMoa1809983.

Vila, M., Vukosavic, S., Jackson-Lewis, V., Neystat, M., Jakowec, M., and Przedborski, S. (2000). Alpha-synuclein up-regulation in substantia nigra dopaminergic neurons following administration of the parkinsonian toxin MPTP. J. Neurochem. *74*, 721–729. https://doi.org/10.1046/j.1471-4159.2000.740721.x.

Vilariño-Güell, C., Rajput, A., Milnerwood, A.J., Shah, B., Szu-Tu, C., Trinh, J., Yu, I., Encarnacion, M., Munsie, L.N., Tapia, L., et al. (2014). DNAJC13 mutations in Parkinson disease. Hum. Mol. Genet. *23*, 1794–1801. https://doi.org/10.1093/hmg/ddt570.

Vranas, M., Lu, Y., Rasool, S., Croteau, N., Krett, J.D., Sauvé, V., Gehring, K., Fon, E.A., Durcan, T.M., and Trempe, J.-F. (2022). Selective localization of Mfn2 near PINK1 enables its preferential ubiquitination by Parkin on mitochondria. Open Biol. *12*, 210255. https://doi.org/10.1098/rsob.210255.

Wakabayashi, K., Tanji, K., Odagiri, S., Miki, Y., Mori, F., and Takahashi, H. (2013). The Lewy Body in Parkinson's Disease and Related Neurodegenerative Disorders. Mol. Neurobiol. *47*, 495–508. https://doi.org/10.1007/s12035-012-8280-y.

Wang, W., Perovic, I., Chittuluru, J., Kaganovich, A., Nguyen, L.T.T., Liao, J., Auclair, J.R., Johnson, D., Landeru, A., Simorellis, A.K., et al. (2011). A soluble α-synuclein construct forms a dynamic tetramer. Proc. Natl. Acad. Sci. U. S. A. *108*, 17797–17802. https://doi.org/10.1073/pnas.1113260108.

Wang, Y., Spincemaille, P., Liu, Z., Dimov, A., Deh, K., Li, J., Zhang, Y., Yao, Y., Gillen, K.M., Wilman, A.H., et al. (2017). Clinical quantitative susceptibility mapping (QSM): Biometal imaging and its emerging roles in patient care. J. Magn. Reson. Imaging JMRI *46*, 951–971. https://doi.org/10.1002/jmri.25693.

Wang, Y., Liu, Y., Liu, J., Kang, R., and Tang, D. (2020). NEDD4L-mediated LTF protein degradation limits ferroptosis. Biochem. Biophys. Res. Commun. *531*, 581–587. https://doi.org/10.1016/j.bbrc.2020.07.032.

Wang, Y.-Q., Chang, S.-Y., Wu, Q., Gou, Y.-J., Jia, L., Cui, Y.-M., Yu, P., Shi, Z.-H., Wu, W.-S., Gao, G., et al. (2016). The Protective Role of Mitochondrial Ferritin on Erastin-Induced Ferroptosis. Front. Aging Neurosci. *8*, 308. https://doi.org/10.3389/fnagi.2016.00308.

Ward, R.J., Zucca, F.A., Duyn, J.H., Crichton, R.R., and Zecca, L. (2014). The role of iron in brain ageing and neurodegenerative disorders. Lancet Neurol. *13*, 1045–1060. https://doi.org/10.1016/S1474-4422(14)70117-6.

Watts, J.L., and Browse, J. (2006). Dietary manipulation implicates lipid signaling in the regulation of germ cell maintenance in C. elegans. Dev. Biol. *292*, 381–392. https://doi.org/10.1016/j.ydbio.2006.01.013.

Waxman, E.A., and Giasson, B.I. (2008). Specificity and regulation of casein kinase-mediated phosphorylation of alpha-synuclein. J. Neuropathol. Exp. Neurol. *67*, 402–416. https://doi.org/10.1097/NEN.0b013e31816fc995.

Weisskopf, M.G., Knekt, P., O'Reilly, E.J., Lyytinen, J., Reunanen, A., Laden, F., Altshul, L., and Ascherio, A. (2010). Persistent organochlorine pesticides in serum and risk of Parkinson disease. Neurology *74*, 1055–1061. https://doi.org/10.1212/WNL.0b013e3181d76a93.

Wenzel, S.E., Tyurina, Y.Y., Zhao, J., St Croix, C.M., Dar, H.H., Mao, G., Tyurin, V.A., Anthonymuthu, T.S., Kapralov, A.A., Amoscato, A.A., et al. (2017). PEBP1 Wardens Ferroptosis by Enabling Lipoxygenase Generation of Lipid Death Signals. Cell *171*, 628-641.e26. https://doi.org/10.1016/j.cell.2017.09.044.

Wenzelburger, R., Kopper, F., Zhang, B.-R., Witt, K., Hamel, W., Weinert, D., Kuhtz-Buschbeck, J., Gölge, M., Illert, M., Deuschl, G., et al. (2003). Subthalamic nucleus stimulation for Parkinson's disease preferentially improves akinesia of proximal arm movements compared to finger movements. Mov. Disord. Off. J. Mov. Disord. Soc. *18*, 1162–1169. https://doi.org/10.1002/mds.10501.

Wersinger, C., and Sidhu, A. (2003). Attenuation of dopamine transporter activity by alpha-synuclein. Neurosci. Lett. *340*, 189–192. https://doi.org/10.1016/s0304-3940(03)00097-1.

Wersinger, C., Prou, D., Vernier, P., Niznik, H.B., and Sidhu, A. (2003). Mutations in the lipid-binding domain of alpha-synuclein confer overlapping, yet distinct, functional properties in the regulation of dopamine transporter activity. Mol. Cell. Neurosci. *24*, 91–105. https://doi.org/10.1016/s1044-7431(03)00124-6.

Wersinger, C., Vernier, P., and Sidhu, A. (2004). Trypsin disrupts the trafficking of the human dopamine transporter by alpha-synuclein and its A30P mutant. Biochemistry *43*, 1242–1253. https://doi.org/10.1021/bi035308s.

Williams, E.T., Chen, X., and Moore, D.J. (2017). VPS35, the Retromer Complex and Parkinson's Disease. J. Park. Dis. *7*, 219–233. https://doi.org/10.3233/JPD-161020.

Withers, G.S., George, J.M., Banker, G.A., and Clayton, D.F. (1997). Delayed localization of synelfin (synuclein, NACP) to presynaptic terminals in cultured rat hippocampal neurons. Brain Res. Dev. Brain Res. *99*, 87–94. https://doi.org/10.1016/s0165-3806(96)00210-6.

Wolf, R.A., and Gross, R.W. (1985). Identification of neutral active phospholipase C which hydrolyzes choline glycerophospholipids and plasmalogen selective phospholipase A2 in canine myocardium. J. Biol. Chem. *260*, 7295–7303. .

Wu, B., Liu, Q., Duan, C., Li, Y., Yu, S., Chan, P., Uéda, K., and Yang, H. (2011). Phosphorylation of α-synuclein upregulates tyrosine hydroxylase activity in MN9D cells. Acta Histochem. *113*, 32–35. https://doi.org/10.1016/j.acthis.2009.07.007.

Wu, J.-R., Wang, J., Zhou, S.-K., Yang, L., Yin, J., Cao, J.-P., and Cheng, Y.-B. (2015). Necrostatin-1 protection of dopaminergic neurons. Neural Regen. Res. *10*, 1120–1124. https://doi.org/10.4103/1673-5374.160108.

Wu, Q., Shaikh, M.A., Meymand, E.S., Zhang, B., Luk, K.C., Trojanowski, J.Q., and Lee, V.M.-Y. (2020). Neuronal activity modulates alpha-synuclein aggregation and spreading in organotypic brain slice cultures and in vivo. Acta Neuropathol. (Berl.) *140*, 831–849. https://doi.org/10.1007/s00401-020-02227-6.

Xiao, X., Jiang, Y., Liang, W., Wang, Y., Cao, S., Yan, H., Gao, L., and Zhang, L. (2019). miR-212-5p attenuates ferroptotic neuronal death after traumatic brain injury by targeting Ptgs2. Mol. Brain *12*, 78. https://doi.org/10.1186/s13041-019-0501-0.

Xu, X., Pin, S., Gathinji, M., Fuchs, R., and Harris, Z.L. (2004). Aceruloplasminemia: an inherited neurodegenerative disease with impairment of iron homeostasis. Ann. N. Y. Acad. Sci. *1012*, 299–305. https://doi.org/10.1196/annals.1306.024.

Yahr, M.D., Duvoisin, R.C., Schear, M.J., Barrett, R.E., and Hoehn, M.M. (1969). Treatment of parkinsonism with levodopa. Arch. Neurol. *21*, 343–354. https://doi.org/10.1001/archneur.1969.00480160015001.

Yakunin, E., Kisos, H., Kulik, W., Grigoletto, J., Wanders, R.J.A., and Sharon, R. (2014). The regulation of catalase activity by PPAR γ is affected by α -synuclein. Ann. Clin. Transl. Neurol. *1*, 145–159. https://doi.org/10.1002/acn3.38.

Yan, S., Yang, X.-F., Liu, H.-L., Fu, N., Ouyang, Y., and Qing, K. (2015). Long-chain acyl-CoA synthetase in fatty acid metabolism involved in liver and other diseases: an update. World J. Gastroenterol. *21*, 3492–3498. https://doi.org/10.3748/wjg.v21.i12.3492.

Yang, W.S., and Stockwell, B.R. (2016). Ferroptosis: Death by Lipid Peroxidation. Trends Cell Biol. *26*, 165–176. https://doi.org/10.1016/j.tcb.2015.10.014.

Yang, H.C., Farooqui, A.A., and Horrocks, L.A. (1996). Characterization of plasmalogen-selective phospholipase A2 from bovine brain. Adv. Exp. Med. Biol. *416*, 309–313. https://doi.org/10.1007/978-1-4899-0179-8_49.

Yang, W.S., SriRamaratnam, R., Welsch, M.E., Shimada, K., Skouta, R., Viswanathan, V.S., Cheah, J.H., Clemons, P.A., Shamji, A.F., Clish, C.B., et al. (2014). Regulation of ferroptotic cancer cell death by GPX4. Cell *156*, 317–331. https://doi.org/10.1016/j.cell.2013.12.010.

Yang, W.S., Kim, K.J., Gaschler, M.M., Patel, M., Shchepinov, M.S., and Stockwell, B.R. (2016). Peroxidation of polyunsaturated fatty acids by lipoxygenases drives ferroptosis. Proc. Natl. Acad. Sci. *113*, E4966–E4975. https://doi.org/10.1073/pnas.1603244113.

Yavich, L., Tanila, H., Vepsäläinen, S., and Jäkälä, P. (2004). Role of alpha-synuclein in presynaptic dopamine recruitment. J. Neurosci. Off. J. Soc. Neurosci. *24*, 11165–11170. https://doi.org/10.1523/JNEUROSCI.2559-04.2004.

Yavich, L., Jäkälä, P., and Tanila, H. (2006). Abnormal compartmentalization of norepinephrine in mouse dentate gyrus in alpha-synuclein knockout and A30P transgenic mice. J. Neurochem. *99*, 724–732. https://doi.org/10.1111/j.1471-4159.2006.04098.x.

Yonetani, M., Nonaka, T., Masuda, M., Inukai, Y., Oikawa, T., Hisanaga, S.-I., and Hasegawa, M. (2009). Conversion of wild-type alpha-synuclein into mutant-type fibrils and

its propagation in the presence of A30P mutant. J. Biol. Chem. *284*, 7940–7950. https://doi.org/10.1074/jbc.M807482200.

Yoritaka, A., Hattori, N., Uchida, K., Tanaka, M., Stadtman, E.R., and Mizuno, Y. (1996). Immunohistochemical detection of 4-hydroxynonenal protein adducts in Parkinson disease. Proc. Natl. Acad. Sci. U. S. A. *93*, 2696–2701. https://doi.org/10.1073/pnas.93.7.2696.

Yu, S., Uéda, K., and Chan, P. (2005). α-Synuclein and Dopamine Metabolism. Mol. Neurobiol. *31*, 243–254. https://doi.org/10.1385/MN:31:1-3:243.

Zambon, F., Cherubini, M., Fernandes, H.J.R., Lang, C., Ryan, B.J., Volpato, V., Bengoa-Vergniory, N., Vingill, S., Attar, M., Booth, H.D.E., et al. (2019). Cellular α-synuclein pathology is associated with bioenergetic dysfunction in Parkinson's iPSC-derived dopamine neurons. Hum. Mol. Genet. *28*, 2001–2013. https://doi.org/10.1093/hmg/ddz038.

Zarranz, J.J., Alegre, J., Gómez-Esteban, J.C., Lezcano, E., Ros, R., Ampuero, I., Vidal, L., Hoenicka, J., Rodriguez, O., Atarés, B., et al. (2004). The new mutation, E46K, of alpha-synuclein causes Parkinson and Lewy body dementia. Ann. Neurol. *55*, 164–173. https://doi.org/10.1002/ana.10795.

Zawada, W.M., Mrak, R.E., Biedermann, J., Palmer, Q.D., Gentleman, S.M., Aboud, O., and Griffin, W.S.T. (2015). Loss of angiotensin II receptor expression in dopamine neurons in Parkinson's disease correlates with pathological progression and is accompanied by increases in Nox4- and 8-OH guanosine-related nucleic acid oxidation and caspase-3 activation. Acta Neuropathol. Commun. *3*, 9. https://doi.org/10.1186/s40478-015-0189-z.

Zhang, J., Su, L., Ye, Q., Zhang, S., Kung, H., Jiang, F., Jiang, G., Miao, J., and Zhao, B. (2016). Discovery of a novel Nrf2 inhibitor that induces apoptosis of human acute myeloid leukemia cells. Oncotarget *8*, 7625–7636. https://doi.org/10.18632/oncotarget.13825.

Zhang, L., Zhang, C., Zhu, Y., Cai, Q., Chan, P., Uéda, K., Yu, S., and Yang, H. (2008). Semi-quantitative analysis of alpha-synuclein in subcellular pools of rat brain neurons: an immunogold electron microscopic study using a C-terminal specific monoclonal antibody. Brain Res. *1244*, 40–52. https://doi.org/10.1016/j.brainres.2008.08.067.

Zhang, X.-M., Yin, M., and Zhang, M.-H. (2014). Cell-based assays for Parkinson's disease using differentiated human LUHMES cells. Acta Pharmacol. Sin. *35*, 945–956. https://doi.org/10.1038/aps.2014.36.

Zhang, Y., Shu, L., Sun, Q., Pan, H., Guo, J., and Tang, B. (2018a). A Comprehensive Analysis of the Association Between SNCA Polymorphisms and the Risk of Parkinson's Disease. Front. Mol. Neurosci. *11*. https://doi.org/10.3389/fnmol.2018.00391.

Zhang, Y., Shi, J., Liu, X., Feng, L., Gong, Z., Koppula, P., Sirohi, K., Li, X., Wei, Y., Lee, H., et al. (2018b). BAP1 links metabolic regulation of ferroptosis to tumour suppression. Nat. Cell Biol. *20*, 1181–1192. https://doi.org/10.1038/s41556-018-0178-0.

Zhang, Y., Chen, L., Luo, Y., Wang, K., Liu, X., Xiao, Z., Zhao, G., Yao, Y., and Lu, Z. (2022). Pink1/Parkin-Mediated Mitophagy Regulated the Apoptosis of Dendritic Cells in Sepsis. Inflammation https://doi.org/10.1007/s10753-022-01628-x.

Zhang, Z., Wu, Y., Yuan, S., Zhang, P., Zhang, J., Li, H., Li, X., Shen, H., Wang, Z., and Chen, G. (2018c). Glutathione peroxidase 4 participates in secondary brain injury through mediating ferroptosis in a rat model of intracerebral hemorrhage. Brain Res. *1701*, 112–125. https://doi.org/10.1016/j.brainres.2018.09.012.

Zhao, H., Li, Y., He, L., Pu, W., Yu, W., Li, Y., Wu, Y.-T., Xu, C., Wei, Y., Ding, Q., et al. (2020). In Vivo AAV-CRISPR/Cas9-Mediated Gene Editing Ameliorates Atherosclerosis in Familial Hypercholesterolemia. Circulation *141*, 67–79. https://doi.org/10.1161/CIRCULATIONAHA.119.042476.

Zhao, X., Shao, Z., Zhang, Y., Liu, F., Liu, Z., and Liu, Z. (2018). Ceruloplasmin in Parkinson's disease and the nonmotor symptoms. Brain Behav. *8*, e00995. https://doi.org/10.1002/brb3.995.

Zhu, Z.-J., Wu, K.-C., Yung, W.-H., Qian, Z.-M., and Ke, Y. (2016). Differential interaction between iron and mutant alpha-synuclein causes distinctive Parkinsonian phenotypes in Drosophila. Biochim. Biophys. Acta *1862*, 518–525. https://doi.org/10.1016/j.bbadis.2016.01.002.

Zigoneanu, I.G., Yang, Y.J., Krois, A.S., Haque, E., and Pielak, G.J. (2012). Interaction of α-synuclein with vesicles that mimic mitochondrial membranes. Biochim. Biophys. Acta *1818*, 512–519. https://doi.org/10.1016/j.bbamem.2011.11.024.

Zille, M., Karuppagounder, S.S., Chen, Y., Gough, P.J., Bertin, J., Finger, J., Milner, T.A., Jonas, E.A., and Ratan, R.R. (2017). Neuronal Death After Hemorrhagic Stroke In Vitro and In Vivo Shares Features of Ferroptosis and Necroptosis. Stroke *48*, 1033–1043. https://doi.org/10.1161/STROKEAHA.116.015609.

Ziv, I., Shirvan, A., Offen, D., Barzilai, A., and Melamed, E. (2001). Molecular biology of dopamine-induced apoptosis : possible implications for Parkinson's disease. Methods Mol. Med. *62*, 73–87. https://doi.org/10.1385/1-59259-142-6:73.

Zondler, L., Miller-Fleming, L., Repici, M., Gonçalves, S., Tenreiro, S., Rosado-Ramos, R., Betzer, C., Straatman, K.R., Jensen, P.H., Giorgini, F., et al. (2014). DJ-1 interactions with α-synuclein attenuate aggregation and cellular toxicity in models of Parkinson's disease. Cell Death Dis. *5*, e1350. https://doi.org/10.1038/cddis.2014.307.

Zorov, D.B., Juhaszova, M., and Sollott, S.J. (2014). Mitochondrial reactive oxygen species (ROS) and ROS-induced ROS release. Physiol. Rev. *94*, 909–950. https://doi.org/10.1152/physrev.00026.2013.

Zou, Y., Henry, W.S., Ricq, E.L., Graham, E.T., Phadnis, V.V., Maretich, P., Paradkar, S., Boehnke, N., Deik, A.A., Reinhardt, F., et al. (2020a). Plasticity of ether lipids promotes ferroptosis susceptibility and evasion. Nature *585*, 603–608. https://doi.org/10.1038/s41586-020-2732-8.

Zou, Y., Li, H., Graham, E.T., Deik, A.A., Eaton, J.K., Wang, W., Sandoval-Gomez, G., Clish, C.B., Doench, J.G., and Schreiber, S.L. (2020b). Cytochrome P450 oxidoreductase contributes to phospholipid peroxidation in ferroptosis. Nat. Chem. Biol. *16*, 302–309. https://doi.org/10.1038/s41589-020-0472-6.

Statistics.

Annexe 1

Supplementary figures and tables

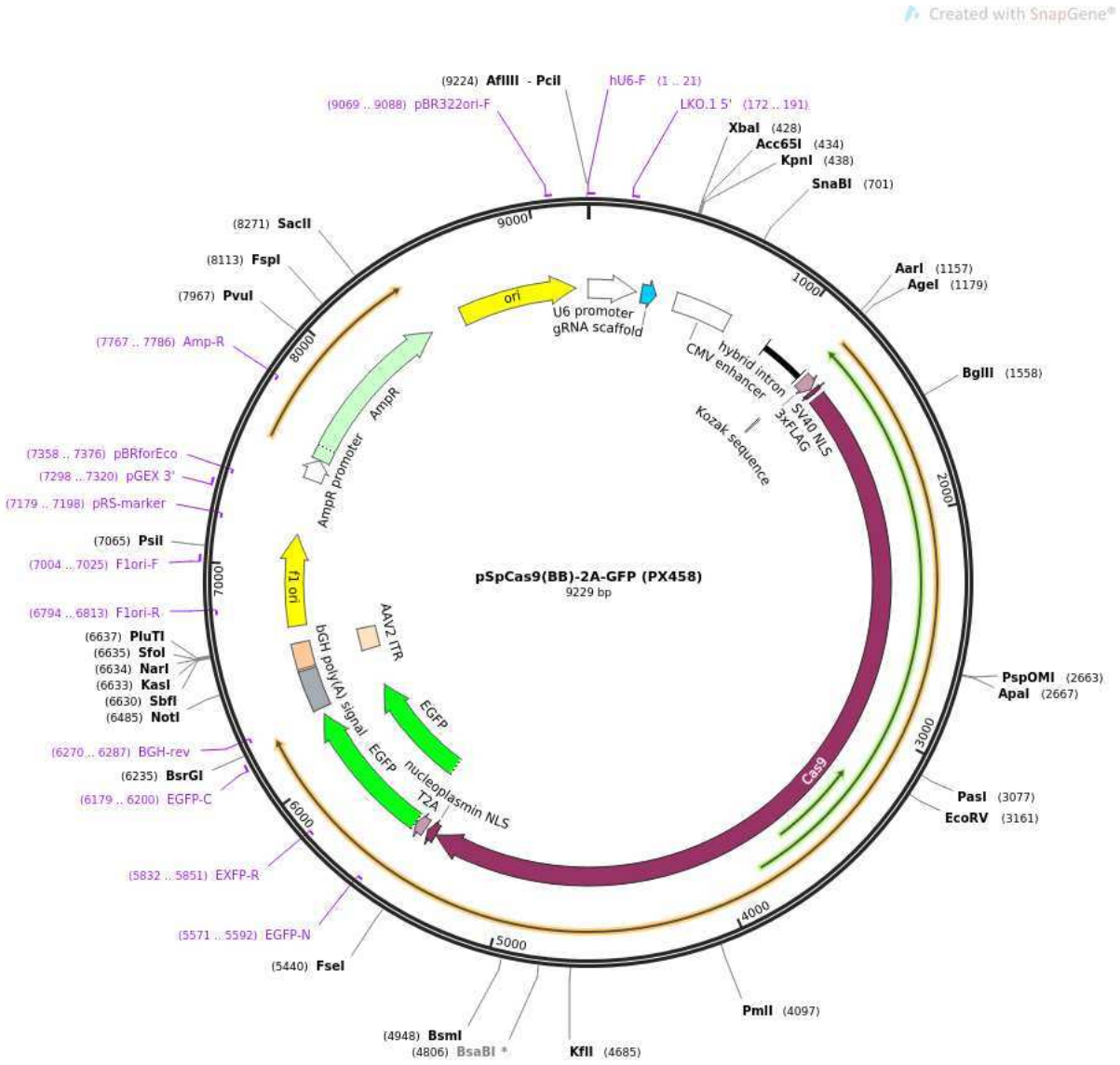

Supplementary figure 1: Addgene full sequence map for pSpCas9(bb)-2A-GFP (px458).
Plasmid used to generate the A53T, 140 α-syn KO and full α-syn KO CRISPR/Cas9 sub-clones throughout this PhD project

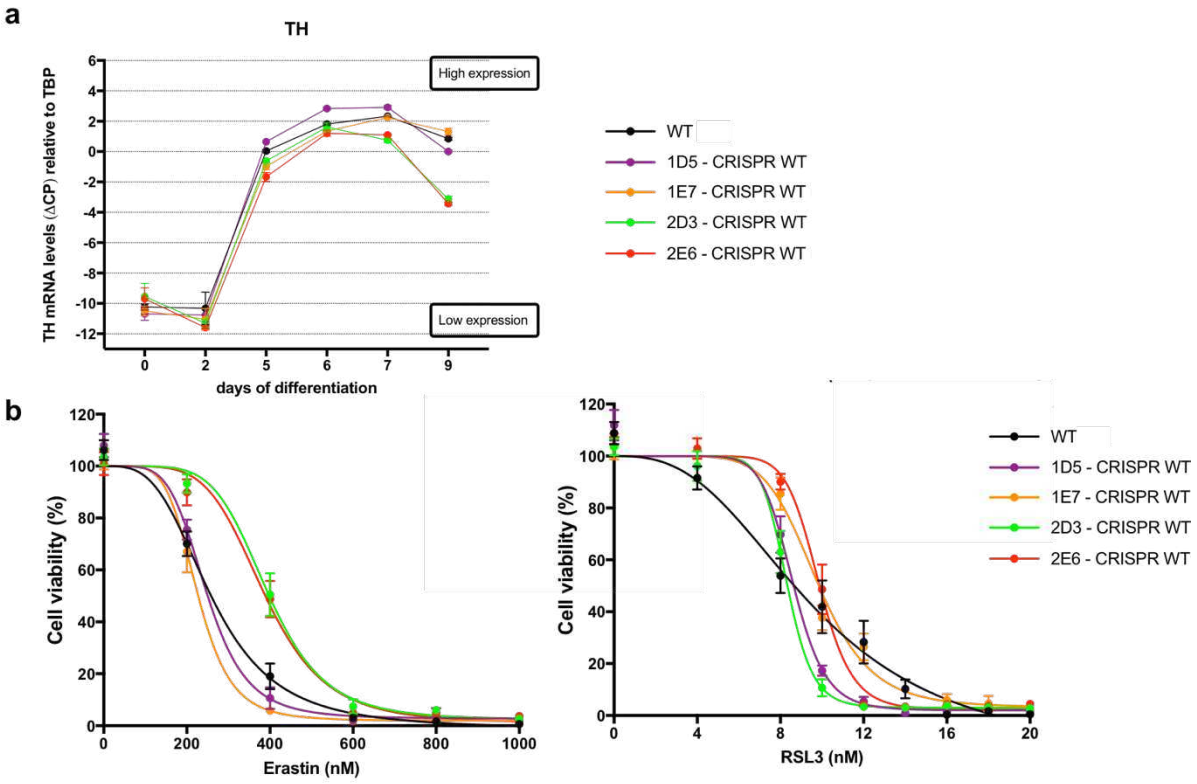

Supplementary figure 2. CRISPR WT characterisation and ferroptosis sensitivity. **a.** TH mRNA levels determined by qRT-PCR in the parental WT and four CRISPR WT subclones throughout several differentiation days. Data represented as relative expression to the house keeping gene TBP. **b.** Erastin and RSL3 dose response viability curves in WT and four CRISPR WT clones. Data represented as mean ± SEM of at least three independent experiments.

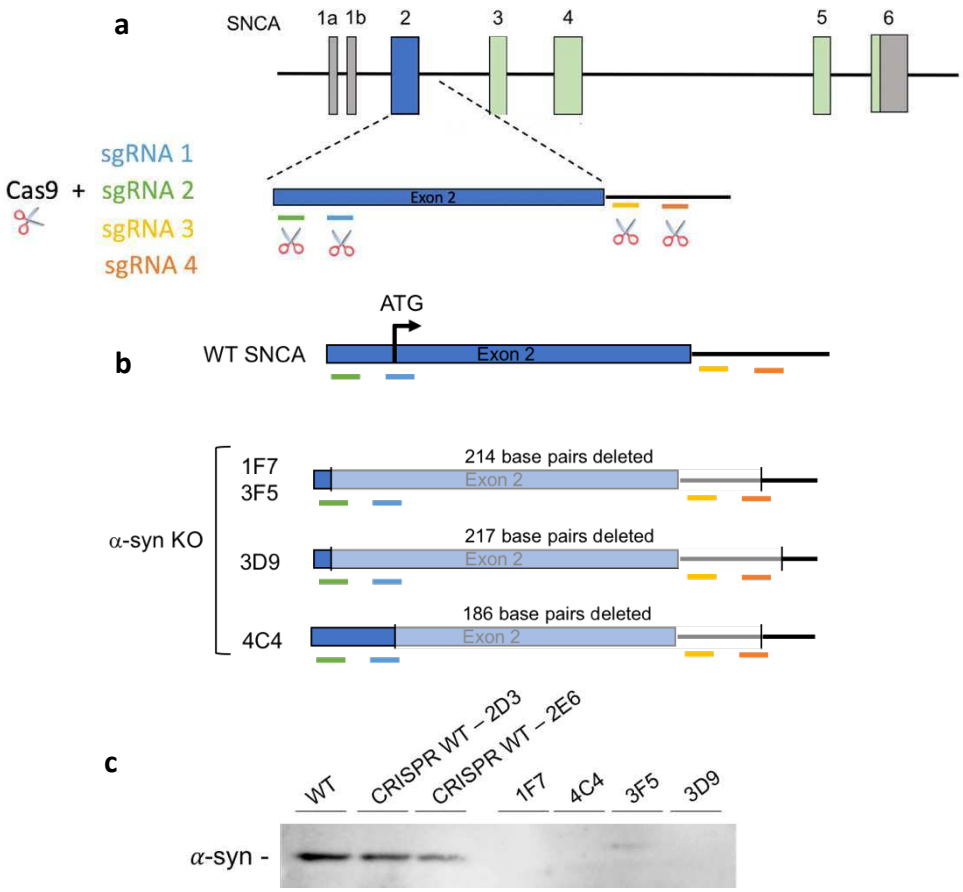

Supplementary figure 3: Generation of α-syn KO CRISPR/Cas9 LUHMES sub-clones. a*. Schematic representation of the SNCA gene and the location of the four sgRNA targeted against exon 2.* ***b.*** *Schematic summary of sequencing results of the four α-syn KO clones.* ***c.*** *Western blot results for α-syn in the parental WT Luhmes cells, two CRISPR WT and four homozygous α-syn KO clones.*

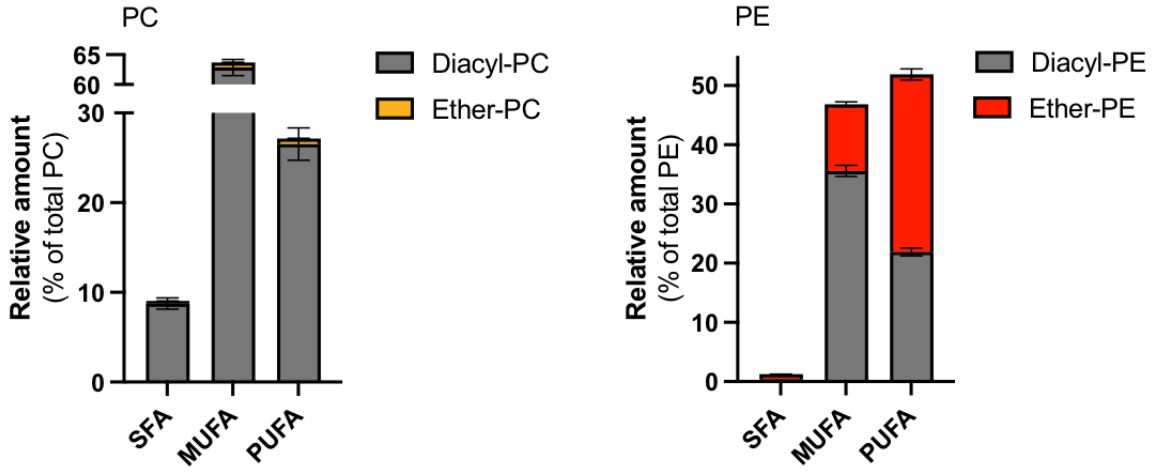

	Diacyl-PL	Ether-PL
Phosphatidylcholine (PC) :		
SFA	8.75 ± 0.62	0.28 ± 0.02
MUFA	62.84 ± 1.35	0.85 ± 0.06
PUFA	26.54 ± 1.8	0.59 ± 0.04
Phosphatidylethanolamine (PE):		
SFA	0.45 ± 0.008	0.8 ± 0.028
MUFA	35.59 ± 0.93	11.26 ± 0.38
PUFA	21.89 ± 0.65	30 ± 0.95

Supplementary figure 4: Proportion of dyacil- and ether-phospholipids in LUHMES dopaminergic neurons. Relative amount and table of percentage of total diacyl- vs ether-PC and PE separated based on the FA content (SFA, MUFA or PUFA). Data represents mean ± SEM of six biological replicates.

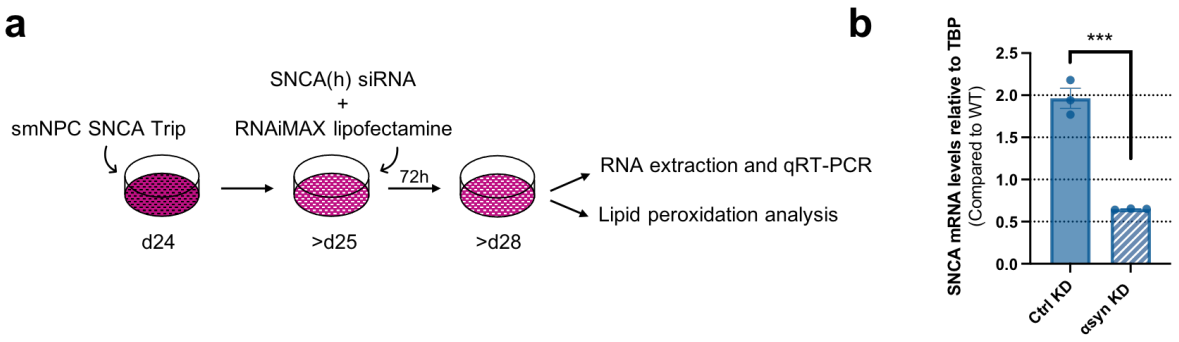

Supplementary Figure 5: siRNA mediated α-syn knock-down in SNCA Trip mDANs. a *Schematic representation of the siRNA protocol to knock-down SNCA mRNA expression in the SNCA Trip mDANs.* ***b*** *qRT-PCR analysis of SNCA levels in SNCA Trip mDANs following α-syn KD. The relative expression is normalized to TBP and represented as mean ± SEM of three independent experiments. Comparisons were made using the two-tailed, unpaired Student's t-test; *** p<0.001.*

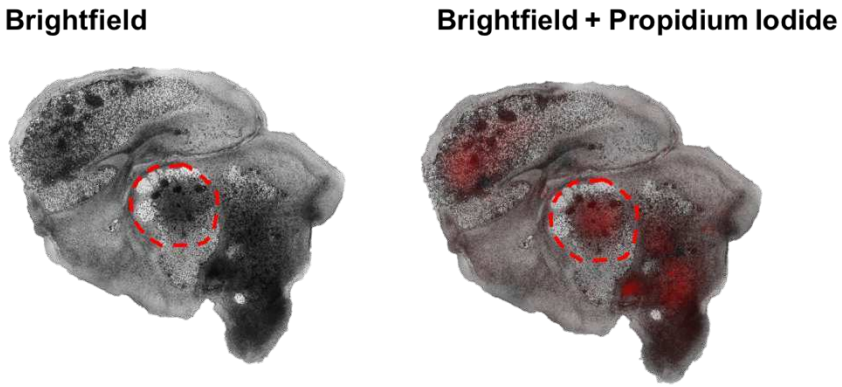

Supplementary Figure 6: Degeneration of thalamus in mice organotypic brain slices. *Bright field and Propidium Iodide staining on mice OBS depicturing the dryness and death of the thalamus in the centre of the slices.*

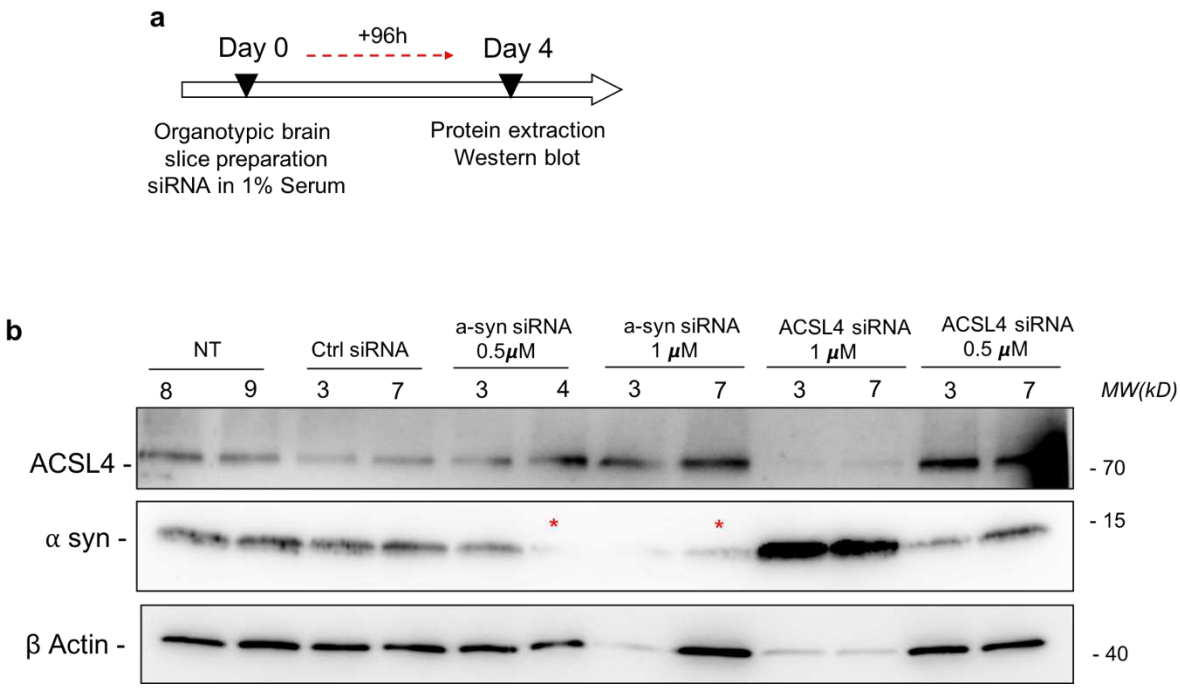

Supplementary figure 7. Protocol 1- siRNA-mediated knock-down of α-syn and ACSL4 in mice organotypic brain slices. **a.** Timeline of the Accell siRNA protocol in OBSs. **b.** Representative WB of α-syn and ACSL4 KD in mice OBS using two different siRNA concentrations.

Plasmid name	Transcription modulator	Transcription effect
dCas9-VP160-2A-puro	dCas9 fused with VP160 activation domain	Upregulation
dCas9-KRAB-pHAGE	dCas9 fused with KRAB transcription repressor	Downregulation
dCas9-KRAB-pLVhu6	gRNA + dCas9 fused with KRAB transcription repressor	Downregulation

Supplementary table 1. CRISPR dCas9 plasmids generated and sequenced for upregulation or downregulation of endogenous α-syn.

Annexe 2 :

Review article: Ferroptosis and its potential role in the physiopathology of Parkinson's Disease.

Ferroptosis and its potential role in the physiopathology of Parkinson's Disease

Laura Mahoney-Sánchez[1#], Hind Bouchaoui[1#], Scott Ayton[2], David Devos[1#], James A. Duce[2,3#], Jean-Christophe Devedjian[1, 4#].

Affiliations:

[1] Department of Medical Pharmacology, Lille University, INSERM UMRS_1172, University Hospital Centre, LICEND COEN Centre, LilNCog – Lille Neuroscience & Cognition, 59000, France.

[2] The Florey Institute of Neuroscience and Mental Health, The University of Melbourne, 30 Royal Parade, Parkville, Victoria 3052, Australia.

[3] ALBORADA Drug Discovery Institute, University of Cambridge, Cambridge Biomedical Campus, Hills Road, Cambridge, CB2 0AH, United Kingdom.

[4] Université du Littoral Côte d'Opale-1, place de l'Yser, BP 72033, 59375, Dunkerque Cedex, France.

[#]Authors have equally contributed to this work

Corresponding authors: David Devos (david.devos@chru-lille.fr) and James Duce (jad205@cam.ac.uk)

Keywords: Parkinson's disease – non apoptotic cell death – Ferroptosis – iron metabolism – oxidative stress– lipid peroxidation - alpha synuclein

Title: 70 characters, **6826 words**, abstract **232 words**: ; 3 figures; 1 Table

ABSTRACT

Parkinson's Disease (PD) is a common and progressive neurodegenerative disorder characterised by motor impairments as well as non-motor symptoms. While dopamine-based therapies are effective in fighting the symptoms in the early stages of the disease, a lack of neuroprotective drugs means that the disease continues to progress. Along with the traditionally recognised pathological hallmarks of dopaminergic neuronal death and intracellular α-synuclein (α-syn) depositions, iron accumulation, elevated oxidative stress and lipid peroxidation damage are further conspicuous features of PD pathophysiology. However, the underlying mechanisms linking these pathological hallmarks with neurodegeneration still remain unclear. Ferroptosis, a regulated iron dependent cell death pathway involving a lethal accumulation of lipid peroxides, shares several features with PD pathophysiology. Interestingly, α-syn has been functionally linked with the metabolism of both iron and lipid, suggesting a possible interplay between dysregulated α-syn and other PD pathological hallmarks related to ferroptosis. This review will address the importance for understanding these disease mechanisms that could be targeted therapeutically. Anti-ferroptosis molecules are neuroprotective in PD animal models and the anti-ferroptotic iron chelator, deferiprone, slowed disease progression and improved motor function in two independent clinical trials for PD. An ongoing larger multi-centre phase 2 clinical trial will confirm the therapeutic potential of deferiprone and the relevance of ferroptosis in PD. This review addresses the known pathological features of PD in relation to the ferroptosis pathway with therapeutic implications of targeting this cell death pathway.

1. INTRODUCTION

Parkinson's Disease (PD) is the second most common neurodegenerative disorder after Alzheimer's Disease. Clinically, PD patients present with motor impairments such as bradykinesia and rigidity, as well as non-motor symptoms including anosmia, constipation, pain, anxiety, depression, psychosis and cognitive disorders that may progress to dementia [1–3]. The main pathological hallmarks of the sporadic and familial forms of the disease are a predominant and progressive degeneration of the dopaminergic neurons of the substantia nigra pars compacta (SNpc) associated with a systematic progressive iron accumulation,

leading to a dopamine depletion in the striatum, disappearance of neuromelanin and appearance of intracellular Lewy Bodies with the major component consisting of aggregated α-synuclein. [4–7].

Current treatments **aim to increase dopamine neurotransmission, which offers symptomatic relief. The therapeutic arsenal includes the dopamine precursor Levodopa (L-DOPA), dopamine agonists and dopamine metabolism inhibitors [8]. L-DOPA remains the standard most effective treatment in combination with decarboxylase inhibitors[9,10]. Evidence from a randomized, double-blind, placebo-controlled trial suggested that L-DOPA slowed progression (as measured by UPDRS) between baseline and 42 weeks compared to the placebo group [11]. However, a more recent and larger study found no evidence of a disease-modifying effect of L-DOPA[12]. Disparity in the potential neuroprotective actions of this drug may arise from L-DOPA's interference with the striatal presynaptic dopamine transporter; standardly used as a reporter for nigro-striatal degeneration by DAT SPECT in clinical trials [11,13]. The powerful symptomatic action and short half-life of L-DOPA also weakens its clinical use with motor complications such as "wearing off" and dyskinesia occurring 4-6 years after chronic use, depending on disease severity [1–3]. To delay the onset of such complications, dopamine agonists, monoamine oxidase-B (MAO-B) inhibitors or catechol-O-methyltransferase (COMT) inhibitors are prescribed as concomitant therapies. The ADAGIO study clinically assessed the potential disease modifying effects of Rasagiline, an irreversible MAO-B inhibitor using a delayed-start protocol aimed at preventing the confounding symptomatic benefits of this drug. Although early treatment with rasagiline at a daily dose of 1mg slowed the rate of UPDRS deterioration in the early-start group, a similar response was not observed with the dose of 2mg [14,15]. Furthermore, a follow-up study failed to demonstrate long-term benefits for early-start rasagiline treatment [16].**

Over the last few years, several compounds have shown promising neuroprotective effects in *in vitro* and *in vivo* models but failed to translate to patient studies due to efficiency or safety concerns (reviewed in more detail in [17]). A huge unmet need remains for efficient neuroprotective or disease-modifying therapies. To overcome this demand, a better understanding of the mechanisms involved in producing the pathological hallmarks associated with the disease and their dynamic relationship to neuronal cell death is required. For many years, the pathological process involved in PD related

neuronal death was considered to be apoptosis. This was mainly due to the fact that until recently, only a few types of programmed cell death were known, and these were identified predominantly by using oncogenic cell lines (i.e. neuroblastoma). Since then, multiple cell death mechanisms have been studied and implicated in PD pathogenesis (reviewed in [18]), including anoikis [19,20], autophagy [21,22], necroptosis [23,24], parthanatos [25,26] and pyroptosis [27]. More recently, ferroptosis has been established as a regulated necrosis that is morphologically and mechanistically distinct from apoptosis and other known cell death pathways [28]. Ferroptosis is characterised by iron dependent lipid peroxidation[29]. Interestingly, several PD pathological hallmarks are known key **features and/or triggers** in the ferroptotic cell death pathway. These include **iron overload** [6,30–33], **elevated lipid peroxidation** [34–36], **reduced GSH levels** [37–40], **XCT downregulation** [41], **DJ-1 depletion** [42,43] **and CoQ10 reduction** [44–46]**. Together, these well-established diseases features strongly** implicate this regulated cell death pathway in the neurodegeneration observed in PD.

In this review we propose that ferroptosis may represent the missing piece to the puzzle in explaining the vicious cycle between synucleinopathy, iron accumulation, oxidative stress and related cell death in PD. Establishing the implication of ferroptosis in neurodegenerative diseases such as PD will promote interest in generating a range of anti-ferroptosis based therapies that could delay disease onset and slow progression. The aim of this paper is to review the current understanding of ferroptosis and present the evidence for the involvement of this newly defined cell death in PD neuropathology.

2. FERROPTOSIS – AN IRON DEPENDENT FORM OF REGULATED CELL DEATH

The term ferroptosis was coined in 2012 to describe a novel regulated form of caspase-independent cell death resulting from iron induced lipid peroxides that accumulate to toxic levels [28]. Although the precise metabolic pathways are still currently being elucidated, the past few years of extensive research have deciphered several regulatory mechanisms as well as numerous specific inducer and inhibitor reagents (Figure 1).

Keeping lipid hydroperoxides (LOOH) within physiological parameters is a key component in minimizing susceptibility to ferroptosis. Lipophilic antioxidants and lipid peroxide scavengers can block ferroptosis by preventing lipid peroxidation [47,48]. Under physiological conditions, the cell combats lipid peroxidation with glutathione peroxidase 4 (GPX4), an essential selenoprotein that reduces LOOH to lipid alcohols (LOH). Importantly, GPX4 is the only member of the glutathione peroxidase family capable of reducing LOOH, supporting its

central enzymatic role in the ferroptotic pathway [49,50]. Direct inactivation of GPX4 by RSL3 is one of the most common strategies to induce ferroptosis experimentally. Deletion of GPX4 in mice is embryonically lethal [51], whilst conditionally knocking out GPX4 in mice leads to acute renal failure, hippocampal and motor neuron neurodegeneration and early death of mice [47]. In addition, overexpression of GPX4 protects against cell death induced by RSL3 [52]. For the reduction of LOOH to LOH, GPX4 requires reduced glutathione (GSH) as an electron donor, releasing oxidised glutathione (GSSG). GSH is synthesised in the cell from glutamate and cysteine, the latter being the rate-limiting substrate. Cysteine can either be synthesised from methionine via the transsulfuration pathway or taken up in the form of an oxidised cystine dimer via the XcT antiporter before being reduced into the amino acid cystine. A heterodimer of the XcT unit (encoded by SLC7A11), that forms the Xc^- system, and the 4F2 unit (encoded by SLC3A2) that localizes the Xc^- system to the plasma membrane, are required for intracellular cystine transport [53]. An impairment of the XcT unit leads to a depletion in the intracellular cysteine pool, with consequential impairment of GSH biosynthesis and GPX4 activity. The subsequent lipid peroxide accumulation results in cell death by ferroptosis. Blocking GSH bioavailability through erastin-induced inhibition of the XcT antiporter or buthionine sulfoximine (BSO) induced inhibition of glutamate-cystein ligase (GCL); the rate-limiting enzyme in the first step of GHS synthesis, suffices to trigger ferroptosis (Figure 1). Elevating intracellular glutathione (GSH) levels with cysteine precursors such as n-acetylcysteine can protect against ferroptosis [52]. Recently in an attempt to uncover genes able to protect against ferroptosis through glutathione-independent pathways, the flavoprotein "apoptosis inducing factor mitochondria-associated 2" (AIFM2), was identified to rescue cell death caused by GPX4 deletion [46,54]. Renamed "ferroptosis suppressor-protein 1" (FSP1), it suppresses ferroptosis by catalysing the regeneration of Coenzyme Q10 (CoQ10, also known as ubiquinone) to its reduced form CoQ10-H_2 or ubiquinol; a potent mitochondria and lipid peroxyl radical trapping antioxidant (Figure 1 and 2).

As the name implies, iron plays a central role in ferroptosis. Co-treatment with several sources of iron sensitizes cells to ferroptosis triggered by erastin or RSL3 [28,55] and depletion of iron using drugs such as deferiprone (DFP) or genetically silencing transferrin receptor 1 (TfR1) to prevent cellular iron import protects cells against ferroptosis [55,56]. Although the exact mechanisms through which iron promotes ferroptosis remain unclear, it has been

suggested that i. ferrous iron directly induces lipid peroxidation[57], ii. iron loads the iron-dependent 12/15 lipoxygenase which enzymatically induces lipid peroxidation [40,58,59], and iii. iron loading of the hypoxia inducible factor prolyl-hydroxylase 1 induces ATF4-dependent pro-death gene transcription [60]. In biofluids such as cerebrospinal fluid (CSF), iron is predominantly bound to transferrin (Tf). Iron-loaded Tf (holo-Tf) incorporates two ferric (Fe^{3+}) atoms and is internalized into a cell through clathrin-mediated TfR1-dependent endocytosis (Belaidi and Bush 2016). Once in the endosome, iron is released from Tf due to its acidic environment and the metalloreductase STEAP3 reduces the bound insoluble Fe^{3+} to its soluble ferrous (Fe^{2+}) form [62]. Iron is then released into the cytosol through the divalent metal transporter 1 (DMT1), with Tf and TfR1 being recycled back to the membrane for further use. Neuronal uptake of iron can also occur directly through the DMT1 channel on the plasma membrane, allowing for a less regulated import pathway [61] (Figure 1). The free cytosolic Fe^{2+} that constitutes the labile iron pool (LIP) participates in the Fenton reaction producing highly reactive hydroxyl radicals (·OH) from hydrogen peroxide (H_2O_2)[57]. It is thus essential that appropriate levels of free iron in the LIP are tightly maintained to avoid the excess generation of free ·OH and other radicals (see section 3.2. for further details). The function of ferritin is in part to safely store excess iron in the cytosol but neuromelanin also serves as a key iron storage protein specifically in dopaminergic neurons. The only known export pathway for iron is through the transmembrane channel ferroportin (FPN) in which iron, oxidized to Fe^{3+} by a ferroxidase such as ceruloplasmin, can exit the cell[63]. In select cells (including neurons) β-amyloid precursor protein (APP) is required to facilitate iron efflux by stabilising FPN on the plasma membrane [64–67] (Figure 1).

In addition to the Fenton reaction, iron can mediate the generation of lipid peroxides by serving as a cofactor to the family of Lipoxygenase enzymes (LOX). Of particular interest to ferroptosis, 15-LOX can enzymatically generate additional LOOH on long-chain polyunsaturated fatty acids (PUFA); mainly phosphatidylethanolamines containing arachidonic acid (AA) or adrenic acid (AdA) present on the plasma membrane (Shintoku et al. 2017; Shah, Shchepinov, and Pratt 2018). The lipid composition of the plasma membrane can therefore determine cellular susceptibility to ferroptosis whereby long chain PUFAs containing AA increase the risk for lipid peroxidation whilst monounsaturated fatty acids (MUFAs) appear to decrease such risk [70]. For PUFAs to be incorporated into the phospholipids (PL) of the plasma membrane, they first need to be conjugated to Coenzyme-A

(CoA) by the enzyme acyl-CoA synthetase long-chain family member 4 (ACSL4). PUFA-CoAs can then be incorporated into the plasma membrane by lysophosphatidylcholine acyltransferase 3 (LPCAT3) where 15-LOX specifically oxidise the PLs rendering the plasma membrane more permeable and fragile. ACSL4, but not other members of the ACSL family, is a key player in the ferroptosis pathway as it enriches cellular membranes with long chain ω6 fatty acids. Inhibiting or genetically depleting ACSL4 prevents ferroptotic lipid peroxidation and subsequent associated cell death [71]. The selectivity of ACSL4 over the other ACSLs in regulating the ferroptosis pathway is likely to be due to its substrate preference for AA, the main fatty acid implicated in ferroptosis [72]. The importance of LPCAT3 in the ferroptosis pathway was initially pointed out by Dixon *et al* [73] but later confirmed by Doll *et al* [71] where LPCAT3 deletion mildly protected fibroblast against ferroptosis (Figure 1).

The initial discovery of ferroptosis occurred within the context of certain oncogenic Ras-dependent cancer types. However, thanks to extensive ongoing research since its emergence, this type of cell death has now also been implicated in an array of other pathological conditions. These include ischemia-reperfusion injury (IRI) of the liver, kidney, brain and heart [74–81], **stroke** [82–86] and multiple neurodegenerative disorders including PD [56], Alzheimer's disease [87] and amyotrophic lateral sclerosis [88].

3. FERROPTOSIS IN PARKINSON'S DISEASE

Ferroptosis has been shown to be a prevalent type of cell death in *in vitro*, *ex vivo* and *in vivo* models of PD [56]. Dopaminergic neurons within a differentiated cellular model (Lund human mesencephalic cells; LUHMES) or *ex vivo* organotypic slice cultures are sensitive to erastin induced ferroptosis which can be rescued by the ferroptosis specific inhibitors ferostatin-1 (Fer-1) and liproxstatin-1 (Lpx-1) as well as the iron chelator DFP. These specific inhibitors are also protective against neurotoxin induced cell death associated with sporadic PD (e.g. rotenone, paraquat and MPP+). *In vivo*, 1-methyl-4-phenyl-1,2,3,6-tetrahydropyridine (MPTP) associated neuropathology has been identified to have a ferroptosis component as inhibition by Fer-1 and Lpx-1 prevents dopaminergic neuronal loss in the SN and striatum as well as behavioural and motor impairments [56]. **These results further** provide promise that inhibition of ferroptosis may alleviate and/or prevent PD associated neuropathology.

3.1 The role of iron in PD pathology

Iron serves as a cofactor in a myriad of metabolic processes throughout the body, and is particularly essential for brain health as it is involved in neurotransmitter synthesis, mitochondrial respiration, myelin synthesis and sulfur-cluster protein synthesis amongst other processes [89,90]. Due to the high metabolic activity and reliance on iron for many of these processes it should not be a surprise that this metal accumulates in the brain through age. However, this accumulation is even greater in regions of the brain that happen to be associated with neurodegenerative disorders [61,91]. In PD, iron elevation is especially observed in glia and dopaminergic neurons of the SNpc, where levels correlate with disease severity[6,31,32,92]. In patients, this has been measured by iron-sensitive high-field MRI [32,93] and quantitative susceptibility mapping (QSM) analyses [94] as well as post-mortem tissue and is strongly supported in many parkinsonian animal models [33,95–97]. In PD, abnormal iron accumulation is most likely due to an imbalance in the iron homeostatic pathway caused by alterations in iron regulatory proteins [98,99]. Patients carrying mutations that cause iron-related proteins to be dysfunctional (e.g. transferrin) have an increased a risk of developing PD [100,101]. Increased levels of DMT1, reported in the SNpc of PD patients as well as several mouse models of PD, are likely to contribute to an increased cellular iron import [102,103]. Ferritin levels are also decreased in the SN of post-mortem brains of PD patients [104], and FPN is decreased in several models of PD including MPTP and 6-hydroxydopamine (6-OHDA)[105]. Of relevance to impaired neuronal efflux through ferroportin, rare variants of APP with loss of membrane function predispose humans to develop PD [106]. In addition, APP expression is decreased in the SN of PD patients, leading to a similar iron-associated phenotype as APP knockout mice [65,67]. Furthermore, the ferroxidase activity of CP required to facilitate iron efflux through FPN is decreased in both patients and animal models of PD[107,108]. Further support for iron elevation as a cause of parkinsonian pathology comes from the genetic disorder aceruloplasminemia, in which CP is mutated, often leading to a parkinsonian phenotype including gait difficulties, ataxia, involuntary movements and cognitive decline that correlate with brain iron deposition [109,110]. It is likely that an unregulated modulation of iron import and efflux contribute towards the elevation of intracellular iron required for increased vulnerability to free radical formation and ferroptosis.

Based on the extensive evidence supporting the impact of iron on PD pathology, iron chelation has been investigated as a possible therapeutic strategy[99,111,112]. Iron chelation in the MPTP mouse model restores iron to physiological levels in correlation with preventing cell toxicity and behavioural deficits [96,97]. DFP is currently used clinically for systemic iron

overload disorders such as beta thalassemia and was recently investigated in a double-blind, randomized, placebo-controlled clinical trial of early-stage PD [97]. Over 12 months, patients receiving daily doses of DFP showed a promising decrease in motor handicap progression as well as reduced iron deposition in the SN [97]. The potential of DFP as a disease modifying treatment for PD is now being assessed in a phase 3 multicentre clinical trial with outcomes expected within the near future (FAIRPARK II – NCT01539837). Importantly, similar results have been observed in an independent phase 2 randomised double-blind placebo controlled clinical trial [113].

3.2 The role of oxidative stress in PD Pathology

Oxidative stress (OS) is considered a major contributor to the pathophysiology underlying PD and is well reported in patients as well as all PD animal models [39,40,114,115]. Indeed, a number of parkinsonian models induce an OS response that results in a phenotype similar to PD. Cellular damage caused by OS comprises of protein oxidation, leading to protein dysfunction and structural changes, DNA oxidation and cell membrane disruption due to lipid peroxidation. OS is induced by an imbalance in the redox state caused not only by an excessive reactive oxygen species (ROS) production but also by an insufficient antioxidant system response to reduce these reactive species. ROS are defined as highly reactive molecules derived from oxygen and include free radicals such as superoxide (O_2^-) and ·OH as well as non-radical molecules like H_2O_2 [115]. ·OH are considered one of the most volatile ROS responsible for the cytotoxicity effect underlying oxidative stress and are predominantly generated from H_2O_2 and free cytosolic Fe^{2+} through the Fenton Reaction. Mitochondria are one of the main sites of H_2O_2 and ROS production, particularly O_2^-, via the respiratory chain complexes used to transport electrons [116,117]. In the brain, the majority of the O_2^- is produced by Complex I, and it is not a coincidence that this is the primary location from which ROS is generated in various neurodegenerative diseases [118]. Indeed, in PD patients a dysfunctional Complex I is present in the SN and frontal cortex as well as fibroblast and platelets from these patients; all of which may lead to increased superoxide production [117,118]. The deficiency in complex I is related to a CoQ10 deficit, further contributing to ROS production in mitochondria and lipid peroxidation in membranes. Interestingly, CoQ10 was recently reported to play an important anti-ferroptosis role on an FSP1-NAD(P)H-CoQ10 axis [46,54]. Cells are equipped with an antioxidant system to maintain a balanced redox state, which, if compromised, can result in excessive oxidative stress and subsequent cell death. The

maintenance of glutathione GSH is one such antioxidant system heavily used by the brain to remove ROS by directly interacting and removing the highly reactive O_2^- and ·OH radicals [119,120]. Oxidative stress in PD may in part be due to a reduction in GSH levels that appear to be particularly evident in the SN of PD [37–39]. **The** Sian *et al* **study measured GSH levels in several port-mortem brain regions from PD, progressive supranuclear palsy, multiple-system atrophy and Huntington's disease patients, and the only significant change observed was a specific 40% reduction in the SN from PD patients. The fact that no changes were reported in the other diseases suggests that the alterations in GSH levels were not a general consequence of neurodegeneration** [38]. Interestingly, a recent analysis of DNA methylation in 1132 PD cases and 999 controls associated hypermethylation in the promoter region of the SLC7A11 gene (encoding the cysteine-glutamate antiporter XcT-) with risk of PD. This hypermethylation of SLC7A11 results in a downregulation of system XcT- which could contribute to the decreased intracellular GSH levels observed in PD and increase a susceptibility to ferroptosis[41]. A similar reduction in GSH level has been shown to trigger the activation of neuronal 12-lipoxygenase (12-LOX) and subsequent accumulation of LOOH [40]. These observations further support the concept that the decrease of GSH in the SN from PD patients is not simply a consequence of neuronal death but a direct indication of oxidative stress. Moreover, as GSH is a natural ligand for Fe^{2+} [121], its reduction in the SN of PD patients would not only impair the antioxidant capacity of dopaminergic neurons but also increase the LIP, further contributing to the generation of ·OH and other ROS. The aforesaid intracellular environment would render the dopaminergic neurons particularly vulnerable to ferroptotic cell death.

DJ-1 is another cellular antioxidant enzyme known to play a key role in regulating oxidative stress, ROS formation and mitochondrial function. Loss of function mutations in the DJ-1 gene (PARK7) have been linked to autosomal-recessive early onset PD with increased mitochondrial oxidant stress, a drop in basal cellular respiration and oxidized dopamine accumulation[122]. Recently, Cao *et al* have shown that DJ-1 acts as a ferroptosis inhibitor by preserving the transsulfuration pathway, and thereby the biosynthesis of cysteine and GSH. DJ-1 depletion leads to lipid ROS accumulation and a heightened sensitivity to ferroptosis cell death [43]. The discovery of DJ-1 as a ferroptosis suppressor further supports that ferroptosis is implicated in PD pathology.

One would anticipate that such changes to GSH levels and the increase in LOOH would impact upon the expression and activity of key antioxidant enzymes such as GPX4. In post-

mortem tissue from PD patients' brains, protein levels of GPX4 are increased compared to control subjects [123]. More recently, GPX4 levels were confirmed to be increased relative to cell density of surviving neurons, despite the apparent reduction when measuring against total tissue [124]**. This implies that it is only the remaining neurons in the SN of PD patients that were able to counter an oxidative and pro-ferroptotic environment through an appropriate GPX4 response to prevent cell death** [124]**Interestingly, this phenomenon has also been reported in *in vitro* and *in vivo* models of stroke** [82,83].

Recent advances in imaging technology are increasing our capability to measure oxidative stress in living PD patients using positron emission tomography (PET). Copper(II)-diacetyl-bis(4-methylthiosemicarbazonato) (Cu-ATSM) is a PET tracer initially developed for hypoxia imaging but has recently shown potential in reflecting the redox state within the body [125]. Interestingly, this brain blood barrier penetrant imaging agent was identified as being neuroprotective in multiple animal models of Parkinson's disease [126] and prevent lipid peroxidation without altering the oxidation state of iron. Similar to Fer-1 and Lpx-1, Cu-ATSM may block ferroptosis by preventing the propagation of lipid radicals rather than preventing iron oxidation [127] and could offer an opportunity to monitor disease progression as well as efficacy in PD patients during treatment. While functional imaging of oxidative stress is currently considered to mainly detect mitochondrial dysfunction, it still appears sensitive enough to show an elevation of striatal oxidative stress in PD patients when compared to controls [128].

Despite the strong evidence implicating oxidative stress in PD pathology and the neuroprotective properties of antioxidants reported in models of PD, outcomes from clinical trials have remained inconsistent (reviewed in [115]). Clinical studies with exogenous antioxidant therapies are mixed with some reporting efficacy [129–131] whilst others fail to demonstrate a significant effect [132]. A major component of this disparity could lie with many clinical trials not having the appropriate pharmacokinetic measurements taken, a lack of confirmation in target engagement in the brain, inappropriate treatment duration and/or uncontrolled variances in endogenous antioxidant potential within the patient.

3.2.1 The role of lipid peroxidation in PD pathology

Lipid metabolism and cellular lipid composition can determine cellular sensitivity to ferroptosis. Lipidomic analyses revealed that polyunsaturated-fatty-acid-containing phospholipids (PUFA-PLs), and in particular phosphatidylethanolamines (PE) containing

arachidonic acid (AA) or adrenic acid (AdA) in the plasma membrane, are the lipids most susceptible to ferroptosis-related peroxidation [133,134]. The ability of cells to undergo ferroptosis is therefore determined by the abundance and cellular localisation of PUFA, as confirmed by the fact that human cells enriched with AA are sensitised to ferroptosis [58]. As previously mentioned, free PUFAs undergo esterification by ACSL4 before incorporation into the plasma membrane phospholipids by LPCAT3 [73]. The bis-allylic carbons, adjacent to two carbon atoms with double bonds, are the key positions within lipids that drive ferroptosis as they increase susceptibility to attack from reactive radicals, lipoxygenases and surrounding lipid peroxides [58]. Thus, the peroxidation potential of a PUFA is linearly dependent on their number of double bonds [135]. The process of lipid peroxidation takes place via three steps: initiation, propagation and termination. Firstly, reactive radicals abstract a hydrogen atom from a bis-allylic carbon to form the carbon-centred lipid radical (PL·). Such radicals rapidly react with oxygen forming lipid peroxyl radicals (PLOO·), which can subsequently abstract further hydrogens from neighbouring lipids to propagate the generation of new PLOO· and lipid hydroperoxides (PLOOH) [136].The lipid peroxidation reaction can be inhibited by the FSP1-CoQ10H_2 system or when antioxidant enzymes, such as GPX4, donate electrons and reduce the pLOOH to PLOH (Figure 2). In ferroptosis, an insufficient GPX4 activity leads to an overwhelming accumulation of LOOH.

Noteworthy, the brain has the second highest concentration of lipids, after adipose tissue. The proportion of these lipids are largely AA and docosahexaenoic acid (DHA) which contain four and six double bonds respectively [137]. Furthermore, the high oxygen consumption of the brain makes it particularly sensitive to lipid peroxidation. Dexter *et al*, were the first to demonstrate the involvement of lipid peroxidation in PD as a cause of nigral cell death [34]. Brain post-mortem analyses revealed a reduction in PUFAs but not MUFAs in the SN of PD patients compared to controls (D. Dexter et al. 1986). Conversely, levels of malondialdehyde (MDA), a toxic by-product of lipid peroxidation, were elevated in the same tissue [35] and LOOH increased in plasma [138]. MDA levels were increased both in early and late PD patients whilst LOOH levels were only significantly increased in later stages of the disease. This suggests that while MDA could be a useful biomarker for PD, changes in LOOH levels may correlate better with disease progression [36]. Further studies have revealed a correlative increase in another lipid peroxidation metabolite, 4-hydroxy-2-nonenal (HNE), as well as HNE-protein adducts, with pathology from Lewy bodies in the SN of PD patients and

brainstem of DLB [139]. Interestingly, in the CSF of PD patients, elevated HNE correlates with an accumulation of iron in the SN [139,140].

The mechanism by which lipid peroxidation is involved with PD pathology was expanded upon by Shchepinov *et al* whereby MPTP treated mice were protected against nigrostriatal injury upon supplementation with deuterated-PUFAs (D-PUFAs) [141]. D-PUFAs have deuterium in the place of the bis-allylic hydrogens, which slows radical generation compared to Hydrogenate-PUFAs [141]. More recently, *Yang et al* confirmed that pre-treating cells with D-PUFA prevents PUFA oxidation and ferroptosis[58].

The 85-kDa group VI calcium-independent phospholipase A2 beta (PLA2G6) is another key enzyme with possible implications to ferroptosis. This enzyme hydrolyses the sn-2 acyl chain of glycerophospholipids to release free fatty acids and lysophospholipids. PLA2G6 localizes to the mitochondria and has proposed roles in the remodeling of membrane phospholipids, signal transduction, calcium signaling, cell proliferation and cell death[142]. Patients with homozygous PLA2G6 mutations present a form of neurodegeneration with brain iron accumulation (NBIA) that has neuropathological similarities to both Parkinson's and Alzheimer's disease: as well as iron accumulation, these include widespread Lewy bodies, dystrophic neurites and cortical neuronal neurofibrillary tangles[143]. In a recent study, Kinghorn *et al*, showed that knocking-out the *drosophila* homologue of the PLA2G6 gene, iPLA2-VIA, resulted in reduced survival, locomotor deficits, organismal hypersensitivity to oxidative stress (in particular the mitochondria) and a strong association with increased lipid peroxidation levels [144]. D-PUFA has also shown to rescue the aged-associated locomotor abnormalities and restore mitochondrial membrane potential in this model.

An elevation of iron in combination with high levels of PUFAs within dopaminergic neurons creates an environment particularly sensitive to lipid peroxidation meaning that a slight imbalance in iron, dopamine or lipid homeostasis could sensitise dopaminergic neurons to ferroptosis. Characterising the distinct and regulated pathways of lipid peroxidation sheds light in deciphering the neuropathology involved in nigral cell death in PD and encourages the pursuit of therapeutic strategies that will inhibit ferroptosis.

3.3 The role of other ferroptosis regulators in PD pathology

Nuclear factor erythroid-2-related factor 2 (Nrf2), a master regulator of the antioxidant **response, was recently shown to protect against ferroptosis** [145,146]**.** Under

oxidative stress, Nrf2 is translocated to the nucleus to induce the expression of endogenous antioxidant **proteins responsible for preventing lipid peroxidation. Of relevance to ferroptosis, continuous exposure to erastin results in Nrf2-dependent upregulation of cystathionine β-synthase (CBS), the enzyme responsible for the biosynthesis of cysteine, in an attempt to counter cell death** [146]**. Nrf2 also controls the expression of NAD(P)H:quinone oxidoreductase 1** [147]**, several iron metabolism proteins (e.g. ferritin and ferroportin), GPX4** [148] **and other key ferroptosis proteins involved in GSH biosynthesis (e.g. XcT, glutamate-cystein ligase and gluthathione synthetase)** [146,148,149] **(reviewed by** [150]**).** Nrf2 has been extensively studied in the context of PD pathology where an age-related decline in activity leads to reduced GSH levels [151,152]**. In PD patients, Nrf2 and downstream effectors are highly transcribed in blood leukocytes compared to controls** [153]**. Interestingly, these Nrf2 transcripts correlate with PD duration, suggesting that Nrf2 plays a role in fighting the intrinsic oxidative stress observed during disease pathology. Furthermore, the cellular localisation of Nrf2 appears to be predominantly nuclei in the SN of PD patients, in contrast to the cytoplasmic location in affected brain regions from other neurodegenerative diseases such as AD or Lewy body variant of AD** [154]**. Such nuclear translocation in PD indicates a cellular and/or disease dependent recruitment of Nrf2 caused by an intrinsic vulnerability of dopaminergic neurons to oxidative stress.** *In vitro*, activation and nucleus translocation of Nrf2 is also protective against MPP+ insult [155], **and sufficient in preventing locomotor impairment as well as neuronal loss in a *drosophila* model of PD** [156]**. It is worth noting that Nrf2 response to oxidative stress is not unique to ferroptosis as Nrf2 inhibition has also been implicated in apoptosis cell death** [157]**. Therefore, the role of Nrf2 in PD may be associated with several forms of cell death.**

NADPH is an intracellular reductant involved in the elimination of LOOH. Intracellular NADPH levels are considered a biomarker for ferroptosis sensitivity, but accurate measurement of NADPH levels is difficult in patients. Several studies with biofluids from PD patients have demonstrated an altered level of NADPH oxidase; an enzymatic complex which oxidises NADPH to generate oxygen species. The NADPH oxidase subunits NADPH oxidase 1 (NOX1) and 4 (NOX4) are both increased in the SN in several PD mammalian models [158,159] as well as PD patients [160].

CoQ10 and its reduced form CoQ10-H_2 are potent mitochondria and lipid ROS antioxidants also considered as endogenous ferroptosis inhibitors [29]. The role of **CoQ10 as a ferroptosis inhibitor** has been further established by the two recent studies that show FSP1 as being instrumental in regenerating CoQ10 from NADPH and having an ability to suppress both phospholipid peroxidation and ferroptosis independent of GPX4 [46,54]. Interestingly, CoQ10 is reduced in patients and animal models of PD [44, 45], resulting in increased ROS production. CoQ10 supplementation can decrease lipid peroxidation markers in the plasma, liver and brain of PD mouse models [161] as well as protect against MPTP induced dopaminergic neurodegeneration and α-syn aggregation [162]. The lack of a beneficial outcome of CoQ10 in a randomized early PD clinical trial [132] may have arisen from challenges around its **biodistribution in the central nervous system. Duration of treatment is another factor to take into consideration as the CARE-HD (Coenzyme 10 and Remacemide Evaluation in Huntington's Disease) study only indicated a benefit after two years of treatment [163]. A related alternative treatment rationale could be** CoQ10-H_2 , as a **3-fold higher plasma concentration can be achieved compared to oxidised CoQ10** [164], or the introduction of a combinatorial therapy with currently used drugs and/or **ferroptosis inhibitors.**

Selenium (Se) is considered a key element in the cellular antioxidant machinery as it is crucial for selenocysteine formation and the synthesis of selenoproteins such as GPX4[165]. Se abundance can thus impact upon ferroptosis sensitivity, whereby supplementation promotes ferroptosis resistance and a deficit leads to increased sensitivity, presumably through modulating GPX4 levels and activity [166]. In line with an intrinsically high oxidative environment, the level of Se in the brain is highest in the SN and caudate[167]. Multiple studies report a protective role of Se in several PD models: Se supplementation reduces motor impairments and DNA damage in a rat model in which Paraquat induces parkinsonism [168] and a single dose of Se was sufficient to reverse the depletion of striatal dopamine and its metabolites in the MPTP mouse model [169]. In line with GPX4 expression levels, Selenoprotein P, a peptide with a high content of selenium in the form of selenocysteine, was reportedly reduced in PD SN compared to control brains but increased relative to cell density (Bellinger et al. 2012).

Extensive research has independently linked several components of the ferroptotic pathway to the pathology underlying neuronal degeneration in PD. In serum, the significant

diagnostic ability, measured using ROC analysis (AUC: 0,94), has been used to identify the combination of NOX1 and Se as a promising diagnostic biomarker for PD (Hemmati-Dinarvand et al. 2017.

3.4 Implications on the role of α-synuclein in ferroptosis

Aggregated α-synuclein (α-syn), one of the main components in intracellular Lewy Bodies [7], has long been considered a key pathological hallmark of the disease. The relationship of α-syn to disease pathology has been confirmed by genome wide association studies, where single nucleotide polymorphisms associate with sporadic PD risk whilst confirmed mutations and duplication/triplication in the *SNCA* gene (encoding α-syn) lead to various clinical manifestations ranging from classical to early onset familial PD [172,173]. Despite the involvement of α-syn in PD pathology, the exact physiological function of this protein and the mechanisms linking it to neurodegeneration remain elusive**. Establishing a synucleinopathy link to ferroptosis would strengthen the implication of this novel type of cell death in PD.** To this end, multiple studies have increasingly shown α-syn to have a role in regulating both iron and lipid metabolisms with inference to the ferroptosis pathway (Figure 3). **Interestingly, iron chelators, D-PUFAs, and ferrostatin all suppress cell death induced by toxic α-syn oligomers, meeting the basic criteria set out to define ferroptosis** [29,133,174]**.**

3.4.1 α-synuclein and iron metabolism

Over the past two decades, the interactions between α-syn and iron metabolism have been extensively studied and reviewed (e.g. [112,175,176]). However, since the emergence of ferroptosis, this relationship should be reassessed and placed in the ferroptosis context. Both Fe^{2+} and Fe^{3+} strongly bind to α-syn and promote its oligomerization by converting this intrinsically disordered protein into a β-sheet structure [177–181]. Iron exposure to neuronal cultures overexpressing α-syn with a familial mutation (A53T α-syn) increase aggregate formation and vulnerability to iron induced toxicity [182]. Furthermore, α-syn oligomers interacting with iron in neurons induce ROS and lipid peroxidation production, reduce GSH levels [183], abd have subsequently been shown to induce ferroptosis via iron-dependent oxidation [174]. This is particularly poignant with the knowledge that the dopaminergic neurons, susceptible in PD, are high in iron and have an intrinsically high oxidative environment due

to their dopamine metabolism. Iron chelation has not only been shown to be neuroprotective against PD related neurotoxin insult (i.e MPTP, 6-OHDA and Paraquat) but can reduced α-syn aggregation *in vitro* and rescue behavioural deficits induced by iron exposure in a mouse model of α-syn aggregation [184].

While iron can modulate the biophysical nature of α-syn, this protein may also have a role in neuronal iron homeostasis. α-Syn contains an iron response element (IRE) within its 5'UTR mRNA region; a binding site involved in regulating the translation of the protein upon modulation of neuronal iron load [185]. As an iron regulated protein, iron depletion causes a decrease in translation of α-syn[186] whilst overexpression of α-syn in neurons results in higher levels of Fe^{2+} [187]. It has been suggested that α-syn acts as a ferrireductase reducing Fe^{3+} to Fe^{2+} [183] and increases susceptibility to iron-dependent ROS and LOOH production [187]. More recently, Baksi and colleagues have proposed that α-syn directly mediates iron metabolism by facilitating the uptake of transferrin-bound iron, and colocalizes with TfR1 in the plasma membrane. Depletion of α-syn results in TfR retention in recycling endosomes and subsequent depletion of cellular iron stores [188] whilst an increase in α-syn can afect lysosomal activity by disrupting the trafficking of lysosomal hydrolases and impairing ferritinophagy [189]; a process linked to ferroptosis [190,191]. An alternative mechanism in which α-syn is proposed to modulate cellular iron import is through an ability to upregulate the iron transport protein DMT1. Bi *el al*, showed that α-syn-induced p38 mitogen-activated protein kinase (MAPK) phosphorylation of parkin inactivates its E3 ubiquitin ligase activity and reduces DMT1 degradation via ubiquitylation [103].

3.4.2 α-syn and lipid metabolism

Substantial evidence linking α-syn with cellular lipid **metabolism further implicates α-syn in ferroptosis**. Firstly, α-syn has a high degree of sequence homology with apolipoproteins and binds lipids through its N-terminal region. Of particularly high binding affinity are the PUFAs α-linolenic acid, DHA and eicosapentaenoic acid[192,193]. When exposed to free or phospholipid-bound PUFAs, α-syn undergoes structural changes including an increased propensity to oligomerize [194–197], whereas monosaturated fatty acids (MUFAs) have no effect on α-syn aggregation [193]. Lipid peroxidation products from PUFA, such as HNE, also induce modifications to α-syn and equally promote the formation of toxic oligomers in human neuroblastoma cells [198]. Conversely, α-syn modulates the metabolism of certain membrane PUFAs including **linoleic acid, dihomo-gamma-linoleic acid, AdA and AA.**

Both the lipid ratio of these PUFAs in the plasma membrane and the membrane fluidity are increased when α-syn **is overexpressed in neuronal cultures as well as in brain tissue from PD and DLB patients** [138]**. In contrast, the** cytosolic fatty acid composition is altered and the membrane fluidity reduced in brains of α-syn KO mouse [138]. A separate study also suggests that α-syn contributes to membrane remodelling by sensing lipid packing defects and inducing lateral expansion of lipids [199]. These findings strongly indicate that α-syn has a role in membrane fatty acid compositions and thereby regulating membrane fluidity, vesicle assembly and subsequent synaptic transmission. [200]Finally, technological advances in transmission electron microscopy (TEM) in association with light microscopy imaging has enabled a clearer understanding of Lewy Body composition, revealing a high level of membranous content, fragmented organelles and vesicles at the core of α-syn immunoreactivity [5].

Overall, iron and PUFA dependent studies suggest that α-syn's physiological and/or pathological functions may generate, over time, a pro-ferroptotic environment in dopaminergic neurons. Specifically how α-syn functionally regulates membrane composition remains unclear but Golovko and colleagues have shown *in vivo* that α-syn plays a key role in the metabolism of brain AA [200]; **the main substrate of LOX-15 and ACSL4, two enzymes implicated in the ferroptosis pathway. Direct or indirect enrichment of cellular membranes with AA, amongst other PUFAs, by** α-syn **under the pathological conditions of elevated free labile iron and oxidative stress, may lead to further lipid peroxidation and drive neurons towards ferroptosis. The recent finding that α-syn oligomers bind the plasma membrane to drive ferroptosis cell death through lipid peroxide generation provide the first direct evidence to support ferroptosis as a pathological mechanism in synucleinopathies** [174]**. However, further research is essential to strengthen this hypothesis and establish whether α-syn's ability to regulate both iron and lipid homeostasis in neurons are also implicated in the ferroptosis pathway.**

4. CONCLUSION AND FUTURE PERSPECTIVES

New disease modifying therapies and novel therapeutic strategies are in high demand for PD patients. An emerging knowledge on ferroptosis is shedding a different perspective on several physiological and pathophysiological conditions. Indeed, for decades, researchers have been heavily characterising several aspects of PD pathology as independent

components, which now may be linked in conferring susceptibility to ferroptosis. These include elevated lipid peroxidation, glutathione depletion**, DJ-1 and CoQ10 deficiency, GPX4 reduction,** mitochondriopathy, iron accumulation and α-synuclein aggregation. Based on this information **it is hard to believe that the extensive similarities between** PD neuropathology **and aspects of the ferroptosis cell death pathway are due to a mere coincidence**. We therefore propose ferroptosis as a key contributor to PD progression with broader implications in synucleinopathies. **Deciphering the role of α-synuclein in the iron and/or lipid components of the ferroptotic pathway now represents an area of increased research focus that is hoped to not only provide a greater understanding to the physiological function of the protein but also elucidate one of its neuropathological features in PD.**

The fact that iron chelation, an established anti-ferroptotic strategy, has shown the first clinical benefits in two independent clinical trials on early-PD [97,113] should encourage further progress in targeting ferroptosis. Ultimately, the role of ferroptosis in neurodegenerative disorders will only be confirmed when additional anti-ferroptotic therapies advance successfully to clinical trial.

ACKNOWLEDGMENTS

The authors wish to thank the support of the Lille University Hospital and NS-Park/FCRIN clinical research network, the European commission for the grant N° 633190 of the H2020 program; NCT02655315. The authors also thank the Fédération de la Recherche Clinique du CHU de Lille, Pauline Guyon, Lucile Marguet, Stéphanie Le Naour, Florence Nosal, Amelie Michon, Aurélie Rabier for the support and ApoPharma for the drug provision in the clinical trials.

FULL FINANCIAL DISCLOSURE

James Duce has received research funding from Alzheimer's Society, Alzheimer's Research UK, European Commission, Parkinson's UK and NHMRC. He serves as a scientific advisor on the FAIR-PARK II but has no financial disclosures.

David Devos has received PHRC grants from the French Ministry of Health and research funding from the ARSLA charity, France Parkinson charity, Credit Agricole Fundation. He has led two pilot investigator driven studies with DFP provided for free by ApoPharma (FAIRPARK-I and SAFE-FAIR ALS-I). He is leading two large investigator driven studies

with DFP provided for free by ApoPharma (FAIRPARK-II and FAIR ALS-II). He served on advisory boards, served as a consultant and given lectures for pharmaceutical companies such as Orkyn, Aguettant, Abbvie, Medtronic, Novartis, Teva, UCB, Lundbeck.
Laura Mahoney-Sanchez, Hind Bouchaoui, Scott Ayton and Jean Christophe Devedjian have nothing to declare.

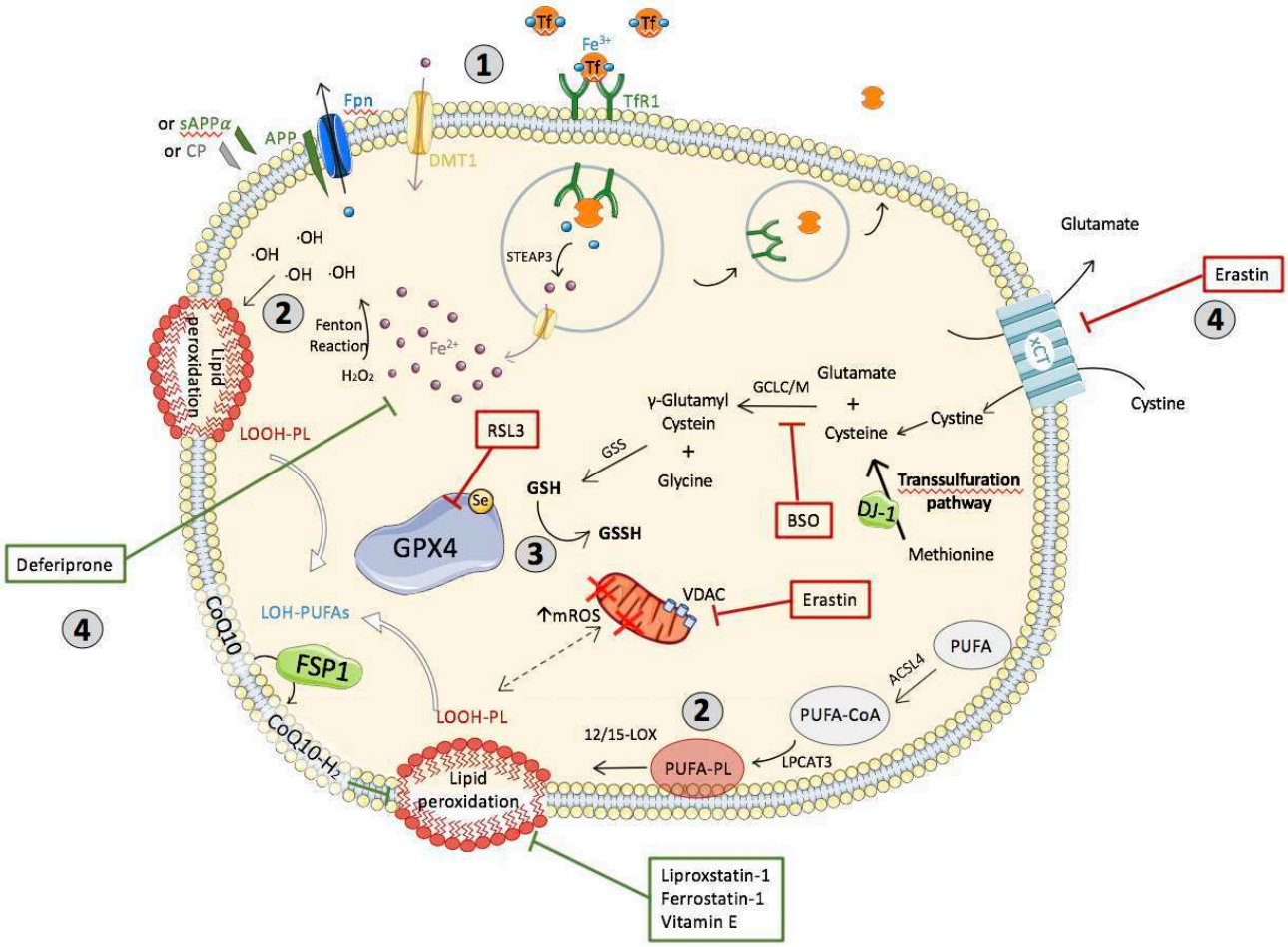

Figure 1: The ferroptosis pathway. Alterations in the iron regulatory pathway and phospholipid oxidation are implicated in Parkinson's disease pathology. **1.** Increased intracellular iron occurs by enhanced import of iron within transferrin (Tf) through Transferrin receptor (TfR), and increased import of Fe^{2+} through the divalent metal transporter 1 (DMT1). In addition, iron export is impaired through the destabilization of ferroportin (Fpn) on the cell surface by β-amyloid precursor protein (APP) or ceruloplasmin (CP). **2.** An elevated labile iron pool catalyzes the formation of

phospholipid hydroperoxides. Free cytosolic polyunsaturated fatty acids (PUFA) are conjugated to coenzyme-A (CoA) by acyl-CoA synthetase long-chain family member 4 (ACSL4) allowing PUFA-CoA to be incorporated into the phospholipids in the plasma membrane. Phospholipid-PUFA are oxidised by lipoxygenases 12/15, contributing to the accumulation of phospholipid hydroperoxides at the plasma membrane level. Mitochondrial dysfunction result in increased ROS production which may also contribute to lipid peroxidation in the plasma membrane. **3.** Cystine uptake through the X_{c-} antiporter is required for biosynthesis of glutathione (GSH). Glutathione peroxidase 4 (Gpx4) uses 2 GSH molecules to safely reduce phospholipid hydroperoxides to their corresponding lipid-alcohols, producing H_2O and glutathione disulphide (GSSG) as byproducts. Elevated levels of intracellular iron with depletion of Gpx4, as evidenced in models of PD, promotes the accumulation of phospholipid hydroperoxides leading to a disruption in membrane integrity through a ferroptotic pathway. **4.** Ferroptosis is induced by Erastin that blocks Cystine import, GSH biosynthesis and mitochondrial VDAC, and/or directly inhibiting GPX4 with RSL3. Conversely, reducing the labile iron pool (i.e deferiprone) or depleting the phospholipid hydroperoxides (i.e. liproxstatin-1, ferrostatin-1or vitamin E) are promising targets for inhibiting ferroptosis in PD pathology. FSP1 serves as a ferroptosis suppressor by regenerating CoQ10, whose reduced form – CoQ10-H_2 traps membrane lipid hydroperoxides preventing lipid peroxidation propagation.

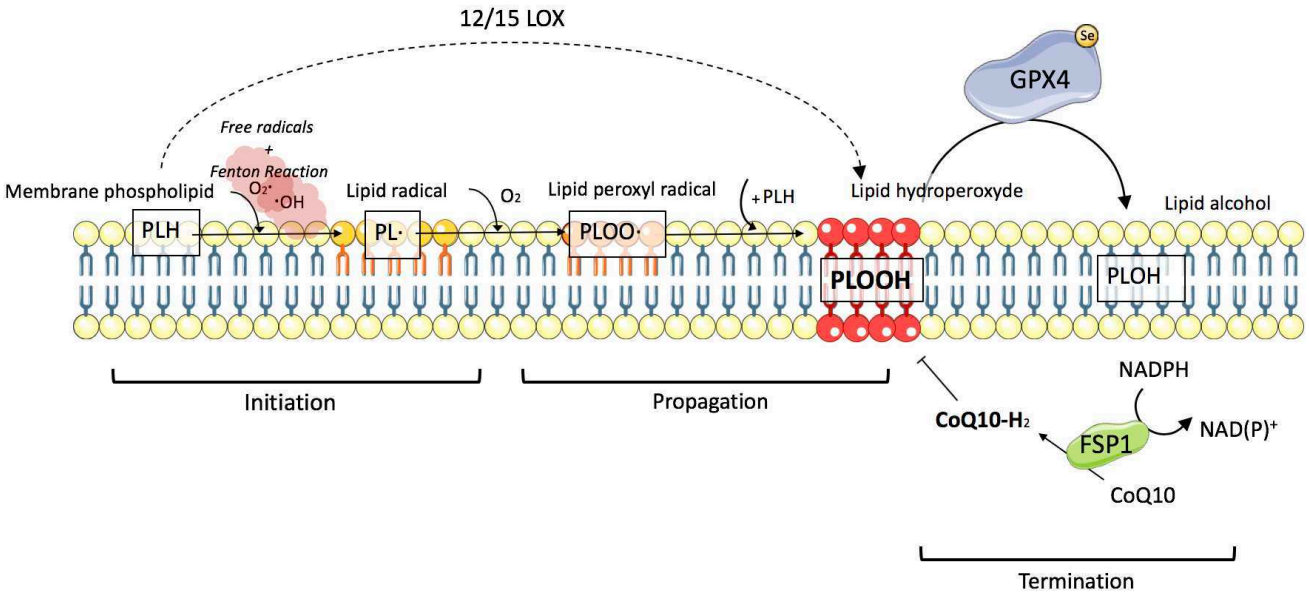

Figure 2: Membrane lipid peroxidation.

The process of membrane phospholipid peroxidation takes place via three steps: initiation, propagation and termination. The Fenton reaction and free reactive radicals abstract a hydrogen atom from the phospholipid carbon chain forming a lipid radical (PL·). These radicals rapidly react with oxygen and form lipid peroxyl radicals (PLOO·), which can subsequently react with neighbouring lipids to propagate the generation of new lipid peroxyl radicals and lipid hydroperoxides (PLOOH). The lipid peroxidation reaction is terminated when antioxidant elements or enzymes, such as GPX4, reduce the lipid peroxides to lipid alcohols (L-OH). The FSP1 - CoQ10 - NAD(P)H system works in parallel to GPX4 in suppressing lipid peroxidation at membranes and subsequent cell death by ferroptosis.

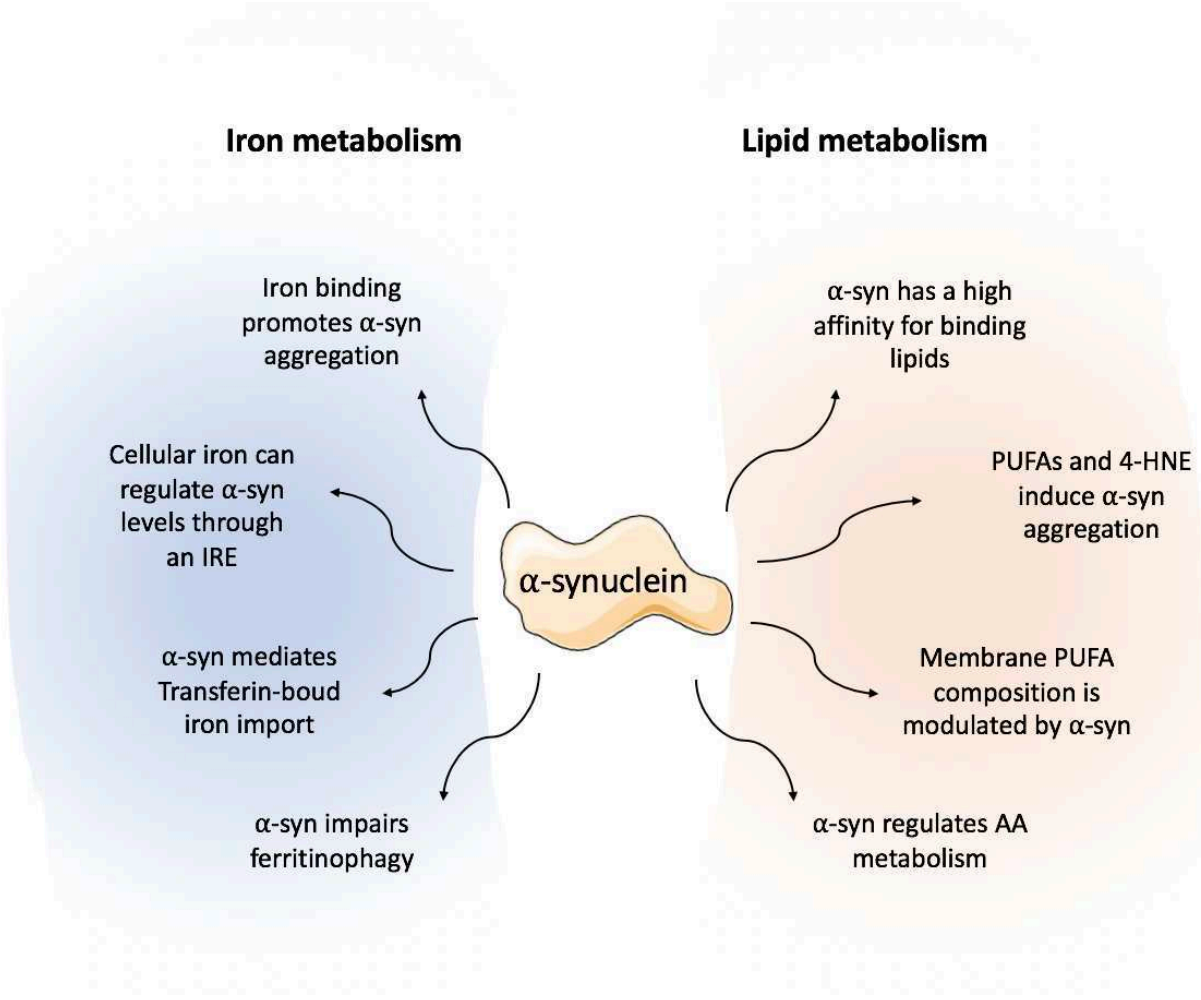

Figure 3: The iron and lipid metabolism interplay with α-synuclein.

Increasing studies are linking α-syn to metabolism of iron and lipid, in particular PUFAs, suggesting a possible role of α-syn in ferroptosis.

Table 1: Features of Parkinson's Disease Pathology consistent with Ferroptosis

A list of known Parkinson's disease pathology hallmarks common to Ferroptosis that support the role of this novel cell death in the disease pathogenesis.

Feature	Comment	References
Decreased XcT- and GSH	DNA methylation analysis revealed downregulation of SLC7A11 gene. Measures in post mortem brain regions from PD revealed reduction in GSH levels in the SN of PD patients	(Vallerga et al, 2020 ; Pearce et al, 1997; Sian et al, 1994; Sofic et al, 1992)
Altered brain PUFA composition	Post-mortem analyses reveal a reduction of PUFAs in the SN of PD patients	(Dexter et al, 1989)
Elevated lipid peroxidation products	HNE and MDA are elevated in the SN of PD brains and associated with iron accumulation. HNE is equally elevated in the CSF of PD patients	(Dexter et al, 1989; Domenico et al, 2017; de Farias et al, 2016)
Decrease GPX4 in Substantia Nigra	In post mortem analysis: reduced GXP4 levels in the SN in PD brains, but increased relative to cell density of surviving neurons	(Bellinger et al, 2011)
Increased iron in SN	MRI and QSM analyses confirm iron accumulation in the SNpc in PD patients. Iron concentrations correlate with disease severity	(Dexter et al, 1987, 1988; Hirsch et al, 1991; Hopes et al., 2016; Wang et al., 2017)
Clinical benefits of Iron Chelation	A double-blind, randomized, placebo-controlled clinical trial of early-stage PD showed a decreased motor handicap progression and reduced iron deposits in the SN of PD patients taking DFP. An ongoing phase 3 multicentre clinical trial will assess DFP as a disease modifying treatment	(Devos et al, 2014)
Decreased CoQ10 levels	Levels of the antioxidant CoQ10 are reduced in PD animal models and PD patients	(Battino et al., 1996; Mischley et al., 2012)
DJ-1 depletion	DJ-1 loss of function mutations are associated with early-onset PD. DJ-1 is a negative ferroptosis regulator as it maintains the cysteine and GSH biosynthesis through the transsulfuration pathway	(Burbulla et al, 2017; Cao et al, 2020)

REFERENCES

1. Agid, Y., Chase, T. & Marsden, D. Adverse reactions to levodopa: drug toxicity or progression of disease? *The Lancet* **351**, 851–852 (1998).

2. Agid, Y., Olanow, C. & Mizuno, Y. Levodopa: why the controversy? *The Lancet* **360**, 575 (2002).

3. Tran, T. N., Vo, T. N. N., Frei, K. & Truong, D. D. Levodopa-induced dyskinesia: clinical features, incidence, and risk factors. *J. Neural Transm. Vienna Austria 1996* **125**, 1109–1117 (2018).

4. Schneider, S. A. & Obeso, J. A. Clinical and pathological features of Parkinson's disease. *Curr. Top. Behav. Neurosci.* **22**, 205–220 (2015).

5. Shahmoradian, S. H. *et al.* Lewy pathology in Parkinson's disease consists of crowded organelles and lipid membranes. *Nat. Neurosci.* **22**, 1099–1109 (2019).

6. Dexter, D. T. *et al.* Increased Nigral Iron Content and Alterations in Other Metal Ions Occurring in Brain in Parkinson's Disease. *J. Neurochem.* **52**, 1830–1836 (1989).

7. Spillantini, M. G. *et al.* Alpha-synuclein in Lewy bodies. *Nature* **388**, 839–840 (1997).

8. Connolly, B. S. & Lang, A. E. Pharmacological treatment of Parkinson disease: a review. *JAMA* **311**, 1670–1683 (2014).

9. Yahr, M. D., Duvoisin, R. C., Schear, M. J., Barrett, R. E. & Hoehn, M. M. Treatment of parkinsonism with levodopa. *Arch. Neurol.* **21**, 343–354 (1969).

10. Nagatsua, T. & Sawadab, M. L-dopa therapy for Parkinson's disease: past, present, and future. *Parkinsonism Relat. Disord.* **15 Suppl 1**, S3-8 (2009).

11. Fahn, S. *et al.* Levodopa and the progression of Parkinson's disease. *N. Engl. J. Med.* **351**, 2498–2508 (2004).

12. Verschuur, C. V. M. *et al.* Randomized Delayed-Start Trial of Levodopa in Parkinson's Disease. *N. Engl. J. Med.* **380**, 315–324 (2019).

13. Fahn, S. & Parkinson Study Group. Does levodopa slow or hasten the rate of progression of Parkinson's disease? *J. Neurol.* **252 Suppl 4**, IV37–IV42 (2005).

14. Olanow, C. W. *et al.* A randomized, double-blind, placebo-controlled, delayed start study to assess rasagiline as a disease modifying therapy in Parkinson's disease (the ADAGIO study): rationale, design, and baseline characteristics. *Mov. Disord. Off. J. Mov. Disord. Soc.* **23**, 2194–2201 (2008).

15. Olanow, C. W. *et al.* A double-blind, delayed-start trial of rasagiline in Parkinson's disease. *N. Engl. J. Med.* **361**, 1268–1278 (2009).

16. Rascol, O. *et al.* Long-term effects of rasagiline and the natural history of treated Parkinson's disease. *Mov. Disord. Off. J. Mov. Disord. Soc.* **31**, 1489–1496 (2016).

17. Kulisevsky, J., Oliveira, L. & Fox, S. H. Update in therapeutic strategies for Parkinson's disease. *Curr. Opin. Neurol.* **31**, 439–447 (2018).

18. Guiney, S. J., Adlard, P. A., Bush, A. I., Finkelstein, D. I. & Ayton, S. Ferroptosis and cell death mechanisms in Parkinson's disease. *Neurochem. Int.* **104**, 34–48 (2017).

19. Li, A. E. *et al.* A role for reactive oxygen species in endothelial cell anoikis. *Circ. Res.* **85**, 304–310 (1999).

20. Saha, A. R. *et al.* Induction of neuronal death by alpha-synuclein. *Eur. J. Neurosci.* **12**, 3073–3077 (2000).

21. Chu, Y., Dodiya, H., Aebischer, P., Olanow, C. W. & Kordower, J. H. Alterations in lysosomal and proteasomal markers in Parkinson's disease: Relationship to alpha-synuclein inclusions. *Neurobiol. Dis.* **35**, 385–398 (2009).

22. Dehay, B. *et al.* Pathogenic lysosomal depletion in Parkinson's disease. *J. Neurosci. Off. J. Soc. Neurosci.* **30**, 12535–12544 (2010).

23. Mogi, M. *et al.* Tumor necrosis factor-α (TNF-α) increases both in the brain and in the cerebrospinal fluid from parkinsonian patients. *Neurosci. Lett.* **165**, 208–210 (1994).

24. Wu, J.-R. *et al.* Necrostatin-1 protection of dopaminergic neurons. *Neural Regen. Res.* **10**, 1120–1124 (2015).

25. Mandir, A. S. *et al.* Poly(ADP-ribose) polymerase activation mediates 1-methyl-4-phenyl-1,2,3,6-tetrahydropyridine (MPTP)-induced parkinsonism. *Proc. Natl. Acad. Sci. U. S. A.* **96**, 5774–5779 (1999).

26. Outeiro, T. F. *et al.* Pharmacological inhibition of PARP-1 reduces alpha-synuclein- and MPP+-induced cytotoxicity in Parkinson's disease in vitro models. *Biochem. Biophys. Res. Commun.* **357**, 596–602 (2007).

27. Koprich, J. B., Reske-Nielsen, C., Mithal, P. & Isacson, O. Neuroinflammation mediated by IL-1beta increases susceptibility of dopamine neurons to degeneration in an animal model of Parkinson's disease. *J. Neuroinflammation* **5**, 8 (2008).

28. Dixon, S. J. *et al.* Ferroptosis: An Iron-Dependent Form of Non-Apoptotic Cell Death. *Cell* **149**, 1060–1072 (2012).

29. Stockwell, B. R. *et al.* Ferroptosis: a regulated cell death nexus linking metabolism, redox biology, and disease. *Cell* **171**, 273–285 (2017).

30. Dexter, D. T. *et al.* INCREASED NIGRAL IRON CONTENT IN POSTMORTEM PARKINSONIAN BRAIN. *The Lancet* **330**, 1219–1220 (1987).

31. Hirsch, E. C., Brandel, J.-P., Galle, P., Javoy-Agid, F. & Agid, Y. Iron and Aluminum Increase in the Substantia Nigra of Patients with Parkinson's Disease: An X-Ray Microanalysis. *J. Neurochem.* **56**, 446–451 (1991).

32. Pyatigorskaya, N. *et al.* High nigral iron deposition in LRRK2 and Parkin mutation carriers using R2* relaxometry. *Mov. Disord. Off. J. Mov. Disord. Soc.* **30**, 1077–1084 (2015).

33. Ayton, S. *et al.* Parkinson's disease iron deposition caused by nitric oxide-induced loss of β-amyloid precursor protein. *J. Neurosci. Off. J. Soc. Neurosci.* **35**, 3591–3597 (2015).

34. Dexter, D. *et al.* Lipid peroxidation as cause of nigral cell death in Parkinson's disease. *Lancet Lond. Engl.* **2**, 639–640 (1986).

35. Dexter, D. T. *et al.* Basal lipid peroxidation in substantia nigra is increased in Parkinson's disease. *J. Neurochem.* **52**, 381–389 (1989).

36. de Farias, C. C. *et al.* Highly specific changes in antioxidant levels and lipid peroxidation in Parkinson's disease and its progression: Disease and staging biomarkers and new drug targets. *Neurosci. Lett.* **617**, 66–71 (2016).

37. Sofic, E., Lange, K. W., Jellinger, K. & Riederer, P. Reduced and oxidized glutathione in the substantia nigra of patients with Parkinson's disease. *Neurosci. Lett.* **142**, 128–130 (1992).

38. Sian, J. *et al.* Alterations in glutathione levels in Parkinson's disease and other neurodegenerative disorders affecting basal ganglia. *Ann. Neurol.* **36**, 348–355 (1994).

39. Pearce, R. K. B., Owen, A., Daniel, S., Jenner, P. & Marsden, C. D. Alterations in the distribution of glutathione in the substantia nigra in Parkinson's disease. *J. Neural Transm.* **104**, 661–677 (1997).

40. Li, Y., Maher, P. & Schubert, D. A Role for 12-lipoxygenase in Nerve Cell Death Caused by Glutathione Depletion. *Neuron* **19**, 453–463 (1997).

41. Vallerga, C. L. *et al.* Analysis of DNA methylation associates the cystine–glutamate antiporter SLC7A11 with risk of Parkinson's disease. *Nat. Commun.* **11**, 1238 (2020).

42. Bonifati, V. *et al.* Mutations in the DJ-1 gene associated with autosomal recessive early-onset parkinsonism. *Science* **299**, 256–259 (2003).

43. Cao, J. *et al.* DJ-1 suppresses ferroptosis through preserving the activity of S-adenosyl homocysteine hydrolase. *Nat. Commun.* **11**, 1251 (2020).

44. Battino, M., Littarru, G. P., Gorini, A. & Villa, R. F. Coenzyme Q, peroxidation and cytochrome oxidase features after Parkinson's-like disease by MPTP toxicity in intra-synaptic and non-synaptic mitochondria fromMacaca Fascicularis cerebral cortex and hippocampus: action of dihydroergocriptine. *Neurochem. Res.* **21**, 1505–1514 (1996).

45. Mischley, L. K., Allen, J. & Bradley, R. Coenzyme Q10 Deficiency in Patients with Parkinson's Disease. *J. Neurol. Sci.* **318**, 72–75 (2012).

46. Bersuker, K. *et al.* The CoQ oxidoreductase FSP1 acts parallel to GPX4 to inhibit ferroptosis. *Nature* **575**, 688–692 (2019).

47. Friedmann Angeli, J. P. *et al.* Inactivation of the ferroptosis regulator Gpx4 triggers acute renal failure in mice. *Nat. Cell Biol.* **16**, 1180–1191 (2014).

48. Skouta, R. *et al.* Ferrostatins inhibit oxidative lipid damage and cell death in diverse disease models. *J. Am. Chem. Soc.* **136**, 4551–4556 (2014).

49. Forcina, G. C. & Dixon, S. J. GPX4 at the Crossroads of Lipid Homeostasis and Ferroptosis. *PROTEOMICS* **19**, 1800311 (2019).

50. Cozza, G. *et al.* Glutathione peroxidase 4-catalyzed reduction of lipid hydroperoxides in membranes: The polar head of membrane phospholipids binds the enzyme and addresses the fatty acid hydroperoxide group toward the redox center. *Free Radic. Biol. Med.* **112**, 1–11 (2017).

51. Seiler, A. *et al.* Glutathione peroxidase 4 senses and translates oxidative stress into 12/15-lipoxygenase dependent- and AIF-mediated cell death. *Cell Metab.* **8**, 237–248 (2008).

52. Yang, W. S. *et al.* Regulation of ferroptotic cancer cell death by GPX4. *Cell* **156**, 317–331 (2014).

53. Oestreicher, J. & Morgan, B. Glutathione: subcellular distribution and membrane transport 1. *Biochem. Cell Biol. Biochim. Biol. Cell.* **97**, 270–289 (2019).

54. Doll, S. *et al.* FSP1 is a glutathione-independent ferroptosis suppressor. *Nature* **575**, 693–698 (2019).

55. Gao, M., Monian, P., Quadri, N., Ramasamy, R. & Jiang, X. Glutaminolysis and Transferrin Regulate Ferroptosis. *Mol. Cell* **59**, 298–308 (2015).

56. Do Van, B. *et al.* Ferroptosis, a newly characterized form of cell death in Parkinson's disease that is regulated by PKC. *Neurobiol. Dis.* **94**, 169–178 (2016).

57. Dixon, S. J. & Stockwell, B. R. The role of iron and reactive oxygen species in cell death. *Nat. Chem. Biol.* **10**, 9–17 (2014).

58. Yang, W. S. *et al.* Peroxidation of polyunsaturated fatty acids by lipoxygenases drives ferroptosis. *Proc. Natl. Acad. Sci. U. S. A.* **113**, E4966-4975 (2016).

59. Wenzel, S. E. *et al.* PEBP1 Wardens Ferroptosis by Enabling Lipoxygenase Generation of Lipid Death Signals. *Cell* **171**, 628-641.e26 (2017).

60. Karuppagounder, S. S. *et al.* Therapeutic targeting of oxygen-sensing prolyl hydroxylases abrogates ATF4-dependent neuronal death and improves outcomes after brain hemorrhage in several rodent models. *Sci. Transl. Med.* **8**, 328ra29 (2016).

61. Belaidi, A. A. & Bush, A. I. Iron neurochemistry in Alzheimer's disease and Parkinson's disease: targets for therapeutics. *J. Neurochem.* **139**, 179–197 (2016).

62. Knutson, M. D. Steap Proteins: Implications for Iron and Copper Metabolism. *Nutr. Rev.* **65**, 335–340 (2007).

63. Hare, D., Ayton, S., Bush, A. & Lei, P. A delicate balance: Iron metabolism and diseases of the brain. *Front. Aging Neurosci.* **5**, 34 (2013).

64. McCarthy, R. C., Park, Y.-H. & Kosman, D. J. sAPP modulates iron efflux from brain microvascular endothelial cells by stabilizing the ferrous iron exporter ferroportin. *EMBO Rep.* **15**, 809–815 (2014).

65. Lei, P. *et al.* Tau deficiency induces parkinsonism with dementia by impairing APP-mediated iron export. *Nat. Med.* **18**, 291–295 (2012).

66. Tsatsanis, A., Dickens, S., Kwok, J. C. F., Wong, B. X. & Duce, J. A. Post Translational Modulation of β-Amyloid Precursor Protein Trafficking to the Cell Surface Alters Neuronal Iron Homeostasis. *Neurochem. Res.* **44**, 1367–1374 (2019).

67. Belaidi, A. A. *et al.* Marked Age-Related Changes in Brain Iron Homeostasis in Amyloid Protein Precursor Knockout Mice. *Neurother. J. Am. Soc. Exp. Neurother.* **15**, 1055–1062 (2018).

68. Shintoku, R. *et al.* Lipoxygenase-mediated generation of lipid peroxides enhances ferroptosis induced by erastin and RSL3. *Cancer Sci.* **108**, 2187–2194 (2017).

69. Shah, R., Shchepinov, M. S. & Pratt, D. A. Resolving the Role of Lipoxygenases in the Initiation and Execution of Ferroptosis. *ACS Cent. Sci.* **4**, 387–396 (2018).

70. Magtanong, L. *et al.* Exogenous Monounsaturated Fatty Acids Promote a Ferroptosis-Resistant Cell State. *Cell Chem. Biol.* **26**, 420-432.e9 (2019).

71. Doll, S. *et al.* ACSL4 dictates ferroptosis sensitivity by shaping cellular lipid composition. *Nat. Chem. Biol.* **13**, 91–98 (2017).

72. Yan, S. *et al.* Long-chain acyl-CoA synthetase in fatty acid metabolism involved in liver and other diseases: An update. *World J. Gastroenterol. WJG* **21**, 3492–3498 (2015).

73. Dixon, S. J. *et al.* Human Haploid Cell Genetics Reveals Roles for Lipid Metabolism Genes in Nonapoptotic Cell Death. *ACS Chem. Biol.* **10**, 1604–1609 (2015).

74. Angeli, J. P. F. *et al.* Inactivation of the ferroptosis regulator Gpx4 triggers acute renal failure in mice. *Nat. Cell Biol.* **16**, 1180–1191 (2014).

75. Linkermann, A. *et al.* Synchronized renal tubular cell death involves ferroptosis. *Proc. Natl. Acad. Sci.* **111**, 16836–16841 (2014).

76. Martin-Sanchez, D. *et al.* Ferroptosis, but Not Necroptosis, Is Important in Nephrotoxic Folic Acid–Induced AKI. *J. Am. Soc. Nephrol.* **28**, 218–229 (2017).

77. Baba, Y. *et al.* Protective effects of the mechanistic target of rapamycin against excess iron and ferroptosis in cardiomyocytes. *Am. J. Physiol. - Heart Circ. Physiol.* **314**, H659–H668 (2018).

78. Feng, Y., Madungwe, N. B., Imam Aliagan, A. D., Tombo, N. & Bopassa, J. C. Liproxstatin-1 protects the mouse myocardium against ischemia/reperfusion injury by decreasing VDAC1 levels and restoring GPX4 levels. *Biochem. Biophys. Res. Commun.* **520**, 606–611 (2019).

79. Li, Y. *et al.* Ischemia-induced ACSL4 activation contributes to ferroptosis-mediated tissue injury in intestinal ischemia/reperfusion. *Cell Death Differ.* **26**, 2284–2299 (2019).

80. Tuo, Q.-Z. *et al.* Tau-mediated iron export prevents ferroptotic damage after ischemic stroke. *Mol. Psychiatry* **22**, 1520–1530 (2017).

81. Guan, X. *et al.* The neuroprotective effects of carvacrol on ischemia/reperfusion-induced hippocampal neuronal impairment by ferroptosis mitigation. *Life Sci.* **235**, 116795 (2019).

82. Alim, I. *et al.* Selenium Drives a Transcriptional Adaptive Program to Block Ferroptosis and Treat Stroke. *Cell* **177**, 1262-1279.e25 (2019).

83. Zille, M. *et al.* Neuronal Death After Hemorrhagic Stroke In Vitro and In Vivo Shares Features of Ferroptosis and Necroptosis. *Stroke* **48**, 1033–1043 (2017).

84. Karuppagounder, S. S. *et al.* N-acetylcysteine targets 5 lipoxygenase-derived, toxic lipids and can synergize with prostaglandin E2 to inhibit ferroptosis and improve outcomes following hemorrhagic stroke in mice. *Ann. Neurol.* **84**, 854–872 (2018).

85. Chen, B. *et al.* Inhibition of neuronal ferroptosis in the acute phase of intracerebral hemorrhage shows long-term cerebroprotective effects. *Brain Res. Bull.* **153**, 122–132 (2019).

86. Zhang, Z. *et al.* Glutathione peroxidase 4 participates in secondary brain injury through mediating ferroptosis in a rat model of intracerebral hemorrhage. *Brain Res.* **1701**, 112–125 (2018).

87. Ayton, S. & Bush, A. I. L-8 - Iron and ferroptosis in the pathogenesis of Alzheimer´s disease. *Free Radic. Biol. Med.* **120**, S8 (2018).

88. Devos, D. *et al.* A ferroptosis–based panel of prognostic biomarkers for Amyotrophic Lateral Sclerosis. *Sci. Rep.* **9**, 1–6 (2019).

89. Ferreira, A., Neves, P. & Gozzelino, R. Multilevel Impacts of Iron in the Brain: The Cross Talk between Neurophysiological Mechanisms, Cognition, and Social Behavior. *Pharm. Basel Switz.* **12**, (2019).

90. Ward, R. J., Zucca, F. A., Duyn, J. H., Crichton, R. R. & Zecca, L. The role of iron in brain ageing and neurodegenerative disorders. *Lancet Neurol.* **13**, 1045–1060 (2014).

91. Haacke, E. M. *et al.* Imaging iron stores in the brain using magnetic resonance imaging. *Magn. Reson. Imaging* **23**, 1–25 (2005).

92. Davies, K. M. *et al.* Comparative Study of Metal Quantification in Neurological Tissue Using Laser Ablation-Inductively Coupled Plasma-Mass Spectrometry Imaging and X-ray Fluorescence Microscopy. *Anal. Chem.* **87**, 6639–6645 (2015).

93. Hopes, L. *et al.* Magnetic Resonance Imaging Features of the Nigrostriatal System: Biomarkers of Parkinson's Disease Stages? *PLOS ONE* **11**, e0147947 (2016).

94. Wang, Y. *et al.* Clinical Quantitative Susceptibility Mapping (QSM) – Biometal Imaging and its Emerging Roles in Patient Care. *J. Magn. Reson. Imaging JMRI* **46**, 951–971 (2017).

95. Kaur, D. *et al.* Genetic or pharmacological iron chelation prevents MPTP-induced neurotoxicity in vivo: a novel therapy for Parkinson's disease. *Neuron* **37**, 899–909 (2003).

96. Ayton, S. *et al.* Ceruloplasmin dysfunction and therapeutic potential for Parkinson disease. *Ann. Neurol.* **73**, 554–559 (2013).

97. Devos, D. *et al.* Targeting Chelatable Iron as a Therapeutic Modality in Parkinson's Disease. *Antioxid. Redox Signal.* **21**, 195–210 (2014).

98. Double, K. L., Gerlach, M., Youdim, M. B. & Riederer, P. Impaired iron homeostasis in Parkinson's disease. *J. Neural Transm. Suppl.* 37–58 (2000) doi:10.1007/978-3-7091-6301-6_3.

99. Masaldan, S., Bush, A. I., Devos, D., Rolland, A. S. & Moreau, C. Striking while the iron is hot: Iron metabolism and ferroptosis in neurodegeneration. *Free Radic. Biol. Med.* **133**, 221–233 (2019).

100. Borie, C. *et al.* Association study between iron-related genes polymorphisms and Parkinson's disease. *J. Neurol.* **249**, 801–804 (2002).

101. Rhodes, S. L. *et al.* Pooled Analysis of Iron-related Genes in Parkinson's Disease: Association with Transferrin. *Neurobiol. Dis.* **62**, 172–178 (2014).

102. Salazar, J. *et al.* Divalent metal transporter 1 (DMT1) contributes to neurodegeneration in animal models of Parkinson's disease. *Proc. Natl. Acad. Sci. U. S. A.* **105**, 18578–18583 (2008).

103. Bi, M., Du, X., Jiao, Q., Liu, Z. & Jiang, H. α-Synuclein regulates iron homeostasis via preventing parkin-mediated DMT1 ubiquitylation in Parkinson's disease models. *ACS Chem. Neurosci.* (2020) doi:10.1021/acschemneuro.0c00196.

104. Dexter, D. T. *et al.* Decreased Ferritin Levels in Brain in Parkinson's Disease. *J. Neurochem.* **55**, 16–20 (1990).

105. Song, N., Wang, J., Jiang, H. & Xie, J. Ferroportin 1 but not hephaestin contributes to iron accumulation in a cell model of Parkinson's disease. *Free Radic. Biol. Med.* **48**, 332–341 (2010).

106. Schulte, E. C. *et al.* Rare variants in β- Amyloid precursor protein (APP) and Parkinson's disease. *Eur. J. Hum. Genet.* **23**, 1328–1333 (2015).

107. Bharucha, K. J., Friedman, J. K., Vincent, A. S. & Ross, E. D. Lower serum ceruloplasmin levels correlate with younger age of onset in Parkinson's disease. *J. Neurol.* **255**, 1957–1962 (2008).

108. Zhao, X. *et al.* Ceruloplasmin in Parkinson's disease and the nonmotor symptoms. *Brain Behav.* **8**, (2018).

109. Costello, D., Walsh, S., Harrington, H. & Walsh, C. Concurrent hereditary haemochromatosis and idiopathic Parkinson's disease: a case report series. *J. Neurol. Neurosurg. Psychiatry* **75**, 631–633 (2004).

110. Miyajima, H., Takahashi, Y. & Kono, S. Aceruloplasminemia, an inherited disorder of iron metabolism. *Biometals Int. J. Role Met. Ions Biol. Biochem. Med.* **16**, 205–213 (2003).

111. Devos, D. *et al.* Conservative iron chelation for neurodegenerative diseases such as Parkinson's disease and amyotrophic lateral sclerosis. *J. Neural Transm.* (2020) doi:10.1007/s00702-019-02138-1.

112. Moreau, C. *et al.* Iron as a therapeutic target for Parkinson's disease. *Mov. Disord. Off. J. Mov. Disord. Soc.* **33**, 568–574 (2018).

113. Martin-Bastida, A. *et al.* Brain iron chelation by deferiprone in a phase 2 randomised double-blinded placebo controlled clinical trial in Parkinson's disease. *Sci. Rep.* **7**, (2017).

114. Blesa, J., Trigo-Damas, I., Quiroga-Varela, A. & Jackson-Lewis, V. R. Oxidative stress and Parkinson's disease. *Front. Neuroanat.* **9**, (2015).

115. Kim, G. H., Kim, J. E., Rhie, S. J. & Yoon, S. The Role of Oxidative Stress in Neurodegenerative Diseases. *Exp. Neurobiol.* **24**, 325–340 (2015).

116. Cadenas, E. & Davies, K. J. A. Mitochondrial free radical generation, oxidative stress, and aging11This article is dedicated to the memory of our dear friend, colleague, and mentor Lars Ernster (1920–1998), in gratitude for all he gave to us. *Free Radic. Biol. Med.* **29**, 222–230 (2000).

117. Mancuso, M., Coppede, F., Migliore, L., Siciliano, G. & Murri, L. Mitochondrial dysfunction, oxidative stress and neurodegeneration. *J. Alzheimers Dis.* **10**, 59–73 (2006).

118. Zorov, D. B., Juhaszova, M. & Sollott, S. J. Mitochondrial Reactive Oxygen Species (ROS) and ROS-Induced ROS Release. *Physiol. Rev.* **94**, 909–950 (2014).

119. Dringen, R., Gutterer, J. M. & Hirrlinger, J. Glutathione metabolism in brain. *Eur. J. Biochem.* **267**, 4912–4916 (2000).

120. Gandhi, S. & Abramov, A. Y. Mechanism of Oxidative Stress in Neurodegeneration. *Oxidative Medicine and Cellular Longevity* https://www.hindawi.com/journals/omcl/2012/428010/ (2012) doi:10.1155/2012/428010.

121. Hider, R. C. & Kong, X. L. Glutathione: a key component of the cytoplasmic labile iron pool. *BioMetals* **24**, 1179–1187 (2011).

122. Burbulla, L. F. *et al.* Dopamine oxidation mediates mitochondrial and lysosomal dysfunction in Parkinson's disease. *Science* **357**, 1255–1261 (2017).

123. Blackinton, J. *et al.* Post-transcriptional regulation of mRNA associated with DJ-1 in sporadic Parkinson disease. *Neurosci. Lett.* **452**, 8–11 (2009).

124. Bellinger, F. P. *et al.* Glutathione Peroxidase 4 is associated with Neuromelanin in Substantia Nigra and Dystrophic Axons in Putamen of Parkinson's brain. *Mol. Neurodegener.* **6**, 8 (2011).

125. Floberg, J. M. *et al.* Altering cellular reducing potential changes 64Cu-ATSM signal with or without hypoxia. *J. Nucl. Med.* jnumed.119.230805 (2019) doi:10.2967/jnumed.119.230805.

126. Hung, L. W. *et al.* The hypoxia imaging agent CuII(atsm) is neuroprotective and improves motor and cognitive functions in multiple animal models of Parkinson's disease. *J. Exp. Med.* **209**, 837–854 (2012).

127. Southon, A. A. *et al.* CuII (atsm) inhibits ferroptosis: implications for treatment of neurodegenerative disease. *Br. J. Pharmacol.* (2019) doi:10.1111/bph.14881.

128. Ikawa, M. *et al.* Evaluation of striatal oxidative stress in patients with Parkinson's disease using [62Cu]ATSM PET. *Nucl. Med. Biol.* **38**, 945–951 (2011).

129. Etminan, M., Gill, S. S. & Samii, A. Intake of vitamin E, vitamin C, and carotenoids and the risk of Parkinson's disease: a meta-analysis. *Lancet Neurol.* **4**, 362–365 (2005).

130. Knekt, P. *et al.* Serum vitamin D and the risk of Parkinson's disease. *Arch. Neurol.* **67**, 808–811 (2010).

131. Spindler, M., Beal, M. F. & Henchcliffe, C. Coenzyme Q10 effects in neurodegenerative disease. *Neuropsychiatr. Dis. Treat.* **5**, 597–610 (2009).

132. Beal, M. F. *et al.* A Randomized Clinical Trial of High-Dosage Coenzyme Q10 in Early Parkinson Disease: No Evidence of Benefit. *JAMA Neurol.* **71**, 543–552 (2014).

133. Yang, W. S. & Stockwell, B. R. Ferroptosis: Death by Lipid Peroxidation. *Trends Cell Biol.* **26**, 165–176 (2016).

134. Kagan, V. E. *et al.* Oxidized arachidonic and adrenic PEs navigate cells to ferroptosis. *Nat. Chem. Biol.* **13**, 81–90 (2017).

135. Ayala, A., Muñoz, M. F. & Argüelles, S. Lipid peroxidation: production, metabolism, and signaling mechanisms of malondialdehyde and 4-hydroxy-2-nonenal. *Oxid. Med. Cell. Longev.* **2014**, 360438 (2014).

136. Girotti, A. W. Lipid hydroperoxide generation, turnover, and effector action in biological systems. *J. Lipid Res.* **39**, 1529–1542 (1998).

137. Larrieu, T. & Layé, S. Food for Mood: Relevance of Nutritional Omega-3 Fatty Acids for Depression and Anxiety. *Front. Physiol.* **9**, (2018).

138. Sharon, R., Bar-Joseph, I., Mirick, G. E., Serhan, C. N. & Selkoe, D. J. Altered Fatty Acid Composition of Dopaminergic Neurons Expressing α-Synuclein and Human Brains with α-Synucleinopathies. *J. Biol. Chem.* **278**, 49874–49881 (2003).

139. Di Domenico, F., Tramutola, A. & Butterfield, D. A. Role of 4-hydroxy-2-nonenal (HNE) in the pathogenesis of alzheimer disease and other selected age-related neurodegenerative disorders. *Free Radic. Biol. Med.* **111**, 253–261 (2017).

140. Selley, M. L. (E)-4-Hydroxy-2-Nonenal May be Involved in the Pathogenesis of Parkinson's Disease. *Free Radic. Biol. Med.* **25**, 169–174 (1998).

141. Shchepinov, M. S. *et al.* Isotopic reinforcement of essential polyunsaturated fatty acids diminishes nigrostriatal degeneration in a mouse model of Parkinson's disease. *Toxicol. Lett.* **207**, 97–103 (2011).

142. Kinghorn, K. J. & Castillo-Quan, J. I. Mitochondrial dysfunction and defects in lipid homeostasis as therapeutic targets in neurodegeneration with brain iron accumulation. *Rare Dis.* **4**, (2016).

143. Gregory, A. *et al.* Neurodegeneration associated with genetic defects in phospholipase A2. *Neurology* **71**, 1402–1409 (2008).

144. Kinghorn, K. J. *et al.* Loss of *PLA2G6* leads to elevated mitochondrial lipid peroxidation and mitochondrial dysfunction. *Brain* **138**, 1801–1816 (2015).

145. Sun, X. *et al.* Activation of the p62-Keap1-NRF2 pathway protects against ferroptosis in hepatocellular carcinoma cells. *Hepatol. Baltim. Md* **63**, 173–184 (2016).

146. Liu, N., Lin, X. & Huang, C. Activation of the reverse transsulfuration pathway through NRF2/CBS confers erastin-induced ferroptosis resistance. *Br. J. Cancer* **122**, 279–292 (2020).

147. Kovac, S. *et al.* Nrf2 regulates ROS production by mitochondria and NADPH oxidase. *Biochim. Biophys. Acta* **1850**, 794–801 (2015).

148. Osburn, W. O. *et al.* Nrf2 Regulates an Adaptive Response Protecting Against Oxidative Damage Following Diquat-Mediated Formation of Superoxide Anion. *Arch. Biochem. Biophys.* **454**, 7–15 (2006).

149. Kerins, M. J. & Ooi, A. The Roles of NRF2 in Modulating Cellular Iron Homeostasis. *Antioxid. Redox Signal.* **29**, 1756–1773 (2018).

150. Song, X. & Long, D. Nrf2 and Ferroptosis: A New Research Direction for Neurodegenerative Diseases. *Front. Neurosci.* **14**, (2020).

151. Suh, J. H. *et al.* Decline in transcriptional activity of Nrf2 causes age-related loss of glutathione synthesis, which is reversible with lipoic acid. *Proc. Natl. Acad. Sci.* **101**, 3381–3386 (2004).

152. Todorovic, M., Wood, S. A. & Mellick, G. D. Nrf2: a modulator of Parkinson's disease? *J. Neural Transm. Vienna Austria 1996* **123**, 611–619 (2016).

153. Petrillo, S. *et al.* Systemic Activation of Nrf2 Pathway in Parkinson's Disease. *Mov. Disord.* **35**, 180–184 (2020).

154. Ramsey, C. P. *et al.* Expression of Nrf2 in Neurodegenerative Diseases. *J. Neuropathol. Exp. Neurol.* **66**, 75–85 (2007).

155. Xiao, H. *et al.* Deprenyl prevents MPP(+)-induced oxidative damage in PC12 cells by the upregulation of Nrf2-mediated NQO1 expression through the activation of PI3K/Akt and Erk. *Toxicology* **290**, 286–294 (2011).

156. Barone, M. C., Sykiotis, G. P. & Bohmann, D. Genetic activation of Nrf2 signaling is sufficient to ameliorate neurodegenerative phenotypes in a Drosophila model of Parkinson's disease. *Dis. Model. Mech.* **4**, 701–707 (2011).

157. Zhang, J. *et al.* Discovery of a novel Nrf2 inhibitor that induces apoptosis of human acute myeloid leukemia cells. *Oncotarget* **8**, 7625–7636 (2016).

158. Cristóvão, A. C., Choi, D.-H., Baltazar, G., Beal, M. F. & Kim, Y.-S. The role of NADPH oxidase 1-derived reactive oxygen species in paraquat-mediated dopaminergic cell death. *Antioxid. Redox Signal.* **11**, 2105–2118 (2009).

159. Choi, D.-H. *et al.* NADPH oxidase 1-mediated oxidative stress leads to dopamine neuron death in Parkinson's disease. *Antioxid. Redox Signal.* **16**, 1033–1045 (2012).

160. Zawada, W. M. *et al.* Loss of angiotensin II receptor expression in dopamine neurons in Parkinson's disease correlates with pathological progression and is accompanied by increases in Nox4- and 8-OH guanosine-related nucleic acid oxidation and caspase-3 activation. *Acta Neuropathol. Commun.* **3**, 9 (2015).

161. Yoshida, Y., Hayakawa, M., Habuchi, Y. & Niki, E. Evaluation of the dietary effects of coenzyme Q in vivo by the oxidative stress marker, hydroxyoctadecadienoic acid and its stereoisomer ratio. *Biochim. Biophys. Acta BBA - Gen. Subj.* **1760**, 1558–1568 (2006).

162. Cleren, C. *et al.* Therapeutic effects of coenzyme Q10 (CoQ10) and reduced CoQ10 in the MPTP model of Parkinsonism. *J. Neurochem.* **104**, 1613–1621 (2008).

163. Huntington Study Group. A randomized, placebo-controlled trial of coenzyme Q10 and remacemide in Huntington's disease. *Neurology* **57**, 397–404 (2001).

164. Bhagavan, H. N. & Chopra, R. K. Plasma coenzyme Q10 response to oral ingestion of coenzyme Q10 formulations. *Mitochondrion* **7 Suppl**, S78-88 (2007).

165. Friedmann Angeli, J. P. & Conrad, M. Selenium and GPX4, a vital symbiosis. *Free Radic. Biol. Med.* **127**, 153–159 (2018).

166. Cardoso, B. R., Hare, D. J., Bush, A. I. & Roberts, B. R. Glutathione peroxidase 4: a new player in neurodegeneration? *Mol. Psychiatry* **22**, 328–335 (2017).

167. Cadet, J. L. The potential use of vitamin E and selenium in Parkinsonism. *Med. Hypotheses* **20**, 87–94 (1986).

168. Ellwanger, J. H. *et al.* Selenium reduces bradykinesia and DNA damage in a rat model of Parkinson's disease. *Nutr. Burbank Los Angel. Cty. Calif* **31**, 359–365 (2015).

169. Khan, H. A. Selenium partially reverses the depletion of striatal dopamine and its metabolites in MPTP-treated C57BL mice. *Neurochem. Int.* **57**, 489–491 (2010).

170. Bellinger, F. P. *et al.* Changes in selenoprotein P in substantia nigra and putamen in Parkinson's disease. *J. Park. Dis.* **2**, 115–126 (2012).

171. Hemmati-Dinarvand, M., Taher-Aghdam, A.-A., Mota, A., Zununi Vahed, S. & Samadi, N. Dysregulation of serum NADPH oxidase1 and ferritin levels provides insights into diagnosis of Parkinson's disease. *Clin. Biochem.* **50**, 1087–1092 (2017).

172. Blauwendraat, C. *et al.* Parkinson's disease age at onset genome-wide association study: Defining heritability, genetic loci, and α-synuclein mechanisms. *Mov. Disord. Off. J. Mov. Disord. Soc.* **34**, 866–875 (2019).

173. Zhang, Y. *et al.* A Comprehensive Analysis of the Association Between SNCA Polymorphisms and the Risk of Parkinson's Disease. *Front. Mol. Neurosci.* **11**, (2018).

174. Angelova, P. R. *et al.* Alpha synuclein aggregation drives ferroptosis: an interplay of iron, calcium and lipid peroxidation. *Cell Death Differ.* 1–16 (2020) doi:10.1038/s41418-020-0542-z.

175. Duce, J. A. *et al.* Post translational changes to α-synuclein control iron and dopamine trafficking; a concept for neuron vulnerability in Parkinson's disease. *Mol. Neurodegener.* **12**, 45 (2017).

176. Chen, B. *et al.* Interactions between iron and α-synuclein pathology in Parkinson's disease. *Free Radic. Biol. Med.* **141**, 253–260 (2019).

177. Hashimoto, M. *et al.* Oxidative stress induces amyloid-like aggregate formation of NACP/alpha-synuclein in vitro. *Neuroreport* **10**, 717–721 (1999).

178. Paik, S. R., Shin, H. J. & Lee, J. H. Metal-catalyzed oxidation of alpha-synuclein in the presence of Copper(II) and hydrogen peroxide. *Arch. Biochem. Biophys.* **378**, 269–277 (2000).

179. Uversky, V. N., Li, J. & Fink, A. L. Metal-triggered structural transformations, aggregation, and fibrillation of human alpha-synuclein. A possible molecular NK between Parkinson's disease and heavy metal exposure. *J. Biol. Chem.* **276**, 44284–44296 (2001).

180. Peng, Y., Wang, C., Xu, H. H., Liu, Y.-N. & Zhou, F. Binding of alpha-synuclein with Fe(III) and with Fe(II) and biological implications of the resultant complexes. *J. Inorg. Biochem.* **104**, 365–370 (2010).

181. Golts, N. *et al.* Magnesium inhibits spontaneous and iron-induced aggregation of alpha-synuclein. *J. Biol. Chem.* **277**, 16116–16123 (2002).

182. Ostrerova-Golts, N. *et al.* The A53T alpha-synuclein mutation increases iron-dependent aggregation and toxicity. *J. Neurosci. Off. J. Soc. Neurosci.* **20**, 6048–6054 (2000).

183. Deas, E. *et al.* Alpha-Synuclein Oligomers Interact with Metal Ions to Induce Oxidative Stress and Neuronal Death in Parkinson's Disease. *Antioxid. Redox Signal.* **24**, 376–391 (2016).

184. Carboni, E. *et al.* Deferiprone Rescues Behavioral Deficits Induced by Mild Iron Exposure in a Mouse Model of Alpha-Synuclein Aggregation. *Neuromolecular Med.* **19**, 309–321 (2017).

185. Friedlich, A. L., Tanzi, R. E. & Rogers, J. T. The 5'-untranslated region of Parkinson's disease α -synuclein messengerRNA contains a predicted iron responsive element. *Mol. Psychiatry* **12**, 222–223 (2007).

186. Febbraro, F., Giorgi, M., Caldarola, S., Loreni, F. & Romero-Ramos, M. α-Synuclein expression is modulated at the translational level by iron: *NeuroReport* **23**, 576–580 (2012).

187. Davies, P., Moualla, D. & Brown, D. R. Alpha-synuclein is a cellular ferrireductase. *PloS One* **6**, e15814 (2011).

188. Baksi, S., Tripathi, A. K. & Singh, N. Alpha-synuclein modulates retinal iron homeostasis by facilitating the uptake of transferrin-bound iron: Implications for visual manifestations of Parkinson's disease. *Free Radic. Biol. Med.* **97**, 292–306 (2016).

189. Baksi, S. & Singh, N. α-Synuclein impairs ferritinophagy in the retinal pigment epithelium: Implications for retinal iron dyshomeostasis in Parkinson's disease. *Sci. Rep.* **7**, 12843 (2017).

190. Latunde-Dada, G. O. Ferroptosis: Role of lipid peroxidation, iron and ferritinophagy. *Biochim. Biophys. Acta Gen. Subj.* **1861**, 1893–1900 (2017).

191. Masaldan, S. *et al.* Iron accumulation in senescent cells is coupled with impaired ferritinophagy and inhibition of ferroptosis. *Redox Biol.* **14**, 100–115 (2018).

192. Ugalde, C. L., Lawson, V. A., Finkelstein, D. I. & Hill, A. F. The role of lipids in α-synuclein misfolding and neurotoxicity. *J. Biol. Chem.* **294**, 9016–9028 (2019).

193. Fecchio, C., Palazzi, L. & de Laureto, P. P. α-Synuclein and Polyunsaturated Fatty Acids: Molecular Basis of the Interaction and Implication in Neurodegeneration. *Mol. Basel Switz.* **23**, (2018).

194. De Franceschi, G. *et al.* Molecular insights into the interaction between alpha-synuclein and docosahexaenoic acid. *J. Mol. Biol.* **394**, 94–107 (2009).

195. Broersen, K., van den Brink, D., Fraser, G., Goedert, M. & Davletov, B. Alpha-synuclein adopts an alpha-helical conformation in the presence of polyunsaturated fatty acids to hinder micelle formation. *Biochemistry* **45**, 15610–15616 (2006).

196. Sharon, R. *et al.* alpha-Synuclein occurs in lipid-rich high molecular weight complexes, binds fatty acids, and shows homology to the fatty acid-binding proteins. *Proc. Natl. Acad. Sci. U. S. A.* **98**, 9110–9115 (2001).

197. Lücke, C., Gantz, D. L., Klimtchuk, E. & Hamilton, J. A. Interactions between fatty acids and alpha-synuclein. *J. Lipid Res.* **47**, 1714–1724 (2006).

198. Shamoto-Nagai, M., Hisaka, S., Naoi, M. & Maruyama, W. Modification of α-synuclein by lipid peroxidation products derived from polyunsaturated fatty acids promotes toxic oligomerization: its relevance to Parkinson disease. *J. Clin. Biochem. Nutr.* **62**, 207–212 (2018).

199. Ouberai, M. M. *et al.* α-Synuclein Senses Lipid Packing Defects and Induces Lateral Expansion of Lipids Leading to Membrane Remodeling. *J. Biol. Chem.* **288**, 20883–20895 (2013).

200. Golovko, M. Y. *et al.* Acyl-CoA synthetase activity links wild-type but not mutant alpha-synuclein to brain arachidonate metabolism. *Biochemistry* **45**, 6956–6966 (2006).

Annexe 3:

Research article: Alpha synuclein determines ferroptosis sensitivity in dopaminergic neurons via modulation of the ether-phospholipid membrane composition

Cell Reports

Alpha synuclein determines ferroptosis sensitivity in dopaminergic neurons via modulation of ether-phospholipid membrane composition.

--Manuscript Draft--

Manuscript Number:	
Full Title:	Alpha synuclein determines ferroptosis sensitivity in dopaminergic neurons via modulation of ether-phospholipid membrane composition.
Article Type:	Research Article
Keywords:	Parkinson's disease; alpha-synuclein; ferroptosis; arachidonic acid; ether phospholipids
Corresponding Author:	David Devos Universite de Lille FRANCE
First Author:	Laura Mahoney-Sanchez
Order of Authors:	Laura Mahoney-Sanchez
	Hind Bouchaoui
	Ibrahim Boussaad
	Aurélie Jonneaux
	kelly Timmerman
	Olivier Berdeaux
	Scott Ayton
	Rejko Krüger
	James A. Duce
	David Devos
	Jean-Christophe Devedjian
Abstract:	There is a continued unmet need for treatments that can slow Parkinson's disease progression due to the lack of understanding behind the molecular mechanisms underlying neurodegeneration. Since its discovery, ferroptosis has been implicated in several diseases and represents a therapeutic target in Parkinson's disease. Here we use two highly relevant human dopaminergic neuronal models to show that endogenous levels of a-synuclein can determine the sensitivity of dopaminergic neurons to ferroptosis. Using small interfering RNA and CRISPR/Cas9 genome editing, we show that reducing a-synuclein expression in dopaminergic neurons leads to ferroptosis evasion, whilst elevated a-synuclein expression in patient's small molecule-derived neuronal precursor cells with SNCA triplication causes an increased vulnerability to lipid peroxidation and ferroptosis. Lipid profiling reveal that ferroptosis resistance is due to a reduction in ether-linked phospholipids, required for ferroptosis, in neurons depleted of a-syn. These results provide a molecular mechanism linking a-syn levels to the sensitivity of dopaminergic neurons to ferroptosis, suggesting potential therapeutic relevance.
Suggested Reviewers:	Marcus Conrad principal investigator, Helmholtz Zentrum Munchen Deutsches Forschungszentrum fur Gesundheit und Umwelt marcus.conrad@helmholtz-muenchen.de Marcus Conrad is a world expert on ferroptosis regulatory mechanisms. His previous work had characterised the role of ACSL4 in ferroptosis. Since this manuscript suggests a novel ferroptosis regulatory mechanisms, we believe he will be able to provide valuable and enriching review to this article.
	Sharon Ronit Professor, The Hebrew University of Jerusalem Faculty of Medicine

	ronitsh@ekmd.huji.ac.il Sharon Ronit has previsouly shown alterations to the metabolism of lipids associated with synucleinopathies in cell models and patient's brain. Her knowledge on plasma membrane lipid composition in Parkinson's disease makes her highly suitable for revision of this manuscript
	Kay Double Professor, The University of Sydney Faculty of Health Sciences Lidcombe Campus: The University of Sydney School of Health Sciences kay.double@sydney.edu.au Prof. Kay Double has extensive knowledge on molecular pathways underlying neurodegeneration in Parkinson's disease. With a particular focus on iron but also proteinopathies, she's characterised pathological pathways associated with PD.
	James Connor Professor, Penn State Cancer Institute jrc3@psu.edu Prof. James Connor is an expert on iron dyshomeostasis and redox imbalance in neurodegenerative disorders. His in-depth knowledge on the pathological pathways associated to PD make him a valuable reviewer for this manuscript.
	Pier Mastrobernadino Erasmus Universiteit Rotterdam p.g.mastroberardino@erasmusmc.nl The are of expertise of Dr. Mastrobernadino is the molecular pathological pathways underlying nuerodegeneration in Parkinson's Disease. His knowledge on molecular and cellular biology would allow his to provide relevant and valuable feedback on this manuscript
Opposed Reviewers:	
Additional Information:	
Question	**Response**
Standardized datasets A list of datatypes considered standardized under Cell Press policy is available here. Does this manuscript report new standardized datasets?	No
Original code Does this manuscript report original code?	No
Mendeley Data If your paper is accepted, we encourage you to publish the original, unprocessed data alongside your Cell Press paper through Mendeley Data. For more information, please refer to our detailed instructions.	I do not wish to publish my original data.

Title: Alpha synuclein determines ferroptosis sensitivity in dopaminergic neurons via modulation of ether-phospholipid membrane composition.

Authors:

Laura Mahoney-Sanchez[1], Hind Bouchaoui[1], Ibrahim Boussaad[2], Aurélie Jonneaux[1], Kelly Timmerman[1], Olivier Berdeaux[3], Scott Ayton[4], Rejko Krüger[2,5,6], James A. Duce[4,7,*,+], David Devos[1,*,+], Jean-Christophe Devedjian[1,8,9,+]

Affiliations:

[1] Department of Medical Pharmacology, Lille University, INSERM UMRS_1772, Lille University hospital, LICEND COEN Centre, LilNCog – Lille Neuroscience & Cognition, 59000, France

[2] Translational Neuroscience, Luxembourg Centre for Systems Biomedicine (LCSB), University of Luxembourg, 4365 Esch-sur-Alzette, Luxembourg.

[3] Lipid-Aroma Platform, Centre des Sciences du Goût et de l'Alimentation, UMR6265 CNRS, UMR1324 INRA, Université de Bourgogne, Agrosup Dijon, F-21000 Dijon, France

[4] Melbourne Dementia Research Centre, Florey Institute of Neuroscience and Mental Health, The University of Melbourne, Victoria, Australia

[5] Transversal Translational Medicine, Luxembourg Institute of Health (LIH), 1445 Strassen, Luxembourg

[6] Parkinson Reserch Clinic, Centre Hospitalier de Luxembourg (CHL), 1210 Luxembourg (Belair), Luxembourg.

[7] The ALBORADA Drug Discovery Institute, University of Cambridge, Cambridge Biomedical Campus, Cambridge, UK.

[8] Université du Litoral Côte d'Opale, 1, Place de l'Yser, Dunkerque Cedex, France

[9] Lead contact

[+] Equally contributed

[*] Correspondence: David.DEVOS@CHRU-LILLE.FR (D.D.), james.duce@florey.edu.au (J.D.).

Keywords: Parkinson's disease – alpha-synuclein – ferroptosis –arachidonic acid– ether-phospholipids

Abstract

There is a continued unmet need for treatments that can slow Parkinson's disease progression due to the lack of understanding behind the molecular mechanisms underlying neurodegeneration. Since its discovery, ferroptosis has been implicated in several diseases and represents a therapeutic target in Parkinson's disease. Here we use two highly relevant human dopaminergic neuronal models to show that endogenous levels of α-synuclein can determine the sensitivity of dopaminergic neurons to ferroptosis. Using small interfering RNA and CRISPR/Cas9 genome editing, we show that reducing α-synuclein expression in dopaminergic neurons leads to ferroptosis evasion, whilst elevated α-synuclein expression in patient's small molecule-derived neuronal precursor cells with SNCA triplication causes an increased vulnerability to lipid peroxidation and ferroptosis. Lipid profiling reveal that ferroptosis resistance is due to a reduction in ether-linked phospholipids, required for ferroptosis, in neurons depleted of α-syn. These results provide a molecular mechanism linking α-syn levels to the sensitivity of dopaminergic neurons to ferroptosis, suggesting potential therapeutic relevance.

Introduction

Parkinson's disease (PD) is pathologically defined by dopaminergic neurodegeneration, alpha synuclein (α-syn) aggregation and deposition within Lewy bodies as well as iron accumulation in the substantia nigra pars compacta (SNpc) (Dexter et al., 1989a; Spillantini et al., 1997; Schneider and Obeso, 2015). These pathological hallmarks have encouraged the progress of therapeutic avenues towards dopamine restoration, mitigating the aggregation of α-syn and iron chelation. Despite symptomatic relief, a huge unmet need remains for efficient disease-modifying therapies that can reduce dopaminergic neuron death and thus disease progression. To overcome this demand, a better understanding of the mechanisms involved in the development of these pathological hallmarks and their dynamic relationship to cell death is required. For many years, neuronal death in PD was considered to be caused via apoptosis (Ziv et al., 2001). This was mainly due to the fact that until recently, the use of oncogenic cell lines (e.g. neuroblastoma) greatly limited the types of regulated cell death that were able to be identified (Galluzzi et al., 2018). Since the field continue to expand, novel mechanisms that orchestrate multiple cell death pathways are unveiled. This is in part due to a greater use of primary cultures and the capacity to separate key differences in cell death mechanisms, which has resulted in more cell death processes implicated with disease mechanisms (Guiney et al., 2017; Galluzzi et al., 2018). More recently, ferroptosis was identified as a novel cell death pathway characterized by iron dependent lipid peroxide accumulation (Dixon et al., 2012; Stockwell et al., 2017) and is increasingly implicated in various human diseases as well as *in vivo* disease models (Friedmann Angeli et al., 2014; Do Van et al., 2016; Martin-Sanchez et al., 2017; Karuppagounder et al., 2018; Alim et al., 2019; Devos et al., 2019). The initiation, execution and inhibition of ferroptosis lies at the intersection of the metabolism of amino acids, lipids and iron (Tang et al., 2021). The peroxidation of polyunsaturated fatty acids (PUFAs) in the membrane phospholipids (PL) is a key step in promoting ferroptosis (Yang et al., 2016). Therefore, the lipid composition of the plasma membrane can determine cellular susceptibility to ferroptosis whereby long chain PUFAs increase the risk for lipid peroxidation whilst monounsaturated fatty acids (MUFAs) appear to decrease such risk (Magtanong et al., 2019). We have previously shown that ferroptosis is indeed a prevalent mechanism for neuronal cell death in *in vitro* and *in vivo* pro-oxidant models of Parkinson's Disease (Do Van et al., 2016; Mahoney-Sánchez et al., 2020) and there is an indication that some familial PD patients carry mutations in proteins

important in modulating pathways that alter ferroptosis sensitivity (Cao et al., 2020; Vallerga et al., 2020).

In addition to being a major component of Lewy body pathology, α-syn is implicated in PD causality by genome wide association studies of sporadic PD and autosomal dominantly inherited mutations and duplication/triplication in the *SNCA* gene that lead to various clinical phenotypes ranging from typical late-onset to rapid progressive early-onset familial PD (Zhang et al., 2018a; Blauwendraat et al., 2019). Despite the genetic support for the involvement of α-syn in PD pathology, neither the physiological function nor the neuropathological mechanisms of this protein are fully understood. In this study, we sought to investigate the potential implication of endogenous α-syn in ferroptosis sensitivity given the evidence implicating α-syn with an altered lipid metabolism, particularly the plasma membrane PUFA composition (Sharon et al., 2001, 2003; Golovko et al., 2005, 2006, 2007; Barceló-Coblijn et al., 2007). Here, we demonstrate that α-syn plays a pivotal role in dopaminergic neuron survival by regulating PL membrane composition; specifically the ether-linked phospholipids (ether-PL) essential for ferroptotic cell death (Zou et al., 2020a; Cui et al., 2021). Suppression of α-syn expression markedly decreases the proportion of ether-PL in the plasma membrane of dopaminergic neurons, increasing the resistance to ferroptosis in neurons to a comparable level as when the major ferroptotic regulator acyl-coA synthetase long-chain family member 4 (ACSL4) is reduced. Conversely, elevated levels of α-syn in human small-molecule derived neuronal precursor cells (smNPC)-derived midbrain neurons with SNCA triplication render neurons more vulnerable to ferroptosis induced lipid peroxidation and cell death. The discovery of α-syn as a positive modulator of ferroptosis in two distinct dopaminergic neuronal models supports ferroptosis as a key mechanism involved in the pathology of PD and provides novel ferroptosis-based therapeutic opportunities in the disease.

Results

Depletion of α-synuclein selectively protects neurons against ferroptosis. To investigate the impact of α-syn on ferroptosis, α-syn was knocked-down (KD) by small interfering RNA (siRNA) in LUHMES cells (Fig. 1a & supplementary fig. 1a&b), a relevant human neuronal precursor cell line which can be differentiated into a mature, post-mitotic homogenous dopaminergic cell population. As ACSL4 is a well-established pro-ferroptotic modulator involved in enriching cellular membrane with PUFAs (Doll et al., 2017), all readouts were

compared to KD of this enzyme in the same dopaminergic cell line. Reducing both α-syn and ACSL4 expression significantly protected neurons against both RSL3 and erastin-induced ferroptosis, whilst no difference in sensitivity was observed against staurosporin (STS) triggered apoptosis (Fig. 1b), suggesting a ferroptosis specific effect. Of note, since α-syn modulation was still observed when ferroptosis was triggered through a downstream component (e.g. Glutathione peroxidase 4 (GPX4) inhibition via RSL3), it is likely that the ferroptosis associated mechanism involving α-syn is not upstream of GPX4. Ferroptotic cell death ultimately occurs due to a cellular imbalance in elevated lipid peroxides that outweigh the capacity for GPX4 to act as a reductant in the presence of glutathione, and thus lipid peroxidation is a classic ferroptosis biomarker. Using the specific ferroptosis inducer -RSL3, and the fluorescent probe C-11 BODIPY to measure lipid ROS by flow cytometry, a depletion of α-syn levels was shown to mitigate ferroptosis-dependent lipid peroxidation to a similar level as ACSL4 KD (Fig. 1c).

To support the initial findings observed with acute KD of α-syn by siRNA, we established two stable cell lines that lack the main 140 amino-acid isoform of α-syn (referred to as F6 and G5 -140 α-syn KO) (Fig. 1d and supplementary fig.2). These two isoform specific KO cell lines were generated by CRISPR/Cas9 genome modification, whereby exon 3 in the *SNCA* locus was targeted in LUHMES cells and through non-homologous end joining (NHEJ) repair the insertion of an extra guanidine caused a shift in the reading frame (clone F6) or a deletion of 7 nucleotides (clone G5) led to alternative splicing of the *SNCA* gene (supplementary fig. 2a) that deleted the full length 140 α-syn isoform (supplementary fig. 2b, c&d). In line with our previous findings, both 140 α-syn KO clones, were found to be more resistant to ferroptosis induced by erastin and RSL3 but had no effect on apoptosis sensitivity (Fig. 1e). Consistent with the KD experiments, both 140 α-syn KO subclones also exhibited reduced RSL3-induced lipid peroxidation accumulation compared to the WT parental line (Fig. 1f).

Arachidonic acid and iron induced ferroptosis is mediated by α-synuclein expression.

Two key pathological hallmark of PD include iron overload (Dexter et al., 1989a; Ayton et al., 2015; Moreau et al., 2018) and elevated lipid peroxidation (Dexter et al., 1986, 1989b; de Farias et al., 2016) in the SNpc. Of note, impaired metabolism of fatty acids (FAs) with higher levels of membrane polyunsaturated fatty acids (PUFAs) are evident in both PD and DLB post-mortem brain (Sharon et al., 2003). In an attempt to model a more physiologically

relevant environment to induce ferroptosis that also has relevance to PD, the abundant brain PUFA arachidonic acid (AA) and FeCl3 were studied in combination at doses that were sub-toxic when administered separately (Fig. 2a). Specific induction of ferroptosis cell death and lipid peroxidation has recently been confirmed in this model and a range of known ferroptosis inhibitors (e.g. deferiprone, ferrostatin-1, and liproxstatin) as well as genetic depletion of ACSL4 or 15/15B lipoxygenases (ALOX15/15B) protect neurons against ferroptotic cell death and lipid peroxidation (Bouchaoui et al, in review).
The depletion of α-syn in LUHMES neurons co-treated with AA and Fe protected against both lipid peroxide generation (Fig. 2b) and cell death (Fig. 2c), similar to that observed with pharmacologically induced ferroptosis (Fig. 1). Levels of protection by α-syn depletion were comparable to KD of ACSL4 (Fig. 2b&c). A similar protection against AA and Fe induced cell death was also observed in both 140 α-syn KO subclones (Fig. 2d). Taken together, these findings in addition to prior studies support α-syn having a role in the metabolisms of PUFAs and iron (Sharon et al., 2003; Barceló-Coblijn et al., 2007; Baksi et al., 2016; Baksi and Singh, 2017) and subsequently indicates that α-syn specifically mediates the sensitivity of dopaminergic neurons to ferroptosis induced by the toxic combination of AA and Fe.

α-Synuclein levels determine ferroptosis sensitivity in patient derived midbrain neurons. To determine that observations in the LUHMES neurons were not due to a cell specific phenotype, a second *in vitro* human cell model was studied. Human midbrain dopaminergic neurons (mDANs) differentiated from smNPC (Fig. 3a) were either genetically modified by CRISPR/Cas9 to knock-out α-syn (C4 - SNCA KO) or derived from a patient with a triplication in *SNCA* (SNCA Trip) (Fig. 3b). Comparing C4 - SNCA KO to the C4 - WT isogenic control confirmed that an absence of α-syn rendered mDANs more resistant to RSL3-induced ferroptosis but had no effect on sensitivity to STS-induced apoptosis (Fig. 3c). In contrast, mDANs carrying SNCA triplication were more vulnerable to RSL3 toxicity when compared to their isogenic control (Iso WT) despite having no observable difference in their response to STS (Fig 3d). Paralleling the selective changes to ferroptotic cell death, lipid peroxidation levels in response to ferroptosis induction was lower in the C4 - SNCA KO mDANS (Fig 3e) and higher in the SNCA Trip mDANS (Fig 3f) when compared to their respective WT isogenic controls. Importantly, the triplication of SNCA alone sufficed to trigger lipid peroxidation under basal control conditions, indicating that an increase in α-syn levels could prime the cells to be more sensitive to ferroptosis (Fig 3f). To further confirm

that the observed changes to lipid peroxidation in the SNCA Trip neurons were specifically due to an elevation of α-syn, we performed siRNA to reduce α-syn expression back to similar levels observed in the isogenic control (Fig. 3g and supplementary fig 3a&b.). As expected, knocking-down α-syn in the SNCA Trip neurons significantly reduced the levels of ferroptosis induced lipid peroxidation (Fig. 3g). Taken together, these findings further support α-syn as a positive modulator of ferroptosis in midbrain dopaminergic neurons.

α-Synuclein modulates the composition of ether-phospholipids in the plasma membrane. Prior studies have shown altered fatty acid composition in response to abnormal α-syn levels in both *in vitro* and *in vivo* models as well as human brain (Sharon et al., 2001, 2003; Golovko et al., 2005, 2006, 2007; Barceló-Coblijn et al., 2007). Overexpression of α-syn increases levels of AA, linoleic acid and dihomo-γ-linoleic acid, whilst the absence of α-syn reduces the PUFA content in brain PLs (Sharon et al., 2003; Golovko et al., 2006). Based on these findings, we hypothesized that the ferroptosis resistant phenotype observed in α-syn depleted neurons could be due to a reduction in PUFAs present in the PLs.
In search of potential mechanisms that underlie the observed evasion from ferroptosis in the α-syn depleted neurons, PL membrane composition in the α-syn KD neurons was measured by mass spectrometry and compared to the effects caused by a reduction in ACSL4 expression. Similar to previous reports in other cell types (Doll et al., 2017), the percentages of total phosphatidylcholine (PC) and phosphatidylethanolamine (PE) containing PUFAs (PC PUFAs or PE PUFAs) were reduced in the ACSL4 depleted dopaminergic neurons (Fig. 4a). A similar profile was observed when α-syn levels were reduced (Fig. 4a) with no significant changes to MUFAs content (supplementary fig 4), indicating that α-syn may mediate the phospholipid PUFA content in dopaminergic neurons through a similar pathway as ACSL4. To elucidate how these changes in PC and PE would impact on the generation of lipid peroxides, an index of peroxidability (PI) (Naudí et al., 2017) was calculated for each condition (PI = (% monoenoic FA × 0.025) + (% dienoic FA × 1) + (% trienoic FA × 2) + (% tetraenoic FA × 4) + (% pentaenoic FA×6) + (% hexaenoic FA × 8)). This index, that takes into account the number of double bonds in the PUFAs to determine the risk of PLs to oxidize, was reduced in LUHMES neurons with either α-syn or ACSL4 depleted by siRNA (Fig. 4b).

Taking more in-depth lipidomic profiling of the different PC and PE molecular species in both α-syn and ACSL4-depleted neurons revealed a prominent and selective loss of ether-linked phospholipids (ether-PL) (highlighted in Fig. 4c). Unlike ester-linked diacyl-PL, ether-PL possess an ether bond at the glycerol sn-1 position. Ether-PL comprise two subclasses: alkyl-ether phospholipids (ePL) and vinyl-ether phospholipids, also known as plasmalogens (pPL). In the sn-2 position, ether-PL most often contain a PUFA, which is prone to peroxidation. Finally, in the sn-3 position, ether-PL present a polar head group, commonly a phosphoethanolamine and phosphocholine (Fig. 4d&e). Of note, recent studies have shown that ether-PL are essential for ferroptosis and a reduction in ether-PLs suffices to protect cells against this unique cell death pathway (Zou et al., 2020a; Cui et al., 2021). In line with these findings, reduced α-syn or ACSL4 expression in LUHMES cells resulted in a specific downregulation of ether-linked PC (ether-PC) and PE (ether-PE) (Fig. 4c&f). Upon evaluating specific ether-PLs species previously associated with an increased vulnerability to ferroptosis (Cui et al., 2021), several were observed to be consistently downregulated in LUHMES dopaminergic neurons where α-syn or ACSL4 was depleted (Supplementary fig 5a&b). Taken together, these findings indicate that a key factor in α-syn's capability to mediate the sensitivity of dopaminergic neurons to ferroptosis-induced lipid peroxidation and cell death is through ether-PL modulation in the plasma membrane.

The level of ether-PL in α-syn depleted neurons is restored upon arachidonic acid treatment. A reduction in ether-PL upon α-syn depletion could be explained by; *i*. greater peroxidation of the PUFAs within the ether-PL, *ii*. increased removal from the plasma membrane by the relevant phospholipase, and/or *iii*. impaired biosynthesis. The loss of all molecular species of ether-PL, regardless of fatty acid length or saturation status (Fig. 4c) indicates an unlikelihood that reduced α-syn caused greater peroxidation of the PUFA in the ether-PL and thus this avenue of investigation was not pursued further. The calcium-independent phospholipase A2 (iPLA2) has been implicated in the removal of ether-PL from the plasma membrane (Wolf and Gross, 1985; Ford et al., 1991; Yang et al., 1996). However, a lack of change to iPLA2 in the α-syn depleted neurons makes increased enzymatic removal of ether-PL from the plasma membrane also an unlikely protective mechanism (Fig. 5a).
To assess whether the observed downregulation of ether-PLs in the α-syn KD cells might be driven by defective biogenesis at the peroxisome, established peroxisome markers (Peroxisomal biogenesis factor 3 and 14 - PEX3 and PEX14), were assessed along with the

enzymes (Fatty Acyl-CoA Reductase 1 - FAR1, Glyceronephosphate O-Acyltransferase - GNPAT, Alkyldihydroxyacetonephosphate synthase - AGPS and 1-Acylglycerol-3-Phosphate O-Acyltransferase 3 - AGPAT3) required for the synthesis of the ether-PL precursor 1-*O*-alkyl-glycerol-3-phosphate (AGP) (Fig. 5a, b&c). Again, similar to ACSL4 KD, neither levels of peroxisome markers or the relevant upstream proteins required for ether-PL biogenesis were altered (Fig. 5a&b), suggesting the initial stages of ether-PL synthesis were not impaired.

The role of ACSL4 is essential for the generation and incorporation of PUFA-CoA into the ferroptosis-relevant ether-PL in the ER (Fig. 5c). Supplementation of AA (20 μM), the preferential substrate of ACSL4, restored ether-PLs back to control levels in LUHMES depleted of ACSL4 (Fig 5d & e). Similarly, AA supplementation restored the levels of ether-PLs upon a-syn depletion (Fig. 5d & e) despite no observable changes in ACSL4 expression (Fig 5a & Supplementary fig 1a&b), suggesting the changes in ether-PL may be due to a lack of the PUFA-CoA required for ether-PL synthesis.

These results provide evidence to support a requirement for ether-PL in ferroptotic cell death not only in cancer cells (Zou et al., 2020a; Cui et al., 2021) but also dopaminergic neurons which have a greater of PUFA containing ether-PL (PUFA-ether-PL) than PUFA containing diacyl PL (PUFA-diacyl-PL) (Supplementary fig 6a&b). Furthermore, α-syn appears to play a critical role in ferroptosis sensitivity in dopaminergic neurons through modulation of ether-PL synthesis, strengthening a mechanistic link between endogenous α-syn and ferroptosis in neurons.

Discussion

Ferroptosis has been established as a regulated cell death pathway with implications in several diseases (Friedmann Angeli et al., 2014; Linkermann et al., 2014; Do Van et al., 2016; Martin-Sanchez et al., 2017; Zhang et al., 2018c; Alim et al., 2019). Although the precise molecular pathways associated with ferroptosis continue to expand and evolve, extensive research to date has deciphered several key regulatory mechanisms. Here, we reveal that α-syn mediates the sensitivity of dopaminergic neurons to ferroptosis by enriching cellular membranes with ether-PL. These findings further implicate ferroptosis in PD, which is supported by prior studies that reveal changes in PD consistent with ferroptosis, including iron overload (Dexter et al., 1987, 1989a; Hirsch et al., 1991; Ayton et al., 2015), elevated lipid peroxidation (Dexter et al., 1986, 1989b; de Farias et al., 2016), reduced glutathione (GSH) levels (Sofic et al., 1992; Sian et al., 1994; Pearce et al., 1997; Li et al., 1997), XcT

downregulation (Vallerga et al., 2020), and CoQ10 reduction (Battino et al., 1996; Mischley et al., 2012; Bersuker et al., 2019). The potential role of ferroptosis in PD pathology is further strengthened by the recent finding that DJ-1, a gene linked to autosomal-recessive early-onset PD (Bonifati et al., 2003), acts as a ferroptosis inhibitor by preserving the transsulfuration pathway, and thereby the biosynthesis of cysteine and GSH (Cao et al., 2020). Furthermore, a recent analysis associated DNA hypermethylation in the promotor region of the SLC7A11 gene (encoding the cysteine-glutamate antiporter XcT) to risk of PD. This hypermethylation of SLC7A11 results in a downregulation of XcT which contributes to the decreased intracellular GSH levels observed in PD and increased susceptibility to ferroptosis (Vallerga et al., 2020). Together, these well-established disease features strongly implicate ferroptosis in the neurodegeneration observed in PD. To this extent, we have previously shown that ferroptosis is a prevalent cell death pathway in several oxidative stress models of Parkinsonism (Do Van et al., 2016). Despite this growing evidence, the implication as to whether ferroptosis is present in synucleinopathy models remains less clear. The recent findings that exogenous α-syn oligomers bind the plasma membrane to drive ferroptotic cell death through lipid peroxide generation, and that this can be rescued by iron chelators, D-PUFAs or ferrostatin-1, provide the first evidence to support ferroptosis as a pathological mechanisms in synucleinopathies (Angelova et al., 2020). However, our study now goes further in implicating endogenous α-syn in the ferroptosis pathway by demonstrating that cellular α-syn expression can modulate the sensitivity of dopaminergic neurons to ferroptotic cell death in a similar way as the pro-ferroptotic enzyme ACSL4. Using two relevant human dopaminergic neuron *in vitro* models, we show that a reduction in α-syn expression protects neurons from ferroptosis induced lipid peroxidation accumulation and subsequent cell death. Of relevance, human smNPC derived midbrain neurons carrying a familial PD multiplication in *SNCA* (SNCA Trip) that results in elevated levels of α-syn has an opposing effect: increasing the vulnerability of neurons to ferroptosis induced lipid peroxidation and cell death. An elevated basal lipid peroxidation in these SNCA Trip neurons supports similar observations in lipid ROS levels in SNCA Trip iPSC derived cortical neurons (Angelova et al., 2020) and suggests a residual priming effect that increases ferroptosis susceptibility in synucleinopathy conditions where there is an imbalance in redox homeostasis. Indeed, elevated oxidative stress and more specifically lipid peroxidation markers, including the metabolite 4-hydroxy-2-nonenal (4-HNE), are conspicuous features of sporadic PD pathology (Dexter et al., 1986)(Di Domenico et al., 2017). In this study, α-syn was shown to

determine the sensitivity of neurons to ferroptosis cell death whilst no effect was observed against apoptosis, suggesting a ferroptosis specific effect. However, the implication of α-syn in other cell death mechanisms such as pyroptosis, parthanatos or necroptosis remains unanswered and provide a prospect for future research.

The role of ether-PL in health and disease has gained increasing attention, especially since they were recently shown to drive ferroptosis in cancer cells (Zou et al., 2020a; Cui et al., 2021). Recent studies have shown that depletion of ether-PL biosynthesis enzymes (GNPAT, FAR1, AGPS and AGPAT3) decreases the level of PUFA containing ether-PL (PUFA-ether-PL) and markedly promotes ferroptosis resistance., whilst supplementation of PUFA-ether-PL in cells with deficiency in ether-PL synthesis resensitize these cells to ferroptosis (Zou et al., 2020a). Of note, supplementing cells with either PUFA-ether-PL or their non-ether-linked PL counterparts have similar sensitizing effect on ferroptosis suggesting that PUFA-ether-PL are not intrinsically more sensitive to peroxidation than other PUFA-PLs. However, ether-PL are essential in driving ferroptosis perhaps because they represent an abundant pool of PUFA-PLs that are available for peroxidation. This is particularly relevant in neurons as the brain has the highest proportion of ether-PL, more specifically ether-PE which represent >50% of total PE (Brites et al., 2004). In line with this, SH-SY5Y neuroblastoma cells acquire sensitivity to ferroptosis as the levels of ether-PL increase during differentiation (Zou et al., 2020a). Furthermore, the observation that LUHMES dopaminergic neurons have a greater proportion of PUFA-ether-PE than PUFA-diacyl-PE (supplementary fig. 6a&b) suggests that ferroptosis unfolding in neurons may be governed by peroxidation of ether-PL. Here we describe the importance in α-syn modulation of ether-PL membrane composition to regulate ferroptosis sensitivity in dopaminergic neurons. Similar to ACSL4, this function of α-syn is not related to the upstream enzymes involved with the early stages of biosynthesis at the peroxisome or an abnormal removal from the plasma membrane via iPLA2 since no alteration in protein or mRNA levels were detected. However, a modulation of the enzymatic activity of such enzymes cannot be excluded. The restoration of ether-PL levels by AA in neurons depleted of α-syn paralleled that observed with ACSL4 depletion and suggests an impaired activity of ACSL4 in dopaminergic neurons lacking α-syn. This hypothesis is strengthened by Golovko and colleagues who reported a reduction in AA-CoA mass and AA incorporation into PLs in the brains of SNCA KO mice due to a reduction in total ACSL activity (Golovko et al., 2006). This ACSL activity was restored upon addition of exogenous α-syn, indicating a role of α-syn in the control of ACSL4 in AA-CoA formation.

Furthermore, we now also strengthen a link between α-syn and ether-PL that was previously reported in brains of a synucleinopathy mouse model (A53T α-syn) with higher levels of plasmalogens, specifically derivates of either C16:0 or C18:0 (Yakunin et al., 2014). α-Synuclein has a high degree of sequence homology with apolipoproteins (Eichmann et al., 2017; Fecchio et al., 2018), is implicated in the metabolism of lipids (most prevalently membrane PUFAs including AA, adrenic acid, linoleic acid and dihomo-gamma-linoleic acid) (Sharon et al., 2003; Golovko et al., 2006; Barceló-Coblijn et al., 2007) and has a high binding affinity to PUFAs (α-linolenic acid, DHA and eicosapentaenoic acid) through its N-terminal domain. Both the lipid ratio of these PUFAs in the plasma membrane and the membrane fluidity are increased when α-syn levels are elevated both in neuronal cultures and brain tissue from PD and DLB patients (Sharon et al., 2003). Conversely, when exposed to free or phospholipid-bound PUFAs, α-syn undergoes structural changes including an increased propensity to oligomerize (Sharon et al., 2001; Broersen et al., 2006; De Franceschi et al., 2009). Direct or indirect enrichment of cellular membranes with diacyl- and ether-PL containing PUFAs by α-syn under the PD pathological conditions of elevated free labile iron and oxidative stress, may lead to further lipid peroxidation and drive neurons towards ferroptotic cell death.

For the first time, the implicated role of endogenous α-syn with the metabolism of ether-PL, provides a direct link to an established pathway involved in lipid peroxidation that is essential for ferroptosis. These observations also reveal a cell death mechanism in dopaminergic neurons from patients where α-syn levels are dysregulated, including synucleinopathies such as in PD. This provides further support to that already presented (Sofic et al., 1992; Sian et al., 1994; Pearce et al., 1997; Li et al., 1997; Devos et al., 2014) (Vallerga et al., 2020)(Bonifati et al., 2003; Cao et al., 2020)(Battino et al., 1996; Mischley et al., 2012; Bersuker et al., 2019) for targeting ferroptosis as a therapeutic strategy in synucleinopathies.

Acknowledgement

The authors wish to thank the BioImaging Center Lille (BiCel) platform, and in particular Nathalie Jouy, for the support given in the flow cytometry experiments. The authors wish to thank the support of the Lille University Hospital and NS-Park/FCRIN clinical research network, the European commission for the grant Nº 633190 of the H2020 program; NCT02655315.Work of I.B and R.K were supported by grants from Luxembourg National

Research Fund (FNR) for the PEARL program (FNR/P13/6682797 to R.K), MotaSYN (12719684) and MAMasyn.

Conflict of interest

David Devos has received PHRC grants from the French Ministry of Health and research funding from the ARSLA charity, France Parkinson charity, Credit Agricole Foundation. He has led two pilot investigator driven studies with DFP provided for free by ApoPharma (FAIRPARK-I and SAFE-FAIR ALS-I). He is leading two large investigator driven studies with DFP provided for free by ApoPharma (FAIRPARK-II and FAIR ALS-II). He served on advisory boards, served as a consultant and given lectures for pharmaceutical companies such as Orkyn, Aguettant, Abbvie, Medtronic, Novartis, Teva, UCB, Lundbeck. James Duce has received research funding from Alzheimer's Society, Alzheimer's Research UK, European Commission, Parkinson's UK and NHMRC. He serves as a scientific advisor on the FAIR-PARK II but has no financial disclosures. The remaining authors have nothing to declare.

Author contributions

Experimentation, L.M.S., H.B., A.J, and I.B.; analysis, L.M.S and O.B.; manuscript preparation, L.M.S., J.D., and S.A.; supervision, J.D., D.D., and J-C.D.; funding acquisition, D.D., and R.K. All authors reviewed the manuscript.

Methods

Antibodies and reagents. The antibodies to α-syn (MJFR1 ab138501 and Biolegend), ACSL4 (EPR8640 ab155282), PEX14 (ab183885), AGPS (ab236621) were obtained from abcam. The antibodies against GNPAT (14931-1-AP) and PLA2G6 (22030-1-AP) were purchased from Proteintech. Erastin (E7781), staurosporin (S4400), N6, 2'-O-dibutyryl cAMP sodium (cAMP – D0627), tetracyclin (T-7660), Poly-L-ornithune (P3655), fibronectin (F1141) and arachidonic acid (10931) were purchased from Sigma. RSL3 (S8155) was obtained from Selleckhem. N2 supplement (17502048), advanced DMEM/F12 (12634-028), Glutamine 2mM (25030-123), BODIPY 581/591 C11 (D3861), LIVE/DEAD (L23105) lipofectamine RNAiMAX (13778150), optimum reduced serum media (10149832) were obtained from Thermo Fisher Scientific. bFGF (4114-TC) and GDNF (212-GT) were purchased from R&D Systems.

Cell culture. LUHMES cells were a kind gift from Pr. Marcel Leist from the University of Konstanz. For LUHMES cell culture, Nunclon™ cell culture flasks and well-plates were coated with 50µg/ml of PLO and 1µg/ml fibronectin. Cells were grown at 37ºC in a humidified 95% air, 5% CO2 atmosphere. Proliferating cells are maintained in advanced DMEM/F12 media supplemented with 1x N2, 2mM L-glut and 40ng/ml bFGF. For dopaminergic neuron differentiation, the proliferative media was replaced by differentiation media (advanced DMEM/F12, 1x N2, 2mM L-glut, 1mM dibutyryl cAMP, 1µg/ml tetracycline and 2ng/ml recombinant human GDNF). After 2 days of pre-differentiation, cells were harvested with trypsin, centrifuged for 5 minutes at 300g, counted and seeded in plates. LUHMES cells were left to fully differentiate for another 3 days in order to start every experimental protocol at day 5 of differentiation. All media were supplemented with 1% penicillin and streptomycin.

Small molecule derived neuronal precursor cells (smNPC) were differentiated from iPSC as described in (Reinhardt et al., 2013). smNPC expansion medium consisted of N2B27 supplemented with CHIR, PMA and ascorbic acid (AA), with a medium change every other day. For splitting, cells were digested into single cells with a 15 minutes incubation at 37ºC with prewarmed accutase (PAA). Cells were diluted and collected with DMEM and centrifuged at 200g for 5 minutes. The cell pellets were resuspended in fresh smNPC expansion medium and plated on Matrigel-coated culture plates. For generation of midbrain dopaminergic neurons, smNPC expansion medium was changed to N2B27 with 100ng/ml FGF8, 1µM PMA and 200µM AA. After 8 days, media was changed to maturation medium: N2B27 with 10ng/ml BDNF, 10ng/ml GDNF, 1ng/ml TGF-b3, 200µM AA and 500µM cAMP. Neuronal maturation and differentiation of smNPC was performed for at least 28 days to generate midbrain-specific dopaminergic neurons. The SNCA triplication line was obtained from EBISC (cell line Edi001-A) and the isogenic gene corrected line (Iso WT) was generated and kindly provided by Dr Tilo Kunath from the University of Edinburgh (Mohamed et al., 2021).

siRNA-mediated knock-down of α-syn and ACSL4. siRNA transfection was performed by preparing solution A - RNAiMAX lipofectamine (ThermoFisher Scientific, 10601435) and OptiMEM (ThermoFisher Scientific, 10149832), and solution B consisting of siRNA (10µM) and OptiMEM. The siRNA control-A (sc-37007), control-B (sc-44230), α-syn (sc-29619) and ACSL4 (sc-60619) were purchased from SantaCruz Biotechnology. After 5 minutes of incubation, both solutions were combined and transferred to plates before seeding day 2 pre-

differentiated LUHMES cells. Cells were left to fully differentiate for an additional 3 days before treatments. siRNA-mediated KD efficiency was measured by PCR and western blot 72h post transfection.

For smNPC derived midbrain, the media was removed from seeded cells in 24-well plates and replaced by 400µl maturation media per well. The siRNA mix was prepared as follow: for 1 well, 1,5µl RNAiMAX lipofectamimne was carefully mixed with 50µl OptiMEM and separately, 1,5µl of the control or α-syn siRNA were mixed with 50µl OptiMEM. The two solutions were left to incubate at room temperature for 5 minutes before carefully mixing vol:vol. The transfection solution was left to incubate at room temperature for an additional 15 minutes before adding 100µl per well. 6h later, 500µl of maturation was added to each well and cells were left for 72h before conducting any experimentation or extracting the RNA.

CRISPR/Cas9-mediated KO of 140 α-syn. The experimental procedure for generating CRISPR/Cas9 clones on LUHMES cells was adapted from *Shah et al, 2016*, with some minor alterations. CRISPR gRNA were designed by http://crispor.tefor.net/. The gRNA targeting exon 3 were inserted into pSpCas9(BB)-2A-GFP (PX458) plasmid from Addgene (#48138).

Following gRNA ligation, OneShot *E.Coli* bacteria were transformed and spread on separate labelled LB agar plates in the presence of 50µg/ml ampicillin. Colonies were left to grow overnight at 37ºC. The following day, 25 individual colonies were picked and PCR analysis was conducted to validate the plasmid sequence. The SNCA Ex3 gRNA oligonucleotide sequences are as follows:

Sense (5' to 3'): CACCgTggTgCATggTgTggCAAC

Antisense (5' to 3'): AAACgTTgCCACACCATgCACCAC

To generate 140 α-syn KO clones, LUHMES cells were electroporated with PX458-SNCAEx3 gRNA plasmids using the Amaxa P3 primary cell kit (V4XP-3024) on a nucleic acid transfection apparatus (4D Nucleofector device) with EM-110 program. Transfected cells were FACS sorted by fluorescence (FACSAria II, BD) into several 96-well plates. Single cell colonies were left to grow in proliferation media and amplified until frozen. The DNA was extracted for PCR amplification before sequence verification using the following primers:

Forward: 5' - gCTTgAgACTTATgTCTTgAATTTg

Reverse: 5'- TCTTgAATACTgggCCACAC

Successfully edited clones were verified using western blot.

CRISPR/Cas9-mediated SNCA KO in smNPC. Control smNPC line C4 - WT was previously described and characterised in (Boussaad et al., 2020). C4 - SNCA KO iPSC were generated as described in (Barbuti et al., 2020a). The Cas9 plasmid pX330 (Addgene, 42230) containing a sgRNA targeting the human *SNCA* sequence gctgctgagaaaaccaaaca was transfected into C4 -WT cells. Briefly, iPSCs were dissociated to single cells using PAA and plated in iPS media as described in (Barbuti et al., 2020b; Boussaad et al., 2020), plus Rho-Kinase Inhibitor Y-27632 (10µM, Abcam ab120129). 1 x 10^6 cells were then electroporated using the 2D-Amaxa nucleofector unit (Lonza, Basel, Switzerland) with program B16. After electroporation, 1mL of E8 was added to the cuvette before being placed at 37ºC for 10 minutes. Cells were then plated into 6-well plates and cell selection was achieved using antibiotic resistance to puromycin when small to medium-sized colonies began to appear.

Cell viability. Briefly, a stock solution was prepared at a concentration of 10mg/ml by dissolving resazurin dye (7-hydroxy-3H-phenoxazin-3-one 10-oxide) in dH_2O. Approximately 4x10^4 LUHMES or mDANs were plated on coated 96-well plates in appropriate medium. Cytotoxicity was assayed 24 or 48h post treatment by adding resazurin solution (10% of cell culture volume per well – final concentration 100µg/ml) and cells were left to incubate for 2h at 37ºC. Samples were analysed fluorometrically on a microplate reader (Mithras LB950 or BioTek citation 5 imaging reader, Ex= 540nM, Em= 600nM). Background signals obtained from cell-free wells were subtracted from each sample. Cell viability under treatment conditions were reported as a percentage relative to untreated control cells.

Lipid peroxidation analysis. LUHMES cells were seeded at day 2 of differentiation in 24 well-plates at a density of 300 000 cells per well and left to complete the differentiation until day 5. Following ferroptosis induction, cells were collected after the addition of trypsin, centrifuged for 5 minutes at 300g and resuspended in 200µl PBS containing the LIVE/DEAD (Thermo Fisher - L23105) probe for cell viability measurements. Following a 15 minutes incubation at 37ºC, an additional 200µl of PBS containing C11-BODIPY (Thermo Fisher - D3861) probe was added to the cells at a final concentration of 1µM. Cells were incubated for another 15 minutes at 37ºC and analysed using the FORTESSA X20 flow cytometer (BD Biosciences). Data were collected from at least 10 000 cells and C11-BODIPY staining was analysed from the living cell population. Data was analysed using the Kaluza software. For

smNPC derived midbrain neurons, lipid peroxidation measurements were conducted as described above with some minor alterations: Following treatment, cells were collected with prewarmed accutase and centrifuged at 500g for 5 minutes. Cells were resuspended in 300µl of PBS containing 2µM C11-BODIPY and incubated for 20 minutes at 37ºC. For staining of viable cells, 17µg/ml DAPI was added to the cells immediately before measurement.

Lipid extraction. Lipids were extracted from cells according to the method of *Folch et al, 1957* (Folch et al., 1957). Briefly, 3 million cells were homogenized with 2mL of NaCl solution in water (0.73%). Lipids were extracted with 10 ml of $CHCl_3$/CH_3OH (2:1, v/v), and vortexed for 1 minute. Mixture was centrifuged at 3000 rpm for 3 minutes. The upper phase was discarded and the lower phase collected through a protein interface using a Pasteur pipette. After evaporation, the lipid extract (lower phase) was re-dissolved in 200μL of $CHCl_3$/CH_3OH (2:1, v/v) and stored, under nitrogen, at -20°C until further analyses.

Analysis of phospholipid molecular species. In the 200µl lipid extract, 10µl of internal standards mixture containing 320µg/ml PC(14:0/14:0) and 160µg/ml PE(14:0/14:0) were added. The process of identification and quantification of phospholipids species was performed on a Thermo UltiMate™ 3000 coupled to an Orbitrap Fusion™ Tribrid Mass Spectrometer equipped with an EASY-MAX NG™ Ion Source (H-ESI) (Thermo Scientific). Separation of phospholipid classes was achieved under HILIC conditions using Kinetex Hilic 100 x 2.1 mm, 1.7μm column (Phenomenex), with a flow of 0.500 mL.min^{-1}. The mobile phase consisted of (A) CH_3CN/H_2O (96/4, v/v) containing 10 mM ammonium acetate and (B) CH_3CN/H_2O (50/50, v/v) containing 10 mM ammonium acetate. The injection volume was 10 μL and the column was maintained at 50°C. PL species were detected by high resolution mass spectrometry (HRMS) analysis, and H-ESI source parameters were optimized and set as follows: ion transfer tube temperature of 285°C, vaporizer temperature of 370°C, sheath gas flow rate of 35 au, sweep gas of 1 au and auxiliary gas flow rate of 25 au. Positive and negative ions were monitored alternatively by switching polarity approach with a static spray voltage at 3500V and 2800V in positive and negative respectively. Mass spectra in full scan mode were obtained using the Orbitrap mass analyzer with the normal mass range and a target resolution of 240,000 (FWHM at m/z 200), on a mass range to charge ratio m/z form 200-1600 using a Quadrupole isolation on a normal mass range. All MS data were recorded using a max injection time of 100 ms, automated gain AGC target (%) at 112.5, RF lens (%) at 50 and one microscan. An Intensity Threshold filter of 1.10^3 counts was applied. For

MS/MS analyses, data-dependent mode was used for the characterization of PL species. Precursor isolation was performed in the Quadrupole analyzer with an isolation width of m/z 1.6. Higher-energy Collisional Dissociation (HCD) was employed for the fragmentation of PL species with optimized stepped collision energy of 27%. The linear ion trap (LIT) was used to acquire spectra for fragment ions in data-dependent mode. The AGC target was set to 2.10^4 with a max injection time of 50 ms. All MS and MS/MS data were acquired in the profile mode.

The Orbitrap Fusion was controlled by Xcalibur™ 4.1 software. Data of high accuracy and the information collected from fragmentation spectra, with the help of the LipidSearch™ software (Thermo) and the LIPID MAPS® database (https://www.lipidmaps.org/) were used for PL species identification.

The index of peroxidability for PC and PE (PI = (% monoenoic FA × 0.025) + (% dienoic FA × 1) + (% trienoic FA × 2) + (% tetraenoic FA × 4) + (% pentaenoic FA×6) + (% hexaenoic FA × 8)) was calculated according to (Naudí et al., 2017).

Western blot analysis. Cells were lysed in RIPA buffer containing 1% phosphatase and protease inhibitors for 15minutes at 4ºC. Cells were fully lysed by sonicating for 15 seconds with 1 second impulses every 0,5s with an amplitude of 20%. Cell debris was removed by centrifugation at 1000g for 10 minutes, 4ºC and protein concentration was determined using the Pierce™ BCA protein assay kit (ThermoFisher Scientific, 23225). For western blot analysis, samples were denaturated by heating at 90ºC for 10 minutes in standard loading dye for SDS-Page and loaded on 4-20% SDS gels. Proteins were transferred onto nitrocellulose membranes. For optimal α-syn detection, blots were then fixed with 4%PFA for 30 minutes at room temperature before blocking with either 5% BSA TBS-Tween 20 (TBS-T) 0.1% or 5% NFDM TBS-T 0.05% (non-fat dry milk) for 1 hour at room temperature. The blots were incubated with the indicated primary antibodies diluted in either 5% BSA TBS-T 0.1% or 5% NFDM TBS-T 0.05%, according to manufacturer's instructions, overnight at 4ºC. The following day, primary antibodies were washed 3x 5 minutes with TBS-T 0.1% and 3x 5 minutes with TBS. Membranes were incubated with species-specific secondary antibodies conjugated to horseradish peroxidase which was detected by enhanced chemiluminescence with Amersham ECL detection reagents. Chemiluminescence signals were visualised with Fujifilm LAS (4000), and quantification of the signals was done using ImageJ with protein quantification normalized to β-actin signals.

Quantitative reverse transcription PCR. Total RNA was extracted from differentiated cells in either 6 well-plates or 24 well-plates using the QIAGEN RNAeasy extraction kit according to manufacturer's instructions. Total RNA was dosed with BioSpec-nanodrop and a DNase step was performed on 2µg of total RNA before reverse transcription with Superscript II reverse Transcriptase (ThermoFisher Scientific, 18064022) using random primers (ThermoFisher Scientific, 48190011) in a 40µl reaction. PCR amplification of the cDNA was quantified using the LightCycler FastStart DNA Master SYBR Green I (Roche, 3003230). The housekeeping gene control was TBP. Primers were designed using NCBI primer design and purchased from TibMolBio. Threshold cycles were determined for each gene and expression levels were calculated relative to TBP. The sequences of the primers used for the qPCR are listed in Supplementary table 1.

Statistical analysis. All statistical analyses were performed using the Prism 9 GraphPad Software. The number of biological replicates for each experiment is indicates in the figure legends. Unless otherwise stated, differences between means were determined using the parametric two-tailed Student's *t*-tests and following data normality verification, and were considered significant at $p < 0.05$.

References

Alim, I., Caulfield, J.T., Chen, Y., Swarup, V., Geschwind, D.H., Ivanova, E., Seravalli, J., Ai, Y., Sansing, L.H., Ste Marie, E.J., et al. (2019). Selenium Drives a Transcriptional Adaptive Program to Block Ferroptosis and Treat Stroke. Cell 177, 1262-1279.e25. https://doi.org/10.1016/j.cell.2019.03.032.

Angelova, P.R., Choi, M.L., Berezhnov, A.V., Horrocks, M.H., Hughes, C.D., De, S., Rodrigues, M., Yapom, R., Little, D., Dolt, K.S., et al. (2020). Alpha synuclein aggregation drives ferroptosis: an interplay of iron, calcium and lipid peroxidation. Cell Death Differ. 1–16. https://doi.org/10.1038/s41418-020-0542-z.

Ayton, S., Lei, P., Hare, D.J., Duce, J.A., George, J.L., Adlard, P.A., McLean, C., Rogers, J.T., Cherny, R.A., Finkelstein, D.I., et al. (2015). Parkinson's disease iron deposition caused by nitric oxide-induced loss of β-amyloid precursor protein. J. Neurosci. Off. J. Soc. Neurosci. 35, 3591–3597. https://doi.org/10.1523/JNEUROSCI.3439-14.2015.

Baksi, S., and Singh, N. (2017). α-Synuclein impairs ferritinophagy in the retinal pigment epithelium: Implications for retinal iron dyshomeostasis in Parkinson's disease. Sci. Rep. 7,

12843. https://doi.org/10.1038/s41598-017-12862-x.

Baksi, S., Tripathi, A.K., and Singh, N. (2016). Alpha-synuclein modulates retinal iron homeostasis by facilitating the uptake of transferrin-bound iron: Implications for visual manifestations of Parkinson's disease. Free Radic. Biol. Med. 97, 292–306. https://doi.org/10.1016/j.freeradbiomed.2016.06.025.

Barbuti, P., Antony, P., Santos, B., Massart, F., Cruciani, G., Dording, C., Arias, J., Schwamborn, J., and Krüger, R. (2020a). Using High-Content Screening to Generate Single-Cell Gene-Corrected Patient-Derived iPS Clones Reveals Excess Alpha-Synuclein with Familial Parkinson's Disease Point Mutation A30P. Cells 9, 2065. https://doi.org/10.3390/cells9092065.

Barbuti, P.A., Santos, B.F.R., Dording, C.M., Cruciani, G., Massart, F., Hummel, A., and Krüger, R. (2020b). Generation of two iPS cell lines (HIHDNDi001-A and HIHDNDi001-B) from a Parkinson's disease patient carrying the heterozygous p.A30P mutation in SNCA. Stem Cell Res. 48, 101951. https://doi.org/10.1016/j.scr.2020.101951.

Barceló-Coblijn, G., Golovko, M.Y., Weinhofer, I., Berger, J., and Murphy, E.J. (2007). Brain neutral lipids mass is increased in alpha-synuclein gene-ablated mice. J. Neurochem. 101, 132–141. https://doi.org/10.1111/j.1471-4159.2006.04348.x.

Battino, M., Littarru, G.P., Gorini, A., and Villa, R.F. (1996). Coenzyme Q, peroxidation and cytochrome oxidase features after parkinson's-like disease by MPTP toxicity in intra-synaptic and non-synaptic mitochondria from Macaca fascicularis cerebral cortex and hippocampus: action of dihydroergocriptine. Neurochem. Res. 21, 1505–1514. https://doi.org/10.1007/BF02533098.

Bersuker, K., Hendricks, J.M., Li, Z., Magtanong, L., Ford, B., Tang, P.H., Roberts, M.A., Tong, B., Maimone, T.J., Zoncu, R., et al. (2019). The CoQ oxidoreductase FSP1 acts parallel to GPX4 to inhibit ferroptosis. Nature 575, 688–692. https://doi.org/10.1038/s41586-019-1705-2.

Blauwendraat, C., Heilbron, K., Vallerga, C.L., Bandres-Ciga, S., von Coelln, R., Pihlstrøm, L., Simón-Sánchez, J., Schulte, C., Sharma, M., Krohn, L., et al. (2019). Parkinson's disease age at onset genome-wide association study: Defining heritability, genetic loci, and α-synuclein mechanisms. Mov. Disord. Off. J. Mov. Disord. Soc. 34, 866–875. https://doi.org/10.1002/mds.27659.

Bonifati, V., Rizzu, P., van Baren, M.J., Schaap, O., Breedveld, G.J., Krieger, E., Dekker, M.C.J., Squitieri, F., Ibanez, P., Joosse, M., et al. (2003). Mutations in the DJ-1 gene associated with autosomal recessive early-onset parkinsonism. Science 299, 256–259. https://doi.org/10.1126/science.1077209.

Boussaad, I., Obermaier, C.D., Hanss, Z., Bobbili, D.R., Bolognin, S., Glaab, E., Wołyńska, K., Weisschuh, N., Conti, L.D., May, C., et al. (2020). A patient-based model of RNA mis-splicing uncovers treatment targets in Parkinson's disease. Sci. Transl. Med. https://doi.org/10.1126/scitranslmed.aau3960.

Brites, P., Waterham, H.R., and Wanders, R.J.A. (2004). Functions and biosynthesis of plasmalogens in health and disease. Biochim. Biophys. Acta BBA - Mol. Cell Biol. Lipids 1636, 219–231. https://doi.org/10.1016/j.bbalip.2003.12.010.

Broersen, K., van den Brink, D., Fraser, G., Goedert, M., and Davletov, B. (2006). Alpha-synuclein adopts an alpha-helical conformation in the presence of polyunsaturated fatty acids to hinder micelle formation. Biochemistry 45, 15610–15616. https://doi.org/10.1021/bi061743l.

Cao, J., Chen, X., Jiang, L., Lu, B., Yuan, M., Zhu, D., Zhu, H., He, Q., Yang, B., and Ying, M. (2020). DJ-1 suppresses ferroptosis through preserving the activity of S-adenosyl homocysteine hydrolase. Nat. Commun. 11, 1251. https://doi.org/10.1038/s41467-020-15109-y.

Cui, W., Liu, D., Gu, W., and Chu, B. (2021). Peroxisome-driven ether-linked phospholipids biosynthesis is essential for ferroptosis. Cell Death Differ. 28, 2536–2551. https://doi.org/10.1038/s41418-021-00769-0.

De Franceschi, G., Frare, E., Bubacco, L., Mammi, S., Fontana, A., and de Laureto, P.P. (2009). Molecular insights into the interaction between alpha-synuclein and docosahexaenoic acid. J. Mol. Biol. 394, 94–107. https://doi.org/10.1016/j.jmb.2009.09.008.

Devos, D., Moreau, C., Devedjian, J.C., Kluza, J., Petrault, M., Laloux, C., Jonneaux, A., Ryckewaert, G., Garçon, G., Rouaix, N., et al. (2014). Targeting chelatable iron as a therapeutic modality in Parkinson's disease. Antioxid. Redox Signal. 21, 195–210. https://doi.org/10.1089/ars.2013.5593.

Devos, D., Moreau, C., Kyheng, M., Garçon, G., Rolland, A.S., Blasco, H., Gelé, P., Timothée Lenglet, T., Veyrat-Durebex, C., Corcia, P., et al. (2019). A ferroptosis–based

panel of prognostic biomarkers for Amyotrophic Lateral Sclerosis. Sci. Rep. 9, 1–6. https://doi.org/10.1038/s41598-019-39739-5.

Dexter, D., Carter, C., Agid, F., Agid, Y., Lees, A.J., Jenner, P., and Marsden, C.D. (1986). Lipid peroxidation as cause of nigral cell death in Parkinson's disease. Lancet Lond. Engl. 2, 639–640. https://doi.org/10.1016/s0140-6736(86)92471-2.

Dexter, D.T., Wells, F.R., Agid, F., Agid, Y., Lees, A.J., Jenner, P., and Marsden, C.D. (1987). Increased nigral iron content in postmortem parkinsonian brain. Lancet Lond. Engl. 2, 1219–1220. https://doi.org/10.1016/s0140-6736(87)91361-4.

Dexter, D.T., Wells, F.R., Lees, A.J., Agid, F., Agid, Y., Jenner, P., and Marsden, C.D. (1989a). Increased nigral iron content and alterations in other metal ions occurring in brain in Parkinson's disease. J. Neurochem. 52, 1830–1836. https://doi.org/10.1111/j.1471-4159.1989.tb07264.x.

Dexter, D.T., Carter, C.J., Wells, F.R., Javoy-Agid, F., Agid, Y., Lees, A., Jenner, P., and Marsden, C.D. (1989b). Basal lipid peroxidation in substantia nigra is increased in Parkinson's disease. J. Neurochem. 52, 381–389. https://doi.org/10.1111/j.1471-4159.1989.tb09133.x.

Di Domenico, F., Tramutola, A., and Butterfield, D.A. (2017). Role of 4-hydroxy-2-nonenal (HNE) in the pathogenesis of alzheimer disease and other selected age-related neurodegenerative disorders. Free Radic. Biol. Med. 111, 253–261. https://doi.org/10.1016/j.freeradbiomed.2016.10.490.

Dixon, S.J., Lemberg, K.M., Lamprecht, M.R., Skouta, R., Zaitsev, E.M., Gleason, C.E., Patel, D.N., Bauer, A.J., Cantley, A.M., Yang, W.S., et al. (2012). Ferroptosis: an iron-dependent form of nonapoptotic cell death. Cell 149, 1060–1072. https://doi.org/10.1016/j.cell.2012.03.042.

Do Van, B., Gouel, F., Jonneaux, A., Timmerman, K., Gelé, P., Pétrault, M., Bastide, M., Laloux, C., Moreau, C., Bordet, R., et al. (2016). Ferroptosis, a newly characterized form of cell death in Parkinson's disease that is regulated by PKC. Neurobiol. Dis. 94, 169–178. https://doi.org/10.1016/j.nbd.2016.05.011.

Doll, S., Proneth, B., Tyurina, Y.Y., Panzilius, E., Kobayashi, S., Ingold, I., Irmler, M., Beckers, J., Aichler, M., Walch, A., et al. (2017). ACSL4 dictates ferroptosis sensitivity by shaping cellular lipid composition. Nat. Chem. Biol. 13, 91–98.

https://doi.org/10.1038/nchembio.2239.

Eichmann, C., Kumari, P., and Riek, R. (2017). High-density lipoprotein-like particle formation of Synuclein variants. FEBS Lett. 591, 304–311. https://doi.org/10.1002/1873-3468.12543.

de Farias, C.C., Maes, M., Bonifácio, K.L., Bortolasci, C.C., de Souza Nogueira, A., Brinholi, F.F., Matsumoto, A.K., do Nascimento, M.A., de Melo, L.B., Nixdorf, S.L., et al. (2016). Highly specific changes in antioxidant levels and lipid peroxidation in Parkinson's disease and its progression: Disease and staging biomarkers and new drug targets. Neurosci. Lett. 617, 66–71. https://doi.org/10.1016/j.neulet.2016.02.011.

Fecchio, C., Palazzi, L., and de Laureto, P.P. (2018). α-Synuclein and Polyunsaturated Fatty Acids: Molecular Basis of the Interaction and Implication in Neurodegeneration. Mol. Basel Switz. 23. https://doi.org/10.3390/molecules23071531.

Folch, J., Lees, M., and Sloane Stanley, G.H. (1957). A simple method for the isolation and purification of total lipides from animal tissues. J. Biol. Chem. 226, 497–509.

Ford, D.A., Hazen, S.L., Saffitz, J.E., and Gross, R.W. (1991). The rapid and reversible activation of a calcium-independent plasmalogen-selective phospholipase A2 during myocardial ischemia. J. Clin. Invest. 88, 331–335. https://doi.org/10.1172/JCI115296.

Friedmann Angeli, J.P., Schneider, M., Proneth, B., Tyurina, Y.Y., Tyurin, V.A., Hammond, V.J., Herbach, N., Aichler, M., Walch, A., Eggenhofer, E., et al. (2014). Inactivation of the ferroptosis regulator Gpx4 triggers acute renal failure in mice. Nat. Cell Biol. 16, 1180–1191. https://doi.org/10.1038/ncb3064.

Galluzzi, L., Vitale, I., Aaronson, S.A., Abrams, J.M., Adam, D., Agostinis, P., Alnemri, E.S., Altucci, L., Amelio, I., Andrews, D.W., et al. (2018). Molecular mechanisms of cell death: recommendations of the Nomenclature Committee on Cell Death 2018. Cell Death Differ. 25, 486–541. https://doi.org/10.1038/s41418-017-0012-4.

Golovko, M.Y., Faergeman, N.J., Cole, N.B., Castagnet, P.I., Nussbaum, R.L., and Murphy, E.J. (2005). Alpha-synuclein gene deletion decreases brain palmitate uptake and alters the palmitate metabolism in the absence of alpha-synuclein palmitate binding. Biochemistry 44, 8251–8259. https://doi.org/10.1021/bi0502137.

Golovko, M.Y., Rosenberger, T.A., Faergeman, N.J., Feddersen, S., Cole, N.B., Pribill, I., Berger, J., Nussbaum, R.L., and Murphy, E.J. (2006). Acyl-CoA synthetase activity links

wild-type but not mutant alpha-synuclein to brain arachidonate metabolism. Biochemistry 45, 6956–6966. https://doi.org/10.1021/bi0600289.

Golovko, M.Y., Rosenberger, T.A., Feddersen, S., Faergeman, N.J., and Murphy, E.J. (2007). Alpha-synuclein gene ablation increases docosahexaenoic acid incorporation and turnover in brain phospholipids. J. Neurochem. 101, 201–211. https://doi.org/10.1111/j.1471-4159.2006.04357.x.

Guiney, S.J., Adlard, P.A., Bush, A.I., Finkelstein, D.I., and Ayton, S. (2017). Ferroptosis and cell death mechanisms in Parkinson's disease. Neurochem. Int. 104, 34–48. https://doi.org/10.1016/j.neuint.2017.01.004.

Hirsch, E.C., Brandel, J.P., Galle, P., Javoy-Agid, F., and Agid, Y. (1991). Iron and aluminum increase in the substantia nigra of patients with Parkinson's disease: an X-ray microanalysis. J. Neurochem. 56, 446–451. https://doi.org/10.1111/j.1471-4159.1991.tb08170.x.

Karuppagounder, S.S., Alin, L., Chen, Y., Brand, D., Bourassa, M.W., Dietrich, K., Wilkinson, C.M., Nadeau, C.A., Kumar, A., Perry, S., et al. (2018). N-acetylcysteine targets 5 lipoxygenase-derived, toxic lipids and can synergize with prostaglandin E2 to inhibit ferroptosis and improve outcomes following hemorrhagic stroke in mice. Ann. Neurol. 84, 854–872. https://doi.org/10.1002/ana.25356.

Li, Y., Maher, P., and Schubert, D. (1997). A role for 12-lipoxygenase in nerve cell death caused by glutathione depletion. Neuron 19, 453–463. https://doi.org/10.1016/s0896-6273(00)80953-8.

Linkermann, A., Skouta, R., Himmerkus, N., Mulay, S.R., Dewitz, C., De Zen, F., Prokai, A., Zuchtriegel, G., Krombach, F., Welz, P.-S., et al. (2014). Synchronized renal tubular cell death involves ferroptosis. Proc. Natl. Acad. Sci. U. S. A. 111, 16836–16841. https://doi.org/10.1073/pnas.1415518111.

Magtanong, L., Ko, P.-J., To, M., Cao, J.Y., Forcina, G.C., Tarangelo, A., Ward, C.C., Cho, K., Patti, G.J., Nomura, D.K., et al. (2019). Exogenous Monounsaturated Fatty Acids Promote a Ferroptosis-Resistant Cell State. Cell Chem. Biol. 26, 420-432.e9. https://doi.org/10.1016/j.chembiol.2018.11.016.

Mahoney-Sánchez, L., Bouchaoui, H., Ayton, S., Devos, D., Duce, J.A., and Devedjian, J.-C. (2020). Ferroptosis and its potential role in the physiopathology of Parkinson's Disease. Prog.

Neurobiol. 101890. https://doi.org/10.1016/j.pneurobio.2020.101890.

Martin-Sanchez, D., Ruiz-Andres, O., Poveda, J., Carrasco, S., Cannata-Ortiz, P., Sanchez-Niño, M.D., Ruiz Ortega, M., Egido, J., Linkermann, A., Ortiz, A., et al. (2017). Ferroptosis, but Not Necroptosis, Is Important in Nephrotoxic Folic Acid-Induced AKI. J. Am. Soc. Nephrol. JASN 28, 218–229. https://doi.org/10.1681/ASN.2015121376.

Mischley, L.K., Allen, J., and Bradley, R. (2012). Coenzyme Q10 Deficiency in Patients with Parkinson's Disease. J. Neurol. Sci. 318, 72–75. https://doi.org/10.1016/j.jns.2012.03.023.

Mohamed, N.-V., Sirois, J., Ramamurthy, J., Mathur, M., Lépine, P., Deneault, E., Maussion, G., Nicouleau, M., Chen, C.X.-Q., Abdian, N., et al. (2021). Midbrain organoids with an SNCA gene triplication model key features of synucleinopathy. Brain Commun. 3, fcab223. https://doi.org/10.1093/braincomms/fcab223.

Moreau, C., Duce, J.A., Rascol, O., Devedjian, J.-C., Berg, D., Dexter, D., Cabantchik, Z.I., Bush, A.I., and Devos, D. (2018). Iron as a therapeutic target for Parkinson's disease. Mov. Disord. 33, 568–574. https://doi.org/10.1002/mds.27275.

Naudí, A., Cabré, R., Dominguez-Gonzalez, M., Ayala, V., Jové, M., Mota-Martorell, N., Piñol-Ripoll, G., Gil-Villar, M.P., Rué, M., Portero-Otín, M., et al. (2017). Region-specific vulnerability to lipid peroxidation and evidence of neuronal mechanisms for polyunsaturated fatty acid biosynthesis in the healthy adult human central nervous system. Biochim. Biophys. Acta Mol. Cell Biol. Lipids 1862, 485–495. https://doi.org/10.1016/j.bbalip.2017.02.001.

Pearce, R.K., Owen, A., Daniel, S., Jenner, P., and Marsden, C.D. (1997). Alterations in the distribution of glutathione in the substantia nigra in Parkinson's disease. J. Neural Transm. Vienna Austria 1996 104, 661–677. https://doi.org/10.1007/BF01291884.

Reinhardt, P., Glatza, M., Hemmer, K., Tsytsyura, Y., Thiel, C.S., Höing, S., Moritz, S., Parga, J.A., Wagner, L., Bruder, J.M., et al. (2013). Derivation and Expansion Using Only Small Molecules of Human Neural Progenitors for Neurodegenerative Disease Modeling. PLOS ONE 8, e59252. https://doi.org/10.1371/journal.pone.0059252.

Schneider, S.A., and Obeso, J.A. (2015). Clinical and pathological features of Parkinson's disease. Curr. Top. Behav. Neurosci. 22, 205–220. https://doi.org/10.1007/7854_2014_317.

Sharon, R., Goldberg, M.S., Bar-Josef, I., Betensky, R.A., Shen, J., and Selkoe, D.J. (2001). alpha-Synuclein occurs in lipid-rich high molecular weight complexes, binds fatty acids, and shows homology to the fatty acid-binding proteins. Proc. Natl. Acad. Sci. U. S. A. 98, 9110–

9115. https://doi.org/10.1073/pnas.171300598.

Sharon, R., Bar-Joseph, I., Mirick, G.E., Serhan, C.N., and Selkoe, D.J. (2003). Altered fatty acid composition of dopaminergic neurons expressing alpha-synuclein and human brains with alpha-synucleinopathies. J. Biol. Chem. 278, 49874–49881. https://doi.org/10.1074/jbc.M309127200.

Sian, J., Dexter, D.T., Lees, A.J., Daniel, S., Agid, Y., Javoy-Agid, F., Jenner, P., and Marsden, C.D. (1994). Alterations in glutathione levels in Parkinson's disease and other neurodegenerative disorders affecting basal ganglia. Ann. Neurol. 36, 348–355. https://doi.org/10.1002/ana.410360305.

Sofic, E., Lange, K.W., Jellinger, K., and Riederer, P. (1992). Reduced and oxidized glutathione in the substantia nigra of patients with Parkinson's disease. Neurosci. Lett. 142, 128–130. https://doi.org/10.1016/0304-3940(92)90355-b.

Spillantini, M.G., Schmidt, M.L., Lee, V.M., Trojanowski, J.Q., Jakes, R., and Goedert, M. (1997). Alpha-synuclein in Lewy bodies. Nature 388, 839–840. https://doi.org/10.1038/42166.

Stockwell, B.R., Friedmann Angeli, J.P., Bayir, H., Bush, A.I., Conrad, M., Dixon, S.J., Fulda, S., Gascón, S., Hatzios, S.K., Kagan, V.E., et al. (2017). Ferroptosis: A Regulated Cell Death Nexus Linking Metabolism, Redox Biology, and Disease. Cell 171, 273–285. https://doi.org/10.1016/j.cell.2017.09.021.

Tang, D., Chen, X., Kang, R., and Kroemer, G. (2021). Ferroptosis: molecular mechanisms and health implications. Cell Res. 31, 107–125. https://doi.org/10.1038/s41422-020-00441-1.

Vallerga, C.L., Zhang, F., Fowdar, J., McRae, A.F., Qi, T., Nabais, M.F., Zhang, Q., Kassam, I., Henders, A.K., Wallace, L., et al. (2020). Analysis of DNA methylation associates the cystine–glutamate antiporter SLC7A11 with risk of Parkinson's disease. Nat. Commun. 11, 1238. https://doi.org/10.1038/s41467-020-15065-7.

Wolf, R.A., and Gross, R.W. (1985). Identification of neutral active phospholipase C which hydrolyzes choline glycerophospholipids and plasmalogen selective phospholipase A2 in canine myocardium. J. Biol. Chem. 260, 7295–7303.

Yakunin, E., Kisos, H., Kulik, W., Grigoletto, J., Wanders, R.J.A., and Sharon, R. (2014). The regulation of catalase activity by PPAR γ is affected by α -synuclein. Ann. Clin. Transl. Neurol. 1, 145–159. https://doi.org/10.1002/acn3.38.

Yang, H.C., Farooqui, A.A., and Horrocks, L.A. (1996). Characterization of plasmalogen-selective phospholipase A2 from bovine brain. Adv. Exp. Med. Biol. 416, 309–313. https://doi.org/10.1007/978-1-4899-0179-8_49.

Yang, W.S., Kim, K.J., Gaschler, M.M., Patel, M., Shchepinov, M.S., and Stockwell, B.R. (2016). Peroxidation of polyunsaturated fatty acids by lipoxygenases drives ferroptosis. Proc. Natl. Acad. Sci. 113, E4966–E4975. https://doi.org/10.1073/pnas.1603244113.

Zhang, Y., Shu, L., Sun, Q., Pan, H., Guo, J., and Tang, B. (2018a). A Comprehensive Analysis of the Association Between SNCA Polymorphisms and the Risk of Parkinson's Disease. Front. Mol. Neurosci. 11. https://doi.org/10.3389/fnmol.2018.00391.

Zhang, Z., Wu, Y., Yuan, S., Zhang, P., Zhang, J., Li, H., Li, X., Shen, H., Wang, Z., and Chen, G. (2018b). Glutathione peroxidase 4 participates in secondary brain injury through mediating ferroptosis in a rat model of intracerebral hemorrhage. Brain Res. 1701, 112–125. https://doi.org/10.1016/j.brainres.2018.09.012.

Ziv, I., Shirvan, A., Offen, D., Barzilai, A., and Melamed, E. (2001). Molecular biology of dopamine-induced apoptosis : possible implications for Parkinson's disease. Methods Mol. Med. 62, 73–87. https://doi.org/10.1385/1-59259-142-6:73.

Zou, Y., Henry, W.S., Ricq, E.L., Graham, E.T., Phadnis, V.V., Maretich, P., Paradkar, S., Boehnke, N., Deik, A.A., Reinhardt, F., et al. (2020). Plasticity of ether lipids promotes ferroptosis susceptibility and evasion. Nature 585, 603–608. https://doi.org/10.1038/s41586-020-2732-8.

Figures

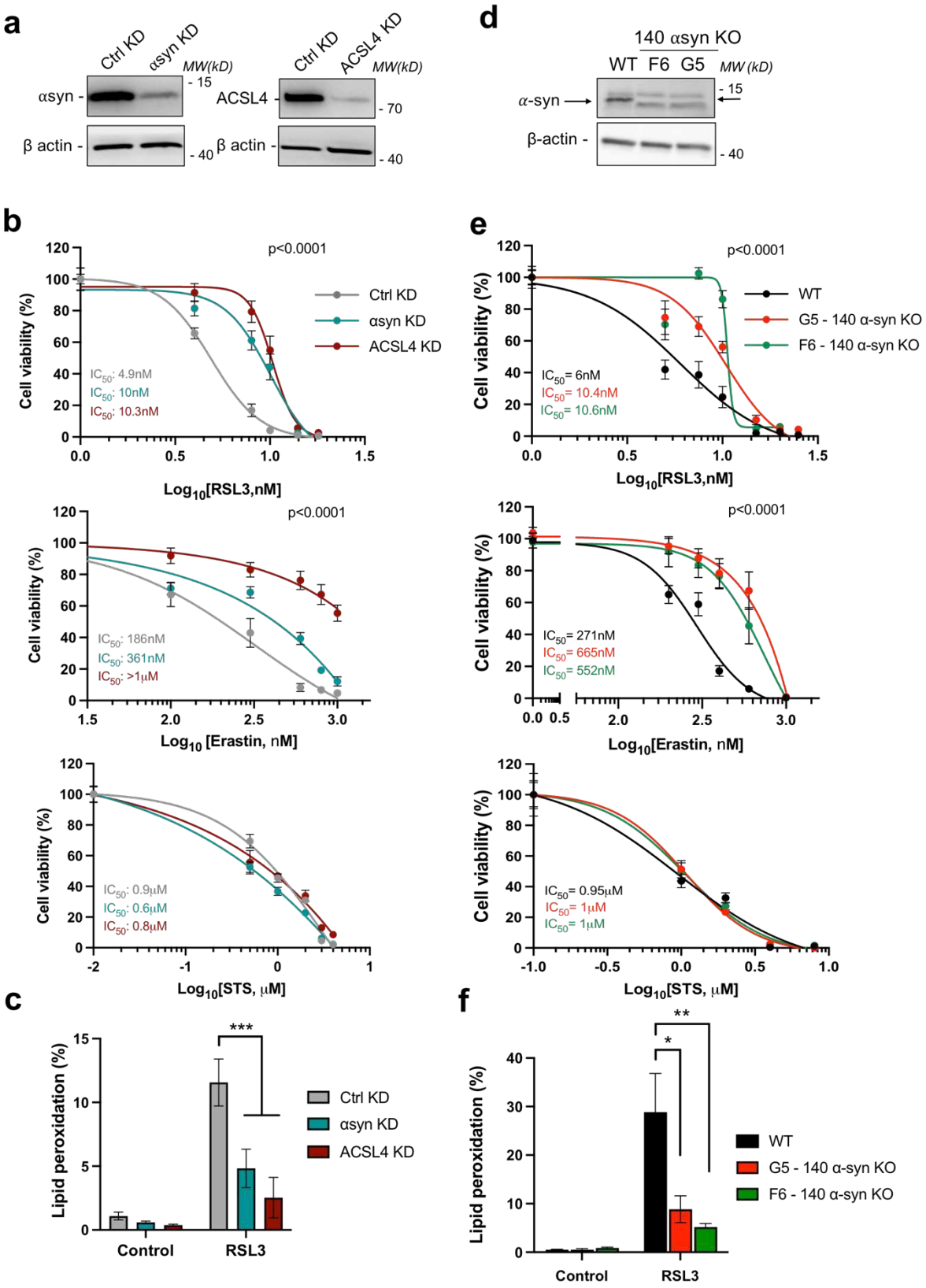

Fig. 1 Depletion of α-synuclein selectively protects dopaminergic neurons from ferroptosis comparative to ACSL4. a. Representative western blot analysis of α-syn and

ACSL4 KD in LUHMES cells compared to control siRNA KD. **b.** Non-linear regression dose curves for viability in Ctrl, α-syn and ACSL4 KD LUHMES cell upon treatment (24h) with the ferroptosis inducers RSL3 and erastin or the apoptosis inducer, staurosporine (STS). Curves were fitted and extra sum-of-squares F tests were performed to assess whether differences were statistically significance. **c.** Lipid peroxidation as assayed by flow cytometry using the C11-BODIPY probe, in Ctrl, α-syn or ACSL4 KD LUHMES cells treated with RSL3 (20nM; 6h). **d.** Representative western blot analysis of LUHMES with wild type α-syn (WT) or the two 140 α-syn KO clones. **e.** Viability curves for WT and 140 α-syn KO clones in response to treatment (24h) with RSL3, erastin or STS. Curves were fitted and extra sum-of-squares F tests were performed to assess whether differences were statistically significance. **f.** Lipid peroxidation analysis of WT and 140 α-syn KO clones after treatment with RSL3 (15nM; 24h). All data is represented as mean ± SEM of three independent experiments. Comparisons in **c&f** were made using the two-tailed, unpaired Student's *t*-test; * $p<0.05$, ** $p> 0.01$, *** $p<0.001$.

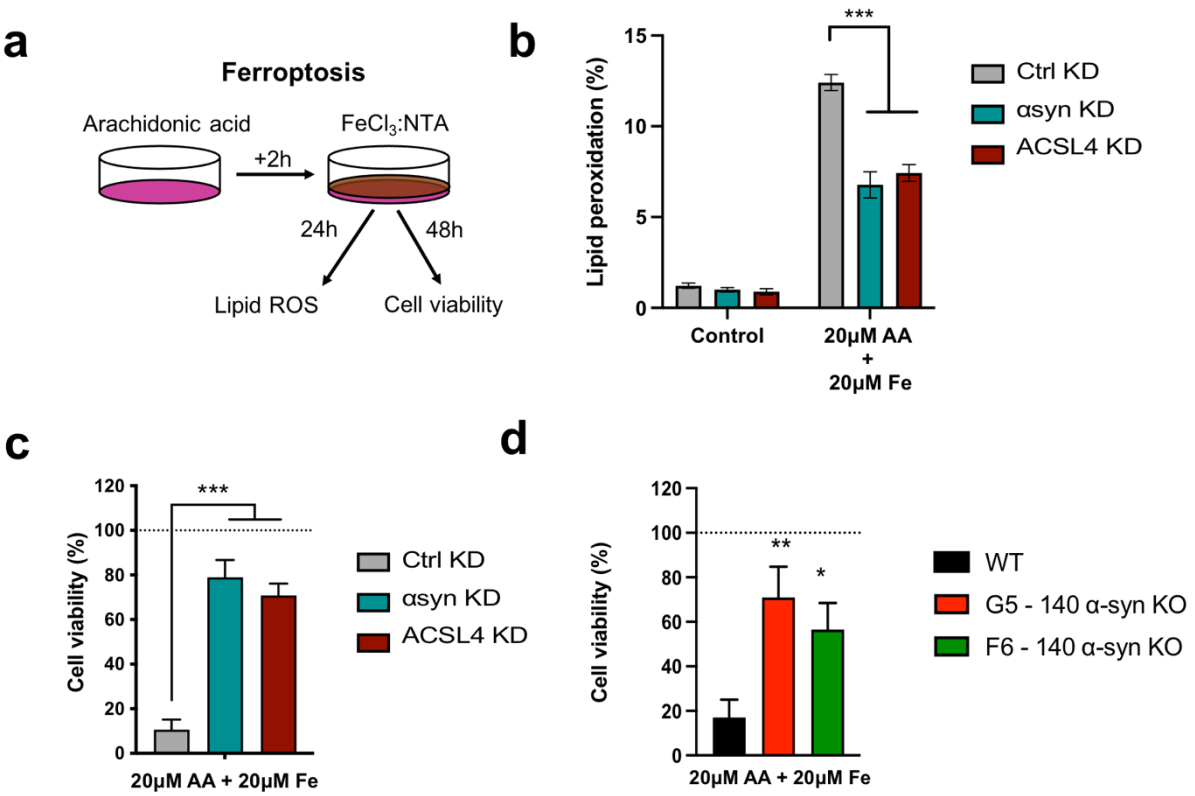

Fig. 2 α-synuclein and ACSL4 mediate dopaminergic neuron sensitivity to ferroptosis induced by arachidonic acid and iron. a. Schematic representation of a more physiologically relevant model of ferroptosis in which differentiated LUHMES cells were treated with arachidonic acid (AA) (20µM) followed by FeCl3:NTA (20µM) before measuring lipid peroxidation or cell viability at 24h and 48h respectively. NTA, nitrilotriacetic acid. **b&c.** Lipid peroxidation (**b**) and cell viability (**c**) in Ctrl, α-syn or ACSL4 KD LUHMES cells with the AA + Fe model of ferroptosis. **d.** Cell viability for WT and 140 α-syn KO LUHMES clones in response to AA + Fe co-treatment (48h). Results expressed as mean ± SEM of three independent experiments. Statistical comparisons were made using two-tailed, unpaired Student's *t*-test; * p<0.05, ** p<0.01, *** p< 0.001.

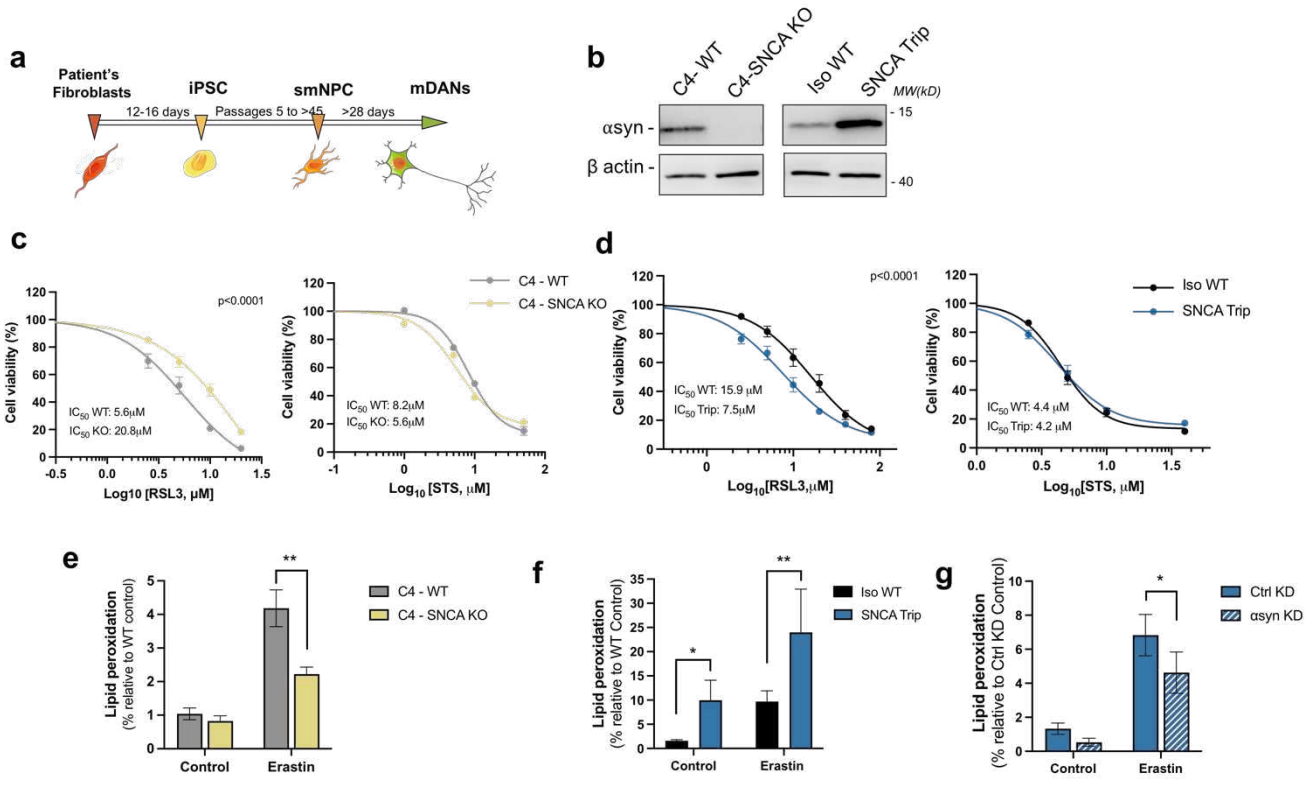

Fig. 3 α-synuclein enhances ferroptosis cell death in human smNPC-derived midbrain neurons. a. Differentiation protocol of human fibroblast into midbrain dopaminergic neurons (mDANs). **b.** Western blot confirmation of α-syn expression in smNPC derived midbrain neurons comparing the isogenic control (C4 – WT) to a CRISPR/Cas9 generated SNCA KO (C4 – SNCA KO) or familial SNCA triplication to its isogenic control. **c&d.** Cell viability curves in response to RSL3 or STS (24h) in WT vs SNCA KO (**c**) and SNCA Trip vs isogenic WT (**d**) mDANs. Curves were fitted and extra sum-of-squares F tests were performed to assess whether differences were statistically significance. **e-f.** Lipid peroxidation relative to WT control after erastin treatment in WT and SNCA KO as well as isogenic WT and SNCA Trip human mDANs (80μM; 6h). **g.** Lipid peroxidation in SNCA Trip mDANs transfected with α-syn siRNA in response to erastin (80μM; 6h) relative to Ctrl KD SNCA Trip mDANs. Data represent mean ± SEM in a minimum of three independent experiments. Statistical comparisons were made the one-tailed, unpaired *t*-test (**f**) or two-tailed *t*-test (**e&g**); * p<0.05, ** p< 0.01, *** p<0.001.

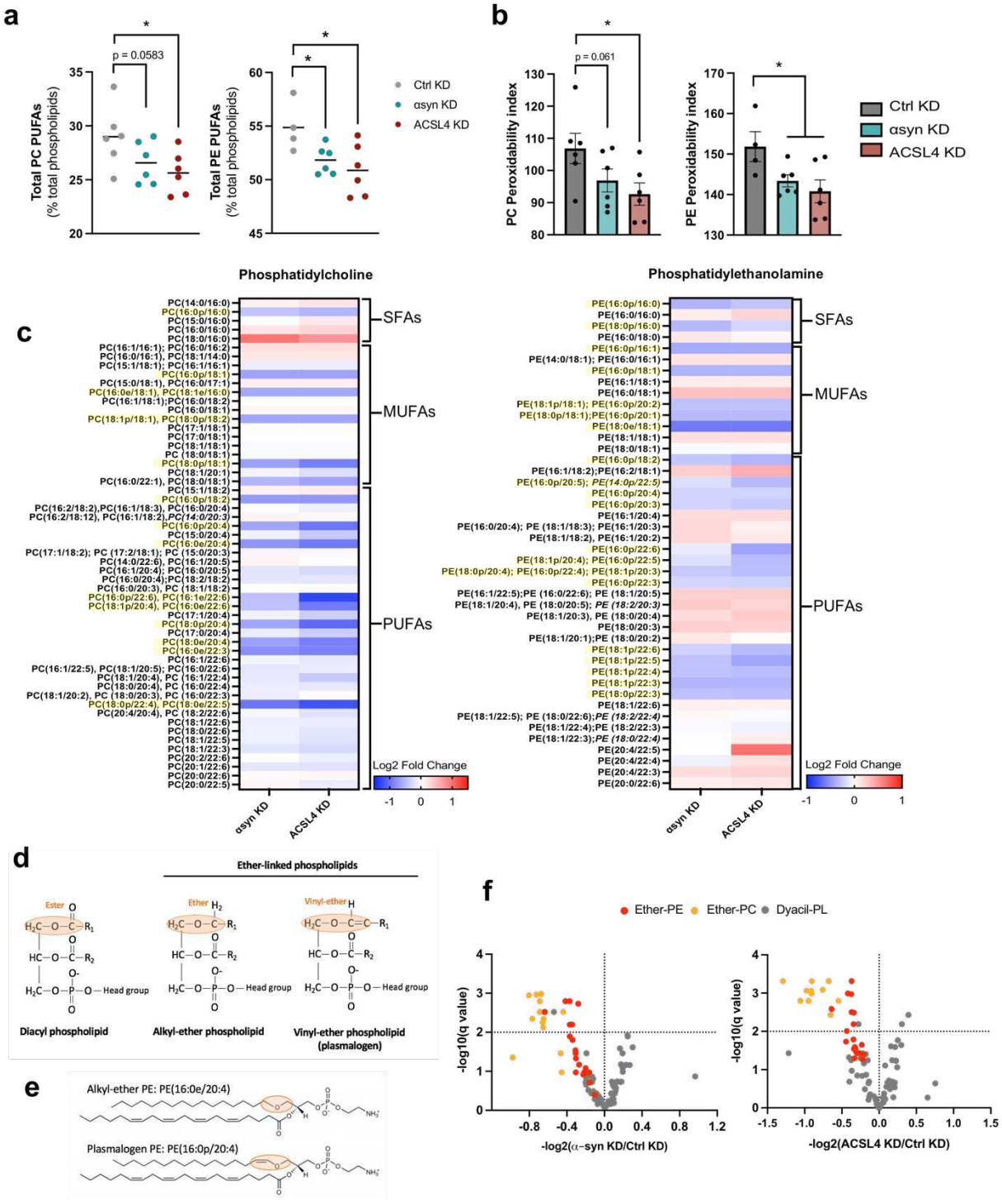

Fig. 4 Modulated ether-linked phospholipid composition by α-synuclein and ACSL4 expression in dopaminergic neurons. a&b. Total levels (**a**) and the peroxidability index (see methods for equation) (**b**) of phosphatidylcholine (PC) and phosphatidylethanolamine (PE) phospholipid containing PUFAs measured in α-syn and ACSL4 KD LUHMES cells. Data represents mean of six replicates **c.** Heat maps comparing the abundance of the different

PC and PE molecular species in α-syn and ACSL4 KD LUHMES cells relative to Ctrl KD. Highlighted in yellow are ether-linked phospholipids shown to be reduced in both the α-syn and ACSL4 KD conditions. **d** Schematic representation of the distinct structures of diacyl phospholipids and the two subtypes of ether-linked phospholipids. **e** The chemical structure of an example alkyl-ether PL, PE(16:0e/20:4), and a plasmalogen, PE(16:0p/20:4). **f** Volcano plots of the expression changes of the phospholipids, with each subtype grouped by colour, for α-syn vs Ctrl KD (left) and ACSL4 vs Ctrl KD (right) LUHMES cells. Data represents mean of six replicates. Statistical mean comparisons in **a&b** were made using the unpaired one-tailed Student's *t*-test (* $p<0.05$) and data in **c** is represented as a $\log_2$ fold change.

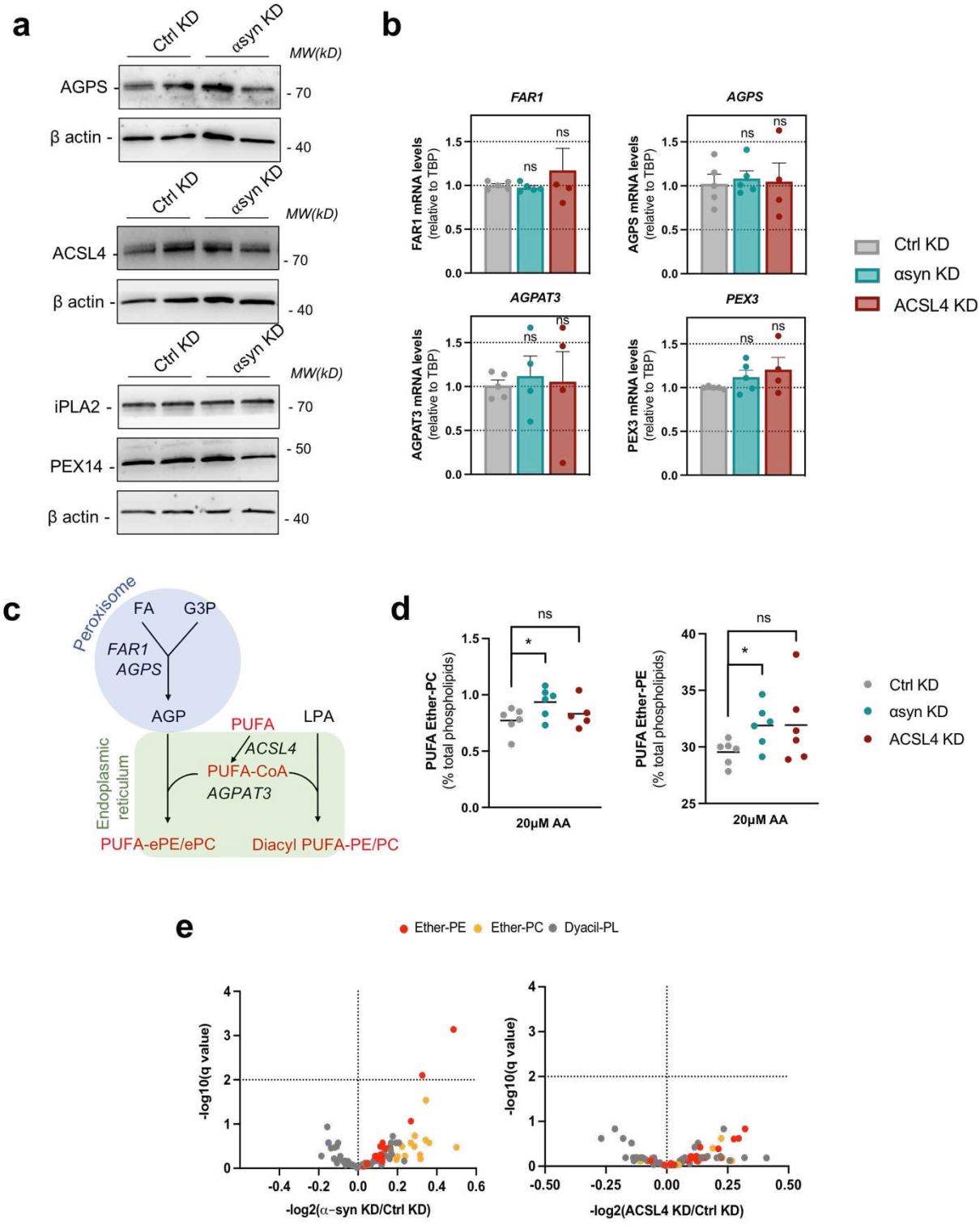

Fig. 5 Arachidonic acid treatment restores ether-PL levels in neurons that have a depletion in α-syn or ACSL4. a&b. Protein (**a**) and mRNA (**b**) expression of several key enzymes involved in the ether-PL biosynthesis pathway in α-syn and ACSL4 KD LUHMES. The relative gene expression was normalized to TBP. **c.** Schematic representation of the

ether-PL biosynthesis pathway starting at the peroxisomal level through to the ER. FA, fatty acid; LPA, lysophosphatidic acid; G3P, glycerol-3-phosphate. **d.** PUFA ether-PC and PUFA ether-PE proportion measured in α-syn and ACSL4 after AA (20μM; 24h) supplementation. **e** Volcano plots illustrating changes in the neuronal PE and PC phospholipid composition upon KD of α-syn or ACSL4 KD and treatment with AA (20μM;24h). Data represents the mean ± SEM from three independent experiments. Statistical mean comparisons in **b&d** were made using the unpaired two-tailed Student's *t*-test (* $p<0.05$